

Some pages of this thesis may have been removed for copyright restrictions.

If you have discovered material in Aston Research Explorer which is unlawful e.g. breaches copyright, (either yours or that of a third party) or any other law, including but not limited to those relating to patent, trademark, confidentiality, data protection, obscenity, defamation, libel, then please read our [Takedown policy](#) and contact the service immediately (openaccess@aston.ac.uk)

**DEVELOPMENT OF A NOVEL DEFORMABLE LIPOSOMAL FORMULATION FOR THE
DERMAL DRUG DELIVERY OF ANTICANCER AGENTS IN THE TREATMENT OF NON-
MELANOMA SKIN CANCERS**

MANDEEP KAUR MARWAH

Doctor of philosophy

ASTON UNIVERSITY

July 2017

© Mandeep Kaur Marwah, 2017

**Mandeep Kaur Marwah asserts her moral right to be identified as the author of this
thesis**

**This copy of the thesis has been supplied on condition that anyone who consults it is
understood to recognise that its copyright rests with its author and that no quotation
from the thesis and no information derived from it may be published without
appropriate permission or acknowledgement.**

Aston University

Development of a novel deformable liposomal formulation for the dermal drug delivery of an anticancer agents

Mandeep Kaur Marwah

Doctor of philosophy

2017

Thesis Summary

The incidence of skin cancer is increasing and conventional treatments such as surgery are not suitable for all patients. This study aimed to develop an elastic liposomal gel to be applied directly to the tumour for the controlled release of anti-cancer agents to the dermal layer. The proposed anti-cancer flavonoids EGCG and naringenin as well as the novel potent cytotoxic agent MTL-004 were loaded into the bilayer of liposomes. Furthermore, aqueous gels HEC and HPMC were investigated as carriers for the liposomes to be applied topically.

Liposomes loaded with either Tween 80, Tween 20 or sodium cholate were found to have increased elastic properties, liposomes with an average size of 400 nm were able to pass through a pore size of 100 nm. Release studies from liposomes loaded with either EGCG, naringenin and MTL-004 as well as varying ratios of Tween 20 were carried out. Within 24 hours, EGCG liposomes loaded with 0% or 10% w/w Tween 20 gave a release of 13.7 ± 1.1 % and 94.4 ± 4.9 % respectively; naringenin liposomes loaded with 0% or 10% w/w Tween 20 gave a release of 109.7 ± 5.0 % and 48.5 ± 2.1 % respectively; MTL-004 liposomes loaded with 0% or 10% w/w Tween 20 gave a release of 59.8 ± 1.2 % and 74.0 ± 1.8 % respectively. This indicates a compounds individual physiochemical properties influences release of compound from liposomes.

EGCG, naringenin and MTL-004 loaded liposomes added into the aqueous gel HEC or HPMC gels may have had an additive effect in terms of retarding drug release. Release was faster from HEC gels and liposomes formulated with Tween 20.

In vitro cellular uptake of liposome uptake into HDFa and HaCat cells was apparent. Thus it appears elastic liposomes are useful in enhancing drug penetration into dermal cells and furthermore may be useful in the development of a controlled release formulation.

Skin cancer, deformable liposomes, dermal release, controlled release, elastic liposomes

Acknowledgements

Firstly, I would like to express my sincere gratitude to my supervisors Dr. Deborah Lowry and Dr. Raj K Singh Badhan for their invaluable guidance, encouragement and constant support throughout this PhD, thank you for everything. I am thankful to my associate supervisor Prof Yvonne Perrie for showing interest in my project and providing invaluable additional support. Additionally Prof Afzal Mohammed and Prof Richard Knox for their advice.

Thank you to all the lab technicians for providing all the lab and technical support throughout my project.

I would like to thank my group colleagues Onyii, Fadi and Mohammed as well as other group colleagues/ fellow researchers Manjit, Eman, Affiong, Swapnil, Carla and Craig for their direct or indirect help.

Thanks to ARCHA for providing training and allowing use of their facility. I would also like to thank the MRC for providing the funding for this PhD as well as Morvus for the supply of MTL-004.

Finally, I reserve my greatest expression of gratitude to my family; Mom and Dad as well as Kuldeep, Kuldeep, Jasdeep, Simren and Ram for their support and encouragement.

TABLE OF CONTENTS

1	Introduction.....	17
1.1	Background.....	18
1.1.1	Cancer.....	18
1.1.2	Skin cancers.....	19
1.1.3	Skin structure.....	21
1.1.4	Common skin cancer therapies	22
1.1.4.1	Topical skin cancer formulations	23
1.2	Topical, dermal and transdermal drug delivery formulation considerations.....	26
1.2.1	Drug physicochemical considerations.....	27
1.2.2	Overcoming the barrier function of the skin	28
1.2.2.1	Passive drug penetration enhancers.....	28
1.2.2.2	Active drug penetration enhancers	30
1.2.2.3	Nanoparticle carriers as penetration enhancers.....	30
1.3	Liposomes.....	32
1.3.1	Lipids	32
1.3.2	Topical liposomes.....	36
1.3.3	Deformable liposomes.....	37
1.3.4	Ethosomes.....	39
1.3.5	Liposome preparation techniques.....	39
1.3.5.1	Freeze drying method	40
1.3.5.2	Extrusion method.....	40
1.3.5.3	Hydration of a thin lipid film	40
1.3.5.4	Reverse-phase evaporation technique.....	40
1.3.5.5	Solvent injection technique.....	40
1.3.6	Characterising liposomes	41
1.3.6.1	Zeta potential.....	41
1.3.6.2	Liposome size	41
1.3.6.3	Confocal laser scanning microscopy	42
1.3.6.4	Encapsulation efficiency	42
1.3.6.5	Stability.....	42
1.4	Gel formulation for topical and transdermal delivery.....	43
1.5	Models of skin absorption.....	45
1.5.1	<i>In silico</i> approaches.....	45
1.5.2	<i>In vitro</i> approaches	46
1.5.2.1	Franz cell	46
1.5.2.2	Cell culture techniques.....	47

1.6	Novel compounds for the treatment of skin cancer	49
1.6.1	MTL-004	49
1.6.2	Flavonoids	51
1.7	Aims and objectives	55
2	Formulation development of elastic liposomes for controlled dermal drug delivery 56	
2.1	Introduction	57
2.2	Aims and objectives	60
2.3	Materials and method	61
2.3.1	Materials	61
2.3.2	Elastic liposome preparation	61
2.3.3	Liposome characterisation: particle size, polydispersity index and zeta potential	62
2.3.4	Liposomes stability	62
2.3.5	Assessment of liposomal deformability	63
2.3.5.1	Assessment of liposomal deformability following extrusion	63
2.3.5.2	Assessment of liposomal deformability following the mechanistic determination of energy contained within the liposomal bilayer	63
2.3.5.3	Assessment of liposomal deformability following lipid quantification after extrusion	64
2.3.6	Development of an <i>in vitro</i> skin model: growth and passage of cells	64
2.3.7	Impact of liposomal formulation on <i>In vitro</i> cytotoxicity on HDFa and HaCat cells	65
2.3.7.1	Haemocytometer counting protocol	65
2.3.8	Cellular liposomal uptake assay on HDFa and HaCat cells	66
2.3.9	Statistical analysis	67
2.4	Results and discussion	68
2.4.1	Liposome characterisation: particle size and polydispersity and zeta potential	68
2.4.2	Stability of deformable liposomes	75
2.4.3	Assessment of liposomal deformability	79
2.4.3.1	Assessment of liposomal deformability following extrusion	79
2.4.3.2	Assessment of the impact of pore size on the deformability of Tween 20 liposomes	82
2.4.3.3	Assessment of liposomal deformability following the mechanistic determination of energy contained within the liposomal bilayer	84
2.4.3.4	Assessment of liposomal deformability following lipid quantification following extrusion	89
2.4.4	Impact of liposomal formulation on <i>In vitro</i> cytotoxicity on HDFa and HaCat cells	94

2.4.5	Cellular liposomal uptake assay on HDFa and HaCat cells	96
2.5	Conclusion	100
3	Development of sustained release EGCG liposomal gel formulations for dermal drug delivery.....	102
3.1	Introduction.....	103
3.2	Aims and objectives	104
3.3	Materials and methods	106
3.3.1	Materials	106
3.3.2	Elastic liposome preparation	106
3.3.3	Liposome characterisation: particle size and polydispersity and zeta potential.....	106
3.3.4	Assessment of liposomal deformability.....	106
3.3.5	HPLC Methodology.....	107
3.3.5.1	HPLC validation	107
3.3.6	Determination of entrapment efficiency	108
3.3.7	Differential scanning calorimetry investigations of EGCG and EGCG lipid blends	108
3.3.8	EGCG loaded aqueous gel formulation.....	109
3.3.9	<i>In vitro</i> EGCG release studies.....	109
3.3.9.1	One compartment release model.....	109
3.3.9.2	Two compartment release model.....	109
3.3.9.3	Liposomal gel release study	110
3.3.10	Release kinetics	110
3.3.11	Growth and passage of cells.....	112
3.3.12	Impact of liposomal formulation on <i>In vitro</i> cytotoxicity on HDFa and HaCat cells.....	112
3.3.13	Cellular liposomal uptake assay on HDFa and HaCat cells	113
3.3.14	Liposome stability.....	113
3.3.15	Statistical analysis	113
3.4	Results and discussion	114
3.4.1	Liposome characterisation: particle size and polydispersity and zeta potential.....	114
3.4.2	HPLC calibration and validation of EGCG detection	118
3.4.3	Determination of entrapment efficiency	120
3.4.4	Assessment of liposomal deformability.....	122
3.4.5	Differential scanning calorimetry investigations of EGCG and EGCG lipid blends	126
3.4.6	Development of a suitable dermal dissolution media	128
3.4.7	<i>In vitro</i> EGCG release studies.....	129

3.4.7.1	EGCG release studies from gel formulations	129
3.4.7.1.1	One compartment release studies.....	129
3.4.7.1.1.1	Kinetic assessment of drug release.....	133
3.4.7.1.2	Two compartment release.....	136
3.4.7.1.2.1	Kinetic assessment.....	138
3.4.7.2	Comparison of EGCG release from HEC and HPMC gels at formulated at 3% w/v of polymer	141
3.4.7.3	EGCG release from liposomes.....	142
3.4.7.3.1	Kinetic assessment of EGCG release from liposomal formulations	144
3.4.7.4	Liposomal gel EGCG release studies.....	146
3.4.8	Impact of liposomal formulation on <i>In vitro</i> cytotoxicity on HDFa and HaCat cells.....	150
3.4.9	Cellular liposomal uptake assay on HDFa and HaCat cells	151
3.4.10	Stability of deformable liposomes	155
3.5	Conclusion	159
4	Development of sustained release naringenin liposomal gel formulations for dermal drug delivery	161
4.1	Introduction.....	162
4.2	Aims and objectives	163
4.3	Materials and methods	165
4.3.1	Materials	165
4.3.2	Elastic liposome preparation	165
4.3.3	Liposome characterisation: particle size and polydispersity and zeta potential.....	165
4.3.4	Assessment of liposomal deformability.....	165
4.3.5	HPLC methodology.....	165
4.3.5.1	HPLC validation	166
4.3.6	Determination of entrapment efficiency	166
4.3.7	Differential scanning calorimetry investigations of naringenin and naringenin-lipid blends.....	166
4.3.8	Naringenin loaded aqueous gel formulation.....	166
4.3.9	<i>In vitro</i> release studies	166
4.3.9.1	One compartment release model.....	166
4.3.9.2	Two compartment release model.....	166
4.3.9.3	Liposomal gel release study	167
4.3.10	Release kinetics	167
4.3.11	Growth and passage of cells.....	167

4.3.12	Impact of liposomal formulation on <i>in vitro</i> cytotoxicity on HDFa and HaCat cells.....	167
4.3.13	Cellular liposomal uptake assay on HDFa and HaCat cells	167
4.3.14	Liposome stability.....	168
4.3.15	Statistical analysis	168
4.4	Results and discussion	169
4.4.1	Liposome characterisation: particle size and polydispersity and zeta potential.....	169
4.4.2	HPLC calibration and validation	174
4.4.3	Determination of entrapment efficiency	176
4.4.4	Assessment of liposomal deformability	177
4.4.5	Differential scanning calorimetry investigations of naringenin and Naringenin lipid blends.....	181
4.4.6	Naringenin release studies.....	184
4.4.6.1	Naringenin release studies from gel formulations	184
4.4.6.1.1	One compartment release studies.....	184
4.4.6.1.1.1	Kinetic assessment.....	186
4.4.6.1.2	Two compartment release.....	188
4.4.6.1.2.1	Kinetic assessment.....	190
4.4.6.2	Naringenin release from liposomes.....	192
4.4.6.2.1	Kinetic assessment of naringenin release from liposomal formulations	194
4.4.6.3	Liposomal gel naringenin release studies	196
4.4.7	Impact of liposomal formulation on <i>In vitro</i> cytotoxicity on HDFa and HaCat cells.....	198
4.4.8	Cellular uptake assay on HDFa and HaCat cells.....	200
4.4.9	Stability of deformable liposomes	203
4.5	Conclusion	207
5	Development of sustained release MTL-004 liposomal gel formulations for dermal drug delivery.....	209
5.1	Introduction.....	210
5.2	Aims and objectives	211
5.3	Materials and methods	212
5.3.1	Materials	212
5.3.2	Elastic liposome preparation	212
5.3.3	Liposome characterisation: particle size and polydispersity and zeta potential.....	212
5.3.4	Assessment of liposomal deformability.....	212
5.3.5	HPLC methodology.....	212

5.3.5.1	HPLC method establishment.....	213
5.3.5.2	UV spectrometry	213
5.3.5.3	Chromatographic separation	213
5.3.5.4	Fluorescence detection	213
5.3.5.5	HPLC validation	213
5.3.6	Physicochemical properties.....	213
5.3.6.1	Solubility determination	213
5.3.6.2	Log P determination	214
5.3.7	Determination of entrapment efficiency	214
5.3.8	Differential scanning calorimetry investigations of MTL-004 and MTL-004 lipid blends	214
5.3.9	MTL-004 loaded aqueous gel formulation.....	214
5.3.10	<i>In vitro</i> release studies	214
5.3.10.1	One compartment release model.....	214
5.3.10.2	Two compartment release model.....	215
5.3.11	Liposomal gel release study	215
5.3.12	Release kinetics	215
5.3.13	Growth and passage of cells.....	215
5.3.14	Impact of liposomal formulation on <i>In vitro</i> cytotoxicity on HDFa and HaCat cells.....	215
5.3.15	Cellular liposomal uptake assay on HDFa and HaCat cells	215
5.3.16	Liposome stability.....	216
5.3.17	Statistical analysis	216
5.4	Results and discussion	217
5.4.1	MTL-004 concerns and supply issues	218
5.4.2	Liposome characterisation: particle size and polydispersity and zeta potential.....	218
5.4.3	HPLC methodology establishment.....	221
5.4.3.1	UV spectroscopy.....	221
5.4.3.2	HPLC method optimisation	221
5.4.3.3	HPLC calibration	223
5.4.3.4	HPLC Validation.....	223
5.4.3.5	Fluorescence detection	225
5.4.4	Physicochemical properties.....	227
5.4.4.1	Solubility.....	227
5.4.4.2	Log P determination	227
5.4.5	Determination of entrapment efficiency	227
5.4.6	Assessment of liposomal deformability	229

5.4.7	Differential scanning calorimetry investigations of MTL-004 and MTL-004 lipid blends	232
5.4.8	MTL-004 release studies	234
5.4.8.1	MTL-004 release studies from gel formulations.....	234
5.4.8.2	One compartment release studies	235
5.4.8.2.1	Kinetic assessment	236
5.4.8.3	Two compartment release	237
5.4.8.3.1	Kinetic assessment	239
5.4.9	MTL-004 release from liposomes	240
5.4.9.1	Kinetic assessment of MTL-004 release from liposomal formulations 242	
5.4.10	Liposomal gel MTL-004 release studies	243
5.4.11	Impact of liposomal formulation on <i>In vitro</i> cytotoxicity on HDFa and HaCat cells.....	245
5.4.12	Cellular liposomal uptake assay on HDFa and HaCat cells	246
5.4.13	Stability of deformable liposomes	250
5.5	Conclusion	254
6	General conclusions.....	256
6.1	General conclusions.....	257
6.2	Future studies	260
7	References	261

LIST OF ABBREVIATIONS

A	Area
ANOVA	Analysis of variance
C	Celsius
CO ₂	Carbon dioxide
Da	Daltons
DI	Deformability index
DiIc	1,1'-Dioctadecyl-3,3',3'-Tetramethylindocarbocyanine Perchlorate
DMSO	Dimethylsulphoxide
DSC	Differential scanning calorimetry
F	force
g	Gram
h	Hour
HEC	Hydroxyethyl cellulose
HPLC	High performance liquid chromatography
HPMC	Hydroxyl propyl methyl cellulose
LOD	Limit of detection
LOQ	Limit of quantification
MEM	Eagle's minimal essential medium
mg	Milligram
min	Minute
μL	Microliter
mL	Millilitre
μM	Micromolar
mM	Millimolar
MSC	Melanoma skin cancer
MW	molecular weight
nm	Nanometer
NMSC	Non-melanoma skin cancer
P	pressure
PBS	phosphate buffered saline
RH	Relative humidity
RPM	Revolutions per minute
SC	stratum corneum
SD	Standard deviation
UV	Ultraviolet
XTT	2,3-Bis-(2-Methoxy-4-Nitro-5-Sulfophenyl)-2H-Tetrazolium-5-Carboxanilide
v	Volume
w	Weight

LIST OF FIGURES

Figure 1.1: Illustrations of the various sub classifications of skin cancer	20
Figure 1.2: Anatomy of the skin	21
Figure 1.3: Imiquimod mechanism of action	24
Figure 1.4: Diagrammatic representation of potential drug penetration pathways	27
Figure 1.5: Liposome structure in aqueous media summary.	32
Figure 1.6: Lipid shape influence on lipid aggregate formation.	34
Figure 1.7: Diagram of liposome subtypes.....	36
Figure 1.8: Representation of how liposomes may interact with the skin	37
Figure 1.9: Deformable liposome movement thought the intact stratum coreum into the dermal layer.....	38
Figure 1.10: Aqueous gel structure	44
Figure 1.11: Franz cell diagram	47
Figure 1.12: Mechanism of action of MTL-004.....	50
Figure 2.1: Chemical structures of a) Tween 80, b) Tween 20, c) sodium cholate.....	59
Figure 2.2: Hemocytometer gridlines.	66
Figure 2.3: Impact of surfactants on liposome size distribution	69
Figure 2.4: Impact of surfactants on polydispersity of liposomes	72
Figure 2.5: Confocal images of MLV liposomes.....	76
Figure 2.6: The stability of blank and deformable liposomes	78
Figure 2.7: Deformability index following extrusion.....	79
Figure 2.8: Deformability index of liposomes following extrusion through a membrane with pore size of 200 nm, 100 nm and 50 nm	83
Figure 2.9: Mechanistic determination of energy stored in the liposome as determined by extrusion	86
Figure 2.10: Stress – strain graph	88
Figure 2.11: The difference in cholesterol concentration in pre- and post- liposomal extrusion	91
Figure 2.12: The difference in PC concentration in pre- and post- liposomal extrusion	92
Figure 2.13: Cellular toxicity of liposomal formulations towards HDFa cells.	95
Figure 2.14: Cellular toxicity of liposomal formulations towards HDFa cells.	95
Figure 2.15: Localisation of DiIC loaded liposomes in HaCat cells.....	97
Figure 2.16: Localisation of DiIC loaded liposomes in HDFa cells.....	98
Figure 3.1: Molecular structure of EGCG	103
Figure 3.2: Liposome size distribution.	116
Figure 3.3: Polydispersity of blank and EGCG loaded liposomes.....	117
Figure 3.4: HPLC-UV calibration curve for EGCG	118
Figure 3.5: Calibration data of EGCG obtained over 3 days	119
Figure 3.6: Entrapment efficiency of EGCG in liposomes formulated with up to 10% w/w Tween 20.....	120
Figure 3.7: Structure and MW of EGCG, cholesterol, Tween 20 and PC	121
Figure 3.8: Deformability index for blank and EGCG loaded liposomes	123
Figure 3.9: DSC scan of EGCG.....	126
Figure 3.10: DSC analysis scans of PC, cholesterol and Tween 20 and EGCG blends.	127
Figure 3.11: In vitro percentage EGCG release profiles from HEC gel.....	130
Figure 3.12: In vitro percentage EGCG release profiles from HPMC gels.....	131

Figure 3.13: Methods of drug release from a pharmaceutical formulation.....	133
Figure 3.14: In vitro percentage EGCG release profiles from HEC gels and EGCG solution	137
Figure 3.15: In vitro percentage EGCG release profiles from HPMC gels and EGCG solution	138
Figure 3.16: In vitro percentage EGCG release profiles from HEC and HPMC gel	142
Figure 3.17: In vitro percentage EGCG release profiles from solution and liposomal formulations.....	143
Figure 3.18: Diagram representing drug release kinetics from liposomes by dynamic dialysis.	146
Figure 3.19: In vitro percentage EGCG release profiles from liposomal gels.....	147
Figure 3.20: Cellular toxicity of EGCG on a) HDFa and b) HaCat cells.	150
Figure 3.21: Localisation of DiIC labelled liposomes loaded with EGCG and 2% w/w Tween 20 in HaCat cells.	151
Figure 3.22: Localisation of DiIC labelled liposomes loaded with EGCG and 2% w/w Tween 20 in HDFa cells.	152
Figure 3.23: z-dimension cellular localisation of DiIC-EGCG loaded liposomes formulated with 2% w/w Tween 20 in HaCat cells.	153
Figure 3.24: z-dimension cellular localisation of DiIC-EGCG loaded liposomes formulated with 2% w/w Tween 20 in HDFa cells	154
Figure 3.25: Confocal images of MLV liposomes formulated with 4% w/w of Tween 20.....	155
Figure 3.26: Stability of EGCG loaded liposomes as determined by size.....	156
Figure 3.27: Liposome encapsulation efficiency for EGCG.....	157
Figure 4.1: Molecular structure of naringenin	162
Figure 4.2: Liposome size distribution, comparing blank and naringenin loaded formulations.	170
Figure 4.3: Polydispersity of blank and naringenin loaded liposomes	172
Figure 4.4: Calibration data for naringenin as determined by HPLC-UV analysis	174
Figure 4.5: Calibration data of naringenin obtained over 3 days as determined by HPLC-UV analysis	175
Figure 4.6: Entrapment efficiency of naringenin in liposomes formulated with up to 10% w/w Tween 20.....	176
Figure 4.7: Structure and MW of naringenin, cholesterol, Tween 20 and PC	177
Figure 4.8: Deformability index following extrusion for blank and naringenin loaded liposomes.....	179
Figure 4.9: DSC scan of naringenin and lipid blends.	183
Figure 4.10: Naringenin release profiles from aqueous gels.....	185
Figure 4.11: In vitro percentage naringenin release profiles from aqueous gels	189
Figure 4.12: In vitro percentage naringenin release profiles from solution and liposomes ..	193
Figure 4.13: In vitro percentage naringenin release profiles from liposomal gels.....	197
Figure 4.14: Cellular toxicity of naringenin towards HDFa and HaCat cells.	199
Figure 4.15: Localisation of DiIC-naringenin loaded liposomes in HaCat cells	200
Figure 4.16: Localisation of DiIC-naringenin loaded liposomes in HDFa cells	200
Figure 4.17: z-dimension cellular localisation of DiIC-naringenin loaded liposomes formulated with 2% w/w Tween 20 in HaCat cells	201
Figure 4.18: z-dimension cellular localisation of DiIC-naringenin loaded liposomes formulated with 2% w/w Tween 20 in HDFa cells	202
Figure 4.19: Confocal images of MLV liposomes formulated with 4% w/w Tween 20	203

Figure 4.20: Stability of naringenin loaded liposomes as determined by size	204
Figure 4.21: Liposome encapsulation efficiency for naringenin over 28 days.....	205
Figure 5.1: Molecular structure and relative molecular weight of MTL-004	210
Figure 5.2: Images of MTL-004 batches.....	218
Figure 5.3: Liposome size distribution comparing blank and MTL-004 loaded formulations.....	219
Figure 5.4: Polydispersity of blank and MTL-004 loaded liposomes.....	220
Figure 5.5: Calibration data for MTL-004 as determined by HPLC-UV analysis.....	223
Figure 5.6: Calibration data of MTL-004 as determined by HPLC-UV analysis obtained over 3 days.....	224
Figure 5.7: Fluorescence scans of MTL-004	226
Figure 5.8: Entrapment efficiency of MTL-004 in liposomes formulated with up to 10% w/w Tween 20	228
Figure 5.9: Structure and MW of MTL-004, cholesterol, Tween 20 and PC	229
Figure 5.10: Deformability index of liposomes following extrusion.....	230
Figure 5.11: DSC scan of MTL-004 and lipid blends.....	233
Figure 5.12: In vitro percentage MTL-004 release profiles from HEC and HPMC gels	235
Figure 5.13: In vitro percentage MTL-004 release profiles from HEC and HPMC.....	238
Figure 5.14: In vitro percentage MTL-004 release profiles from solution and liposomes	241
Figure 5.15: In vitro percentage MTL-004 release profiles from liposomal gels	244
Figure 5.16: Cellular toxicity of MTL-004 on HDFa and HaCat cells.	246
Figure 5.17: Localisation DiIC-liposomes loaded with MTL-004 and 2% w/w Tween 20 in HaCat cells	247
Figure 5.18: Localisation of DiIC-liposomes loaded with MTL-004 and 2% w/w Tween 20 in HDFa cells.....	247
Figure 5.19: z-dimension cellular localisation of DiIC-MTL-004 loaded liposomes formulated with 2% w/w Tween 20 in HaCat cells	248
Figure 5.20: z-dimension cellular localisation of DiIC-MTL-004 loaded liposomes formulated with 2% w/w Tween 20 in HDFa cells	249
Figure 5.21: Confocal images of MLV liposomes formulated with MTL-004	250
Figure 5.22: Stability of MTL-004 loaded liposomes as determined by size.....	251
Figure 5.23: Liposome encapsulation efficiency for MTL-004 over 28 days.....	253

LIST OF TABLES

Table 1-1: Summary of drug characteristics required for transdermal drug delivery	28
Table 1-2: Classification and attributes of polar lipids.....	34
Table 2-1: Details of liposome formulation composition.....	62
Table 2-2: Gradient elution method for quantitative analysis of cholesterol, phosphatidylcholine (PC). TFA: trifluoroacetic acid.	64
Table 2-3: Zeta potential of liposomal formulations formulated with up to 10% w/w loading of Tween 80, Tween 20 and sodium cholate.....	74
Table 2-4: Cholesterol quantification pre- and post- extrusion of liposomal formulations through membranes of pore size 200 nm, 100 nm, and 50 nm formulated with up to 10% w/w Tween 20.....	89
Table 2-5: PC quantification pre- and post- extrusion of liposomal formulations through membranes of pore size 200 nm, 100 nm, and 50 nm formulated with up to 10% w/w Tween 20.....	90
Table 3-1: Details of liposome formulation composition.....	106
Table 3-2: Description of how the diffusional exponent n may be used to characterise release for cylindrical shaped matrices.....	112
Table 3-3: Zeta potential of liposomal formulations formulated with and without drug with up to 10% w/w loading of Tween 20	117
Table 3-4: Kinetic assessment of release data of EGCG from HEC and HPMC aqueous gels.	134
Table 3-5: First order kinetics rate constant for EGCG release from formulations.	135
Table 3-6: Diffusional exponent n calculated from the Korsmeyer-Peppas model of drug release for EGCG release data from aqueous gels with the corresponding release mechanism.....	135
Table 3-7: Kinetic assessment of release data of EGCG from solution and aqueous gels.	139
Table 3-8: First order kinetics rate constant for EGCG release from formulations	140
Table 3-9: Diffusional exponent n for EGCG release data with the corresponding release mechanism.....	141
Table 3-10: Kinetic assessment of release data of EGCG from solution and aqueous gels.	144
Table 3-11: First order kinetics rate constant for EGCG release from all formulations except liposomes formulated with 0% w/w Tween 20 where the zero order rate constant was observed.....	145
Table 4-1: Zeta potential of liposomal formulations formulated with and without naringenin with up to 10% w/w loading of Tween 20	173
Table 4-2: Kinetic assessment of release data of naringenin from HEC and HPMC aqueous gels.	187
Table 4-3: First order kinetics rate constant for naringenin release from formulations.....	187
Table 4-4: Diffusional exponent n calculated from the Korsmeyer-Peppas model of drug release for naringenin release data from aqueous gels with the corresponding release mechanism.....	188
Table 4-5: Kinetic assessment of release data of naringenin from solution and aqueous gels.	190
Table 4-6: First order kinetics rate constant for naringenin release from formulations.....	191
Table 4-7: Diffusional exponent n for naringenin release data with the corresponding release mechanism.....	191

Table 4-8: Kinetic assessment of release data of naringenin from solution and liposomal formulations.....	195
Table 4-9: First order kinetics rate constant for naringenin release from formulations.....	195
Table 5-1: Zeta potential of liposomal formulations formulated with and without drug with up to 10% w/w loading of Tween 20	220
Table 5-2: Effect of variations in the mobile phase ratio of the elution of MTL-004 in water where A is 0.1% TFA in water and B in acetonitrile	222
Table 5-3: Effect of variations in the mobile phase ratio of the elution of MTL-004 in water where A is 0.1% TFA in water and B in methanol.....	222
Table 5-4: Kinetic assessment of release data of MTL-004 from HEC and HPMC aqueous gels.	236
Table 5-5: First order kinetics rate constant for MTL-004 release from formulations	237
Table 5-6: Diffusional exponent n calculated from the Korsmeyer-Peppas model of drug release for MTL-004 release data from aqueous gels with the corresponding release mechanism.	237
Table 5-7: Kinetic assessment of release data of MTL-004 from solution and aqueous gels.	239
Table 5-8: First order kinetics rate constant for MTL-004 release from formulations.	239
Table 5-9: Diffusional exponent n for MTL-004 release data with the corresponding release mechanism.	240
Table 5-10: Kinetic assessment of release data of MTL-004 from solution and liposomal formulations.....	242
Table 5-11: First order kinetics rate constant for MTL-004 release from formulations.....	243

1 Introduction

1.1 Background

Skin cancer is emerging as an increasing public health problem especially in developed countries (Lomas et al., 2012). The large number of cases diagnosed present as a substantial burden to healthcare services in the U.K (Diepgen and Mahler, 2002; Donaldson and Coldiron, 2011). There were around 15,400 new cases of skin cancer in the UK in 2014 and is the fifth most common cancer (CancerResearchUK, 2014).

Skin cancer can be categorised as either non melanoma skin cancer (NMSC) or melanoma skin cancer (MSC), with the former being more common than the latter. NMSC is an increasing problem for health care services worldwide (Lomas et al., 2012). NMSC is the most common cancer affecting Caucasians and the incidence is rapidly increasing worldwide (Lomas et al., 2012). In Caucasian populations in Europe, the U.S., Canada, and Australia the average annual increase of NMSC since 1960 was 3–8% (Glass and Hoover, 1989; Green, 1992). Additionally, the incidence rates in the U.K. appear to be increasing at a faster rate when compared with the rest of Europe. The increase in the incidence of NMSC can be attributed to an amalgamation of increased sun exposure or exposure to ultraviolet (UV) light, increased life span, and ozone depletion (Gloster and Brodland, 1996). In fact, the incidence of NMSC in the Caucasian populations increases with closer proximity to the equator (Giles et al., 1988).

Whilst the incidence of MSC is lower compared with NMSC's, it occurs across all ethnicities. However, it's prevalence has been rising in the Caucasian population worldwide for several decades, in fact being the most rapidly rising cancer within this population grouping (Armstrong and Kricger, 1993; MacLennan et al., 1992). Within the U.K., the rate of MSC incidences has doubled every 10–20 years in North Humberside, between 1978 and 1991 (Ko et al., 1994). In comparison to NMSC, which mainly affecting the elderly population, MSC peaks in people aged between 20–45 year (Holme et al., 2000).

The majority of skin cancers are treatable; however poor treatment or particularly malignant forms of cancer results in 2,500 deaths annually (Skin Cancer in the UK, 2011; Cancer Research UK 2011, a, b, c). The most common treatment for both NMSC and MSC is local surgery to remove the tumour. However, it can be the case that surgical removal is not suitable for the patient thus development of alternative treatments is necessary.

1.1.1 Cancer

Cancer can be characterised by the uncontrolled multiplication and spread of atypical body cells. Both benign and malignant forms manifest as uncontrolled cell proliferation, however malignant forms are distinguished by their ability to de-differentiate, invade surrounding tissue

and metastasise. The main treatment for cancer is surgical excision, irradiation or chemotherapy. Cancer cells are in many ways similar to normal cells making them difficult to target and eliminate. Drugs currently used in chemotherapy include cytotoxic agents (such as alkylating agents, anti-metabolites, cytotoxic antibiotics and plant derivatives), hormones (steroids and antagonistic agents) and miscellaneous agents (including more recent treatments e.g. monoclonal antibodies). These drugs however cannot differentiate between fast-growing cancer cells and the other types of fast-growing cells including skin cells, blood cells, and cells inside the stomach. They therefore have a toxic effect on these cells as well causing side effects including nausea, vomiting, lethargy, hair loss, anaemia and even immunosuppression (Coates et al., 1983; Conklin, 2000; Lindley et al., 1999; Sitzia and Huggins, 1998). Therefore, one of the current challenges in cancer treatment is to enhance tumour-specific targeting so as to improve chemotherapy outcomes and reduce side effects.

1.1.2 Skin cancers

Skin cancers are usually caused by a combination of cumulative and intense sun exposure. NMSC develops slowly in the upper layers of the skin whilst MSC spreads faster in the body (Figure 1.1). NMSC can be classified further into either basal cell carcinoma (BCC) or squamous cell carcinoma (SCC). BCC and SCC are the most common tumours in the Caucasian human population, accounting for greater than 95% of NMSCs (Marcil and Stern, 2000; Urosevic and Dummer, 2002).

The BCCs subsect of NMSC can be described as the abnormal, uncontrolled growth arising within the basal cells, which line the deepest layer of the epidermis. BCCs appear as red patches, pink growths, shiny bumps, or scars (Figure 1.1). Nodular BCC presents as a pearly papule or nodule often exhibiting central crusting or ulceration. Superficial BCC presents as a scaly erythematous patch or plaque. Both nodular and superficial forms have a darker colouring as they contain melanin, imparting a brown, blue, or black colour to these tumours. Infiltrative BCC, appears as a white, scar-like plaque with indistinct margins (Rubin et al., 2005). The presentation of skin cancer can influence absorption of the formulation; tough scaly skin is harder to impregnate than an open ulcer.



Figure 1.1: Illustrations of the various sub classifications of skin cancer

a) NMSC basal cell carcinoma b) NMSC squamous cell carcinoma and c) MSC (Sun Spot Melanoma Awareness, 2013)

SCC is generally a proliferative exophytic tumour growing steadily over months. Depending on duration of growth, size ranges from a few millimetres up to centimetres. In the early stage an SCC may resemble a solar keratosis. A clinical indication of malignant transformation is thickening and tenderness of the skin. Sometimes, the tumours can become infiltrating and firm without an exophytic component. Additionally, a verrucous form of SCC may occur on the sole of the foot. The tumours induce an inflammatory reaction thus becoming crusted and erythematous with bleeding possible. A definite edge is difficult to distinguish on stretching the tumour, which is in contrast to a BCC (Figure 1.1) (R. Marks, 1996). Metastasis from cutaneous SCC appears most commonly in the regional lymph nodes followed by the lungs, liver and other organs (Marks, 1996).

MSC can be classified as superficial spreading, lentigo maligna melanoma and acral melanoma. Superficial spreading MSC observes slow cell growth at first which then spread out across the surface of the skin. Nodular melanoma observes faster cell growth than other melanomas. Lentigo maligna melanoma is observed more so in the elderly population and is localised to areas of skin that have experienced greater sun exposure. Acral melanoma is very rare and not thought to be related to sun exposure (Grossman et al., 1999; Katalinic et al., 2003; Madan et al.).

Both types of skin cancer are more likely to occur in light complexion individuals who have had considerable sunlight exposure, and are more common in the Southern latitudes of the Northern hemisphere. Furthermore, the immune system may have a role in pathogenesis of skin cancers thus may be exploited in treatment (de Visser et al., 2006).

1.1.3 Skin structure

The skin limits the passage of chemicals into and out of the body, helps maintain blood pressure and temperature and mediates sensations ranging from heat to pain. The skin is a multilayered organ with three major tissue layers, the epidermis, dermis and subcutaneous tissue (Figure 1.2). The epidermis has five layers, the cells of the basal layer proliferate and migrate upwards to produce the stratum corneum (Alexander et al., 2012). The epidermis is composed of keratinocytes but also includes melanocytes, sensory perception cells and immunological cells (Prow et al., 2011). There are tight junctions between the cells and expression of tight junction proteins are altered in skin diseases such as psoriasis, in which there is a compromised skin barrier (Cevc and Vierl, 2010). As skin ages the lipid packing arrangement is disrupted therefore lowering skin resistance (Cevc and Vierl, 2010) conversely, there is a depletion of skin lipids causing dry patches which can increase skin resistance (Brooks and Idson, 1991).

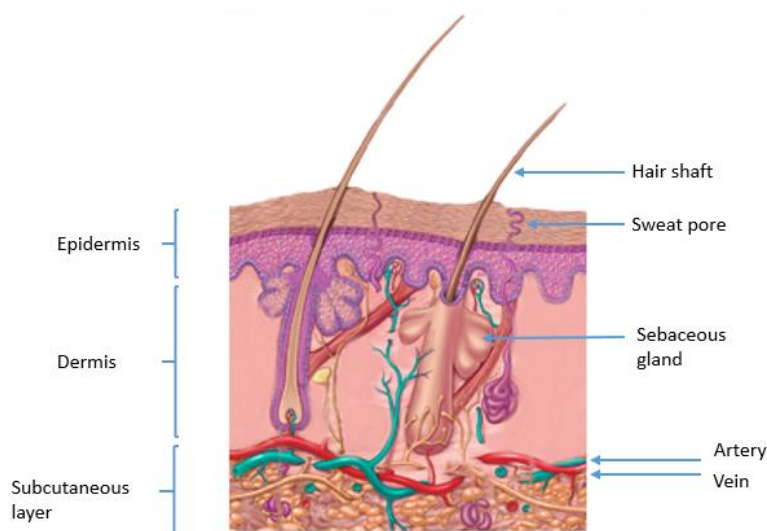


Figure 1.2: Anatomy of the skin

The skin consists of three main layers; the epidermis, dermis and subcutaneous layer (adapted from (McGraw-HillCompanies, 2003)).

The SC is the outermost layer of the epidermis and it is the layer that most limits drug penetration (Thomas and Finnin, 2004), It has a brick and mortar structure (Prow et al., 2011) consisting of corneocytes embedded multiple lipid bilayers of ceramides, cholesterol and fatty acids (Alexander et al., 2012). The dermis is thicker than the epidermis and is composed of connective tissues including collagen and elastic fibres. This layer has a copious blood supply to provide nutrients and remove toxins, thus the skin acts a sink for 'diffusing' molecules by

removing them from the site (Alexander et al., 2012). This can be useful for transdermal drug delivery as a concentration gradient will be maintained encouraging drug delivery by diffusion.

1.1.4 Common skin cancer therapies

The most common treatment to remove both NMSC and MSC are local surgery (curettage and electrodesiccation as well as Mohs micrographic surgery) to excise the tumour (Gaspari and Sauder, 2003; Neville et al., 2007). If the melanoma is identified at an early stage, this is usually the only treatment needed.

In specific circumstances, ionising radiation therapy may be used in skin cancer therapy. Radiation is usually delivered in fractionated doses in the form of superficial X-rays, orthovoltage or deep X-rays, or electron-beam therapy (Neville et al., 2007; Voss and Kim-Sing, 1998).

Additionally, cryosurgery is an option utilising liquid nitrogen at $-196.5\text{ }^{\circ}\text{C}$ to destroy tumour cells *via* freezing and vascular stasis. Ice crystal formation develops intracellularly and extracellularly, resulting in tissue damage and cell death (Kuflik, 1994; Neville et al., 2007; Nguyen and Ho, 2002).

Surgical treatments, radiation therapy and cryotherapy may not be suitable for all patients. Considerable disfigurement can result because of the nature of the tumours and their common localisation on highly visible, cosmetically important areas. That, in turn, represents a serious problem in cases of multiple tumours observed with certain genodermatoses or immunosuppressed patients (Marcil and Stern, 2000). Therefore, development of alternative treatments is important. Topical treatments are available and are effective alternatives for NMSC (Neville et al., 2007; Romero and Morilla, 2013a). These treatments may be useful after surgery when it has not been possible to remove all cancer cells or if there is a high risk of the tumour returning (Felicio et al., 2009; Neville et al., 2007).

Both BCC and SCC occur more so on the head and neck, the rest being divided between other sites of high UV exposure. These include the hands and forearms, upper trunk, and lower leg, in that order (Marks, 1996; Rubin et al., 2005). Thus an appealing aesthetic outcome of treatment is desirable. The choice of treatment approach depends on the location of the cancer, age and health status of the patient, and risk factors for tumour recurrence. Irrespective of the approach used, the treatment goal is to remove the tumour, achieve a high cure rate, preserve the maximal amount of normal surrounding tissue, whilst providing an optimum cosmetic outcome.

1.1.4.1 Topical skin cancer formulations

Topical chemotherapy, topical immunomodulators, or intralesional chemotherapy may be used to treat non-melanoma skin cancer (NMSC). Existing topical therapies have been found to be successful in NMSC treatment, a study found that for topical Imiquimod cure rates ranged from 65 % to 100 %, while for 5-fluorouracil (5-FU) rates ranged from 61 % to 92 %. For intralesional agents, cure rates varied depending on which medication was used and the NMSC subtype treated. Keratoacanthomas (a low grade skin tumour) had high cure rates with intralesional agents: 98 % for 5-FU, 91 % for methotrexate, 100 % for bleomycin, 100 % for interferon α -2, 83 % for interferon α -2a, and 100 % for interferon α -2b (Chitwood et al., 2013).

Topical photodynamic therapy (PDT) refers to topical application of a photosensitizer onto the site of skin disease which is followed by illumination which results in selected cell death. Photodynamic therapy is effective in treating SCC *in situ* and superficial BCCs. Compounds used in this manner include the photosensitizing porphyrin 5-aminolevulinic acid (ALA) and the methyl ester of ALA (mALA), both of which are converted to protoporphyrin IX once absorbed into the skin (Neville et al., 2007). Liposomes have been investigated as carriers for photosensitizers and were found to enhance penetration while decreasing absorption into the systemic circulation (Dragicevic-Curic and Fahr, 2012).

Immunotherapy of NMSC has been attempted with the use of agents such as imiquimod, interferon and interleukins, these treatments however have a lower efficacy compared with surgical approaches (Gaspari and Sauder, 2003; Urosevic and Dummer, 2002).

Imiquimod is a topical immune-response modulator effective when applied topically at the tumour site against superficial BCCs, small nodular BCCs and SCCs. The drug is a novel synthetic imidazoquinolone that modulates the immune system's response to cancer cells (Berman, 2002; Chitwood et al., 2013; Gaspari and Sauder, 2003; Good et al., 2011; Marks et al., 2001; Sauder, 2003). Imiquimod promotes innate and acquired immune responses via secretion of cytokines, and activation of Th-1 cell-mediated immunity (Figure 1.3) (Berman, 2002). This cytokine-induced immune response is responsible for the antiviral and antitumor effects of imiquimod. Additionally, imiquimod stimulates natural killer cells and the proliferation of B-lymphocytes whilst activating Langerhans cells, the key antigen-presenting cell of the skin, and stimulates their migration to regional lymph nodes (Berman, 2002). Responses provide long-term immune memory thus possibly offering future protection against the previously encountered tumour cells. Furthermore, imiquimod may promote cellular apoptosis (Meyer et al., 2003; Sullivan et al., 2003).

Dose-related inflammatory skin reactions such as erythema, burning, impetigo or tenderness at the treatment site at the site of application are common as this is caused by the cell death (Gaspari and Sauder, 2003). Unfortunately, clinical development of local inflammation seems to correlate with the success rate therefore, some degree of local reaction is necessary (Neville et al., 2007).

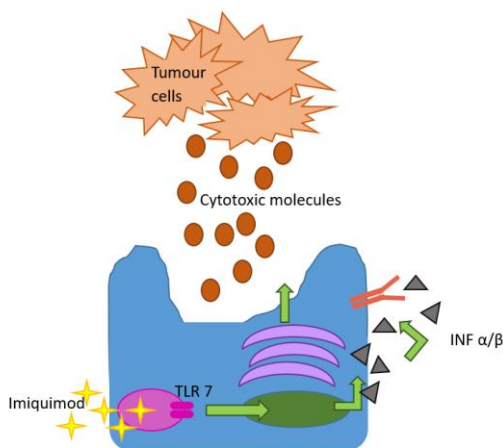


Figure 1.3: Imiquimod mechanism of action

Image depicting how Imiquimod immune responses via secretion of cytokines, and activation of Th-1 cell-mediated immunity. This cytokine-induced immune response is responsible for the antiviral and antitumor effects of imiquimod (adapted from (Drobits et al., 2012)).

Interferon is naturally produced by the body to fight infection. It has been synthesised and formulated into a cream. Though there is no evidence it improves survival rates it may help delay melanoma returning and therefore it may be used as an adjuvant treatment (Chitwood et al., 2013; Good et al., 2011). Interferon initiates apoptosis of BCC cells via the CD-95 ligand-receptor interaction and the stimulation of interleukin (IL)-2 and IL-10 (Chakrabarty and Geisse, 2004). However, treatment may cause flu-like symptoms including headache and fever. Whilst complete response rates of 50–80% have been reported, these results might not be obtained with high-risk tumours (Oguz Acartürk and Edington, 2005). Aside from the low cure rate, a further drawback of interferon therapy is the need for multiple intralesional injections.

Interleukin-2 is a cytokine secreted by CD4+ T lymphocytes following antigen recognition. It has no direct effect on cancer cells, instead, its antitumor activity is accomplished through immunomodulation by stimulating cytotoxicity of T lymphocytes, NK cells, and macrophages (Rogalski et al., 1999). It has been found to be valuable in the treatment of BCC, (Dummer et al., 1992; Mihara et al., 1990). Side effects however include fever, flu-like symptoms, and pain at the injection site (Kaplan and Moy, 2000).

5-FU functions by inhibiting thymidylate synthetase thereby inhibiting DNA synthesis causing cell death (Chitwood et al., 2013; Good et al., 2011; Marks et al., 2001). Its usefulness in treating invasive NMSC is hindered by inability of the topical cream formulation to penetrate into the skin sufficiently. Because of the potential for persistent, deeper, invasive tumours to remain following treatment, application is limited to treating superficial BCC or SCC (Dillaha et al., 1963).

Patients at high risk of developing numerous or invasive NMSC's may be suitable for chemoprevention. Oral retinoids have been proven to be effective in the suppression of new SCC development but require careful monitoring (Neville et al., 2007). Topical retinoids however are not effective for prevention. Further, photodynamic therapy, imiquimod, 5-FU, ingenol mebutate, or diclofenac sodium may theoretically decrease the risk of SCC through treatment of precancerous changes though there is limited data regarding efficacy of these agents. Nonsteroidal anti-inflammatory agents may even have a protective effect against NMSC (Soltani-Arabshahi and Tristani-Firouzi, 2013).

Though there are some effective topical formulations for the treatment of skin cancer, poor patient compliance stemming from perhaps a lack of understanding of needing to adhere to the treatment regimen or unpleasant side effects can result in treatment failure. In addition these treatments may cause skin irritation; the skin may peel, weep, crack or blister. The area treated can become painful, itchy, and ulcerated (Felicio et al., 2009; Kaplan and Moy, 2000; Neville et al., 2007). Therefore development of a treatment with a slow release profile to minimise product application with minimal side effects to normal skin cells would be ideal.

1.2 Topical, dermal and transdermal drug delivery formulation considerations

The skin is an effective route for either local or systemic drug delivery. It is the largest, most easily accessed organ of the body (Thomas and Finnin, 2004). Topical, dermal and transdermal drug delivery are advantageous as the methods employed to delivery drugs are generally pain free and offer dose flexibility with an ease of drug removal (Alexander et al., 2012; Thomas and Finnin, 2004). Topical systems allow medicament to act on the surface of the skin, dermal systems deliver drug to the dermal layer and transdermal systems allow drug to cross the dermal later and enter the blood stream. Dermal and transdermal drug delivery systems are able to deliver drug in a controlled way ensuring steady drug-plasma levels thereby avoiding the peak-trough phenomenon of drug concentration in the plasma seen with multiple drug doses (Alexander et al., 2012). This is especially important for drugs that have a short half-life or those with a narrow therapeutic index (Chaudhary et al., 2013; Thomas and Finnin, 2004). Thus drug concentration remains within the therapeutic window avoiding potentially toxic side effects and sub therapeutic drug concentrations (Alexander et al., 2012). Furthermore the skin has a copious blood supply and drug can be delivered directly into the systemic circulation and avoid first pass metabolism and the variables that affect GI absorption such as pH, enzymes, drug-food interactions, and gastric emptying time (Alexander et al., 2012).

The principle function of mammalian skin is to protect the organism from foreign body invasion including any applied drug formulation (Alexander et al., 2012). Whilst this is not a concern for topical formulations, transdermal and dermal drug delivery systems must be formulated to overcome this barrier function. The extent of drug penetration is dependent on race, skin condition, age, sweat gland density, and skin hydration levels (Thomas and Finnin, 2004). Skin temperature can also affect drug flux and rate of clearance due to the adjustment of cutaneous blood flow (Cevc and Vierl, 2010; Thomas and Finnin, 2004). Further, structural differences in skin, for example stratum coreum (SC) thickness, lipid content and enzyme activity can affect drug delivery across the skin (Thomas and Finnin, 2004). Other aspects to consider when developing transdermal and dermal products include how other external products including soap, creams, and body sprays affect drug delivery and also the potential of dose transfer to another person (Thomas and Finnin, 2004).

Drug delivery *via* the skin offers many benefits over other drug delivery routes including the oral and parenteral routes by avoiding first pass metabolism, delivering the drug at a steady state and being 'user friendly'. Drug penetration however is limited by the stratum corneum (SC), drug formulations are therefore required to penetrate the SC in order reach target locations. Nanoparticulates including liposomes can be employed to carry drug across the skin

and deliver the drug to the dermal layer or even transdermally. Dermal drug delivery may be useful in delivering chemotherapy for treatment of skin cancer.

Drugs are able to penetrate the skin through either intercellular routes or intracellular routes (Figure 1.4). The transcellular route involves the drug moving through the cell. This may be passively by diffusion, being carrier mediated, being actively transported, or being receptor mediated (endocytosis). Drugs are also able to pass through using the follicular pathways which is useful as follicles extend deep into the skin and is well vascularised however, the area available for drug transport is only about 0.1% of the skin (Alexander et al., 2012; Barry, 2001; Brooks and Idson, 1991; Prow et al., 2011).

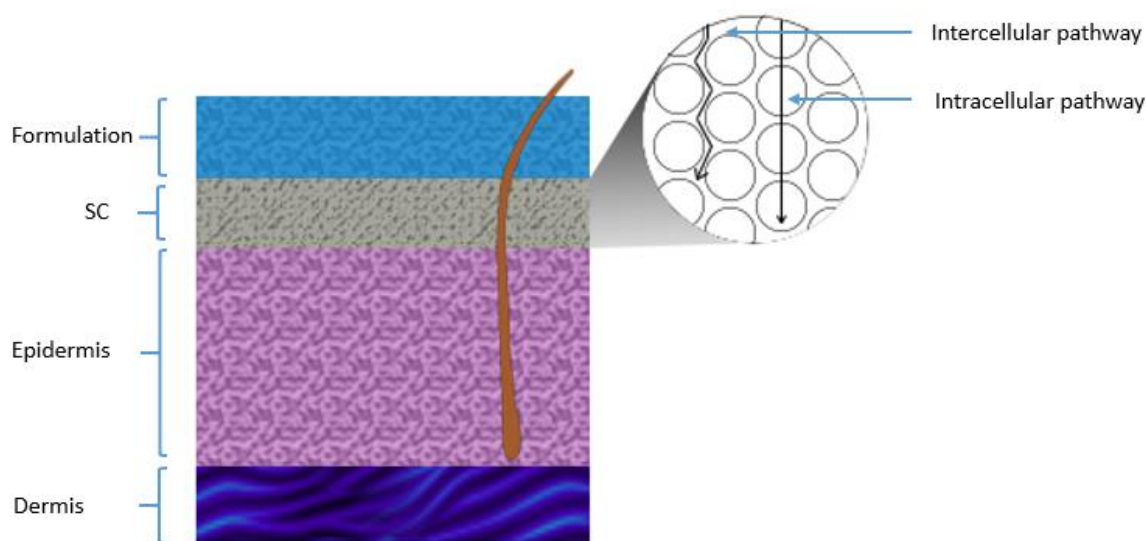


Figure 1.4: Diagrammatic representation of potential drug penetration pathways

The intracellular and intercellular pathways (depicted on the upper right corner) adapted from (Alexander et al., 2012).

1.2.1 Drug physiochemical considerations

When developing transdermal preparations drug physiochemical, pharmacokinetic and pharmacological properties need to be considered. Though smaller drug molecules are ideal for transdermal delivery, if local drug delivery is required, this is not the case as the drug is more likely to be cleared via cutaneous blood flow (Cevc and Vierl, 2010). Drug flux across the skin is influenced by the drug concentration gradient. For a drug to move through the intercellular pathways, it must be able to diffuse through a complex mixture of lipids with hydrophilic and hydrophobic domains. This is determined by ability of drug to partition into the skin and then out of the skin into the underlying tissues; the octanol: water partition coefficient is used to predict this (Thomas and Finnin, 2004). Thus only drugs with suitable

physiochemical properties will be able to pass through this route, usually, only smaller drug molecules (Prow et al., 2011). Ideal properties of a drug intended for the transdermal route are summarised in Table 1-1. Chemical structure of the drug influences diffusivity as the polar head groups of the intracellular lipids can interact with the hydrogen bond forming functional groups in drug structure (Cevc and Vierl, 2010). Therefore, ideal physiochemical properties of a drug for transdermal drug delivery include a low molecular mass, a high diffusion coefficient, high drug concentration and a high but balanced partition coefficient.

Table 1-1: Summary of drug characteristics required for transdermal drug delivery

(Alexander et al., 2012; Guy & Hadgraft, 1985)

Molecular weight	< 500 Da
Log P	< 5
Melting point	200 °C

1.2.2 Overcoming the barrier function of the skin

The most obstructive layer of the skin which must be overcome is the SC. Many methods have been developed to help carry drug across the skin and further the use of skin as a viable drug delivery pathway. Passive drug penetration enhancers may be added to a formulation and may either carry the drug across or decrease the resistance of the skin. These include chemical enhancers, supersaturated solutions, ion pairing techniques, eutectic mixtures, oils and amphipaths and nanoparticles. Active penetration enhancers force the drug across the skin layers by using physical force usually by electrically assisted means. Such methods include iontophoresis, ultrasound (sonophoresis), electroporation, photomechanical waves and electron beam irradiation.

1.2.2.1 Passive drug penetration enhancers

Chemical enhancers temporarily diminish the skin barrier. Few compounds have been successful and it is difficult to correlate *in vitro* to *in vivo* action due to live skin responding differently to the chemicals used (Thomas and Finnin, 2004). Ideally their effect would diminish once the drug has passed through leaving no lasting damage. There is a need to develop the understanding of the mechanism of such substances so predictions can be made to how they would improve drug flux (Barry, 2001). Some solvents, for example ethanol, can remove lipids from the SC thus reducing its barrier capabilities (Naik et al., 2000). Additionally, the effect has been shown to be reversible (Bommaman et al., 1991). Such penetration enhancers may intercalate into the structured lipids of the skin where it can disrupt the packing thus rendering them more 'fluid' thereby increasing the diffusion coefficient of the permeant (Cornwell et al.,

1996; Garrison et al., 1994; Gay et al., 1989; Golden et al., 1986). The second approach in which excipients (for example, propylene glycol) can improve skin permeability is to shift the solubility parameter of the skin in the direction of that of the permeant. The solubility of the permeant in the outer layers of the skin will be increased and this, in turn, improves the flux (Hadgraft, 1999). One of the concerns however is that this type of molecule usually has irritant properties (Hadgraft, 1999).

A supersaturated formulation is a solution that has exceeded equilibrium solubility. As drug concentration increases, the thermodynamic activity of the drug increases thus drug flux across the skin increases (Alexander et al., 2012). A saturated formulation of the drug will in fact provide the maximal flux, irrespective of the selected vehicle and drug solubility therein (Naik et al., 2000). They are, however known to be inherently unstable due to crystallization over increased time periods (Hadgraft, 1999). Co-solvents able to decrease drug solubility are useful in the formulation of super saturated solutions to keep the drug from reaching potentially toxic levels (Thomas and Finnin, 2004; Valenta and Auner, 2004).

The ion pairing technique enables the permeation of ionisable drugs. Charged molecules are unable to easily penetrate the skin due to the lipids in which the cells are surrounded thus the formation of a neutral ion pair can aid the penetration of a charged drug (Alexander et al., 2012). This has been proved to be successful in the delivery of retinoic acid and glipizide (Tan et al., 2009; Trotta et al., 2003).

Eutectic mixtures transform solid drugs into an oily state at ambient temperature thereby increasing the thermodynamic activity and thus the drug flux across the skin. Skin permeability is enhanced by the formation of a low melting mixture and also by directly disrupting the skin structure to allow passage of the drug (Alexander et al., 2012). EMLA cream is a eutectic mixture of lignocaine and prilocaine which, when applied under an occlusive film, provides effective local anaesthesia for pain-free venepuncture and other procedures (Ehrenstrom Reiz and Reiz, 1982). Additionally, the delivery of ibuprofen across the skin has been improved with eutectic mixtures (Stott et al., 1998; Yong et al., 2003).

Oils and amphiphiles in polar solvents spontaneously form a plethora of structures including micelles, cyclodextrins, liposomes, micro emulsions, and vesicles depending on the shape of the molecules used (section 1.2.4.3). Some improve transdermal drug delivery acting as drug carriers or skin permeation enhancers. When formulating such structures for application additional factors to consider include how the structure will change as the solvent evaporates and how temperature affects the stability (Cevc and Vierl, 2010).

Liposomes are colloidal particles that consist of phospholipids and cholesterol. These lipid molecules form concentric bimolecular layers in the form of vesicles. The drug can be trapped in this structure and transported across the skin. They can also act as penetration enhancers as the lipid components are able to penetrate into the stratum corneum (Schreier and Bouwstra, 1994; Vázquez-González et al., 2014). As well as the lipid component being able to act as penetration enhancers themselves, chemicals can be added to improve vesicular bilayer fluidity and reduce the SC barrier function (Romero and Morilla, 2013b). Further, in addition to protecting the drug from degradation they can be formulated to provide a controlled release of drug (Alexander et al., 2012).

1.2.2.2 Active drug penetration enhancers

Active penetration enhancers force drug to move across the skin layers by using physical force usually by electrically assisted means. Iontophoresis is the process of using an electrical potential difference to force ions across the skin. The power of iontophoresis depends on polarity, valency, mobility of the drug molecule as well as the formulation (Alexander et al., 2012; Cevc and Vierl, 2010). This method has been successful in the delivery of buspirone (Al-Khalili et al., 2003). Different sources of energy can be used to create pores that remain open for up to 24hrs. The use of ultrasound (sonophoresis) is useful for local drug delivery (Alexander et al., 2012; Cevc and Vierl, 2010). Electroporation is the temporary structural disturbance of the lipid bilayer due to a short high voltage pulse. Other methods include the use of photomechanical waves and electron beam irradiation (Alexander et al., 2012). Effectiveness of such methods is also dependent on the physiochemical properties of the drug (Alexander et al., 2012). Combinational approaches are being investigated and developed using a multidisciplinary approach; scientists from engineering, pharmaceutical sciences, physics, chemistry, biology and medicine are working to lower the skin barrier in a controlled, safe, reversible way.

1.2.2.3 Nanoparticle carriers as penetration enhancers

A nanoparticle is defined as a particle with a size between 1 to 100 nm (Prow et al., 2011). The term nanoparticle can be applied to dendrimers, micelles, liposomes, nanoemulsions and to solid particulates provided they possess a size range of < 100 nm. Benefits of using a nanoparticle include enhanced drug absorption, sustained drug release and drug protection. Additionally, such particles may offer sustained release of drugs, less irritation and moisturising properties (Vázquez-González et al., 2014). Another benefit of nanoparticles is that the use of skin digestion or permeation enhancer substances may be avoided (Alexander et al., 2012). Nanoparticles are increasingly being used in local and targeted delivery (Prow et al., 2011).

Dendrimers are highly branched three-dimensional, immensely branched, well-organized polymer nanoscopic macromolecules (Küchler et al., 2009). A drug can be entrapped within this structure. They have already been investigated as carriers for chemotherapeutics (Teow et al., 2013).

Micelles are lipid molecules that arrange themselves in a spherical form in aqueous solutions. The formation of such structures is a response to the amphipathic nature of fatty acids. Micellular nanoparticles can accommodate water soluble and non-water soluble, crystalline and amorphous drugs and a drug loading of up to 20% w/w can be achieved (Lee et al., 2010).

Solid particulate nanoparticles refer to the nanosizing of solid drug particles, solid polymeric nanoparticles, solid protein nanoparticles and solid lipid nanoparticles. Most drug delivery particle technologies are based on solid lipid carrier's (solid lipid nanoparticles) (Prow et al., 2011). These are colloidal particles made of solid lipids e.g. solid triglycerides, saturated phospholipids. They have an occlusive effect which reduces transepidermal water loss thus enhancing penetration (Bhaskar et al., 2009).

Most environmental nanoparticles for example viruses, dust and bacteria are unable to breach the skin barrier. Studies suggest particles greater than 10 nm are unlikely to penetrate the SC without the aid of penetration enhancers and instead amass in hair follicles (Prow et al., 2011). However in aged or damaged skin the potential for drug penetration increases (for example, ulcerated squamous cell carcinoma) (Prow et al., 2011).

Further, mechanical effects such as flexing of the skin or massage may affect penetration though results are inconclusive. Though some studies have found flexing increased penetration, skin massage did not, however others have found the opposite result. These studies used different methods and different sized particles therefore implying flexing and massage effects are dependent on the drug and formulation used (Prow et al., 2011).

The safety of nanoparticles however is a concern, particularly if they are insoluble and non-biodegradable. These may be taken up and retained by the reticulo-endothelial system or accumulate in target organs and it is unclear as to what effects they may have. They can also cause local toxicity such as keratinocyte apoptosis (Prow et al., 2011).

Interest in the use of nanoparticles for drug delivery has grown considerably over the last decade. They can be designed to control drug release, protect the drug and even provide targeted drug delivery. Improving the understanding of how nanoparticles interact and penetrate through the skin layers is vital to improve transdermal drug delivery.

1.3 Liposomes

Liposomes consist of amphoteric lipid molecules (phospholipids) that form spherical, self-closed structures in aqueous media to minimise the entropically unfavourable interaction between hydrophobic chains and aqueous medium (Figure 1.5). Drugs may be loaded into these vesicles for targeted, controlled release. Hydrophilic drugs with a log P <1.7 are retained well in the aqueous core. Lipophilic drugs with a log P >5 remain trapped with the bilayer. Intermediate drugs with a log P of 1.7-5, partition between the bilayer and aqueous phase resulting in rapid loss from the liposome (Gregoriadis, 1973).

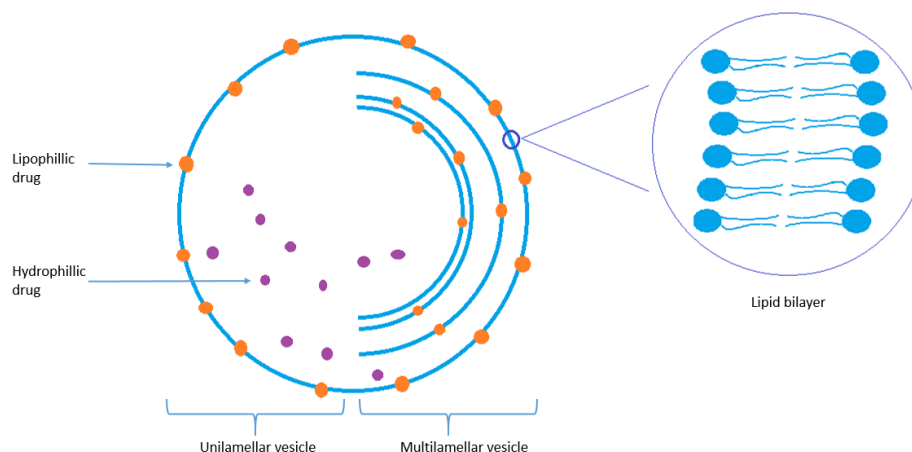


Figure 1.5: Liposome structure in aqueous media summary.

The lipid bilayer is arranged so that the aqueous head group is in contact with the aqueous media and the lipid tails are contained within the bilayer. Hydrophilic drug is contained within the core whilst hydrophobic drug is encapsulated within the bilayer. Surface properties may be modified with the attachment of polymeric groups at the bilayer surface.

Topically applied liposomal formulations are an effective delivery system for the treatment of skin diseases. In the treatment of health related dysfunctions, it is desirable that the drug reaches its site of action at the therapeutic dose range and remains constant over a sufficiently long period of time to elicit an effect. Liposomal formulations provide sustained drug levels in the dermis whilst reducing the incidence of undesirable side effects arising from systemic administration and enhanced systemic absorption of drug after topical application with permeation enhancers which irreversibly disrupt the SC (du Plessis et al., 1994a; Park et al., 2013).

1.3.1 Lipids

Phospholipids are the most important component in liposomes. They consist of two hydrocarbon tails joined to a polar head group with a glycerol backbone. The choice of the head and tail groups will inform the type, size and charge of aggregate formed in polar solvents.

Further, the formation of structures depends on lipid concentration, temperature, and electrostatic and electrodynamic interactions of polar lipids with the solvent and solute molecules. The choice of lipid employed determines the release profile of the drug, lipids with higher transition temperatures are more rigid thus providing slower drug leakage from the liposome (Szoka Jr and Papahadjopoulos, 1980).

When selecting lipids for liposome composition, it is necessary to consider that phospholipids form smectic (liquid crystal) mesophases that undergo a characteristic gel-liquid crystalline phase transition. The phase transition temperature is the temperature at which the lipid changes from being in the ordered gel phase in which the hydrocarbon chains are closely packed, to the disordered liquid crystalline phase in which there is no order and they are fluid. Vesicles composed of phospholipids below this transition temperature are considered "solid" whereas above this temperature they are considered fluid (Chapman, 1975; Lee, 1975; Melchior and Steim, 1976). Controlling the transition temperature of the lipid is useful as it can help determine the properties of the liposome (Szoka Jr and Papahadjopoulos, 1980). As the transition temperature increases a more rigid liposome structure is achieved allowing for less drug leakage and sustained release properties. The transition temperature is influenced by the hydrocarbon chain length, charge, degree of unsaturation, and the head group. As chain length increases, more energy is required to disrupt the ordered packing due to the increase in strength of the van der Waals interaction between the phospholipids whereas the double bond in unsaturated chains puts a kink in the chain which requires less energy to disrupt ordered lipid arrangements (Szoka Jr and Papahadjopoulos, 1980).

Lipids can be classified as either non-polar or polar (Fahy et al., 2011). Polar lipids can be further sub divided as shown in Table 1-2 (Phan and Tso, 2001).

Table 1-2: Classification and attributes of polar lipids

<h1>Class 1</h1>	<ul style="list-style-type: none"> • Insoluble in water, do not swell in water • Form unstructured oil phase or crystals in water, not micelles • Triglycerides, long chain fatty acids, long chain fatty alcohols, cholesterol
<h1>Class 2</h1>	<ul style="list-style-type: none"> • Insoluble in water, do swell • Form liposomes • Phospholipids
<h1>Class 3</h1>	<ul style="list-style-type: none"> • Some solubility in bulk phase, unstable surface films • Form micelles (no aqueous core) • Most anionic, cationic and non-ionic surfactants (polysorbates)

The molecular shape of an amphiphile influences its geometrical packing properties in a given solution environment which governs the type of aggregate produced (Figure 1.6). Mismatched lipids used to form the bilayer can create voids which may be exploited for the inclusion of a hydrophobic drug in the liposomal bilayer (Ali et al., 2013).

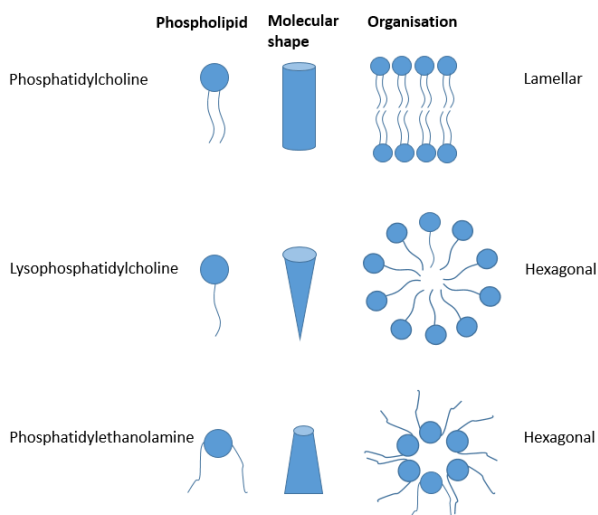


Figure 1.6: Lipid shape influence on lipid aggregate formation.

Lipid shape determines the type aggregate formed in aqueous media (adapted from (Proceedings of the National Academy of Sciences of the United States of America, 2014)).

The shape of a lipid can be expressed as its critical packing parameter (p). It is a ratio of hydrophobic tail volume v , head group area, and chain length (Cullis et al., 1986; Nagarajan, 2002) (Equation 1.1).

Equation 1.1: critical packing parameter (p)

$$p = \frac{v}{a_0 l}$$

where v is the molecular volume of hydrophobic part of polar lipid, a_0 is the surface area per molecule at hydrocarbon water interface and l is the length of hydrocarbon region

Cholesterol is usually included in the liposome membrane (Ali et al., 2013; Doolittle and Chang, 1982; Liu and Krieger, 2002). It provides rigidity to the liposome by modulating the membrane elasticity, fluidity, and permeability. It plugs gaps in the bilayer created by imperfect packing of the lipids (Papahadjopoulos and Kimelberg, 1974; Papahadjopoulos, 1976). However it can cause stability issues for lipid based drug products as it is readily oxidized (Szoka Jr and Papahadjopoulos, 1980).

Phosphatidylcholine (PC), derived from both natural and synthetic sources is a common phospholipid employed in liposomes. At neutral pH, PC is uncharged (zwitter-ionic) (Mashaghi et al., 2012). It can form structures consisting of one or multiple concentric lipid bilayers termed unilamellar (small or large termed SUV's and LUV's correspondingly) or multilamellar (MLV's) respectively with a size range from 25 nm to several micrometres (Figure. 1.7) (Szoka Jr and Papahadjopoulos, 1980). MLV's are formulated following rehydration and shaking whilst SUV's require the additional step of sonication. MLV's can offer a depot effect for release of hydrophilic substances for example, acyclovir (Jain et al., 2005), SUV's have a better bio distribution of drugs and LUV's have a good entrapment efficiency of hydrophilic drugs (Szoka Jr and Papahadjopoulos, 1980).

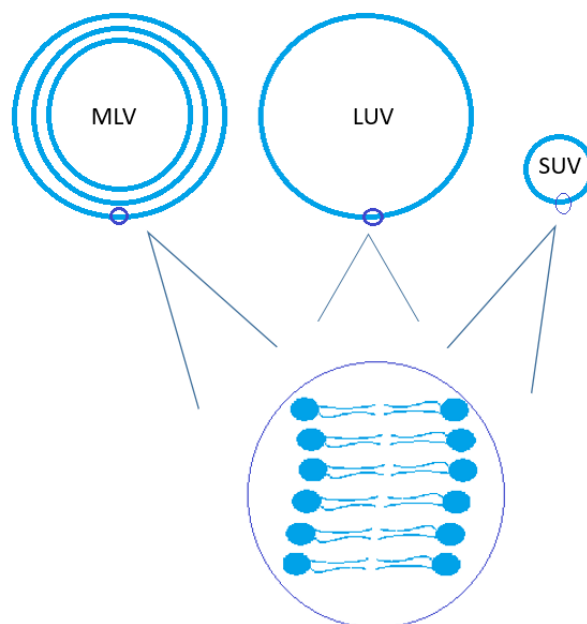


Figure 1.7: Diagram of liposome subtypes

Formulation parameters determine formation of multilamellar (MLV), large unilamellar (LUV) and small unilamellar (SUV) vesicles.

Skin permeation and skin retention has been found to decrease with the amount of PC in formulations for both hydrophilic and hydrophobic drugs (microemulsion > micelles > transfersomes > liposomes). A lipophilic drug would have a higher skin permeability when incorporated into a system containing mainly hydrophilic excipients. Skin retention, however, has not been found to be affected by the drug hydrophilicity to the same extent as skin permeability. Furthermore, occlusion increased both skin retention and skin permeation for model drugs (Ferderber et al., 2009).

1.3.2 Topical liposomes

Liposomes can be very useful for topical drug delivery as the bilayer structure is similar to natural membranes allowing them to fuse (Laouini et al., 2012). Topical liposomes may serve as a solubilisation matrix, as a local depot for sustained release of dermally active compounds, as penetration enhancers, or as rate-limiting membrane barrier for the modulation of systemic absorption of drugs. Advantages of using liposomes as a drug in topical drug formulations include reduced irritation and side effects and improved drug targeting (Egbaria and Weiner, 1990). Further, they have a moisturizing effect which can aid transdermal drug delivery (Laouini et al., 2012). Skin permeability of encapsulated drug is affected by the vesicle structure, size (Verma et al., 2003), membrane fluidity, and the type of anchored polymer (Park et al., 2013).

Liposomes are useful in the topical delivery of lipophilic drugs as they can be contained in the lipid bilayer. A depot effect is formed in the SC liposome by way of transformation into planar lipid bilayers or multilayer structures from which sustained release into the dermis can take place (Fig. 1.8) (Vázquez-González et al., 2014). A study comparing liposomal formulations compared to solutions observed a reduction of percutaneous absorption of hydrocortisone from the liposomal formulation (du Plessis et al., 1994a). These vehicles act as transdermal permeation enhancers without the use of additional permeation enhancers (Shakeel et al., 2010).

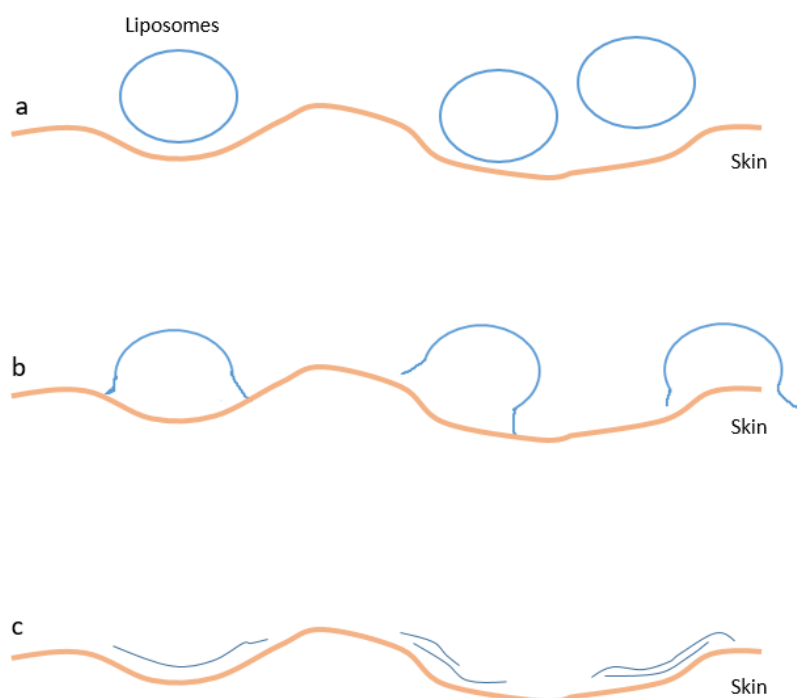


Figure 1.8: Representation of how conventional liposomes may interact with the skin

(a) initial application, (b) liposome deformation (c) planer layer formation. Adapted from (Vázquez-González et al., 2014).

1.3.3 Deformable liposomes

Deformable liposomes are an innovative approach for the non-invasive delivery of active pharmaceuticals. These carriers can transport agents through intact skin by changing their shape to be able to fit through a pore size smaller than their original diameter and then reform to their original shape and size once they have passed through the pore (Figure 1.9). This ability depends on the self-regulating carrier deformability which surpasses that of the related but not optimized lipid aggregates by several orders of magnitude. Conventional lipid suspensions, such as standard liposomes or mixed lipid micelles, do not mediate a systemic biological effect upon epicutaneous applications. Conversely, deformable liposomes are able to transport therapeutic amounts of molecules into the body. This process can be nearly as

efficient as an injection needle, as seen from the results of experiments in mice and humans using such liposomes as insulin-carrying vesicles (Cevc et al., 1998).

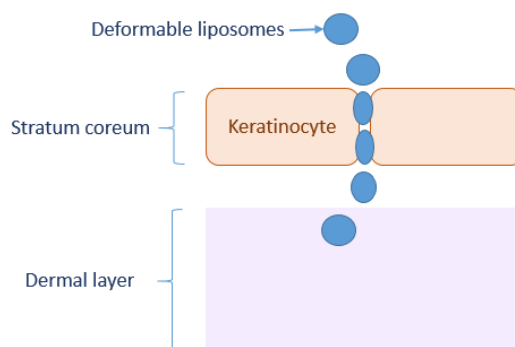


Figure 1.9: Deformable liposome movement through the intact stratum corneum into the dermal layer

Deformable liposomes include single chain surfactants that have a high radius of curvature (examples include sodium cholate, Span 65, and Tween 80 (Cevc, 1996; Ita et al., 2007; Oh et al., 2006)). This extra component destabilizes the vesicle bilayers by reducing the amount of work required to expand the interface allowing the liposome to become more elastic thus increasing the flux across the skin (Cevc, 1996; Ita et al., 2007; Oh et al., 2006). By being able to change shape and volume at minimal energetic cost these structures may even penetrate across hydrophilic pathways of intact skin (Romero and Morilla, 2013a) across the SC to reach the viable epidermis (Warner and Lilly, 1994). Cevc *et al.*, suggested it may be based on concentration intensive, hydrogen based transepidermal gradient. Further it was shown that, modifying the chemical composition of bilayers to decrease the Young's modulus (stress to strain ratio used to describe the stiffness of an elastic material) the resulting deformable liposomes were able to penetrate the SC (Cevc, 1996; Romero and Morilla, 2013a). Additionally, it has been observed that such carriers to the skin may induce changes in the SC resulting in the formation of pores ranging between 50 and 200 nm. This phenomenon is observed as deformable liposomes are able to intercalate into the lipid matrix causing enlarged pores thereby increasing the permeation ability of the drug. Deformable vesicles have already been successfully employed in transdermal delivery of anti-inflammatory agents, plasmid DNA and anti-tumour agents (Cevc and Vierl, 2010; Romero and Morilla, 2013a)

Deformable liposomes have also been produced using nonionic surfactants (L-595 and PEG-8-L with sulfosuccinate as stabilizer) (van den Bergh et al., 1999). These liposomes have been found to quickly partition into the SC, through a fine meshwork of thread-like channels (Honeywell-Nguyen et al., 2002). The liposomes remain in the SC where the drug is released and do not penetrate into the deeper skin layers (Honeywell-Nguyen and Bouwstra, 2003).

However, only mechanistic, not preclinical applications have been studied (Romero and Morilla, 2013b).

Celecoxib applied topically is an effective skin cancer prevention technique, further it has been found to improve anticancer drug effectiveness in tumour treatment. An investigation into the use of liposomes, transfersomes and ethosomes, containing suitable edge activators as penetration enhancers found all formulations improved the drug penetration into the skin with respect to an aqueous suspension (Bragagni et al., 2012).

Ketoconazole is a lipophilic drug with a large molecular weight of 531.44 Da and a low aqueous solubility of 0.04 mg/mL. It has a poor transdermal delivery profile. Elastic vesicles formulated with Span 60 and Tween 80 have showed significantly higher skin penetration and retention compared with free drug suspension. Incorporation into a hydrogel showed a significant retention which was even more than the market formulation. The results of the present study indicate that such elastic liposomes can be used to enhance skin delivery of the model high molecular weight and poorly water-soluble drug ketoconazole (Kakkar and Pal Kaur, 2013).

1.3.4 Ethosomes

Ethosomes are a form of liposomes prepared with ethanol. In comparison to liposomes, ethosomes are less rigid allowing them to penetrate more easily into deeper layers of skin. The ethanol can increase the solubility of the drug in the liposome and disturb the packing of the SC lipid bilayer therefore behaving as a drug permeation enhancer. Further, the high ethanol content results in a negative zeta potential therefore these liposomes have an increased stability with some studies finding that the average size remains constant for at least 2 years at room temperature (Laouini et al., 2012; Touitou et al., 2000).

1.3.5 Liposome preparation techniques

When a lipid mixture is first introduced into a polar liquid, it will first form a monolayer at the air-water interface. As the concentration increases aggregates in which the tails do not have interaction with the polar solvent are formed. The concentration at which aggregates begin to form is termed the critical micelle concentration and is influenced by lipid tail length and surfactants used (Ali et al., 2010; Mohammed et al., 2004; Szoka Jr and Papahadjopoulos, 1980). There are a range of different methods used to prepare liposomes including freeze drying, extrusion method, hydration of a thin film, reverse-phase evaporation technique and the solvent injection technique.

1.3.5.1 Freeze drying method

After dissolving the lipids in chloroform and mixing in the desired ratio the organic solvent must be removed by purging the system with nitrogen. The mixture must be re-suspended in cyclohexane which is then frozen. This must then quickly be placed in a high vacuum system until completely dry and a white powder is produced. This is readily suspended in water thus producing liposomes (Cui et al., 2006; van Winden et al., 1997).

1.3.5.2 Extrusion method

Phospholipid and cholesterol are dissolved in an organic solvent and this suspension is forced through a polycarbonate membrane with a defined pore size to produce liposomes with a diameter similar to the pore size of the membrane used to prepare them (Laouini et al., 2012; Lapinski et al., 2007)

1.3.5.3 Hydration of a thin lipid film

This method was first developed in 1965 by Alec Bangham (Bangham et al., 1965). Phospholipid and cholesterol are dispersed in organic solvent which is removed by evaporation. A dry film is deposited on the flask wall which is then hydrated by adding an aqueous solution under agitation at temperature above the transition temperature. The greater the degree of agitation, the smaller the liposome size produced. Further size reduction techniques include sonication to obtain SUVs or extrusion through polycarbonate filters (Laouini et al., 2012).

1.3.5.4 Reverse-phase evaporation technique

The organic solvent is removed from the lipid solution by evaporation under reduced pressure forming a lipidic film. The system is purged with nitrogen to ensure there is no organic solvent left. The lipids are then re-dissolved in a second organic phase (usually diethyl ether and isopropyl ether). An aqueous buffer is added producing large unilamellar and multilamellar liposomes. The organic solvent is again removed and the system is maintained under nitrogen. These liposomes can also contain large macromolecular assemblies effectively (Szoka and Papahadjopoulos, 1978).

1.3.5.5 Solvent injection technique

The lipid is dissolved in either ethanol or ether which is injected into a heated aqueous solvent forming liposomes with a narrow size distribution. The aqueous phase is heated to above the boiling point of the ether to ensure that upon injection of the organic phase the ether

evaporates. This produces primarily unilamellar liposomes (Laouini et al., 2012; Schubert and Müller-Goymann, 2003).

1.3.6 Characterising liposomes

1.3.6.1 Zeta potential

The zeta potential (ζ) of a particle is the overall charge that a particle acquires in a particular medium. Zeta potential measurements give information about the difference in potential between the static layer and bulk media layer around a particle and how this is affected by changes in the environment for example the pH, presence of counter-ions, adsorption of proteins. Electrostatic interaction is an important force affecting the structure, stability, and function of liposomes (Sou, 2011). Furthermore, zeta potential can also be used to determine the type of interaction between the active substance and the carrier; i.e. whether the drug is encapsulated within the body of the particle or simply adsorbed on the surface (Laouini et al., 2012).

1.3.6.2 Liposome size

Several techniques are available for determining liposome size and size distribution including microscopy techniques, size-exclusion chromatography (SEC) and static or dynamic light scattering (DLS) measurements.

Electron microscopy can offer important information on liposome preparations since they yield a view of morphology and can resolve particles of varying size. However, sample preparation requires removal of liposomes from their native environment and such procedures can cause shrinkage and shape distortion (Sternberg et al., 1994).

Use of HPLC-SEC can provide information on liposome population size distribution. However, use of HPLC for such size determination can destroy the liposome due to adsorption of lipids on to the column (Laouini et al., 2012).

Dynamic light scattering (DLS) is also used in liposome size distribution analysis (Szoka Jr and Papahadjopoulos, 1980). The sample is placed in front of a light source and as the light hits the small particles it scatters. The Brownian motion of the particles causes time-dependent fluctuation in the scattering intensity and this causes a constant change in the distance between particles. Analysis of this fluctuation produces information on particle size. The sample does not need to be modified prior to analysis and this technique is sensitive to small quantities of high molecular weight aggregate (Laouini et al., 2012).

1.3.6.3 Confocal laser scanning microscopy

Confocal laser scanning microscopy (CLSM) uses an increased optical resolution and contrast of a micrograph to enable the reconstruction of three dimensional structures. This imaging technique uses point illumination and a spatial pinhole to eliminate out-of-focus light in specimens. CLSM can be used to determine the extent of liposomes penetration into the skin (Verma et al., 2003). Fluorescent labels are added to the liposome, when light hits the sample these fluoresce and this is what is then detected. Thus this technique does not provide information about the permeation of the entire liposome, but only about the penetration of the fluorescent label (van Kuijk-Meuwissen et al., 1998).

1.3.6.4 Encapsulation efficiency

Liposome preparations consist of encapsulated and un-encapsulated drug. To determine the encapsulation efficiency the encapsulated drug and the free drug must be separated. Several separation techniques have been reported including the mini-column centrifugation and the use of a dialysis membrane with a corresponding cut-off size. Following separation the lipid bilayer is disturbed with methanol or Triton X-100 and the released drug can then be measured (Laouini et al., 2012).

1.3.6.5 Stability

Studies on the stability and the effective storage of liposomes preparations are areas of research assuming increasing importance in liposomal preparation development. Stability encompasses a number of parameters including the chemical stability of the lipids, maintenance of liposome size, examination for aggregation, maintenance of liposomal structure, retention of entrapped drug as well as the influence of biological fluids on the integrity and permeability properties of the liposomes. Therefore stability protocols evaluating these interactions over a period time must be developed and carried out (Laouini et al., 2012; Szoka Jr and Papahadjopoulos, 1980).

A formulation should maintain its physical integrity and the chemical integrity of the drug. The average size distribution of liposomes increases during storage (Szoka Jr and Papahadjopoulos, 1980). Systems tend to decrease the total free energy to reach a more thermodynamically favourable state thus liposomes will aggregate to reduce the interfacial area and fuse into bigger structures. This can affect how the liposome will distribute in the body and could potentially cause drug leakage (Sabin et al., 2006). The presence of excess or bulk water can lead to degradation via hydrolysis. This is influenced by temperature, buffer species, pH, head group and hydrocarbon chain length. The phospholipids used in liposome formulations are often derived from biological sources and contain polyunsaturated fatty acids.

These undergo oxidative reactions which can alter the permeability of the bilayer (Szoka Jr and Papahadjopoulos, 1980). Saturated lipids are less prone to oxidation. Further, the drug may interact with the lipids used affecting either the chemical stability of the drug or the liposome.

1.4 Gel formulations for topical and transdermal delivery

Due to the liquid nature of liposome preparation, an appropriate vehicle must be selected to increase preparation viscosity, for example using creams or gel based formulations. Liposomes have been confirmed to be compatible with viscosity increasing agents including gelling polymers (Foldvari, 1996; Salko et al., 1998).

A gel is a semi-solid jelly-like substance that can display properties ranging from hard and tough to soft and weak. Gels can further be defined as a dilute cross-linked system, exhibiting no flow in the steady-state (Ferry, 1980). By weight, gels are mainly liquid, however due to a three-dimensional cross-linked network, they behave like solids. The crosslinked polymer within the fluid gives the gel its structure and contributes to the adhesive stick. Thus gels are a dispersion of molecules of a liquid within a solid network in which the solid is the continuous phase and the liquid is the discontinuous phase.

Aqueous semi-solid polymeric gels, such as those based on hydroxyethylcellulose (HEC) and hydroxypropyl methylcellulose (HPMC) are often used in transdermal drug delivery and are useful in designing controlled delivery formulations (Ghosal and Nanda, 2013; Valenta and Auner, 2004). Both are cellulose derivatives and have limited solubility for poorly water-soluble compounds (Forbes et al., 2011a; Gupta et al., 2002). These gels are polymeric networks already swollen to equilibrium, and the further addition of fluids results in dilution of the polymeric network (Figure 1.10). These gels may also develop a small degree cross-linking due to a gain in energy under the influence of shear forces, however these are weak, reversible physical forces (Gupta et al., 2002). Drug release from gels usually occurs through the process of diffusion, or swelling caused by water penetration into the polymer followed by diffusion (Kajihara et al., 2001; Mashak and Rahimi, 2009). Additionally aqueous gels are easy to spread therefore suitable for topical application due to their pseudoplastic nature (a decrease in viscosity as the rate of shear stress increases) (Forbes et al., 2011a).

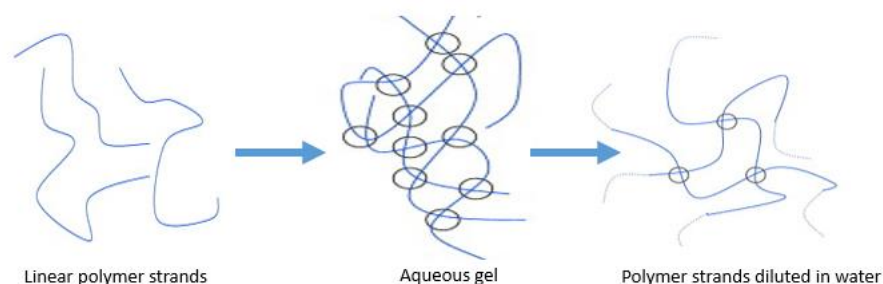


Figure 1.10: Aqueous gel structure

The polymer networks swell following addition of fluid (modified from Gupta, et al., 2002).

Ideally the polymer should be stable, non-reactive with the drug, easily manufactured and fabricated into the desired product, whilst being inexpensive. Additionally, polymer properties (including the molecular weight and glass transition temperature) should be such that the drug diffuses through it and is released appropriately. The polymer should exhibit biocompatibility and chemical compatibility with drug and excipients, whilst providing consistent and effective delivery of a drug throughout the product's life (Keith, 1983).

Drugs administered by the topical route are limited by the SC layer, although topical gels may enhance drug delivery through the skin (Valenta and Auner, 2004). Gels consist of one phase and can either be hydrophilic hydrogels or lipophilic lipogels (Valenta and Auner, 2004). Hydrophilic gels are polymers with a linear structure formed by long-chain monomer units linked by covalent bonds. Further interactions such as hydrogen bonds or Van der Waals forces contribute to achieve the three-dimensional structure which bind the solvent to the polymeric network (Gupta et al., 2002; Valenta and Auner, 2004; Vilar et al., 2012). The majority of drugs formulated as gels do not pass the skin and act on the surface of the epidermis, although this does depend on the physicochemical properties of the drug (Valenta and Auner, 2004).

5-FU is formulated as a cream but is associated with skin irritation, poor skin permeation and retention at the target site. A liposomal gel has been investigated for the delivery of 5-FU with Carbopol 934P used as the gelating agent (Puri and Jain, 2012). An *in vitro* skin permeation and deposition study found an increase in the amount of drug deposition and a larger reduction in tumour density with the gel formulation in comparison with the cream. Further the gel was found to be less irritating. Thus it is clear a liposomal gel may be beneficial in the delivery of chemotherapeutic compounds for the local treatment of NMSC as it can be developed to provide a suitable release of drug whilst being patient friendly.

1.5 Models of skin absorption

1.5.1 *In silico* approaches

Dermal absorption is a multi-factorial multi-step process, affected by many factors including the type of skin, skin pre-treatment, physicochemical properties of the drug and delivery systems, as well as environmental factors. It is notable that in some cases, the pharmacodynamic effect and absorption profiles are higher than could be presumed from *in vitro* permeation data. This may be as a result of efficient clearance of the penetrant by skin microcirculation (Godin and Touitou, 2007). Tissue culture human skin and epidermis equivalents generally possess lower barrier characteristics than human skin, making them questionable for permeation studies. *In vitro* permeation experiments despite their limitations, provide important tools for screening drug delivery systems, skin permeation enhancers and drug delivery carriers

In vitro skin permeation studies are frequently performed for screening of molecules and drug carrier systems aimed at optimising dermal or transdermal delivery. Therefore, one of the main objectives of *in vitro* permeation studies is prediction of *in vivo* absorption. A number of reports present attempts to mathematically correlate or predict from *in vitro* permeation data to *in vivo* drug levels based on a diffusion model (Guy and Hadgraft, 1985; Touitou et al., 1988; Yamashita et al., 1994) or a convolution technique (Sato et al., 1988).

Mathematical modelling of percutaneous absorption of a compound is often applied in an attempt to predict or extrapolate data. Unfortunately, a great number of these interactions is nonlinear, making mathematical modelling of percutaneous absorption problematic. Since the main hindrance of skin permeation of a drug lies in the SC layer, Fick's diffusive law's are generally accepted to describe skin transport of drug (Godin and Touitou, 2007).

Mathematic relationships become more complicated when considering a broad variety of molecules (especially highly hydrophilic ones) due to the heterogeneity of skin structure having at least two parallel diffusion patterns (polar and nonpolar) (Godin and Touitou, 2007).

Fick's first law can be used to describe diffusion (Equation 1.2).

Equation 1.2:

$$J = -D \frac{\partial C}{\partial X}$$

where C is the donor concentration, D is the diffusion coefficient, J is the rate of transfer per unit area (flux) and X is the area. J is a multiple variable and can be expressed as the mass moved per unit time. Therefore Fick's Second Law can also be used to express drug movement

across the skin as it predicts how diffusion causes the concentration to change with time (Equation 1.3).

Equation 1.3:

$$\frac{\partial C}{\partial t} = \left(D \frac{\partial^2 C}{\partial X^2} \right)$$

where t is time

For steady state flux (sink conditions) further equations can be used to describe drug movement across the skin (Equation 1.4 and 1.5). According to this law, diffusion is assumed to be the mass transfer of individual solutes, driven by random molecular movement and the rate of transport

Equation 1.4:

$$\frac{\partial C}{\partial t} = K \times D \times C/h$$

where h is the thickness of the barrier and K is the partition coefficient.

Equation 1.5

$$\frac{Dm}{dt} = \frac{DAC_s}{h}$$

Where m is mass and C_s is the concentration in donor solution.

1.5.2 *In vitro* approaches

1.5.2.1 Franz cell

When designing a study to investigate skin permeation an appropriate mathematical model used to characterise permeation and diffusion apparatus used to conduct the study needs to be selected. An important *in vitro* permeation method is the Franz diffusion cell (Figure 1.11) and it consist of three components; the donor compartment where the drug is uniformly applied, the membrane (synthetic membrane (Cevc et al., 1998), animal skin or human skin (Aungst, 1989)) and a receptor solution (El-Kattan et al., 2000).

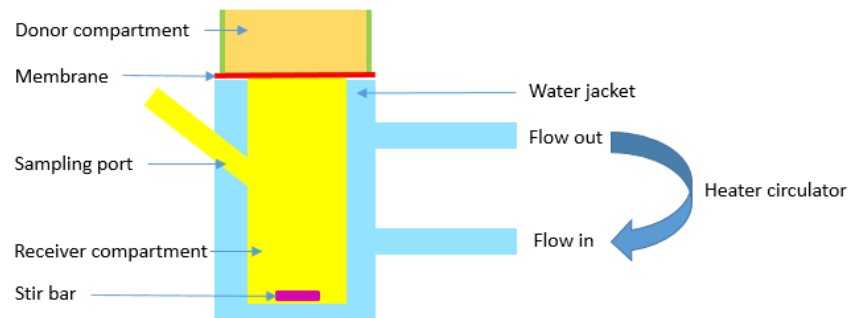


Figure 1.11: Franz cell diagram

Franz cell apparatus used in *in vivo* studies to observe drug diffusion from a formulation across a membrane into a receiver compartment filled with appropriate media.

The topical formulation would be applied to the membrane and samples can be taken from the sampling port at different time points to determine flux of drug across the membrane. When the drug is intended to be delivered topically the use of the Franz cell is useful to investigate the quantity of drug that moves into the systemic circulation.

An additional method to determine drug levels in different layers of the skin the stripping method can be used. A skin patch is mounted on a board and a piece of adhesive tape is used to strip the skin. Each strip is then analysed for drug (du Plessis et al., 1994b).

1.5.2.2 Cell culture techniques

With an increasing desire to limit animal and human exposure to drug testing, cell culture provides an excellent model system for studying the effects of pharmaceuticals on cells. It is useful in drug screening and development and is useful in providing consistent and reproducible results from a batch of cells and may help limit animal and human exposure to drug testing. Additionally, there are significant differences in between human and animal skin for example it is known the lipid composition is not akin (Pappinen et al., 2008).

Cells are removed from human tissue and grown in controlled conditions. Cells are removed directly from the tissue and disaggregated (enzymatically or mechanically) before cultivation, or are derived from an already established cell line. Cell lines derived from primary cultures have a limited life span. As cells are passaged, those with the best growth capacity predominate resulting in a degree of genotypic and phenotypic uniformity in the population.

Each cell type will require its own culture conditions. Usually the artificial environment will contain a substrate or medium that supplies the essential nutrients (amino acids, carbohydrates, vitamins, minerals), growth factors, hormones and gases (O₂, CO₂). Cells may be stored at temperatures below –130°C (cryopreservation) with an appropriate protective agent (e.g., DMSO) until required.

Skin models have been used to predict skin permeation. In a comparative study, organotypic cultures of both transformed and native dermal and epidermal cells were used for permeation studies for a cream and gel formulation containing ibuprofen acid. Results were compared with excised human SC. Studies using excised human stratum corneum showed differences in drug permeability for these two formulations which were also observed with the native organotypic cultures. Organotypic cultures showed a higher permeability for topically applied preparations than excised human stratum corneum (Specht et al., 1998).

SC intercellular lipid composition and organisation of human skin models differ to some extent from that of human SC *ex vivo*, resulting in the models exhibiting less pronounced barrier properties, together with increased hydration of the outermost SC layers. These features may explain the differences observed in vehicle effects in human skin *ex vivo* versus human skin models (Dreher et al., 2002). However due to the homogeneous structure of the SC and the lack of special structures present in human skin, like hair follicles, glands and sebum lipids, cell culture models might be useful for an estimation of the importance of such structures on drug permeation and effects of different formulations particularly in an early stage of evaluation (Kuntsche et al., 2008).

Whilst cells cultured from animal models may be useful, they are with limitations. The dermal drug delivery of various lipid nanoparticle formulations on human skin and rat organotypic cell culture was investigated. Potential alterations of SC lipid domains were studied using fluorescence assays with labelled liposomes and thermal analysis of isolated SC. The results of the permeation and DSC studies differed distinctly in human skin and the rat organotypic culture models. Therefore, it is important to use human cells in culture studies (Kuntsche et al., 2008).

Human Dermal Fibroblasts, adult (HDFa) are primary human dermal fibroblasts isolated from adult skin, cryopreserved at the end of the primary culture. This cell line has previously been used in studies concerning the development of targeted formulations for anticancer drugs (Liu et al., 2007; Wadajkar et al., 2012) for example new magnetic-based core–shell particles (MBCSPs) developed to target skin cancer cells while delivering chemotherapeutic drugs in a controlled fashion (Wadajkar et al., 2012). Human immortalized keratinocytes cells (HaCaT) are a spontaneously transformed aneuploid immortal keratinocyte cell line from adult human skin, used widely in scientific research. HaCaT cells are utilized for their high capacity to

differentiate and proliferate *in vitro*. This cell line has previously been used in the development of targeted skin delivery formulations for example photoinduced intracellular controlled release drug delivery from gold-capped mesoporous silica nanospheres (Vivero-Escoto et al., 2009).

1.6 Novel compounds for the treatment of skin cancer

1.6.1 MTL-004

Morvus (Morvus Technology Ltd © 2013,) has developed MTL-004 [5-(Aziridin-1-yl)-4-hydroxylamino-2-nitrobenzamide], a low-molecular weight (238 g/mol) compound that has been demonstrated to show a lack of systemic toxicity whilst having no effect on slowly dividing (normal) cells. The cytotoxic effect of MTL-004 requires cell division thus there is little effect on non-dividing cells in normal adjacent tissue. Synthesis of hydroxylamine compounds such as MTL-004 is conventionally associated with low yields and potentially explosive reactions. However, Morvus have developed a simple method suitable for the large scale preparation of MTL-004 from a commercially available precursor (Knox et al., 1993). MTL-004 is obtained as a stable yellow powder.

This agent can be applied as a cream for skin cancers. Such administration will deliver the cross-linking agent MTL-004 directly to the tumour to be treated, causing damage to the tumour cells, which will die once they enter the dividing phase (Anlezark et al., 1992).

MTL-004 is the active form of the prodrug Tretazicar, that is reduced to the cytotoxic bifunctional alkylating agent MTL-004 when in the presence of an endogenous enzyme following the mechanism shown in Figure 1.12 (Anlezark et al., 1992). At first, Tretazicar appeared to represent the ideal vision of cancer chemotherapy; a simple, low molecular weight tumour selective compound able to treat tumours with minimal toxic side-effects. Unfortunately, while the drug proved very effective in rat models, it was not active against human cancers (Gusterson et al., 1997).



Figure 1.12: Mechanism of action of MTL-004.

This hydroxylamine derivative can react with thioesters to produce a DNA reactive species. It is postulated that this is the N-acetoxy derivative. Formation of the amine is in competition with reactions with DNA (Knox, 2012).

MTL-004, however, had been previously disregarded as an anti-tumour agent in its own right, as it is rapidly deactivated in serum by serum proteins thus cannot migrate far from the site of administration (Knox et al., 1988). However, it remains that MTL-004 has two main advantages over conventional treatments: a lack of systemic toxicity and lack of toxicity to normal cells. Therefore, Morvus believe that MTL-004 has considerable potential as a topical skin cancer treatment.

The formation of DNA interstrand crosslinks is responsible for the high cytotoxicity of MTL-004 (Anlezark et al., 1992). The interstrand crosslinks are formed with a very high frequency and can contribute up to 70% of the total lesions (Boland et al., 1991; Friedlos et al., 1992). The interstrand crosslink is, in terms of molar efficacy, a more intrinsically toxic lesion than single-strand di-adducts and monofunctional lesions. Furthermore, the crosslinks are poorly repaired which may cause them to be even more intrinsically cytotoxic than those induced by other difunctional agents (Boland et al., 1991; Friedlos et al., 1992). Additionally, the frequency of cross links is much higher than that reported for most other agents. For example, interstrand crosslinks represent 2% or less of the total DNA reactions of Cisplatin or Carboplatin (Knox et al., 1986).

Further, it is advantageous because the compound is deactivated by serum proteins therefore, should the drug permeate through the skin, there would be no systemic toxic side effects. These properties may be useful in the development of a topical skin cancer treatment.

1.6.2 Flavonoids

Flavonoids are a widely distributed group of polyphenolic compounds characterized by a common benzo-pyrone structure. Flavonoids may be further categorised into flavonols, flavones, flavanones, isoflavones, flavonols, and anthocyanidins. These compound occur naturally in fruits and vegetables, mainly as flavonoid glycosides, and are thus important constituents of the human diet (Semalty et al., 2010b).

Flavonoids may be useful in chemoprevention and chemotherapeutic treatment whilst possessing the additional advantages of having good anti-inflammatory activities, free of harmful side-effects and to the skin (Jaeger et al., 1988; Middleton Jr, 1998). Specific oncogenic pathways can be associated with significant changes in the tumour microenvironment. The tumour microenvironment is a complex system of many cell types, including endothelial cells and their precursors, pericytes, smooth-muscle cells, fibroblasts of various phenotypes, myofibroblasts, neutrophils and other granulocytes, mast cells, T, B and natural killer lymphocytes, and antigen presenting cells such as macrophages and dendritic cells. These cells are all able to affect tumour progression. Control of the immediate microenvironment of a developing tumour may therefore be as vital as control of the dysfunctional cells within the tumour (Albini and Sporn, 2007). Several possible agents, including flavonoids, which can potentially inhibit some of these targets have been identified (Casey et al., 2015; Gupta et al., 2004).

Curcumin is a flavonoid isolated from turmeric that has been found to have a positive effect in the treatment of a range of cancerous tumours (Kunnumakkara et al., 2008). A study to investigate the growth inhibition of curcumin on melanoma cells, treated three types of melanoma cell lines (A375, MV3 and M14) with varying concentrations of curcumin for 24, 48, 72 and 96 hours. The control cell line used was normal human lung fibroblast cell line MRC-5. MTT assays were conducted to evaluate cell proliferation. Curcumin-induced growth inhibition was observed to be both time- and dose-dependent in the melanoma cells. The IC₅₀ doses of curcumin for cultured melanoma cells (A375, MV3 and M14) at 48 h were 8.29, 18.29 and 14.25 μ M, respectively. No significant growth inhibition was observed in MRC-5 cells at 5–30 μ M, under similar conditions showing that curcumin at lower concentrations is able to selectively inhibit the growth of melanoma cells without affecting normal cells (Jiang et al., 2015).

Berberine, a compound isolated from plants such as *Berberis*, has been reported with many pharmacological effects related to anti-cancer and anti-inflammation capabilities (Peng et al., 2006). A study observing the effects of berberine on small cell lung cancer found berberine exerted a dose- and time-dependent inhibitory effect on the motility and invasion ability of a highly metastatic A549 cells under non-cytotoxic concentrations. This suggests that berberine possesses an anti-metastatic effect in non-small lung cancer cell and may, therefore, be helpful in clinical treatment (Peng et al., 2006). Additionally, the effects of berberine, on human melanoma cancer cell migration and the molecular mechanisms underlying these effects using melanoma cell lines, A375 and Hs294 has been studied. The treatment of A375 and Hs294 cells with berberine resulted in concentration-dependent inhibition of migration of these cells, which was associated with a reduction in the levels of COX-2, PGE2 and PGE2 receptors. Cell migration is an essential step in invasion and metastasis thus these results indicate for the first time that berberine may have a vital role in the inhibition of cancer progression (Singh et al., 2011b).

Epigallocatechin gallate (EGCG) is a polyphenolic catechin that has been found to have cytotoxic effects in cancerous skin cells as well as cancerous cells in the colon (Chen et al., 2003; Hwang et al., 2007; McLoughlin et al., 2004), pancreas (Shankar et al., 2008), lung (Yang et al., 2002), prostate (Singh et al., 2011a) and breast carcinomas (Singh et al., 2011a). Additionally, it may increase the efficacy of chemotherapeutic treatment as well as have chemo protective effects (Chen et al., 2003; Gupta et al., 2004; Hwang et al., 2007; McLoughlin et al., 2004; Shankar et al., 2008; Siddiqui et al., 2009; Yang et al., 2002). The anti-cancer properties of EGCG are extensively supported by results from epidemiological, cell culture, animal and clinical studies. EGCG is a known antioxidant able to suppress the inflammatory processes that lead to transformation, hyperproliferation, initiation of carcinogenesis as well as suppressing the final steps of carcinogenesis (namely angiogenesis and metastasis) (Mukhtar and Ahmad, 2000; Thawonsuwan et al., 2010).

EGCG has been recognised to suppress colonic tumorigenesis in animal models and epidemiological studies. After oral administration EGCG is retained in the gastrointestinal tract thus creating the potential to function as a chemo preventive agent against colon cancer. Human colorectal carcinoma HT-29 cells have been treated with EGCG to examine the anti-proliferative and pro-apoptotic effects of EGCG, as well as the molecular mechanism underlying these effects. After 36 hours of treatment, EGCG was observed to inhibit HT-29 cell growth with an IC₅₀ of approximately 100 µM. Additionally, HT-29 cells treated with doses higher than 100 µM showed apparent nuclear condensation and fragmentation. EGCG treatment also caused damage to mitochondria, and induced apoptotic cell death (Chen et al., 2003).

Treatment of epidermal carcinoma A431 cells with EGCG (10-40 µg/mL) resulted in dose-dependent inhibition of NF-kappa B/p65, induction of DNA breaks, cleavage of poly (ADP-ribose) polymerase (PARP) and morphological changes consistent with apoptosis. Treatment of cells also resulted in significant activation of caspases and protein expression of caspase-3, -8 and -9. This study found that EGCG-mediated activation of caspases was critical for cell subsequent apoptosis (Gupta et al., 2004).

Naringenin is the predominant flavanone in grapefruit. It is an antioxidant, free radical scavenger, anti-inflammatory agent, and immune system modulator thus may be potentially useful as a pharmacological anti-cancer agent (Casey et al., 2015; Huang et al., 2011).

A study investigating melanogenesis in murine B16-F10 melanoma cells observed exposure of cells to naringenin resulted in morphological changes accompanied by the induction of melanocyte differentiation-related markers, such as melanin synthesis, tyrosinase activity, and the expression of tyrosinase and microphthalmia-associated transcription factor. Additionally an increase in the intracellular accumulation of beta-catenin as well as the phosphorylation of glycogen synthase kinase-3 beta (GSK3 beta) protein was observed after treatment with naringenin. Moreover, the activity of phosphatidylinositol 3-kinase (PI3K) was up-regulated by naringenin since the phosphorylated level of downstream Akt protein was enhanced. Thus naringenin was found to induce melanogenesis through the Wnt-beta-catenin-signalling pathway (Huang et al., 2011).

Additionally, naringenin is able to regulate fibrosis (Du et al., 2009; Lee et al., 2004). Fibroblasts and myofibroblasts play a critical role in the formation of the extra-cellular matrix and inducing fibrosis within growing tumours (Casey et al., 2015; Chtourou et al., 2015). Tissue fibrosis is frequently observed in the tumour microenvironment associated with rapid proliferation of fibroblast cells (Kalluri and Zeisberg, 2006; Kerkar and Restifo, 2012).

A study observing the effect of naringenin on induced pulmonary fibrosis in mice found that increased fibrosis resulted in an increase in the incidence of lung cancer. Furthermore, naringenin was observed to significantly reduce lung metastases in mice with pulmonary fibrosis and increases their survival by improving the immunosuppressive environment through down-regulating transforming growth factor-β1 and reducing regulatory T cells. Therefore, naringenin may be an ideal therapeutic agent in the treatment of both cancer and fibrosis (Du et al., 2009). A study investigating the effect of naringenin on induced hepatic injury in rats observed naringenin to prevent the elevation of serum alanine transaminase, aspartate transaminase, alkaline phosphatase, and bilirubin levels. Naringenin also restored serum albumin and total protein levels, and reduced the hepatic level of malondialdehyde. These results exhibit naringenin displayed in vivo hepatoprotective and anti-fibrogenic effects against

liver injury suggesting suggests that naringenin may be useful in preventing the development of hepatic fibrosis (Lee et al., 2004).

Additionally, naringenin can increase both tyrosinase activity and melanin content, indicating naringenin can be used to prevent oxidative skin damage (Chen et al., 2003; Huang et al., 2011). In previous in vitro studies naringenin has been proven to be a good candidate for employment as a protective agent against photooxidative damage (Kootstra, 1994). An in vitro run-off transcription assay was used to determine if naringenin could prevent the accumulation of UV-B-induced DNA damage. Template plasmid DNA was irradiated with UV-B light, which resulted in a decreased capacity to support transcription. Naringenin was observed to prevent the accumulation of DNA damage. The results support the hypothesis that flavonoids protect DNA from UV-induced DNA damage (Kootstra, 1994). Thus naringenin is a clear candidate for use in the development of a novel skin cancer formulation.

1.7 Aims and objectives

The overall aim of this thesis was to formulate and characterise a drug carrier to deliver anti-cancer agents into the dermal layer of the skin at a controlled rate. Aqueous gel systems loaded with deformable liposome preparations formulated with a surfactant were chosen as administration approaches/vehicles. The formulation of EGCG, naringenin and MTL-004 was considered.

Chapter 2 concerns the basic development and characterisation of deformable liposomes. Liposomes were formulated with PC, cholesterol, and either Tween 80, Tween 20 or sodium cholate. The stability of these liposomes was observed over 28 days. The deformability of these liposomes was then calculated to observe the effect of the surfactant on elasticity of the liposome. An optimal formulation was then selected for application to fibroblast and keratinocyte cell lines to characterise toxicity and observe internalisation.

Chapters 3, 4 and 5 concern liposomes formulated with either EGCG, naringenin or MTL-004 respectively. Compound loaded deformable liposomes were developed and characterised. Release profiles of the compound from the liposomes formulated with and without surfactant was observed and compared. The aqueous gels HEC and HPMC were formulated with up to 5% w/v of polymer and were then loaded with 1% w/w of compound. One compartment and two compartment release was then observed and compared. Aqueous gels loaded with liposomes containing compound formulated both with and without surfactant were then formulated and release observed. Compound and liposomal formulation were then applied to fibroblast and keratinocyte cell lines to characterise toxicity as well as cell localisation.

All compounds were detected with High Performance Liquid Chromatography (HPLC) coupled with Ultra Violet (UV) analysis. HPLC methodology was developed for the detection of MTL-004 and validated. HPLC methods were also validated for EGCG and naringenin.

2 Formulation development of elastic liposomes for controlled dermal drug delivery

2.1 Introduction

The skin is a very efficient and effective physical barrier to the external environment. The barrier function is, in part, a result of the multilayer anatomy, organised as the hypodermis, dermis and finally the non-vascularised epidermal layers which culminate in the stratum corneum (SC). Furthermore, the penetration of small molecular weight molecules is often limited in intact skin, to a molecular weight of < 500 Da (Bos and Meinardi, 2000) and a log P of < 5.

These layers forming the skin are significantly altered in disease states. In particular, NMSC tumours are often accompanied with dry, scaly patches of skin (Mogensen et al., 2009). In inflammatory disorders such as dermatitis and even NMSC the barrier function itself can become compromised with cellular alterations in the SC and keratinocytes (Schmuth et al., 2015). Such disorders may require increased penetration enhancers to be able to permeate the toughened skin however, such skin is usually more sensitive therefore a careful balance must be struck. Furthermore, the release of inflammatory mediator compounds alongside an altered microbial environment often leads to altered local microenvironments (Brandner et al., 2015).

The use of nanoparticle formulations as drug-delivery vehicles provide a novel approach to the delivery and targeting of the dermal layer with benefits for both transport of poorly permeable molecules and larger (often impermeable) biologics. Indeed, reports have identified that smaller nanoparticles (< 200 nm) demonstrate internalisation by keratinocytes and dendritic cells (Vogt and Blume-Peytavi, 2014). The use of nanoparticle carrier technologies specifically allow for the development of novel and often 'responsive' systems which can be developed to possess temperature (Feng et al., 2013) or pH-specific (Baier et al., 2014) trigger release conditions, alongside possessing physical 'flexibility' (Tsai et al., 2015).

Chemotherapy agents are notoriously difficult to formulate, with one of the principle concerns being solubility. Formulations must overcome this limitation with the use of appropriate excipients all the while limiting adverse effects. Unfortunately some of the excipients used in chemotherapy formulations to enhance solubility, including polyoxyethylated castor oil and polysorbates, may cause irritation such as rashes and itchiness (Aungst, 1989; Lorenz et al., 1982; ten Tije et al., 2003; Utreja et al., 2011). Liposomes have successfully been used to limit the use of these excipients, improve drug delivery as well as reduce the side effect profile (Trotta et al., 2004; Utreja et al., 2011).

However, the use of liposomes in dermal drug delivery remains controversial due to their large size (Cevc et al., 1995). Previous studies have demonstrated that liposomes accumulate in the SC, and only rarely penetrate into viable skin (Dayan and Touitou, 2000; Trotta et al., 2004). Elastic liposomes have been reported to penetrate the skin if applied non-occlusively by virtue

of the very high and self-optimizing deformability. They have already been successfully employed in transdermal delivery of lipophilic and hydrophilic drugs including anti-inflammatory agents (Cevc and Blume, 2001), retinol (Oh et al., 2006), anti-tumour agents (Paolino et al., 2008) and hormones (El Maghraby et al., 1999). Liposome adhesion, fusion and penetration into the stratum corneum is possible with potentially deeper penetration into the dermal layer of deformable vesicles compared with traditional liposomes (El Maghraby et al., 1999).

The lipid bilayer of elastic liposomes include single chain surfactants that have a high radius of curvature (examples include Span 65, Tween 80 and sodium cholate (Cevc, 1996; El Maghraby et al., 1999; Ita et al., 2007; Oh et al., 2006). This extra component destabilises the vesicle bilayers by reducing the amount of work required to expand the interface allowing the liposome to become more elastic thus increasing the flux across the skin (Cevc, 1996; Ita et al., 2007; Oh et al., 2006). By being able to change shape and volume at minimal energetic cost these structures may even penetrate across hydrophilic pathways of intact skin (Romero et al., 2013) across the SC to reach the viable epidermis (Warner and Lilly, 1994). This may be based on an osmotic transepidermal gradient created by the difference in the total water concentrations between the skin surface and the skin interior (Cevc et al., 1995). Further it was shown that, modifying the chemical composition of bilayers to decrease the Young's modulus (stress to strain ratio used to describe the stiffness of an elastic material) the resulting deformable liposomes were able to penetrate the SC (Cevc, 1996; Romero et al., 2013).

Reported mechanisms of drug release from liposomes depends on the physicochemical properties of the drug. Drug may be released from liposomes before diffusing through the skin (drug release being the rate-limiting step); or there may be a direct transfer of drug from the liposome to the skin cells (El Maghraby et al., 1999). Entrapment efficiency of the formulation would also affect drug delivery and release (Ganesan et al., 1984). Furthermore, depending on the choice of lipid and other bilayer constituents, liposomes have been found to interact with the SC and destabilise the lipid matrix thus having a penetration enhancing effect (Kirjavainen et al., 1996).

Polysorbates (Tween®) are a class of emulsifiers used in pharmaceuticals. They are oily liquids derived from PEG-ylated sorbitan esterified with fatty acids. As non-ionic surfactants, they have advantages over ionic surfactants including increased stability, and compatibility with a range of other excipients. Chemotherapy agents have commonly been formulated with surfactants to increase solubility. Paclitaxel has been formulated in a vehicle containing polyoxyethylated castor oil, a non-ionic surfactant whilst docetaxel is currently formulated in the polysorbate Tween 80 (ten Tije et al., 2003).

Tween 80, Tween 20 and sodium cholate were selected as surfactants in the present study to improve the elasticity of liposomes. They have all been used in dermal drug delivery and are known to be safe in terms of their lack of toxicity and irritation to the skin (Ita et al., 2007; Oh

et al., 2006; Tsai et al., 2015). Tween 80 (Figure 2.1a) is derived from polyethoxylated sorbitan and oleic acid. Tween 20 (Figure 2.1 b) is a polyoxyethylene derivative of sorbitan monolaurate, and is distinguished from the other members in the polysorbate family by the length of the polyoxyethylene chain and the fatty acid ester moiety lauric acid (Croda Europe Ltd, Span and Tween, 2009). Sodium cholate (Figure 2. 1c) is an anionic emulsifying agent (Sigma-Aldrich(c), 2017).

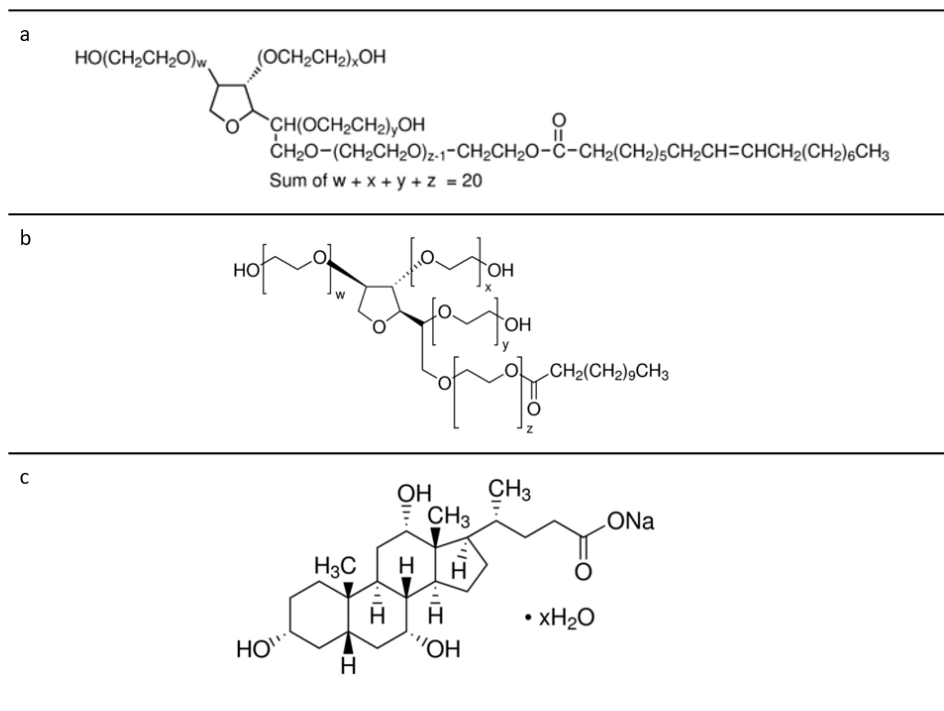


Figure 2.1: Chemical structures of a) Tween 80, b) Tween 20, c) sodium cholate (Sigma-Aldrich(a), 2017; Sigma-Aldrich(b), 2017; Sigma-Aldrich(c), 2017)

2.2 Aims and objectives

The aim of this study was to formulate and characterise deformable liposomes with the aim to be able to load drug into the bilayer for the local sustained release into the dermal layer of the skin.

To achieve the aims, the overall objectives were

- Formulate and characterise liposomes loaded with either Tween 80, Tween 20 and sodium cholate in terms of size and zeta potential.
- Observe the stability of these liposomes over the course of 28 days in terms of liposome size
- Study the deformability index of these liposomes
- Select an optimal formulation for further studies
- Apply formulations to fibroblast (HDFa) and keratinocyte (HaCat) cell lines to characterise toxicity and observe internalisation.

2.3 Materials and method

2.3.1 Materials

Phosphatidylcholine (PC) was obtained from Avanti Polar Lipids. Cholesterol Tween 80, Tween 20 and sodium cholate were all obtained from Sigma-Aldrich. All other reagents including methanol and chloroform were obtained from Fisher Scientific. Ultrapure water was obtained from a Milli-Q purification system (Millipore, Billerica, MA, US). Human dermal fibroblasts (HDFa) isolated from adult skin along with all cell culture reagents (medium 106, Low Serum Growth Supplement. Supplemented medium contained fetal bovine serum, 2% v/v, hydrocortisone 1 µg/mL, human epidermal growth factor, 10 ng/ml, basic fibroblast growth factor, 3 ng/mL, heparin, 10 µg/mL, DMEM media supplemented with 1% L-glutamine, 10% FBS, 1% Penicillin Streptomycin, 0.25% amphotericin) was obtained from Life technologies (Carlsbad, California, US). HaCat cells were a kind gift from Dr Andrew Sanders (Cardiff China Medical Research Collaborative, Cardiff University, Henry Wellcome Building, Heath Park, Cardiff, CF14 4XN).

2.3.2 Elastic liposome preparation

Liposomes were prepared by adapting the film hydration method established by Bangham et al., (1965). Briefly, PC, cholesterol and surfactant were dispersed in an organic solvent mixture consisting of chloroform and methanol in a 9:1 ratio in a round bottomed flask (Table 2.1) (Bangham et al., 1965; Hiruta et al., 2006; Ita et al., 2007; Oh et al., 2006; Tsai et al., 2015). Subsequently, the organic solvent was removed by rotary evaporation for 5 minutes at 35°C, followed by purging with nitrogen gas. The resultant dry film residue was hydrated by the addition of 4 mL water at a temperature above the transition temperature of the phospholipid (between -7 to -15°C) (Pagano and Weinstein, 1978) and vortexed for 5 min to form multilamellar vesicles (MLV). The formed MLV were equilibrated for 30 min above their transition temperatures before being subjected to further characterisation (Ali et al., 2013; Lasic and Barenholz, 1996; Pagano and Weinstein, 1978).

Table 2-1: Details of liposome formulation composition.

Formulation	PC (% w/w)	Cholesterol (% w/w)	Tween 80 (% w/w)	Tween 20 (% w/w)	Sodium cholate (% w/w)
1 (Control)	80	20	0		
2	78	20	2		
3	76	20	4		
4	74	20	6		
5	72	20	8		
6	70	20	10		
7	78	20		2	
8	76	20		4	
9	74	20		6	
10	72	20		8	
11	70	20		10	
12	79.75	20			0.25
13	79.5	20			0.5
14	79	20			1
15	78	20			2
16	76	20			4
17	74	20			6
18	72	20			8
19	70	20			10

2.3.3 Liposome characterisation: particle size, polydispersity index and zeta potential

Mean particle size and the polydispersity index (measurement of the level of homogeneity of particle sizes) of liposomes were measured by dynamic light scattering (DLS) using a Zetaplus (Brookhaven Instruments). A clear cuvette was filled with 3 mL of a 1:4 solution of liposomes to purified water. A small polydispersity value (< 0.2) indicates a homogenous vesicle population, while a larger polydispersity (> 0.3) indicates heterogeneity (Song, Y.-K. and C.-K. Kim, 2006). The particle charge was quantified as zeta potential (ζ). Zeta potential was determined by photon correlation spectroscopy using a Zetaplus (Brookhaven Instruments). The samples were diluted three fold and assessed in triplicate.

2.3.4 Liposomes stability

The stability of liposomes was determined, as prepared in water, through the assessment of particle size over a 28-day period, stored in a stability cabinet maintained at 25 ± 2 °C (Firlabo, France) at a humidity of $60 \% \pm 5 \%$. Mean particle sizes were determined on days 1, 2, 7, 14, 21 and 28 by DLS.

2.3.5 Assessment of liposomal deformability

2.3.5.1 Assessment of liposomal deformability following extrusion

To assess the deformability of elastic liposomes, a liposome suspension (6 mL) was passed through a polycarbonate filter of either 200, 100 or 50 nm using a syringe driver (Cole Parmer, UK) set at 0.6 mL/min for 10 min. The mean particle size and the polydispersity index of liposomes were measured by DLS as described in section 2.3.3. The deformability was quantified through the calculation of a deformability index (equation 2.1) (Goindi et al., 2013):

Equation 2.1:

$$D = 100 - \frac{L_e}{L} \times 100$$

where D is deformability, L_e is size of extruded liposomes, L is size of liposomes prior to extrusion.

2.3.5.2 Assessment of liposomal deformability following the mechanistic determination of energy contained within the liposomal bilayer

The previous method concerns comparing liposome size pre and post extrusion. However, it is unable to distinguish between lipid aggregates and liposomes thus negative DI values were obtained. The following method is an alternate way of determining liposomal elastic properties using the volume of formulation forced through without having to use liposomal size such as the DI determination.

According to the Bernoulli equation (Bernoulli, 1738), pressure is a function of both the force applied and the exertion area, which can be further related to the energy applied per unit volume (Equation 2.2):

Equation 2.2:

$$Pressure = \frac{Force}{Area} = \frac{Energy}{Volume}$$

with force being a product of mass and acceleration (Equation 2.3):

Equation 2.3:

$$Force = Mass \times Acceleration = Mass \times \frac{Speed}{Time}$$

The transit of the syringe driver will be a function of the pore size and the subsequent resistance to the outlet of fluid from the syringe. The 'energy' was therefore calculated by determining the force and pressure under each surfactant condition.

2.3.5.3 Assessment of liposomal deformability following lipid quantification after extrusion

The previous two methods assessing liposome deformability are unable to provide information of the composition of the liposome being extruded. The following method was employed to quantify lipid pre and post extrusion. Quantification of the lipid content, pre- and post- extrusion, was performed by reverse phase high performance liquid chromatography (HPLC) (YL instrument, Anyang, Korea) using a SEDEX 90LT ELSD detector (Sedex Sedere, Alfortville, France) connected to the instrument. A Phenomenex Luna column 5 μm C18(2), 4.60 mm inner diameter and 150 mm length with 100 Å pore size (Phenomenex, Macclesfield, UK) was used. Separation of lipids and surfactant was carried out using an elution gradient analysis as detailed in Table 2.2, with flow rate maintained at 1.5mL/min throughout each run. Mobile phase A consisted of 0.1% TFA in water, and mobile phase B consisted of 100% methanol. Standard lipid solutions were dissolved in chloroform:methanol (9:1 v/v) prior to injection, and liposome formulations were injected both pre- and post- extrusion. 30 μL of sample was injected and the column temperature was maintained at 35 °C, whereas the ELSD temperature was maintained at 52 °C during all runs. Nitrogen was employed as the carrier gas at 3.5 psi inlet pressure. The total run time was 28 minutes. All chromatograms were evaluated with Clarity DataApex version 4.0.3.876 software.

Table 2-2: Gradient elution method for quantitative analysis of cholesterol, phosphatidylcholine (PC). TFA: trifluoroacetic acid.

Time (min)	% Eluent A	% Eluent B
	0.1% TFA in water	Methanol
0	15	85
6	0	100
25	0	100
26	15	85
28	15	85

2.3.6 Development of an *in vitro* skin model: growth and passage of cells

HDFa isolated from adult skin, cryopreserved at the end of the primary culture were revived in Medium 106 supplemented with Low Serum Growth Supplement. Supplemented medium contained fetal bovine serum, 2% v/v, hydrocortisone 1 $\mu\text{g}/\text{ml}$, human epidermal growth factor, 10 ng/mL, basic fibroblast growth factor, 3 ng/mL, heparin, 10 $\mu\text{g}/\text{mL}$.

HaCaT is a spontaneously transformed aneuploid immortal keratinocyte cell line from adult human skin. HaCaT cells are utilised for their high capacity to differentiate and proliferate *in*

vitro. Cells were revived and sustained in high glucose DMEM media supplemented with 1% L-glutamine, 10% FBS, 1% pen-strep, 0.25% amphotericin.

Cells were fed with the supplemented media every 3 days. Once cells reached 70-80% confluency, media was discarded and cells detached using 2 mL of Trypsin/EDTA and incubated for 5-10 min, prior to trypsin neutralization with 3 mL growth media and subsequent centrifugation at 1200 rpm for 10 min. The supernatant was then discarded and the pellet was re-suspended in 2 mL of media and subsequently used for father cell proliferation. Flasks were then placed into a humidified 37 °C incubator with 5 % CO₂.

2.3.7 Impact of liposomal formulation on *In vitro* cytotoxicity on HDFa and HaCat cells

To assess the cytotoxicity of either formulation component or drugs towards HDFa and HaCat cells, an 2,3-Bis-(2-Methoxy-4-Nitro-5-Sulfophenyl)-2H-Tetrazolium-5-Carboxanilide (XTT) assay was performed to measure cell death after exposure of cells to formulation or drug for 24 hours.

Cells suspensions were counted using a hemacytometer following which the cell suspension was diluted with supplemented media to 50000 to 75000 cells/mL. 100 µL of cells suspension were added into each well and incubated overnight (37 °C, 5% CO₂) to attach. Thereafter, media was removed and fresh media added. Each concentration of liposome was assayed in six wells and run in three independent experiments and results expressed as percentage cytotoxicity relative to a control.

Cells were treated with 100 µL of either a 50, 25, 10, 5, 1 or 0.1 % v/v of a liposomal solution in media without serum. The liposomal solution was either a ratio of 16:8 µM of PC : cholesterol loaded with 0 %, 2 % or 10 % w/w of Tween 20. Wells were incubated for 24 hours (37 °C, 5 % CO₂) following which 25 µL of 12.5:1 mixture of XTT to menadione was added each well of a 96 well plate. Plates were subsequently incubated for 3 hours at 37°C and the absorbance read at 450 nm on a Thermo Scientific Multiskan Spectrum. Assessment of EGCG toxicity to these cells was conducted through analysis of changes in XTT absorbance with increasing drug concentration.

2.3.7.1 Haemocytometer counting protocol

A glass hemocytometer and coverslip were cleaned with alcohol before use. The coverslip was moistened with water and affixed to the hemocytometer. The cell suspension was prepared by gently swirling the flask to ensure cells are evenly distributed. Thereafter 0.1 mL of cell suspension was removed into an Eppendorf tube to which Trypan Blue (final concentration 0.2%) was added. 100 µL of Trypan Blue-treated cell suspension was removed and applied to

the haemocytometer, both chambers underneath the coverslip were filled. A microscope with a 10x objective was used to focus on the grid lines of the hemocytometer.

The number of unstained cells (live cells) in each of the four sets of 16 outer squares (Figure 2.2) was counted.

To calculate the number of viable cells/mL the average cell count from each of the sets of 16 corner squares was calculated and then multiplied by 10,000. This was then multiplied by 2 to correct for the 1:1 dilution from the Trypan Blue addition. The final value is the number of viable cells/mL in the original cell suspension.

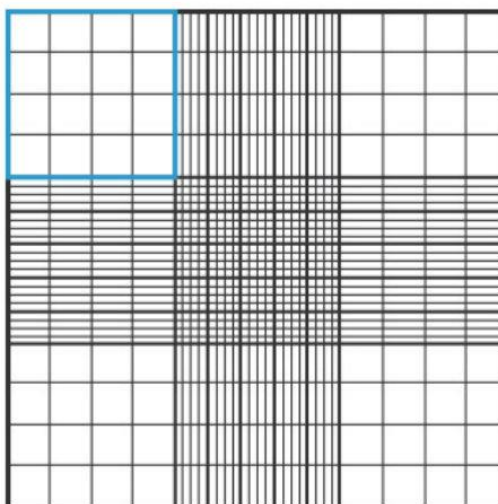


Figure 2.2: Hemocytometer gridlines.

Hemocytometer diagram indicating one of the sets of 16 squares that should be used for counting.

2.3.8 Cellular liposomal uptake assay on HDFa and HaCat cells

Liposomes, both deformable and non-deformable, were formulated with the addition of 0.25 mL of a 0.1mg/mL DiIC fluorescent dye during the lipid mixing stage. The free marker was removed by centrifuging liposomes at 18,000 g for 30 minutes, removing the supernatant, re-suspending in water and centrifuged again. Coverslips were sterilised with ethanol and aseptically coated with 1.0 mL/25 cm² of poly-l-lysine and rocked gently to ensure even coating of the culture surface. After 30 min, solution was removed by aspiration and thoroughly rinsed surface with sterile tissue culture grade water. These were then allowed to dry for 2 hours before introducing cells and medium which were left to attach overnight. DiIC loaded liposomes were diluted with 1 part of supplemented media and were then added to the coverslips and left for 2 hours in a cell culture incubator at 37°C. Supernatant was then removed and the cells washed by adding 1 mL of sterile water, removing, and repeating once more. Paraformaldehyde 4% was used to fix the cells and then the fluroshield DAPI was then added

onto the coverslips and fixed. Cover slips were subsequently analysed in an upright confocal microscope (Leica SP5 TCS II MP) and visualised with a 40x oil immersion objective. Images were acquired using a helium-neon laser at 633 nm to visualise DiIC and a helium–neon laser to visualise DAPI at 461 nm.

2.3.9 Statistical analysis

Unless otherwise stated in the text, a total of three independent experiments were carried out for each study method. The statistical significance was evaluated using one-way ANOVA or a paired two-tail Students t-test employing GraphPad Prism version 6 for Windows (GraphPad Software, La Jolla California USA, www.graphpad.com) for statistical analysis.

A paired T test or a one way repeated measures ANOVA was used to determine any statistically significant difference between means tested. Furthermore, within the ANOVA test the Tukey's multiple comparison test was run to compare between each data set. Unless otherwise stated, data is reported as mean \pm standard deviation (SD). A significance level (P-value) of ≤ 0.05 was considered as statistically significant.

2.4 Results and discussion

Elastic liposomes have been found to be advantageous in the topical administration of drugs. Whilst being able to act as solubilising agents for low solubility drugs, they may also protect the drug from degradation in the body and may be formulated for targeted, sustained drug release.

Blank MLV liposomes were formulated using a dry film method. The PC used in this study was derived from egg and is a mixture of saturated and unsaturated alkyl chains 16-18 carbons in length. The use of cholesterol in liposomes is to stabilise the membrane structure through occupying voids between the phospholipids constituent of the bilayer (Gregoriadis and Davis, 1979). Thereby, it reduces permeability and prevents drug leaching out of the liposome structure (Demel et al., 1972). Surfactant was incorporated with the aim of increasing the deformability of the liposomes by imparting 'elastic' properties to the lipid bilayer by decreasing the interfacial tension. In this study, three different surfactants; Tween 80, Tween 20, and sodium cholate, were investigated in five different ratios for their suitability to form novel deformable liposomes possessing requisite formulation characteristics.

2.4.1 Liposome characterisation: particle size and polydispersity and zeta potential

Liposome size is a key component in determining how nanoparticles will permeate across the skin. The presence of surfactant in the bilayer caused a decrease in size across all three surfactants (Figure 2.3). Liposomes formulated with no surfactant had an average size of 1032.3 ± 182.3 nm, this decreased to 390.6 ± 46.5 nm, 336.5 ± 24.9 nm and 329.2 ± 139.3 nm when formulated with 10% w/w Tween 80 (Figure 2.3a), Tween 20 (Figure 2.3b) and sodium cholate (Figure 2.3c) respectively. For liposomes formulated with Tween 80, the size decrease between liposomes formulated with no surfactant compared with all other loadings of surfactant was significant ($P \leq 0.0001$). The size decrease between liposomes formulated with 2% w/w and 10% w/w of Tween 80 was also significant ($P \leq 0.01$). Finally, the size decrease between liposomes formulated with 2% w/w and both 6 and 8% w/w of Tween 80 was significant ($P \leq 0.05$). For liposomes formulated with Tween 20, only the size decrease between liposomes formulated with no surfactant compared with all other loadings of surfactant was significant ($P \leq 0.0001$).

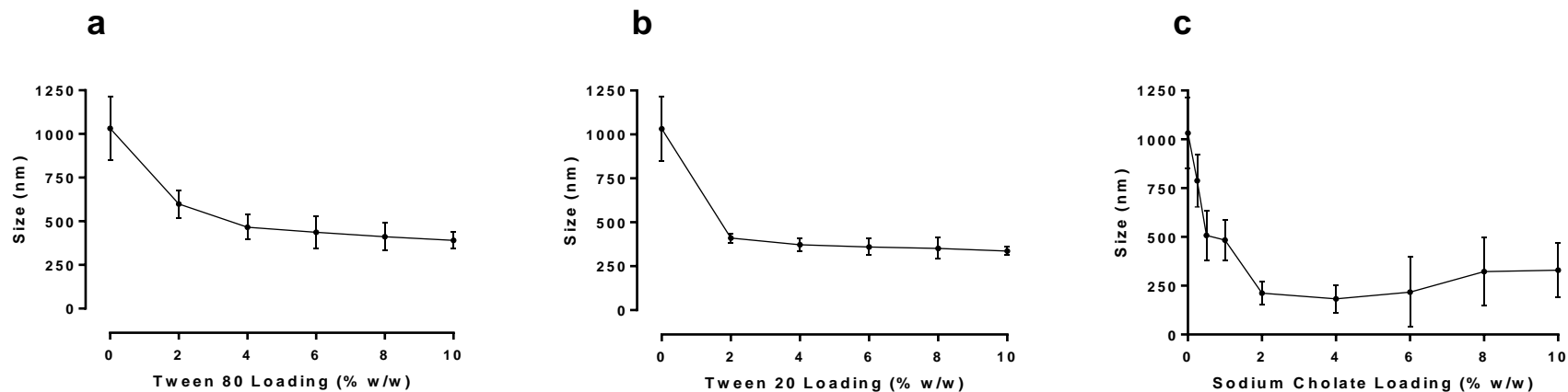


Figure 2.3: Impact of surfactants on liposome size distribution

Liposomes were prepared adapting the dry film method adding the surfactant during the lipid mixing stage. The preparation was then vortexed for 5 minutes. Liposome size was then determined by DLS, comparing up to 10% w/w loadings of either a) Tween 80, b) Tween 20 or c) sodium cholate loaded formulations. Data represents mean \pm SD. n=6 independent batches.

Liposomes formulated with sodium cholate (Figure 2.3c) proved to be problematic in terms of size, polydispersity and DI (discussed in section 2.4.1 and 2.4.4) when formulated beyond 4 % w/w, therefore, additional loadings of 0.25, 0.5 and 1 % w/w of the surfactant were investigated. The size decrease between liposomes formulated with no surfactant compared with 0.5-10 % w/w as well as between 0.25 % and both 4 and 6 % w/w of surfactant was significant ($P \leq 0.0001$). The size decrease between liposomes formulated with 0.25 % and 2, 8 and 10 % w/w of surfactant was significant ($P \leq 0.001$). Finally, the size decrease between 0.25 % and both 0.5 and 1 % w/w of surfactant as well as 0.5 and 4 % w/w loading of surfactant was significant.

The inclusion of surfactant has been previously reported to decrease liposome size in comparison to conventional liposome. A study formulating liposomes with Phospholipon® 90 G and both Tween 80 and Span 80 saw a size reduction from 207 nm to 139 nm following inclusion of the surfactants (Goindi et al., 2013). This may be a result of the surfactant allowing a greater interaction of the phospholipid bilayer with the aqueous phase resulting in the overall formation of a greater number of liposomes of a smaller diameter resulting in a greater surface area in contact with the aqueous phase.

There was no significant differences in the sizes formulated between each of the surfactants (at respective loadings) although sodium cholate appeared to produce the smallest liposomes (up to 182.8 ± 70.8 nm).

Another study has found that the state of aggregation (micellar or vesicular) and the size distribution of micelles or vesicles obtained are a function of the sodium cholate to PC molar ratio (Almog et al., 1986a). When this ratio is higher than 0.4, micelles will be produced, the size of which decreases with an increase in sodium cholate loading. When the ratio is less than 0.3, the dispersion is vesicular, and the mean size of the vesicles is an increasing function of the sodium cholate to PC ratio. Almog *et al.*, (1986) found addition of sodium cholate to vesicular dispersions, resulted in vesicle size growth through a concentration-independent lipid-exchange mechanism; larger liposomes will be formed as the sodium cholate will accumulate in between the two lipid layers that make up the bilayer. Addition of cholate to higher loadings of sodium cholate PC liposomes resulted in a decrease in vesicle size and eventually, micellisation of vesicles.

At lower loadings of sodium cholate, e.g. 0.25 % w/w, an increase in vesicle size was not observed. Thus, at this loading, there may have been insufficient sodium cholate available to act at the lipid bilayer/water interface to reduce interfacial tension and reduce liposome size. However, as the loading of sodium cholate surpassed 4 % w/w, liposome size appeared to increase which goes against the general trend of what was expected. Furthermore, liposomes

loaded with more than 4 % w/w of sodium cholate had a larger standard deviation. This suggests formation of particles other than liposomes including micelles and lipid aggregates.

A liposome preparation homogenous in size is important, as size will determine liposome distribution *in vivo* as well as influencing drug release kinetics. A polydispersity of > 0.3 is considered homogenous (Chen et al., 2012; Goindi et al., 2013; Kang et al., 2013). The general trend observed was that as surfactant was added into the formulation, the polydispersity decreased. The polydispersity of liposomes formulated with no surfactant was 0.33 ± 0.1 , compared with 0.31 ± 0.04 , 0.30 ± 0.02 for a 2% w/w loading of Tween 80 and Tween 20 respectively. The polydispersity for sodium cholate however decreased to 0.31 ± 0.05 at 0.25 % w/w of sodium cholate but then increased to 0.42 ± 0.01 at 10 % w/w (Figure 2.4). This, coupled with the increase in size variability, and cloudy/particulate appearance of sodium cholate liposomal formulations loaded with more than 4% w/w loading provides evidence suggesting the formation of particles other than liposomes such as micelles or lipid aggregates. Studies observing structure formation from PC and sodium cholate (up to 30% w/w loading) formulations found micelles were formed alongside liposomes and noted that these were not as suitable for drug delivery as deformable liposomes (Almog et al., 1986a; El Maghraby et al., 2000). This indicates sodium cholate may not be a suitable surfactant to use in this formulation as it was unable to provide a homogenous mix.

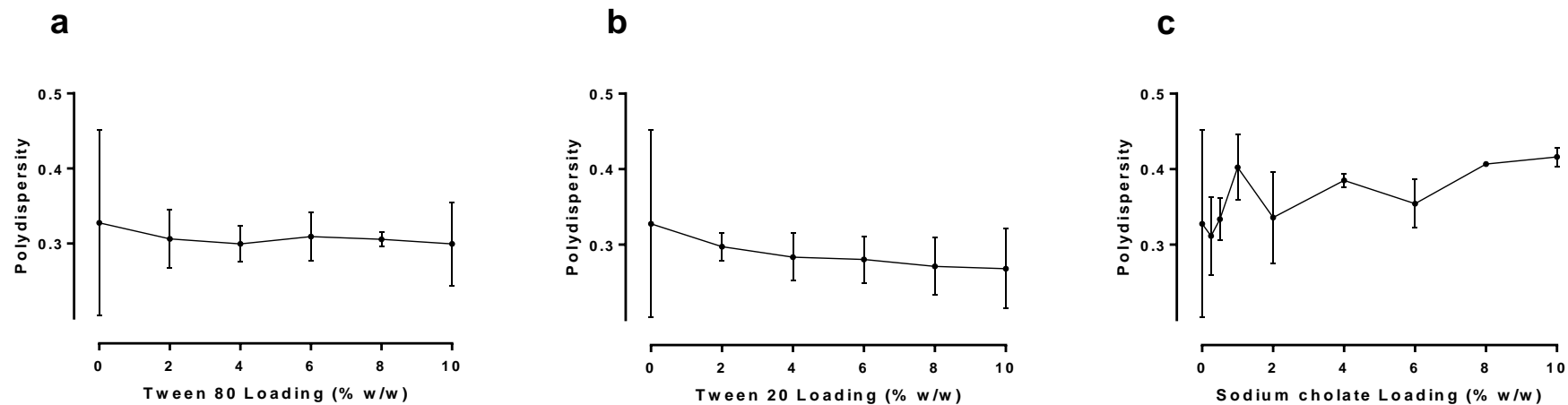


Figure 2.4: Impact of surfactants on polydispersity of liposomes

Liposomes were prepared adapting the dry film method adding the surfactant during the lipid mixing stage. The preparation was then vortexed for 5 minutes. Polydispersity, when formulated with increasing loadings of a) Tween 80, b) Tween 20 and c) sodium cholate up to a maximum of 10% w/w was determined with DLS. Data represents mean \pm SD. n=6 independent batches.

Due to the problems associated with sodium cholate including the large size variability, the range of surfactant loadings was further extended to cover the range of 0.25-10 % w/w. A lower loading of the surfactant was required to decrease the interfacial tension therefore smaller liposomes were produced in comparison to liposomes loaded with the same amount of either Tween 80 or 20 (Figure 2.2). This difference was not found to be significant. Furthermore, a loading of equal to and greater than 4 % w/w sodium cholate seemed to produce unstable liposomes alongside other particles as demonstrated by the increase in size (from 211.9 to 329.2 nm) and polydispersity (from 0.33 to 0.41). However, elastic liposomes loaded with up to 30 % w/w of sodium cholate and Tween 80 have been formulated in another study although they did not include cholesterol in the bilayer (El Maghraby et al., 2000). Sodium cholate has a similar steroidal structure to that of cholesterol and may have displaced cholesterol from the bilayer therefore negating cholesterol's bilayer stabilising property (El Maghraby et al., 2000). (El Maghraby et al., 2004).

The zeta potential is defined as the potential difference between the dispersion medium and the stationary layer of fluid directly surrounding the dispersed particle. The magnitude of the zeta potential indicates the degree of electrostatic repulsion between adjacent, similarly charged particles in a dispersion. Thus it is one of the fundamental parameters known to affect stability. The zeta potential of liposomes formulated with Tween 80, Tween 20 and sodium cholate is displayed in Table 2-3.

Table 2-3: Zeta potential of liposomal formulations formulated with up to 10% w/w loading of Tween 80, Tween 20 and sodium cholate

	Surfactant loading (w/w %)	Zeta potential (mV)	
No surfactant	0	5.03 ± 1.03	
	2	0.51 ± 2.63	
	4	3.14 ± 1.83	
	Tween 80	6	2.12 ± 2.46
		8	7.80 ± 2.61
		10	-6.23 ± 2.45
Tween 20	2	4.67 ± 1.08	
	4	6.67 ± 2.55	
	6	3.71 ± 0.90	
	8	2.56 ± 1.11	
	10	-2.79 ± 0.20	
Sodium cholate	0.25	9.68 ± 9.67	
	0.5	-1.97 ± 12.17	
	1	4.09 ± 11.35	
	2	2.67 ± 10.61	
	4	-2.14 ± 4.91	
	6	12.86 ± 11.31	
	8	7.98 ± 13.87	
10	9.94 ± 13.33		

This study has found the majority of formulations for liposomes to have a near neutral charge. Liposomes formulated with no surfactant had a zeta potential of 5.03 ± 1.03 mV. Liposomes formulated between 2 and 8% w/w of Tween 80 observed a general increase in the zeta potential from 0.51 ± 2.63 mV to 7.80 ± 2.61 mV. At a 10% w/w loading of Tween 80, zeta potential dropped to -6.23 ± 2.45 mV. The difference in zeta potential was not significant across the loadings. Tween 80 is a non-ionic surfactant thus was not expected to influence the surface charge. In a similar study preparing liposomes with PC and Tween 80, the zeta potential value was -6.63 mV. They were unable to conclude why a negative value was obtained as Tween 80 is a non-ionic edge activator and put this down to the chemical structure of Tween 80 and its interaction with their specific formulation parameters (Lee et al., 2005).

Liposomes formulated between 2-10% w/w of Tween 20 observed a general decrease in zeta potential from 4.67 ± 1.08 mV to -2.79 ± 0.2 mV. Again, the difference in zeta potential was not significant across the loadings. Tween 20 is a non-ionic surfactant thus was not expected to influence the surface charge.

Liposomes formulated between 0.25 and 10% w/w of sodium cholate observed no trend in zeta potential, once more, the difference in zeta potential was not significant across the loadings of surfactant. Sodium cholate is an ionic surfactant, thus was expected to influence surface charge. A study formulating liposomes with PC and sodium cholate observed a zeta potential of -2.45 mV (Lee et al., 2005). This is in contrast to a similar study that observed a zeta potential of -29 mV (Essa et al., 2002). These negative values are due to sodium cholate being an anionic detergent. However, in this study, the zeta potential values were less negative. The difference between these studies may be due to several differences in methods between the two studies. For instance, Lee et al. utilised a PBS buffer for measurements whereas Essa et al. utilised the organic solvent ethanol, but in this study water was used.

A key benefit of using liposomes in topical drug delivery system is that they are miscible with the lipids in the skin thus allowing the liposomes to penetrate into deeper layers. Thus a neutral surface charge is ideal (Prausnitz and Langer, 2008). However, neutrally charged liposomes have been found to flocculate and aggregate together due to the lack of like-charge causing repulsion between liposomes (Weiner et al., 1992). Furthermore, positively charged liposomes have been found to be irritating to the skin. Negatively charged liposomes have been found to provide better skin retention for drugs intended for topical use (Katahira et al., 1999). Liposomes formulated with sodium cholate had the highest positive charge therefore would be least likely to flocculate however may also be most irritating to the skin. Use of anionic lipids could be investigated for an enhanced formulation stability as well as increasing the flux across the skin.

2.4.2 Stability of deformable liposomes

The stability of deformable liposomes during storage at 20 °C was studied in terms of size. It is important to assess stability of liposomes in terms of size to assess liposome aggregation and fusion as this may affect compound encapsulation and release. Confocal images were observed on day 1 of formulation to ensure the presence of liposomes (Figure 2.5). The size of blank and surfactant loaded liposomes was measured on days 1, 2, 7, 14, 21 and 28 (Figure 2.6).

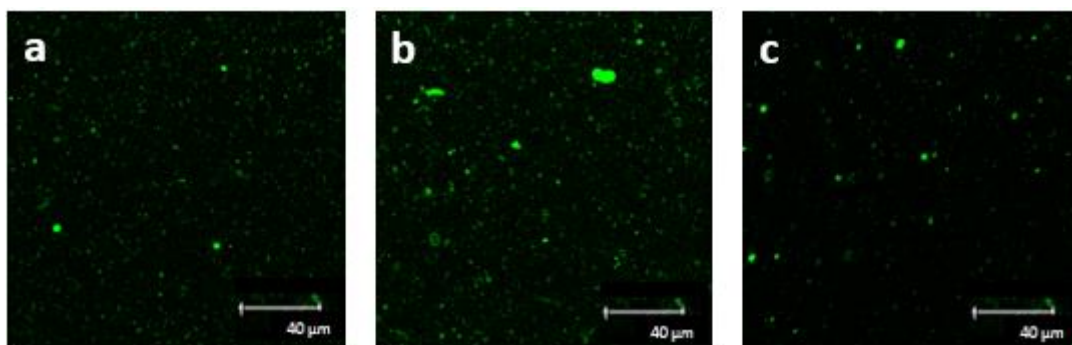


Figure 2.5: Confocal images of MLV liposomes

Confocal images of MLV liposomes formulated with 4% either a) Tween 80, b) Tween 20 or c) sodium cholate. Fluorescently labelled liposomes were formulated by the addition of the fluorescent dye Dil C to the lipid mixing stage. The untrapped marker was removed by centrifuging liposomes, removing the supernatant, re-suspending in water. Liposomes were imaged using an upright confocal microscope (Leica SP5 TCS II MP) and visualised with a 40x oil immersion objective.

Confocal images clearly show the presence of liposomes formulated with Tween 80 (Figure 2.5a), Tween 20 (Figure 2.5b), and sodium cholate (Figure 2.5c).

All liposomal formulations appear to slightly decrease in size over 4 weeks (Figure 2.6). Liposomes formulated with no surfactant decreased in size from 1032.3 ± 126.4 nm to 619.4 ± 16.8 nm. The decrease in size for these liposomes was non-significant up until day 14 where a significant difference in size was noted ($P \leq 0.05$). The decrease in size was significant between days 1 and 21 ($P \leq 0.001$), 1 and 28 ($P \leq 0.0001$), 2 and 21 ($P \leq 0.001$), 2 and 28 ($P \leq 0.0001$), 7 and 14 ($P \leq 0.05$), 7 and 21 ($P \leq 0.001$) and 7 and 28 ($P \leq 0.0001$).

The size decrease in liposomal formulations formulated with 2% w/w of Tween 80 was significant between days 1 and 21 and 1 and 28 ($P \leq 0.05$). The size decrease in liposomal formulations formulated with 4% w/w of Tween 80 was significant between days 1 and 14, 1 and 28 ($P \leq 0.05$), 2 and 14, 21 and 28. ($P \leq 0.01$). The size decrease in liposomal formulations formulated with 6% w/w of Tween 80 was not significant. The size decrease in liposomal formulations formulated with 8% w/w of Tween 80 was not significant. The size decrease in liposomal formulations formulated with 10% w/w of Tween 80 was only significant between days 1 and 28 ($P \leq 0.05$).

The size decrease in liposomal formulations formulated with 2% w/w of Tween 20 was significant between days 1 and 2 ($P \leq 0.05$) as well as days 1 and 7, 14, 21 and 28 ($P \leq 0.01$). The size decrease in liposomal formulations formulated with 4% w/w of Tween 20 was not significant. The size decrease in liposomal formulations formulated with 6% w/w of Tween 20

was significant between days 1 and 7 ($P \leq 0.01$) as well as days 1 and both 14 and 28 ($P \leq 0.05$). The size decrease in liposomal formulations formulated with 8% w/w of Tween 20 was not significant. The size decrease in liposomal formulations formulated with 10% w/w of Tween 20 was not significant.

The size decrease in liposomal formulations formulated with 2% w/w of sodium cholate was not significant. The size decrease in liposomal formulations formulated with 4% w/w of sodium cholate was not significant. The size decrease in liposomal formulations formulated with 6% w/w of sodium cholate was significant between days 1 and 7 ($P \leq 0.01$) as well as days 1 and both 14 and 28 ($P \leq 0.05$). The size decrease in liposomal formulations formulated with 8% w/w of sodium cholate was significant between days 1 and 7, 14, 21 and 28 ($P \leq 0.05$). The size decrease in liposomal formulations formulated with 10% w/w of sodium cholate was only significant between days 1 and 14 ($P \leq 0.05$) and days 1 and both 21 and 28 ($P \leq 0.05$).

The general trend observed, was that liposome size did not significantly alter between days 7 and 28 and that the inclusion of increasing surfactant concentration appears to prevent liposome size changes. Conventional liposomes usually increase in size over time due to aggregation and then fusion of vesicles (Heurtault et al., 2003; Rashidinejad et al., 2014). Liposomes would aggregate and fuse to reduce the interfacial tension and reach a more energetically stable state (Lentz et al., 1987). The inclusion of a surfactant destabilises the bilayer by reducing the amount of work required to expand the interface thus allowing maintenance of smaller structures. It appears the inclusion of surfactant prevents this phenomenon which correlates with similar studies (Seras et al., 1992). This was expected with liposomes loaded with sodium cholate as it is an ionic surfactant thus these structures repel one another in suspension and would not aggregate.

Furthermore, a creamy layer of lipids were observed following formulation, for liposomes formulated with Tween 80 and Tween 20, thus larger liposomes may have settled and aggregated at the bottom of the container resulting in only smaller ones remaining in suspension and being detected. Long-term stability of liposomes depends on the average elastic energy of the membrane being higher than the thermal energy. When this is no longer the case, liposomes will disintegrate (Lipowsky 1991). Thus the elastic energy must be maintained higher than the thermal energy (by use of surfactant), or the thermal energy maintained lower than the elastic energy (temperature control).

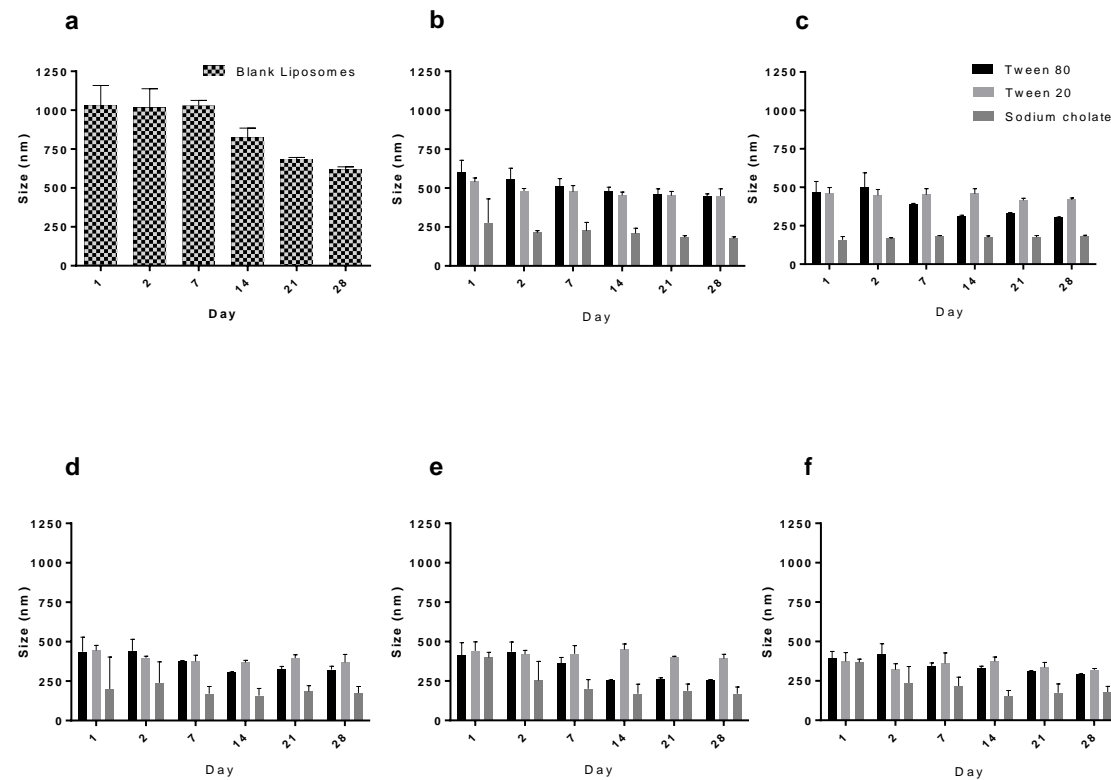


Figure 2.6: The stability of blank and deformable liposomes

The stability of blank and deformable liposomes as determined by size with DLS formulated with loadings varying between 0-10 % w/w of either Tween 80, Tween 20 or sodium cholate. a) blank liposomes, b) liposomes formulated with 2 % w/w of surfactant, c) liposomes formulated with 4 % w/w of surfactant, d) liposomes formulated with 6 % w/w of surfactant, e) liposomes formulated with 8 % w/w of surfactant, f) liposomes formulated with 10 % w/w of surfactant. Data represents mean \pm SD. n=6 independent batches.

2.4.3 Assessment of liposomal deformability

2.4.3.1 Assessment of liposomal deformability following extrusion

The addition of surfactant within the liposomal bilayer has been found to impart elastic properties to the liposome (Almog et al., 1986a; Cevc, 1996; Trotta et al., 2002). This may be beneficial in dermal drug delivery to allow the transport of molecules across the stratum corneum into the dermal layers. Liposomes loaded with up to 10 % w/w of Tween 80, Tween 20 and sodium cholate were formulated and the degree of deformability of each formulation was determined by extruding through a polycarbonate filter with a pore size of 200 nm (Figure 2.7).

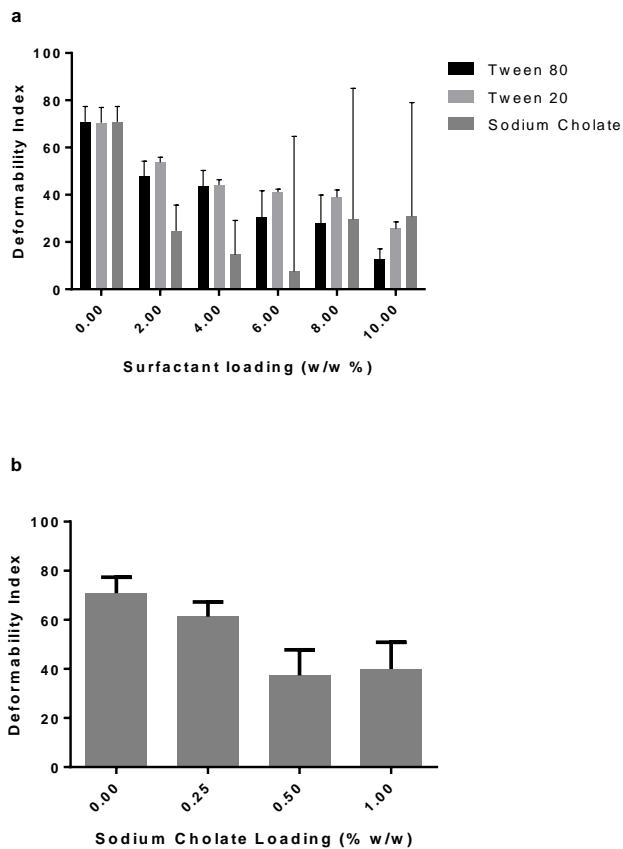


Figure 2.7: Deformability index following extrusion

Blank liposomes and liposomes loaded with a) up to a maximum of 10% w/w of Tween 80, Tween 20 and sodium cholate and additionally, b) up to 1% sodium cholate were extruded through 200 nm filters. Data represents mean \pm SD. n=6 independent batches.

The DI is defined as the degree the liposomes deformed following extrusion and did not regain their original size. The greater the DI the less elastic the liposomes are as they were unable to regain their previous larger size. Blank liposomes were first sonicated to bring the size into range (between 400 and 500 nm). The deformability index was calculated; an index of 100 demonstrating liposomes have deformed by 100% following extrusion and not regained their previous larger size (Figure 2.7).

In general, liposomes were observed to have deformed permanently to a smaller extent when formulated with surfactant. The DI of liposomes formulated with Tween 80 decreased from 70.8 ± 6.5 % to 12.5 ± 4.6 %. This decrease was significant between 0% and 2% w/w of surfactant ($P \leq 0.01$) as well as 0% and 4-10% w/w surfactant ($P \leq 0.0001$). There was also a significant decrease in DI between 2% w/w and 6% w/w of surfactant ($P \leq 0.01$) as well as between 2% and both 8 and 10% w/w of surfactant ($P \leq 0.0001$). Finally, there was a significant decrease in DI between surfactant loadings of 4% and 8% w/w ($P \leq 0.05$), as well as 4% and 10% w/w ($P \leq 0.01$).

Liposomes formulated with Tween 20 observed a decrease in DI from 70.8 ± 6.5 to 25.6 ± 2.9 %. This decrease was significant between 0% and all other loadings of surfactant ($P \leq 0.0001$). There was also a significant decrease between the DI of liposomes formulated with 2% and 4% ($P \leq 0.01$), 2% and 6% ($P \leq 0.001$) as well as between 2% and both 8 and 10% w/w surfactant ($P \leq 0.0001$). There was also a significant decrease in the DI of liposomes formulated with 4% and 10% ($P \leq 0.0001$). Finally there was also a significant difference between 10% and both 6% ($P \leq 0.0001$) and 8% ($P \leq 0.01$) w/w of surfactant.

The DI of liposomes formulated with sodium cholate decreased from 70.85 to 30.9 ± 48.1 %. None of the differences between DI of liposomal formulations was significant ($P \geq 0.05$). Beyond 4% w/w loading of sodium cholate the standard deviation increases showing that the DI values were widely distributed. Due to unreliable data observed at higher loadings of sodium cholate, additional loadings of sodium cholate between 0 and 2% w/w were investigated to observe liposomal behaviour at these loadings (Figure 2.7b).

A consequence of the strong hydrophobic effect of the lipids used to prepare the liposomes is a very high (and negative) internal lateral tension within bilayers. Therefore, rather than complete vesicle destruction, these bilayers have a self-healing effect (Sackmann, 1994). Surfactants may have interacted with the PC with strong affinity but in reversible mode therefore improving their ability to self-heal. The fast reconstruction of liposome spheres after extrusion may be due to the strong affinity between the surfactant, cholesterol and PC. The reversible binding mode might have provided the flexibility upon the application of physical stress (Oh et al., 2006).

Liposomes formulated with PC containing the surfactant dipotassium glycyrrhizinate have been found to retain their size when passed through a membrane with pores narrower than their diameter; liposome size pre and post extrusion through a membrane with a pore size of 100 nm was 352 and 345 nm respectively. These liposomes are able to deform as the surfactant has a propensity for highly curved structures (e.g. micelles), thus accommodating particle shape changes under stress by diminishing the energy required for the particle to deform and then reform its shape (Trotta et al., 2004).

Following 4% w/w loading of sodium cholate, the standard deviation of the DI increased, suggesting these liposomes were not stable and did not deform uniformly. It has already been observed liposomes formulated beyond 4% w/w of sodium cholate were unstable, following extrusion, some smaller liposomes were undoubtedly formed, but also some lipid aggregates. This is in contrast with a study observing the deformability of a liposomal solution containing approximately 87% w/w soya PC and 13% w/w sodium cholate where liposomes could deform when extruded through a pore size one quarter of their size, yet still regain their initial formulation size (Cevc et al., 1995). Considering sodium cholate reduced liposome size to the greatest extent, it would be sensible to assume this surfactant produced the most elastic liposomes in this study. However, it was possible that this molecule was capable of close physicochemical interactions with PC in the lipid membrane bilayer, perhaps displacing cholesterol which is inherently known to provide stability to the liposome structure (Oh et al., 2006).

Following analysis of liposome size, polydispersity, stability and DI, it is clear sodium cholate is not a suitable surfactant to continue for use in these studies. Homogenous preparations were not obtained leading to aggregation, and negative DI values. Studies observing drug delivery from liposomes formulated with PC and sodium cholate found that not only were micelles formed alongside liposomes, but that sodium cholate also led to a lower drug delivery as surfactant decreased the entrapment efficiency and disrupted the lipid membrane so that it became more leaky to the entrapped drug (Almog et al., 1986a; El Maghraby et al., 2000).

There were no significant differences between liposomes formulated with Tween 80 and Tween 20. Tween 80 is formed from polyethoxylated sorbitan and oleic acid. Tween 20 is derived from the ethoxylation of sorbitan before the addition of lauric acid. Whilst Tween 80 has been used in the development of topical liposomes, the oleic acid component has often been found to be more irritating to the skin and cause hypersensitivity reactions (Aungst, 1989; Lorenz et al., 1982; ten Tije et al., 2003). This further drove the selection of Tween 20 for the subsequent studies.

An investigation into the use of liposomes, transfersomes and ethosomes, containing suitable edge activators as penetration enhancers found all formulations improved the drug penetration into the skin with respect to an aqueous suspension (Bragagni et al., 2012). Ethosomes

containing Tween 20 as edge activator demonstrated the best vesicle dimensions and homogeneity, and highest encapsulation efficacy, and enabled the highest increase in drug penetration through the skin due to the presence of both ethanol and Tween 20 which act as permeation enhancers. Thus ethosomes formulated with Tween 20 were found to be the most effective carrier for topical celecoxib applications used in skin cancer prevention and treatment (Bragagni et al., 2012).

Based upon these results, Tween 20 was selected for further liposomal studies at a loading of 0%, 2%, 6% and 10% w/w.

2.4.3.2 Assessment of the impact of pore size on the deformability of Tween 20 liposomes

The DI of liposomes formulated with up to 10% w/w Tween 20 was investigated further by forcing liposomes through pore sizes of 200 nm, 100 nm and 50 nm to observe the ability of the liposome to deform and reform (Figure 2.8).

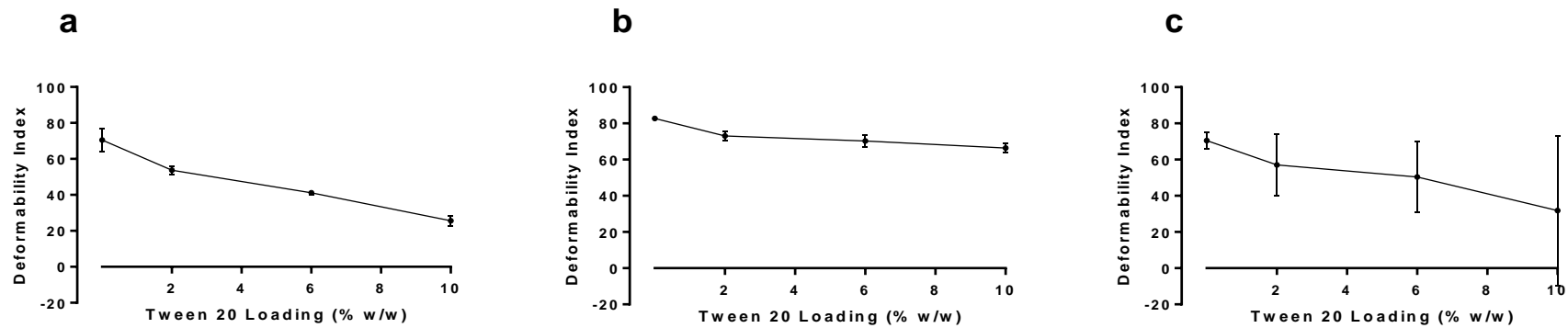


Figure 2.8: Deformability index of liposomes following extrusion through a membrane with pore size of 200 nm, 100 nm and 50 nm

Deformability index of liposomes formulated with loadings of up to 10% w/w of Tween 20 after having been forced through a membrane with a pore size of either a) 50 nm, b) 100 nm or c) 200 nm. Data represents mean \pm SD. n=6 independent batches.

Across the 3 pore sizes, as surfactant loading increased, liposome DI decreased. Liposomes formulated with Tween 20 forced through a 200 nm pore size (Figure 2.8a) saw the DI decrease from 70 to 26% as the Tween 20 loading increased from 0% w/w to 10% w/w, this decrease was significant between all loadings of surfactant ($P \leq 0.0001$). Liposomes formulated with Tween 20 forced through a 100 nm pore size (Figure 2.8b) saw the DI decrease from 83 to 66%. The difference in DI was significant between surfactant loadings of 0% and both 2 and 6% w/w ($P \leq 0.001$) as well as between 0% and 10% ($P \leq 0.0001$) and between 2% and 10% w/w ($P \leq 0.01$). Liposomes formulated with Tween 20 forced through a 50 nm pore size (Figure 2.8c) saw the DI decrease from 71 to 32%. Only the decrease in DI between 0% and 10% w/w of Tween 20 was significant ($P \leq 0.05$). Furthermore, there was no significant difference between the DI of liposomes forced through 200 and both 100 and 50 nm pore sizes, however there was a significant difference between the DI of liposomes forced through a 100 and 50 nm pore size ($P \leq 0.05$).

As expected liposomes deformed the least when forced through 200 nm. Liposomes forced through a pore size of 50 nm would be expected to have the highest deformability index. However this was not observed, instead liposome breakdown and formation of aggregates following extrusion may have occurred. The standard deviation was large for this set of data, up to ± 41.28 at a 10% w/w loading of Tween 20 highlighting variability in the size of structures obtained. These studies indicate liposomes sized around 400 nm in diameter prior to extrusion cannot be forced through a pore size of a quarter of that without destroying some of the structures.

2.4.3.3 Assessment of liposomal deformability following the mechanistic determination of energy contained within the liposomal bilayer

The energy stored within the liposome bilayer was determined to quantify how the presence of Tween 20 influenced energy storage thus liposome elasticity (Figure 2.9). As the loading of Tween 20 increased from 0% to 10% w/w, the energy retained in the formulation increased from 7.53×10^{-8} J to 9.46×10^{-8} J when the formulations were forced through 200 nm pores. This energy increase was significant between 0% w/w and all other loadings of surfactant ($P \leq 0.0001$) as well as between 2% and 10% w/w ($P \leq 0.05$). As the loading of Tween 20 increased from 0% to 10% w/w, the energy retained in the formulation increased from 7.43×10^{-8} to 9.3×10^{-8} J when the formulations were forced through 100 nm pores. This energy increase was significant between 0% w/w and all other loadings of surfactant ($P \leq 0.0001$) as well as between 2% and 10% w/w ($P \leq 0.05$). As the loading of Tween 20 increased from 0% to 10% w/w, the energy retained in the formulation increased from 6.46×10^{-8} to 9.09×10^{-8} J when the formulations were forced through 50 nm pores. This energy increase was significant between 0% w/w and both 2 and 6% w/w loadings of surfactant ($P \leq 0.001$) as well as between 0% and

10% w/w loadings of surfactant ($P \leq 0.0001$). As the pore size decreased, less energy was retained due to more energy being lost as friction, heat and liposome rupture. The increased turbulence in this closed system because of smaller pore size would result in an increase of the aforementioned outcomes.

Liposomes were expected to deform more so as pore size decreased. Deformation can be either elastic (reversible) or plastic (irreversible). This study shows that despite being forced through a pore size as small as 50 nm, some liposomes retained enough elastic energy to maintain the same size as when forced through the 200 nm membrane. Thus, the surfactant retained enough energy to allow liposomes to fit through a smaller gap and reform, at least between a pore size of 50 and 200 nm. Figure 2.9 shows that liposomes formulated with surfactant had the greatest capacity for energy storage. More energy would have gone into deforming the liposomes rather than being lost as friction and heat.

Further it shows liposomes forced through 50 nm pores retained less energy compared with greater pore sizes indicating energy was lost due to liposome rupture. This corresponds with deformation index data (Figure 2.9).

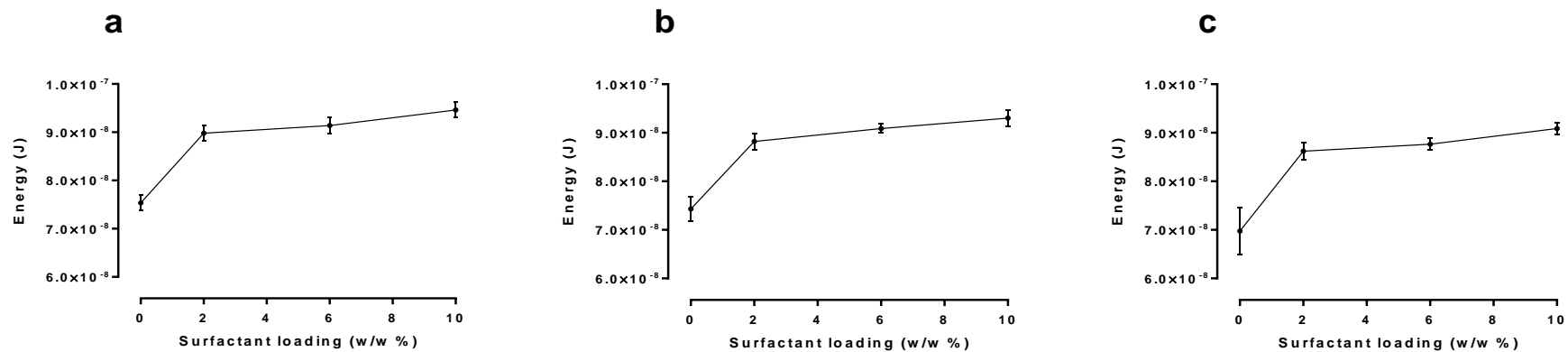


Figure 2.9: Mechanistic determination of energy stored in the liposome as determined by extrusion

Energy stored in the liposome when loaded with up to 10% w/w Tween 20 and forced through a membrane with a pore size of a) 200 nm, b) 100 nm and c) 50 nm. Data represents mean \pm SD. n=6 independent batches.

There is an energy cost to deform the bilayers, and this has been referred to as the 'curvature elastic energy' (Chung and Caffrey, 1994). Energy was supplied to this system in terms of pressure. Further, the temperature of the solution (room temperature) will also contribute to this. This energy will be converted to kinetic (movement and friction) and elastic energy. Elastic energy is defined as the energy stored because of deformation of an elastic object, such as the stretching of a spring or in this case the compression of the liposome to fit through the pore.

The more surfactant included within the bilayer, the more energy the liposome as a whole will be able to retain (Figure 2.9). The energy would be used to bend the surfactant structure, and since all systems gravitate toward minimising the free energy, the energy stored in this structure will be expelled once the liposome has passed the pore (Chung and Caffrey, 1994). This energy can then be expended into reforming the liposome following passage through the pore. Some energy will be lost during passage as heat or non-plastic deformation. Therefore, even at 10% w/w of Tween 20, 100% size was not recovered. Blank liposomes have less capacity to store energy, therefore energy will be used to rupture the membrane causing liposome size to decrease.

It follows that to pass through a pore size of 50 nm, more energy is required to deform the liposome. At this pore size, the amount of energy stored in the liposome membrane was enough to reform some of the liposomes to the same extent as for when forced through a 200 nm membrane. Some energy however will always be lost in the friction of the particles moving through the pores as heat, this energy loss increases with decreasing pore size resulting in the rupture of some liposomes. An increase in surfactant loading may bring allow liposomes to achieve greater reformation. Furthermore, studies observing liposome extrusion through a 50 nm pore size have a larger standard deviation. This indicates there may have been some smaller liposomes that didn't reform alongside some destroyed liposomes clumping together as lipid aggregates. Linear elastic deformation is governed by Hooke's law: the strain (deformation) of an elastic material is proportional to the stress (force) applied to it (Figure 2.10).

As the stress increases, the liposome will deform elastically up until a certain point. Beyond this point plastic deformation will occur and eventually, as the stress is increased further the liposomes will rupture.

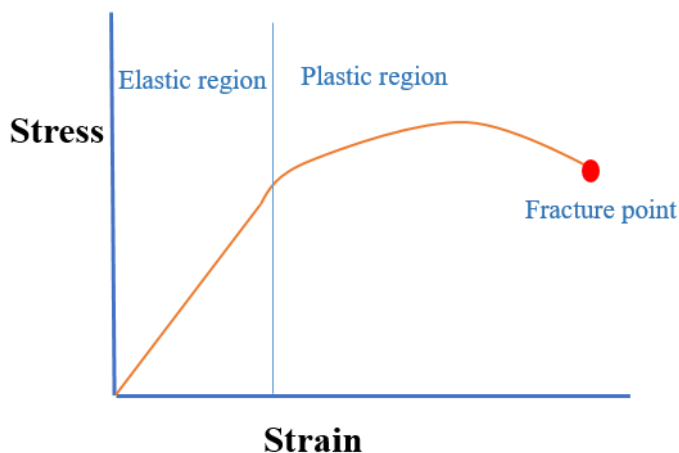


Figure 2.10: Stress – strain graph

Increasing applied force will firstly cause elastic deformation and then plastic deformation and eventually reach fracture point adapted from (Cockcroft and Latham, 1968).

This liposome destruction may not necessarily occur when applied to the skin. This was an *in vitro* study used to aide commentary on liposome deformability, it does not reflect what would happen *in vivo* and suggests liposomes would breakdown following application onto the skin. Liposomes would not be forced through the SC *in vivo* as they were forced through the artificial membrane, they would instead be expected to travel through into the dermal layer based on an osmotic transepidermal gradient (Cevc et al., 1995). When a lipid suspension is placed on the skin surface and partly dehydrated by the water evaporation loss, the lipid vesicles would respond to this gradient and try to avoid complete dehydration by moving along this gradient. Liposomes would only achieve this if they were sufficiently deformable to pass through the narrow pores within in the skin sublayers. Less deformable vesicles, including standard liposomes, would be confined to the skin surface where they would dehydrate and fuse. (Cevc and Blume, 2001; Cevc et al., 1995). Furthermore, due to experimental limitations of this study, the study was carried out at 20°C, the skin has a temperature of 35°C therefore the liposomes would be expected to be more flexible at this temperature and therefore less prone to destruction following passage through smaller gaps. Temperature governs the energy term of enthalpy therefore the liposomes would have more energy to be even more flexible and cross the SC. Furthermore, the bending energy can be drastically reduced by suitable solutes. The SC consists of cells embedded in a lipid mix, the liposomes will be more flexible in a lipid mix as opposed to an aqueous medium as less energy is required to maintain the structure (Sackmann, 1994).

2.4.3.4 Assessment of liposomal deformability following lipid quantification following extrusion

Following extrusion of liposomal formulations, the DI as well as the energy stored in the bilayer was calculated. This does not however provide information on the components of the liposome being passed through the pore. It may be possible that more PC and surfactant passed through as they are more fluid than cholesterol. To clarify this, quantification of the lipid content pre- and post- extrusion was performed by reverse phase HPLC with an ELSD detector connected to the instrument (Table 2-4 and 2-5). Generally, comparison of the concentration in the extruded solution to that in the syringe is lower for both cholesterol and PC across all three pore sizes implying liposomes did resist extrusion.

Table 2-4: Cholesterol quantification pre- and post- extrusion of liposomal formulations through membranes of pore size 200 nm, 100 nm, and 50 nm formulated with up to 10% w/w Tween 20.

Surfactant loading (% w/w)	50 nm		100 nm		200 nm	
	Post- (mg/mL)	Pre- (mg/mL)	Post- (mg/mL)	Pre- (mg/mL)	Post- (mg/mL)	Pre- (mg/mL)
0	0.010 ±	0.210 ±	0.113 ±	0.201 ±	0.140 ±	0.192 ±
	0.008	0.012	0.007	0.013	0.010	0.005
2	0.121 ±	0.184 ±	0.136 ±	0.189 ±	0.173 ±	0.175 ±
	0.006	0.008	0.010	0.007	0.006	0.007
6	0.149 ±	0.168 ±	0.151 ±	0.179 ±	0.179 ±	0.168 ±
	0.007	0.005	0.005	0.004	0.005	0.005
10	0.156 ±	0.160 ±	0.159 ±	0.160 ±	0.173 ±	0.168 ±
	0.004	0.016	0.005	0.008	0.008	0.008

Results are presented as the mean ± standard deviation (n=3)

Table 2-5: PC quantification pre- and post- extrusion of liposomal formulations through membranes of pore size 200 nm, 100 nm, and 50 nm formulated with up to 10% w/w Tween 20.

Surfactant loading (% w/w)	50 nm		100 nm		200 nm	
	Post- (mg/mL)	Pre- (mg/mL)	Post- (mg/mL)	Pre- (mg/mL)	Post- (mg/mL)	Pre- (mg/mL)
0	0.204 ±	0.830 ±	0.283 ±	0.790 ±	0.314 ±	0.726 ±
	0.014	0.018	0.004	0.011	0.011	0.018
2	0.290 ±	0.740 ±	0.315±	0.718 ±	0.338 ±	0.698 ±
	0.023	0.023	0.004	0.013	0.004	0.008
6	0.341 ±	0.680 ±	0.362 ±	0.675 ±	0.415 ±	0.643 ±
	0.028	0.013	0.011	0.010	0.018	0.014
10	0.423 ±	0.632 ±	0.479 ±	0.615 ±	0.488 ±	0.563 ±
	0.010	0.015	0.011	0.0128	0.016	0.019

Results are presented as the mean ± standard deviation (n=3)

The difference between the pre- and post- extrusion concentrations for both cholesterol and PC was then analysed (Figure 2.11 and 2.12). The general trend observed was that the difference in lipid concentrations decreases as surfactant increases and as pore size increases. At 0% w/w loading of surfactant, the difference in cholesterol concentration decreased from 0.11 to 0.05 mg/mL as pore size increased. Furthermore, as surfactant loading increased for liposomes being forced through a 200 nm pore size, the difference in cholesterol concentration decreased from 0.05 to 0.01 mg/ml. This indicates more liposomes were able to move across the membrane as both the pore size and surfactant loading increased.

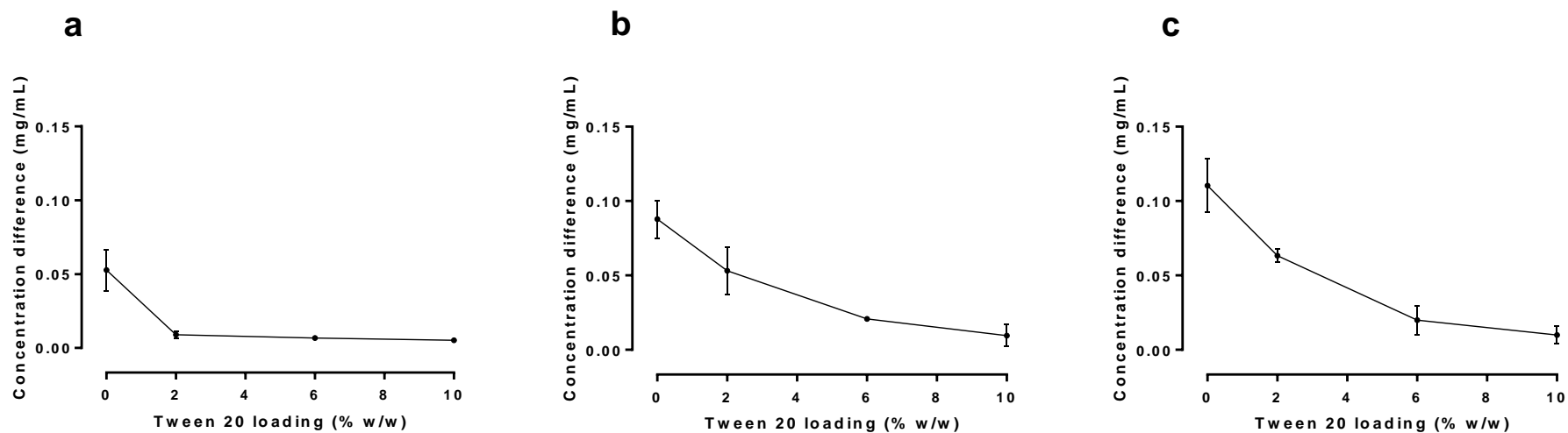


Figure 2.11: The difference in cholesterol concentration in pre- and post-liposomal extrusion

The difference in cholesterol concentration in pre- and post- extrusion of liposomal formulations loaded with up to 10% w/w of Tween 20 when forced through a) 200 nm, b) 100 nm and c) 50 nm. Data represents mean \pm SD. n=6 independent batches.

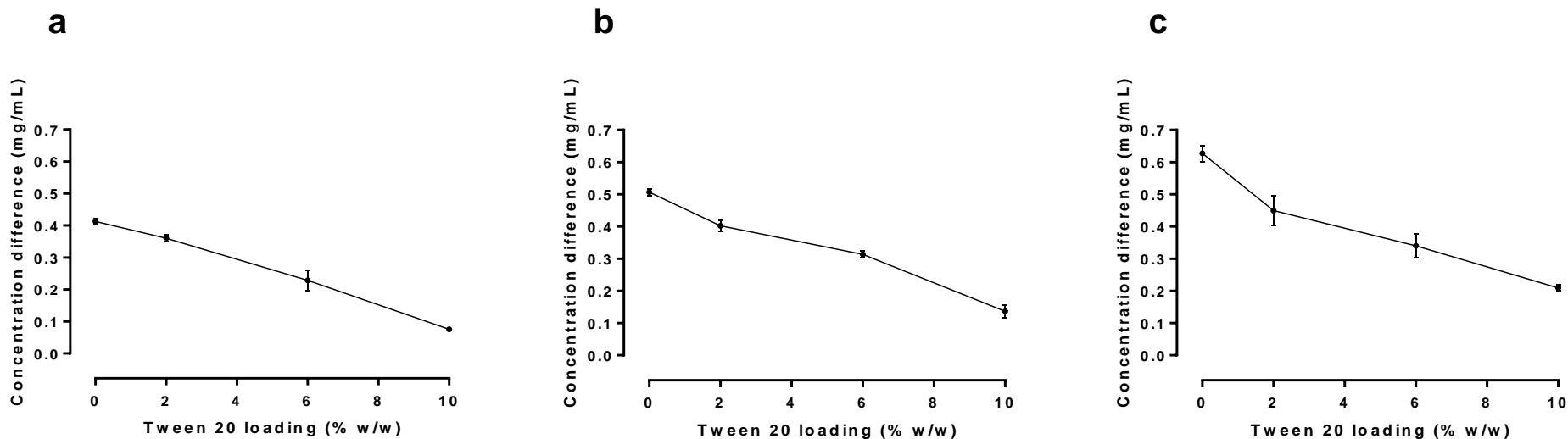


Figure 2.12: The difference in PC concentration in pre- and post- liposomal extrusion

The difference in PC concentration in pre- and post- extrusion liposomal formulations loaded with up to 10% w/w of Tween 20 when forced through a) 200 nm, b) 100 nm and c) 50 nm. Data represents mean \pm SD. n=6 independent batches.

The decrease in the difference of lipid concentration for both cholesterol and PC as surfactant was increased was significant across the three different pore size membranes (200 nm, 100 nm and 50 nm) the formulation was forced through.

The difference in cholesterol concentration for liposomes forced through 200 nm decreased significantly between surfactant loadings of 0% w/w and all other loadings of surfactant ($P \leq 0.001$). The difference in cholesterol concentration for liposomes forced through 100 nm decreased significantly between surfactant loadings of 0% and 2% w/w ($P \leq 0.05$), 0% and both 6 and 10% w/w ($P \leq 0.001$) as well as between 2% and 10% w/w of surfactant ($P \leq 0.01$). The difference in cholesterol concentration for liposomes forced through 50 nm decreased significantly between surfactant loadings of 0% and 2% w/w ($P \leq 0.01$), 0% and both 6 and 10% w/w ($P \leq 0.0001$), 2% and both 6 and 10% w/w ($P \leq 0.01$).

The difference in PC concentration for liposomes forced through 200 nm decreased significantly between surfactant loadings of 0% and 2% w/w ($P \leq 0.05$) as well as between 0% and both 6 and 10% w/w, between 2% and both 6 and 10% w/w and between 6% and 10% w/w ($P \leq 0.0001$). The difference in PC concentration for liposomes forced through 100 nm decreased significantly between surfactant loadings of 0% and 2% w/w ($P \leq 0.001$), 0% and both 6 and 10% w/w ($P \leq 0.0001$) as well as between 2% and 6% w/w of surfactant ($P \leq 0.001$), between 2% and 10% w/w and between 6% and 10% w/w ($P \leq 0.0001$). The difference in PC concentration for liposomes forced through 50 nm decreased significantly between surfactant loadings of 0% and 2% w/w ($P \leq 0.01$), 0% and both 6 and 10% w/w ($P \leq 0.0001$), and finally between 2% and both 6 and 10% w/w ($P \leq 0.01$).

Similar observations were made in a similar study regarding lipid recovery following extrusion of liposomes formulated with PC, L- α -phosphatidyl-L-serine and cholesterol; a decrease in the detection of the phospholipids was observed (Jousma et al., 1987), however their study was limited by the fact that they did not quantify the recovery of cholesterol. Additionally, they attributed some of the loss in lipid recovery to retention of phospholipid or some large vesicles on the Sephadex[®] column. Conversely, another study concerning lipid recovery following extrusion observed 100% lipid recovery (Berger et al., 2001). This may have been due to a lower extrusion pressures employed in their study or water loss from the sample during a thawing process prior to analysis.

This method was unable to detect and quantify differences in surfactant concentration differences pre- and post- extrusion. Further method development would be required and this may be useful in determining the composition of the liposomes passing through the membrane. The difference in cholesterol concentration was lower than that of PC overall, but the initial concentration of cholesterol was around 4 times lower. Furthermore, although PC is more fluid and less rigid than cholesterol (Papahadjopoulos and Kimelberg, 1974; Papahadjopoulos,

1976; Thewalt and Bloom, 1992), it is also a large molecule and may have become lodged within the pores of the membrane and not passaged fully through the membrane. Nonetheless, as the loading of Tween 20 increased, the difference in pre- and post- extrusion lipid concentration decreased implying the liposome, in its original composition was able to pass through the pore. The Tween 20 would increase fluidity of the liposome, thus decreasing liposome destruction, therefore less constituents become stuck within the pores.

2.4.4 Impact of liposomal formulation on *In vitro* cytotoxicity on HDFa and HaCat cells

There is an increasing desire to limit animal and human exposure to drug testing, thus there is a need to develop validated *in vitro* test systems. Whilst animal testing has provided valuable information regarding the pharmacokinetic or pharmacodynamic profile of formulation systems, there are vast differences interspecies difference in the anatomy and physiology of skin.

To determine the cellular toxicity of liposomes to HDFa and HaCat cells to be able to determine the compatibility of these formulations with skin, an XTT assay was performed to measure cell death after exposure of cells to different concentrations of blank liposomal formulations, those loaded with 2% w/w of Tween 20 and those loaded with 10% w/w Tween 20 for 24 hours. Results of cell viability are shown in Figure 2.13 and 2.14.

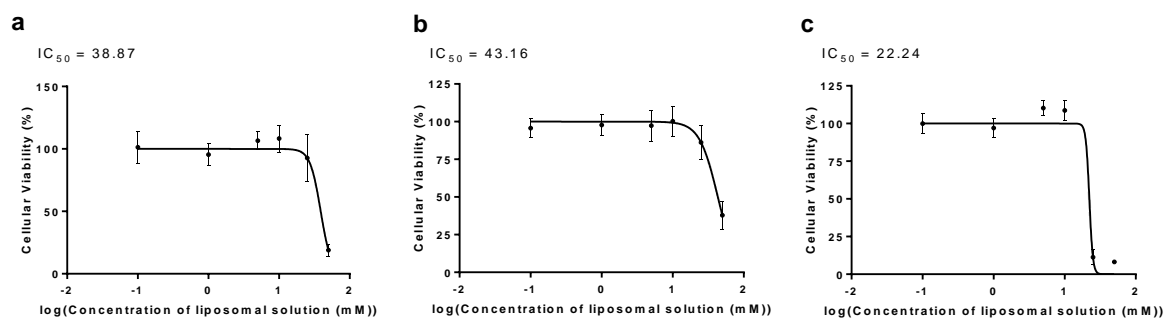


Figure 2.13: Cellular toxicity of liposomal formulations towards HDFa cells.

Cells were grown on a 96-well plate at a density of 50×10^3 cells per well and exposed to various percentages of liposomal solution (up to 50% of a 16:8 mM of PC : cholesterol loaded with a) 0%, b) 2% or c) 10% w/w of Tween 20). After 24 hour incubation following which 25 μ L of a 12.5:1 parts mixture of XTT to menadione was added each well. Plates were incubated for 3 hours at 37°C in a humidified atmosphere of 5% CO₂ in air and the absorbance read at 450 nm. The control cell (without drug) corresponded to a cell viability of 100%. Data is reported as mean \pm SD with 6 replicates per compound in at 3 independent experiments.

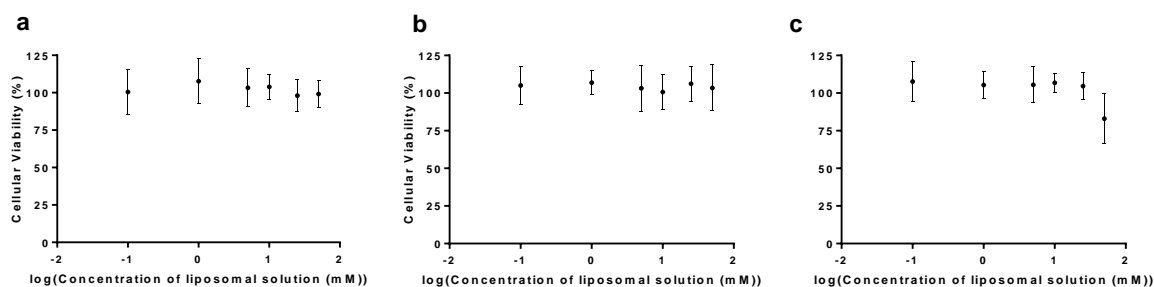


Figure 2.14: Cellular toxicity of liposomal formulations towards HaCat cells.

Cells were grown on a 96-well plate at a density of 50×10^3 cells per well and exposed to various percentages of liposomal solution (up to 50% of a 16:8 mM of PC : cholesterol loaded with a) 0%, b) 2% or c) 10% w/w of Tween 20). After 24 hour incubation following which 25 μ L of a 12.5:1 parts mixture of XTT to menadione was added each well. Plates were incubated for 3 hours at 37°C in a humidified atmosphere of 5% CO₂ in air and the absorbance read at 450 nm. The control cell (without drug) corresponded to a cell viability of 100%. Data is reported as mean \pm SD with 6 replicates per compound in at 3 independent experiments.

HDFa cells treated with blank liposomes maintained cell viability with no significant difference between control cells and cells treated with liposome solution up until 50% of liposome solution (of which stock solution contained 16:8 mM of PC to cholesterol) was applied where viability dropped to $19.0 \pm 4.9 \%$ ($P \leq 0.0001$). The IC_{50} value was 38.87 % of a solution containing 16:8 mM of PC to cholesterol. HDFa cells treated with liposomes loaded with 2% w/w Tween 20 maintained cell viability with no significant difference between control cells and cells treated with liposome solution up until 50% of liposome solution (of which stock solution contained 16:8 mM of PC to cholesterol) was applied where viability dropped to $37.8 \pm 9.2 \%$ ($P \leq 0.0001$). The IC_{50} value was 43.16% of a solution containing 16:8 mM of PC to cholesterol. HDFa cells treated with liposomes loaded with 10% w/w Tween 20 maintained cell viability with no significant difference between control cells and cells treated with liposome solution up until 25% of liposomes where viability dropped to 11% ($P \leq 0.0001$). At 50% of liposome solution, viability dropped furthermore to 8% ($P \leq 0.0001$). The IC_{50} value was 22.24 % of a solution containing 16:8 mM of PC to cholesterol.

HaCat cells treated with blank liposomes maintained cell viability at all concentrations of liposomes. There was no significant difference between the cell viability of the cells treated with the range of liposome concentrations observed in this study. HaCat cells treated with liposomes loaded with 2% w/w Tween 20 maintained cell viability at all concentrations of liposomes. HaCat cells treated with liposomes loaded with 10% w/w Tween 20 also maintained cell viability at all concentrations of liposomes.

Keratinocytes exist in the SC and their primary function is to act as a barrier to foreign objects. They are therefore more resilient than fibroblasts in that they form a part of the SC barrier (Thomas and Finnin, 2004) which explains why fibroblast cell viability decreased at higher liposome concentrations whereas keratinocyte viability did not. Liposomes loaded with 10% w/w of Tween 20 also seemed to have more of a toxic effect on fibroblasts and even the keratinocytes at higher concentrations. Tween 20 is a surfactant that may have interfered with the cell membrane of the cells.

2.4.5 Cellular liposomal uptake assay on HDFa and HaCat cells

Liposomes formulated beyond 2% w/w loading of Tween 20 did not show significant differences between the size, polydispersity, zeta potential and deformability. Therefore, only liposomes formulated with 0 and 2% w/w of Tween 20 were selected for further studies.

Liposomes fluorescently labelled with DiIC, formulated with and without Tween 20, were incubated with both HDFa and HaCat cells to assess the cellular uptake of these formulations. Following a 2-hour incubation with the cells, the labelled liposomes were identified using confocal microscopy (Figure 2.15 and 2.16). Cytoplasmic accumulation of the formulations was apparent, confirming the successful uptake into both HDFa and HaCat cells.

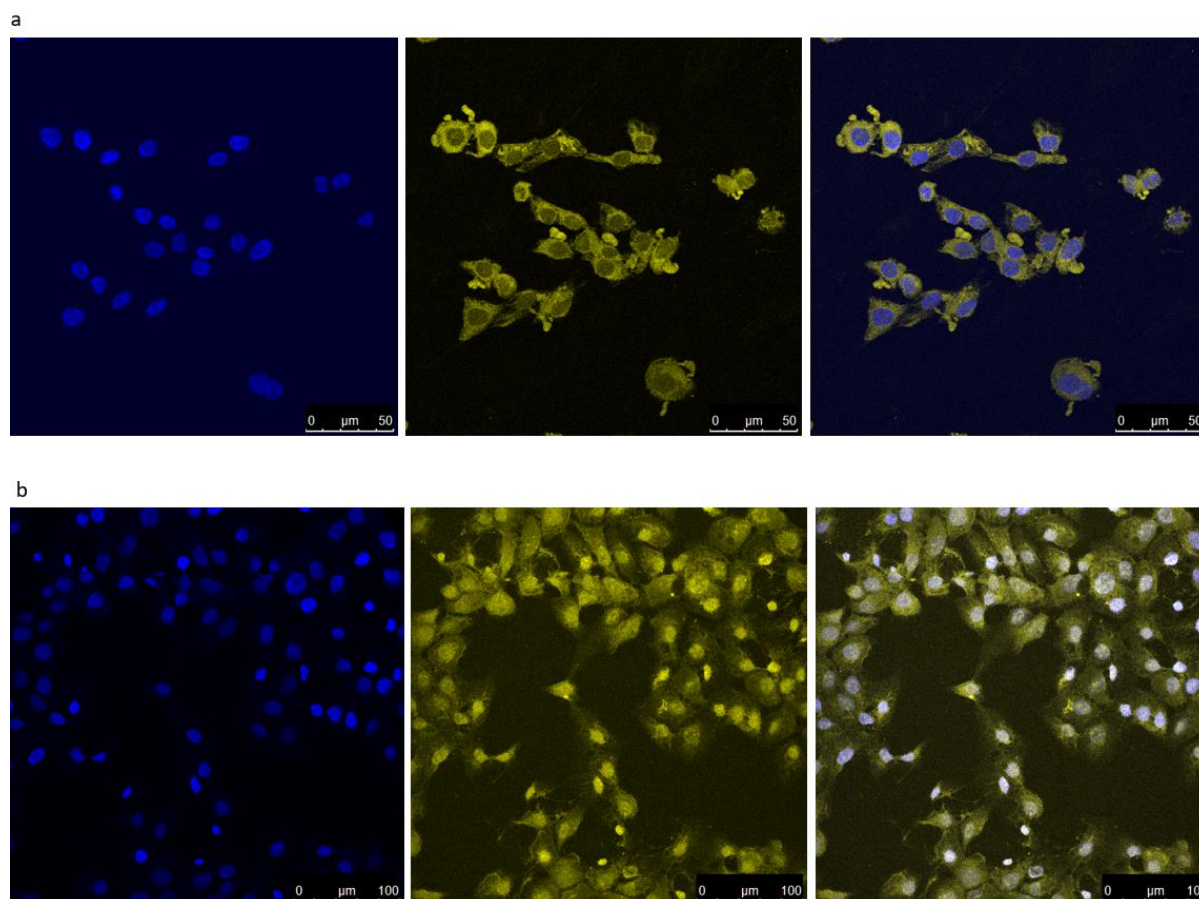


Figure 2.15: Localisation of DiIC loaded liposomes in HaCat cells.

Localisation of DiIC labelled a) blank liposomes b) liposomes loaded with 2% w/w Tween 20 in HaCat cells. Cells were grown on the coverslips for 2 days. Cell nuclei were visualised using DAPI (Blue). Liposomes were formulated with DiIC for visualisation (yellow).

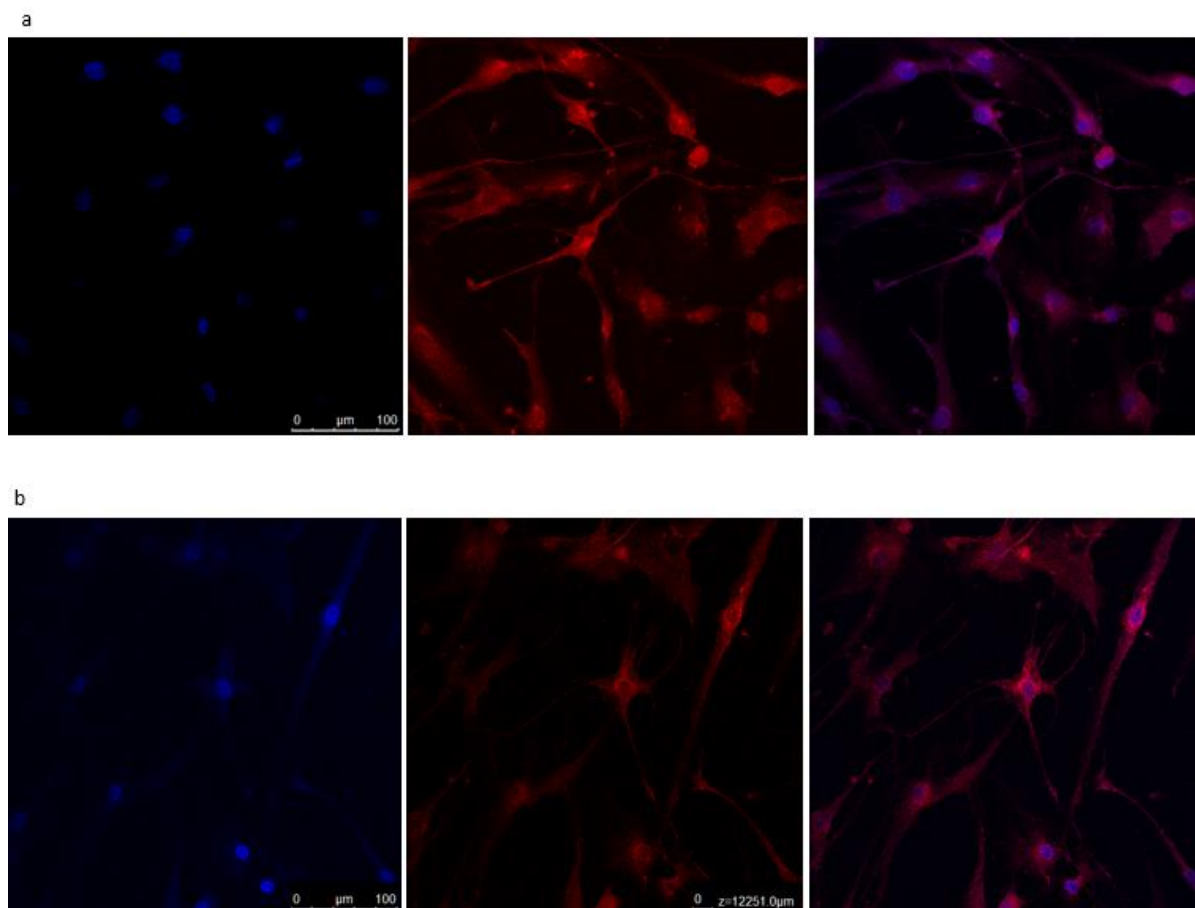


Figure 2.16: Localisation of DiIC loaded liposomes in HDFa cells.

Localisation of DiIC labelled a) blank liposomes b) liposomes loaded with 2% w/w Tween 20 in HDFa cells. Cells were grown on the coverslips for 2 days. Cell nuclei were visualised using DAPI (Blue). Liposomes were formulated with DiIC for visualisation (red).

Liposome uptake was observed within 2 hours of exposure to liposomes formulation with and without Tween 20. There are four proposed methods of liposome interaction with cells. The first one, termed 'stable adsorption' is the association of intact liposomes with the cell surface, without cell uptake. This adsorption may be mediated by specific components (including surface receptors and antibodies), or by nonspecific forces (including electrostatic and hydrophobic interactions). The second proposed interaction of liposomes is endocytosis (Pagano and Weinstein, 1978). This is the uptake of intact liposomes into endocytotic vesicles. Usually, this results in delivery to the lysosomal apparatus, but it is not unusual to see liposome contents escape into the cytoplasm. Both pinocytosis and phagocytosis is capable of mediating liposome uptake (Pagano and Weinstein, 1978). The third method of interaction is fusing of the lipid bilayer with the cell plasma membrane thus the concomitant release of liposome contents into the cytoplasm. Some liposome contents may leak into the medium or deposit

within other intracellular compartments. In the case of MLV, a multilamellar form with one less bilayer than the original should be found in the cytoplasm which may be beneficial when attempting to achieve a controlled release formulation (Martin and MacDonald, 1976). Finally, the fourth proposed method of liposome and cell interaction is lipid transfer. This is defined by the transfer of lipid molecules between liposomal bilayer and cells without actual cell association of aqueous liposome contents (Pagano and Weinstein, 1978). It is difficult to determine which of these occurred in this study, however, these methods of uptake are not mutually exclusive and any combination may be occurring in a given experimental circumstance (Pagano and Weinstein, 1978).

A study observing deformable liposomal uptake into dermal cells using excised human skin from female patients also observed uptake following a 14 hour incubation period. Liposomes were formulated from Phospholipon 90, α -tocopherol and sodium cholate with a size range of 120 -810 nm. Liposomes toward the smaller end of the size range observed greater penetration into the excised skin (Verma et al., 2003). A greater incubation period may have been necessary by Verma *et al.*, due to the presence of surface lipids. Surface lipids (the 'mortar' in the 'brick and mortar' analogy), which are not present to the same extent in the cell culture model than in human epidermis, seem to play an important role in liposomal uptake (Kuntsche et al., 2008). The restricted permeation of nanoparticles in human skin might be caused by the adhesion of the nanoparticles onto the skin surface. Surface lipids appear to play an important role in nanoparticle adhesion, consequently, for restricted drug permeation. Therefore whilst cell culture studies are useful, they are not conclusive (Kuntsche et al., 2008). Occlusion caused by the triglyceride nanoparticles (fat emulsion, solid lipid nanoparticles) was less pronounced in the cell culture model where surface lipids are not present to the same extent as in human skin. Interestingly, corticosterone permeation was nearly comparable in human and rat epidermis when applied in a dispersion of smectic nanoparticles indicating that the surface lipids seem to be less important for this carrier system (Kuntsche et al., 2008).

This formulation is aimed to be targeting the dermal layer. It is unclear whether or not the liposomes would completely pass through the keratinocytes into the dermal layer or whether they would accumulate in the stratum corneum. To be able to determine this, application onto excised skin would be necessary. Nonetheless it is clear liposomes were taken up by the cells, more importantly the fibroblasts where anti-cancer agents are aiming to be delivered.

2.5 Conclusion

The dermal delivery of pharmaceutical actives used in the treatment of skin cancer is limited by the SC. Although cream formulations of chemotherapeutic agents do exist, the side effect profile, high daily dose frequency coupled with dose transference raise compliance and therefore treatment issues. Therefore, there is an inherent need to develop formulations able to penetrate the SC and provide a sustained release of drug delivery.

This study investigated the use of the surfactants Tween 80, Tween 20 and sodium cholate in the development of elastic liposomes intended to pass through the SC and remain in the dermal layer where they would give a sustained release of drug. As the amount of surfactant in the bilayer is increased, liposome size decreases. Furthermore, the inclusion of surfactant within the bilayer seemed to produce a more homogenous formulation as defined by the polydispersity index.

Stability studies concerning liposome size found that over the first 2 days, liposome size decreased although this may have been due to lipid aggregates settling out (as confirmed by creaming at the bottom of the liposome container). Beyond this, over 28 days, the liposome size was maintained for liposomes formulated with Tween 20 and sodium cholate, a slight decrease in size was observed for liposomes formulated with Tween 80.

Inclusion of surfactant in the bilayer decreased the liposome DI and increased the amount of lipid able to pass through a membrane. Increasing the loading of the surfactant decreased the DI across all three surfactants. This implies that inclusion of surfactant would increase the ability of the liposome to pass through the gaps in the SC into the dermal layer. Sodium cholate appears to increase deformability the greatest, however, at the loadings investigated, Tween 80 and Tween 20 appeared the most stable. Furthermore, presence of surfactant appears to aid liposome movement across a membrane with a smaller pore size than liposomal diameter. Liposomes were able to move across a 200 nm pore size easier than a 50 nm pore size which appeared to cause some destruction of the liposomal structure.

Increasing loadings of Tween 20 within the liposomal bilayer appeared to increase the amount of energy stored within the bilayer that allowed the liposome to reform following extrusion rather than deforming permanently into smaller liposomal structures/aggregates. As the loading of Tween 20 increased, the difference in pre- and post- extrusion lipid concentration decreased. The Tween 20 increased fluidity of the liposome, thus decreasing liposome destruction, therefore less constituents become stuck within the pores. This implies that increasing loadings of Tween 20 allow the liposome, closer to its original composition, to pass through the pore.

Following application of liposomes onto dermal cell lines, 50% of the liposome solution (containing 16:8 mM of PC to cholesterol) decreased fibroblast cell viability. This was only the case for liposomes formulated with 10% w/w Tween 20 on the keratinocytes; these cells were

not affected by blank liposomes or those formulated with 2% w/w of Tween 20. This highlights fibroblast cells are more sensitive to the liposomes formulated in this study therefore further formulation development must consider this phenomenon. Cell uptake of both blank and 2% w/w Tween 20 loaded liposomes was apparent into both the keratinocyte cell line and the fibroblast cell line.

It appears elastic liposomes are useful in enhancing drug penetration through the SC into dermal cells and may be useful in the development of a controlled release formulation. Choice of surfactant influences liposomes size and deformability and thus the ability of the liposome to penetrate the SC. Investigation of Tween 80, Tween 20 and sodium cholate found that in terms of liposome stability, Tween 20 was the most suitable surfactant to continue to incorporate into the liposome formulation for all further studies.

3 Development of sustained release EGCG liposomal gel formulations for dermal drug delivery

3.1 Introduction

Epigallocatechin gallate (EGCG) is a polyphenolic catechin (Figure 3.1) that has been reported to possess a variety of anti-tumour effects towards cancerous skin cells including skin tumours (Gupta et al., 2004; Katiyar, 2011) and other neoplastic tumour types (e.g. colon (Chen et al., 2003; Hwang et al., 2007; McLoughlin et al., 2004) pancreas (Shankar et al., 2008), lung, prostate and breast (Yang et al., 2002)).

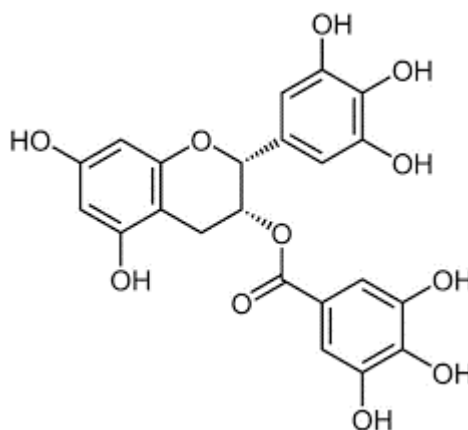


Figure 3.1: Molecular structure of EGCG

The tumour microenvironment is both a cause and consequence of tumorigenesis. This environment affects how the tumour and host cells co-evolve through direct and indirect cellular interactions. This then elicits multistage effects on many biological processes, including cellular proliferation, growth, metabolism, as well as angiogenesis and hypoxia and immunity (Albini and Sporn, 2007).

Emerging strategies for cancer management are primarily focused on chemoprevention and chemoprotection utilising naturally occurring nontoxic agents including EGCG (Hwang et al., 2007; Siddiqui et al., 2009; Singh et al., 2011a). EGCG has been found to affect specific biological processes that could be exploited as targets for the prevention and treatment of cancer (Casey, S. C., et al. 2015). Specific properties include induction of apoptosis (Gupta et al., 2004), promotion of cell growth arrest by altering the expression of cell cycle regulatory proteins (Gupta et al., 2004), activation of killer caspases and the suppression of oncogenic transcription factors (Singh et al., 2011a; Singh et al., 2011b; Thawonsuwan et al., 2010) and pluripotency maintain factors (Sigler and Ruch, 1993). Furthermore, clinical studies have found that treatment with EGCG inhibits tumour incidence and metastasis in additional organ sites (Mukhtar and Ahmad, 2000; Singh et al., 2011a).

The application of the use of naturally occurring compounds as chemopreventative and chemoprotective strategies has so far been received with limited success and this may be largely due to inefficient delivery systems and a limited bioavailability of promising agents.

Consequently, to achieve maximum clinical efficacy, novel approaches are required to enhance the bioavailability. A nanoparticle mediated delivery would be valuable in enhancing the bioavailability of these compounds.

The skin is an efficient and effective physical barrier to the external environment. The barrier function is, a result of the multilayer anatomy of the epidermis, dermal layer, and finally the subcutaneous layer. The use of liposomal nanoparticle formulations as drug-delivery vehicles provide a novel approach to the delivery and targeting of the dermal layer alongside site-specific delivery with benefits for both delivery of existing (poorly permeable) molecules and larger (often impermeable) biologics. Elastic liposomes have been reported to penetrate the skin if applied non-occlusively by the very high and self-optimizing deformability. They have already been successfully employed in the transdermal delivery of lipophilic and hydrophilic drugs including anti-inflammatory agents, plasmid DNA, anti-tumour agents and hormones (Cevc and Blume, 2001; El Maghraby et al., 1999; Oh et al., 2006; Romero et al., 2013). Liposome adhesion, fusion and penetration into the SC is possible with potentially deeper penetration into the dermal layer of deformable vesicles compared with traditional liposomes (El Maghraby et al., 1999).

Furthermore, liposomes intended for topical application are required to be delivered in a carrier due to the liquid nature of the preparation. Liposomes are compatible with viscosity increasing agents such as cellulose based gels including HEC and HPMC (Foldvari, 1996). These are known to be safe in topical, dermal and transdermal delivery (Forbes et al., 2011b; Hascicek et al., 2009; Patton et al., 2007).

3.2 Aims and objectives

In this body of work, a formulation aiming to deliver EGCG to the dermal layer in the management of skin cancer was developed. The effectiveness of the *in vitro* delivery of EGCG encapsulated in liposomes in an aqueous gel system to the dermal layer was assessed. The aim of this study was to formulate and characterise an aqueous gel system loaded with elastic liposomes formulated with Tween 20 for the dermal delivery of EGCG. Liposomes were loaded with up to 10% w/w Tween 20 and 0.25 mg/mL of EGCG. They were characterised by size, zeta potential, DI and stability. EGCG release was observed from these liposomal formulations as well as from HEC and HPMC gels and from gels loaded with liposomes. Toxicity and uptake into HDFa and HaCat cells was subsequently determined.

To achieve the aims, the overall objectives were to

- Validate a HPLC method for EGCG detection.
- Formulate and characterise EGCG loaded liposomes and investigate the release profiles.
- Characterise EGCG loaded deformable liposomes formulated with Tween 20 and investigate the release profiles.
- Formulate and compare EGCG release from EGCG loaded HEC and HMPC aqueous gels
- Formulate and compare EGCG release from aqueous gels loaded with EGCG loaded liposomes
- Apply formulations to fibroblast (HDFa) and keratinocyte (HaCat) cell lines to characterise toxicity as well as cell localisation.

3.3 Materials and methods

3.3.1 Materials

The materials used to prepare liposomes, all reagents as well as materials used to grow HDFa and HaCat cells are detailed in section 2.3.1. EGCG, HEC and HPMC polymers were obtained from Sigma-Aldrich.

3.3.2 Elastic liposome preparation

Liposomes were prepared by using the film hydration method established by Bangham *et al.*, (1965) detailed in section 2.3.2. Briefly, PC, cholesterol and surfactant were dispersed in chloroform and methanol in a 9:1 ratio. Ratios of lipids are detailed in Table 3-1 rational of which has been adapted from previous studies concerning the formulation of elastic liposomes (Hiruta *et al.*, 2006; Ita *et al.*, 2007; Oh *et al.*, 2006; Tsai *et al.*, 2015). EGCG loaded liposomes were prepared by adding the required amount of EGCG to the lipid mixing stage.

Table 3-1: Details of liposome formulation composition.

Formulation	PC (% w/w)	Cholesterol (% w/w)	Tween 20 (% w/w)
1	80	20	0
2	78	20	2
3	76	20	4
4	74	20	6
5	72	20	8
6	70	20	10

Formulation 1 was the control formulation to which no surfactant was added

3.3.3 Liposome characterisation: particle size and polydispersity and zeta potential

Mean particle size, polydispersity index and zeta potential of liposomes was measured as detailed in section 2.3.3 using a Zetaplus (Brookhaven Instruments). Each sample was measured 3 times.

3.3.4 Assessment of liposomal deformability

The deformability index (DI) of the elastic vesicles was determined using a mini filtration technique as detailed in section 2.3.3.

3.3.5 HPLC Methodology

Detection of EGCG was assessed using a reverse phase HPLC methodology. A Waters Alliance separation module HPLC with UV detection was utilised at an operating wavelength of 275 nm (Bradfield and Penney, 1948) with a Waters X select column (5 μ m C18 4.6 x 150 mm). 10 μ L of sample at room temperature was injected. The mobile phase comprised of a 70:30 ratio of 0.1% TFA in water to methanol at a flow rate of 1 mL/min.

Stock solutions and standard solutions of EGCG were prepared with both water and ethanol ranging from 0.5-500 μ g/mL.

3.3.5.1 HPLC validation

The method was validated by assessing the linearity and range, repeatability and sensitivity in terms of the limit of detection (LOD) limit of quantification (LOQ) and precision. The system was flushed with 100% methanol before each use for 30 min.

For the linearity and range assessment, standard solutions ranging between 0.5-500 μ g/mL of EGCG in water were prepared. The mean peak area \pm SD was calculated and plotted against the known concentration of the standard.

The repeatability of the method was assessed by determination of the intraday (same day) and interday (over the course of three days) variability.

A study of the sensitivity of the method was assessed by means of the calculation of the LOD (equation 3.2), and the LOQ (equation 3.3) from the standard deviation (Equation 3.1). Values were determined from the standard deviation of the response (σ) and the slope (S) obtained from the calibration curves carried out during the linearity assessment. According to the ICH guidelines (Guideline, 2005), a signal-to-noise ratio of three was assumed for the quantification of the LOD, whereas for the LOQ, a signal-to-noise ratio of ten was set.

Equation 3.1: Standard deviation

$$\sigma = \frac{\sum(y - y_i)^2}{n^2}$$

Equation 3.2: Detection limit

$$LOD = \frac{3.3 \times \sigma}{s}$$

Equation 3.3: Quantitation limit

$$LOQ = \frac{(10 \times \sigma)}{s}$$

where σ is the standard deviation, y is a data value, y_i is the mean, n is the total sample population, and s is the slope of the curve.

3.3.6 Determination of entrapment efficiency

The entrapment efficiency of EGCG loaded in elastic liposomes was determined by centrifuging samples and quantifying drug in the supernatant. The sample was centrifuged at 18,000 rpm for 30 min at 4°C in an Optima™ MAX-XP ultracentrifuge to separate the incorporated drug from the free form. The supernatant was then analysed using HPLC (section 3.3.5) to determine the drug encapsulation percentage of the total EGCG load. The percentage encapsulation efficiency of EGCG in liposomal formulations was calculated using Equation 3.4:

Equation 3.4:

$$E = \frac{D_t - D_s}{D_t} \times 100\%$$

where E is the encapsulation efficiency, D_t is the total drug content and D_s is drug content in supernatant.

3.3.7 Differential scanning calorimetry investigations of EGCG and EGCG lipid blends

EGCG and ratios of lipid, surfactant and drug mixtures corresponding to liposome ratios were analysed in the solid state using a TA Instruments Q200 Thermal Analysis DSC. 3 mg of EGCG was weighed into T-Zero aluminium pans and then hermetically sealed. All

experimental runs started at an initial temperature of 0°C, purged under nitrogen gas, with a scan rate of 10°C/min to 300°C.

3.3.8 EGCG loaded aqueous gel formulation

Aqueous gels were prepared using HEC (1, 3 and 5% w/v) and HPMC (1, 3 and 5% w/v) which were mixed overnight using a mechanical mixer (Polytron PT 3100 D) at a speed of 3000 rpm. HEC and HPMC gels with a drug loading of 1% w/v polymer were formulated.

3.3.9 *In vitro* EGCG release studies

Drug release from gels, liposomes and liposomal gels over 24 hours was observed using multiple methods.

A one compartment model to observe drug release requires formulation to be placed directly into the release media and aliquots of media removed and quantified for drug release. A two compartment model may be used in which formulation and release media are separated by a membrane. A one compartment model can be used to study release and gel swelling behaviour whilst a two compartment diffusion cell observes drug release across a membrane and allows for the comparison of release from solution (which would require a membrane to separate the donor and receiver compartments) to formulation. A one compartment model and a two compartment model was used to observe release from gels. A one compartment model was not suitable for release from liposomes as the additional step of ultracentrifugation or ultrafiltration to separate free drug must be applied. This however is time consuming and requires greater sample sizes.

3.3.9.1 One compartment release model

To study the *in vitro* release and swelling behaviour of gels over 24 hours 1 g of each EGCG loaded gel was syringed into plastic containers with 20 mL of dermal dissolution media (DDM) and these were then placed into a shaking water bath at 34 °C and 60 rpm. The release media was sampled with volume replacement (0.5 mL) at 15, 30, 60, 120, 180, 240, 300, 360, 420, 480 and 1440 minutes and analysed using HPLC quantification with UV analysis (section 3.3.5).

3.3.9.2 Two compartment release model

A diffusion cell dialysis system (PermeGear diffusion cell, Hellertown, USA) was used to evaluate *in vitro* drug release from aqueous solution (0.1 mg/mL), gels (formulated with 1% w/w of drug) and liposomes into release media. Drug release was quantified over 24 hours using a side by side diffusion chamber maintained at 35 °C. 10 mL of the formulation was placed into the donor side of the diffusion cell with a stirrer and release across a 50 nm membrane into the receiver side containing 100 mL of water with a stirrer was measured.

The release media was sampled with volume replacement (0.5 mL) at 15, 30, 60, 120, 180, 240, 300, 360, 420, 480 and 1440 minutes and analysed using HPLC quantification with UV analysis.

3.3.9.3 Liposomal gel release study

In order to assess drug released from drug-loaded liposomes entrapped within polymer gels, a permeable insert models system was used. A 4 cm² cylindrical cell culture Thincert™ insert (400 µm pore size) was filled with 1 mL of formulation. Release into 4 mL of DDM in a 6-well Thincert™ plate from solution, and gels loaded with liposomes was quantified. HEC and HPMC gels loaded with 3% w/v of polymer were manufactured. These gels were then loaded with non-surfactant loaded liposomes formulated or liposomes formulated with 2% w/w Tween 20. The plates were maintained at 35 °C on a shaking plate. This system was used to investigate if drug/drug loaded liposome was able to diffuse out from the gel rather than to test and compare rates of release.

The release media was sampled with volume replacement (0.5 mL) at 15, 30, 60, 120, 180, 240, 300, 360, 420, 480 and 1440 minutes and analysed using HPLC quantification with UV analysis (section 3.3.5).

3.3.10 Release kinetics

To analyse the mechanism of drug release-rate kinetics, data obtained from *in vitro* release profiles can be quantified in many kinetic models including zero order, first order, Higuchi, and Korsmeyer-Peppas (Higuchi, 1963b; Korsmeyer et al., 1983; Peppas, 1985; Siepmann and Peppas, 2012). Mathematical modelling increases understanding of the release mechanism and can help reduce the number of experiments required to optimize drug formulations.

Zero order release: drug is released at a constant rate independent of the initial concentration (Equation 3.5).

Equation 3.5:

$$C = C_0 - kt$$

where C is the concentration, C_0 is the original concentration, k is the rate constant and t is time.

First order release: drug is released at a constant rate in proportion to the amount of drug available at that time (Equation 3.6).

Equation 3.6:

$$C = C_0 e^{-Kt}$$

where C is the concentration, C_0 is the original concentration, K is the rate constant and t is time.

Higuchi: Higuchi developed several theoretical models to study the release of water soluble and low soluble drugs incorporated into semi-solid and/or solid matrixes (Higuchi, 1961; Higuchi, 1963b). Mathematical expressions were obtained for drug particles dispersed in a uniform matrix behaving as the diffusion media. To study the dissolution from a planar system having a homogeneous matrix, Equation 3.7 is used

Equation 3.7:

$$C = C_0 K \sqrt{t}$$

Where C is the concentration, C_0 is the original concentration, K is the rate constant and t is time

Korsmeyer-Peppas Model: A simple, semi-empirical model that relates exponentially the drug release to the fractional release of the drug (Equation 3.8) (Korsmeyer et al., 1983; Peppas, 1985).

Equation 3.8:

$$\frac{C_t}{C} = Kt^n$$

where C_t/C is fraction of drug released at time t , k is the release rate constant and n is the release exponent. The n value is the diffusional exponent and is used to characterise release for cylindrical shaped matrices, the value of n can be used to describe the release mechanism as described in Table 3-2.

Table 3-2: Description of how the diffusional exponent n may be used to characterise release for cylindrical shaped matrices

< 0.5	0.5 – 1	1	> 1
Fickian diffusion: Case I transport	Non-fickian diffusion	Case II transport	Super case II transport
$t^{0.5}$	t^{n-1}	Zero order	t^{n-1}

Mathematical models to assess release kinetics were fit using Microsoft Excel[®]. Zero order and first order release profiles were applied to release from drug solution and drug loaded liposome solution following which regression analysis techniques were employed to determine the probable drug-release. The release kinetic model displaying with the highest r^2 metric (≥ 0.95) was determined to be the mechanism, by which release occurs. Furthermore, the Higuchi release profile and Korsmeyer-Peppas Model was applied to release data obtained from gel formulations and liposomal gels to describe release from a polymeric system.

3.3.11 Growth and passage of cells

HDFa isolated from adult skin, cryopreserved at the end of the primary culture were revived in medium 106 supplemented with Low Serum Growth Supplement. HaCaT is a spontaneously transformed aneuploid immortal keratinocyte cell line from adult human skin. HDFa and HaCat cells were maintained in a humidified 37 °C incubator with 5 % CO₂, grown, fed and split for further proliferation as detailed in section 2.3.6.

3.3.12 Impact of liposomal formulation on *In vitro* cytotoxicity on HDFa and HaCat cells

To determine the cytotoxicity profile of EGCG towards HDFa and HaCat cells, an XTT assay (Scudiero et al., 1988) was performed to measure cell death after exposure of cells to different concentrations of drug for 24 hours. Cells were trypsinised, centrifuged and re-suspended in fresh media. Cells were then counted and seeded in a 96-well plate as detailed in section 2.3.7. On day 3, media was removed. Cells were treated with 100 μ L of either 100 μ M, 50 μ M, 10 μ M, 5 μ M, 1 μ M and 0.1 μ M of drug in prepared in <1% DMSO / media. Plates were incubated in a humidified incubator for 24 hours at 37°C with 5% CO₂ following which a mixture of 12.5:1 parts of XTT to menadione (25 μ L) was added each well in a 96 well plate. Plates were incubated for 3 hours at 37°C and the absorbance read at 450 nm on a Thermo Scientific

Multiscan spectrum. Assessment of EGCG toxicity to these cells was conducted through analysis of changes in XTT absorbance with increasing drug concentration.

3.3.13 Cellular liposomal uptake assay on HDFa and HaCat cells

Liposomes, both deformable and non-deformable, were formulated with the addition of the fluorescent dye, DiIc, in DMSO as detailed in section 2.3.8. Coverslips were prepared and analysed with an upright confocal microscope (Leica SP5 TCS II MP) as detailed in section 2.3.8.

3.3.14 Liposome stability

The stability of liposomes was determined, as prepared in water, through the assessment of particle size over a 28 day period as detailed in section 2.3.4.

Furthermore, the encapsulation efficiency of drug loaded liposomes was assessed over 4 weeks as detailed in section 3.3.6.

3.3.15 Statistical analysis

Unless otherwise stated, all results are presented as mean \pm SD. Replicates of at least 3 were used for all studies. For multiwell plate assays replicates of 6 were used for each experimental condition with the study replicated 3 times.

A paired T test or a one way ANOVA was used to determine any statistically significant difference between means tested. A post-hoc Tukey's multiple comparisons test was then applied to assess differences between groups. Results were deemed statistically significant if $P < 0.05\%$.

3.4 Results and discussion

EGCG is a flavonoid that is the most abundant catechin (anti-oxidant) in tea, thus may be potentially useful as a pharmacological anti-cancer agent (Casey et al., 2015). This flavonoid has been found to have cytotoxic effects in cancerous skin cells. Additionally, it may also increase the efficacy of chemotherapeutic treatment as well as have chemoprotective effects (Chen et al., 2003; Gupta et al., 2004; Hwang et al., 2007; McLoughlin et al., 2004; Shankar et al., 2008; Siddiqui et al., 2009; Yang et al., 2002).

The use of naturally occurring compound as chemopreventative and chemoprotective strategies has been limited in success due to inefficient delivery systems and a limited bioavailability of promising agents. Liposomes could be valuable in enhancing the bioavailability of these compounds (Nishiyama, 2007; Siddiqui et al., 2009). Elastic liposomes have been found to be advantageous in dermal delivery of drugs (Cevc and Blume, 2001; El Maghraby et al., 1999; Oh et al., 2006; Romero et al., 2013). Whilst being able to act as solubilising agents for low solubility drugs, they may also protect the drug from degradation in the body and may be formulated for targeted, sustained drug release. They can also improve drug deposition within the skin at the site of action where the aim is to reduce systemic absorption thereby reducing side effects (Benson 20016, Cevc 1996).

Elastic liposomes have been reported to penetrate the skin if applied non-occlusively by the very high and self-optimizing deformability. The skin is an efficient and effective physical barrier to the external environment. They have already been successfully employed in transdermal delivery of lipophilic and hydrophilic drugs including anti-inflammatory agents, plasmid DNA, anti-tumour agents and hormones (Cevc and Blume, 2001; El Maghraby et al., 1999; Oh et al., 2006; Romero et al., 2013).

In attempting to delivery nanoparticle formulations to the dermal layer, it is often necessary to employ carrier vehicles such as a gel or cream due to the liquid nature of the preparation. It has been confirmed that liposomes are compatible with viscosity increasing agents such as cellulose based gels including HEC and HPMC (Foldvari, 1996). These are known to be safe in topical, dermal and transdermal delivery (Forbes et al., 2011b; Hascicek et al., 2009; Patton et al., 2007).

3.4.1 Liposome characterisation: particle size and polydispersity and zeta potential

A target goal for the present studies was to increase drug loaded liposome permeation across the epidermal layer; the size of drug carrier is an important determinant of this. EGCG loaded MLV liposomes were formulated using the dry film method, MLV's were formulated by vortexing for 5 min (section 3.3.2). Liposomes were formulated with cholesterol which provides membrane stabilising properties by filling voids in between the phospholipids (Gregoriadis and Davis 1979). The inclusion of cholesterol thereby reduces permeability of the liposome bilayer

and prevents drug leaching out of the liposome structure (Demel *et al.*, 1972). Additionally, various loadings of Tween 20, a polysorbate surfactant, were added to the formulation so as to add elastic properties to the bilayer.

As the surfactant loading in the bilayer of EGCG loaded liposomes increased, a decrease in size was noted (from 1292.2 ± 33.5 nm for liposomes formulated with no surfactant to 524.8 ± 25.1 nm for liposomes formulated with 10% w/w Tween 20 surfactant (Figure 3.2)). The decrease in size was significant for liposomes loaded with no surfactant compared with liposomes loaded with 2, 6 and 10% w/w Tween 20. There was no significant difference between the size of liposomes loaded with 2, 6 and 10% w/w of surfactant. Surfactant has been found to decrease liposome size in comparison to conventional liposomes (Goindi *et al.*, 2013; Tsai *et al.*, 2015). This may be as a result of the surfactant destabilising the bilayer (El Zaafarany *et al.*, 2010) and allowing a greater interaction of the phospholipid bilayer with the aqueous phase resulting in the overall formation of liposomes with a smaller diameter giving a greater surface area in contact with the aqueous phase.

EGCG loaded liposomes were found to have a larger diameter than blank liposomes; 1292.2 ± 33.5 nm compared with 1030.25 ± 182.5 nm for liposomes formulated with no surfactant and 358.1 ± 57.1 nm compared with 524.8 ± 25.1 nm for liposomes formulated with 10% w/w loading of Tween 20 (Figure 3.2). EGCG is amphiphilic in character (Mignet *et al.*, 2013) thus when encapsulated in liposomes it will be bound to the membrane surface rather than being present within the hydrophilic core. Therefore, to increase capsulation within bilayer, encapsulation into liposomes was performed as in the case of lipophilic compounds where the bioactive is added directly to the lipid and solvent mixture (Istenic *et al.*, 2016). The inclusion of drug in the bilayer may have caused an increase in liposome size by increasing bilayer hydrophobicity as it had caused the bilayer to have less interaction with the aqueous phase.

Similar to blank liposomes, as the surfactant loading increased in the EGCG loaded liposomes, the diameter decreased, however, increasing the Tween 20 content beyond 2% w/w demonstrated no statically significant differences in liposome size. This would indicate that either 2% w/w is the maximum loading of Tween 20 that can be added in either formulation or that, simply, between 2% and 10% w/w, the size of liposome does not decrease as there is not sufficient surfactant to decrease the interfacial tension to decrease liposome size.

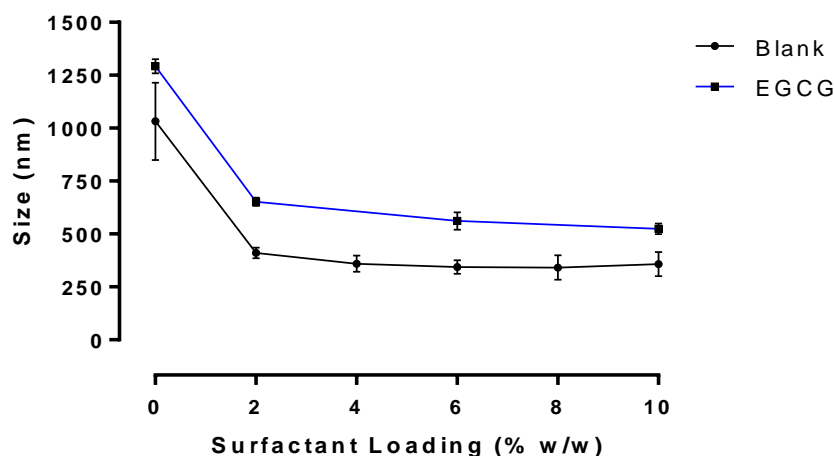


Figure 3.2: Liposome size distribution.

Liposome size distribution, determined by DLS, comparing blank and EGCG loaded formulations with increasing loadings of Tween 20 up to a maximum of 10% w/w. Liposomes were prepared via the dry film hydration method and compound was added during the lipid mixing stage. Data represents mean \pm SD. n=3 independent batches.

A liposome preparation homogenous in size is important as size will determine liposome distribution *in vivo* as well as influence drug release kinetics. A polydispersity of up to 0.3 is considered homogenous (Chen et al., 2012; Goindi et al., 2013; Kang et al., 2013). Liposomes formulated without surfactant were slightly out of this range (0.33 ± 0.09 and 0.32 ± 0.04 for blank and EGCG loaded liposomes respectively) however liposomes formulated with surfactant all had a polydispersity below 0.3 therefore can be considered homogenous (Figure 3.3). The polydispersity for EGCG loaded liposomes formulated with Tween 20 was similar to blank liposomes formulated with Tween 20 ($P \geq 0.05$). The polydispersity of EGCG loaded liposomes however had a greater standard deviation (0.06 compared with 0.02 for liposomes formulated with 2% w/w Tween 20, 0.07 compared with 0.03 for liposomes formulated with 6% w/w Tween 20) showing these liposomes were perhaps less homogenous than blank liposomes. This may be due to EGCG disrupting the bilayer of the membrane resulting in a wider range of liposome diameter. Additionally, as the loading of Tween 20 increased, the polydispersity decreased from 0.322 with no surfactant to 0.221 with 10% w/w of Tween 20. As discussed later on in section 3.4.3, as the loading of Tween 20 increased, the entrapment efficiency decreases. Therefore this indicated that the presence of EGCG with the bilayer led to a wider size range of formulated liposomes.

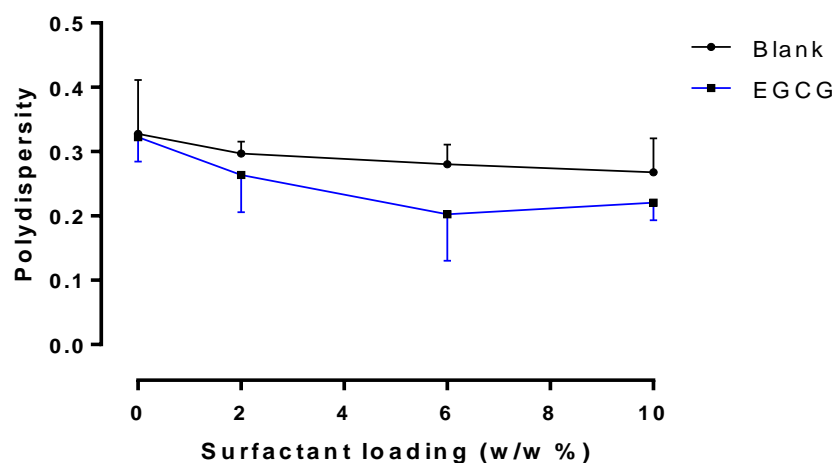


Figure 3.3: Polydispersity of blank and EGCG loaded liposomes.

Polydispersity, determined with DLS, of blank and EGCG loaded liposomes formulated with increasing loadings of Tween 20 up to a maximum of 10% w/w. Liposomes were prepared via the dry film hydration method and compound was added during the lipid mixing stage. Data represents mean \pm SD. n=3 independent batches.

The zeta potential may be defined as the potential difference between the dispersion medium and the stationary layer of fluid attached to the dispersed particle. The magnitude of the zeta potential indicates the degree of electrostatic repulsion between adjacent, similarly charged particles in a dispersion. Thus it is one of the fundamental parameters known to affect stability. The zeta potential of blank and EGCG liposomal formulations is displayed in Table 3-3.

Table 3-3: Zeta potential of liposomal formulations formulated with and without drug with up to 10% w/w loading of Tween 20

Surfactant loading (% w/w)	Zeta potential (mV)	
	Blank Liposomes	EGCG loaded liposomes
0	5.03 \pm 1.03	2.412 \pm 1.08
2	4.67 \pm 1.08	3.667 \pm 0.91
6	3.71 \pm 0.90	-0.985 \pm 1.01
10	-2.79 \pm 0.20	-1.895 \pm 0.88

Results are presented as the mean \pm standard deviation (n=3)

A neutral liposomal surface charge is ideal to avoid skin irritation (Prausnitz and Langer, 2008) however, this may lead to particle flocculation due to the lack of like-charge causing repulsion between liposomes (Weiner et al., 1992). Furthermore, positively charged liposomes have been found to be irritating to the skin therefore negatively charged liposomes may be ideal (Katahira et al., 1999). This study identified that the majority of formulations for both blank and EGCG loaded liposomes to have a near neutral charge however, as the loading of Tween 20 increased from 0 to 10% w/w, there was a general decrease in the zeta potential from 2.4 mV to -1.9 mV (Table 3.3), this was not however statistically significant.

3.4.2 HPLC calibration and validation of EGCG detection

In order to develop a robust HPLC method for the detection of EGCG, validation of the final HPLC-UV method was performed according to the International Conference of Harmonization (ICH) guidelines in terms of linearity and range, limit of detection (LOD), limit of quantification (LOQ) and precision.

Calibration data using the method outlined in section 3.3.5 was then obtained (Figure 3.4).

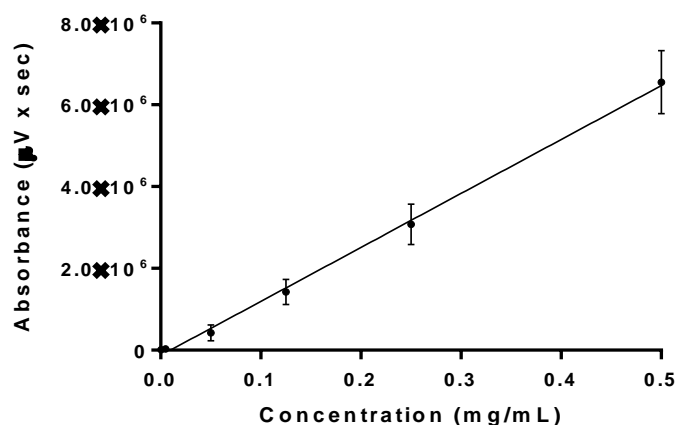


Figure 3.4: HPLC-UV calibration curve for EGCG

Calibration data for EGCG over the concentration range of 0-0.5 mg/mL in water following HPLC-UV analysis. A proportional response was evident versus the analytical concentration over the working concentration range with an r^2 of 0.997 and linear equation of $y = 1 \times 10^7 \cdot x$. Data represents mean \pm SD. $n=9$.

For the linearity and range assessment (Figure 3.4), standard solutions ranging between 0 – 0.5 mg/mL of EGCG in water were prepared. The method developed demonstrated a high correlation with a good linear fit, with the correlation coefficient (r^2) being greater than 0.99. Assessment of repeatability/precision of the developed method was determined by assessing the intraday (same day) and interday (over the course of three days) variability (Figure 3.5). This was done to assess variation caused by temperature fluctuations and any variation in experimental method EGCG standards from 0.5-500 µg/mL carried out intraday and interday

are plotted in Figure 3.5a and b respectively. The results show that the values have no statistically significant difference for all the calibration curves carried out at different times on the same day and also on different days, meaning the method has good precision.

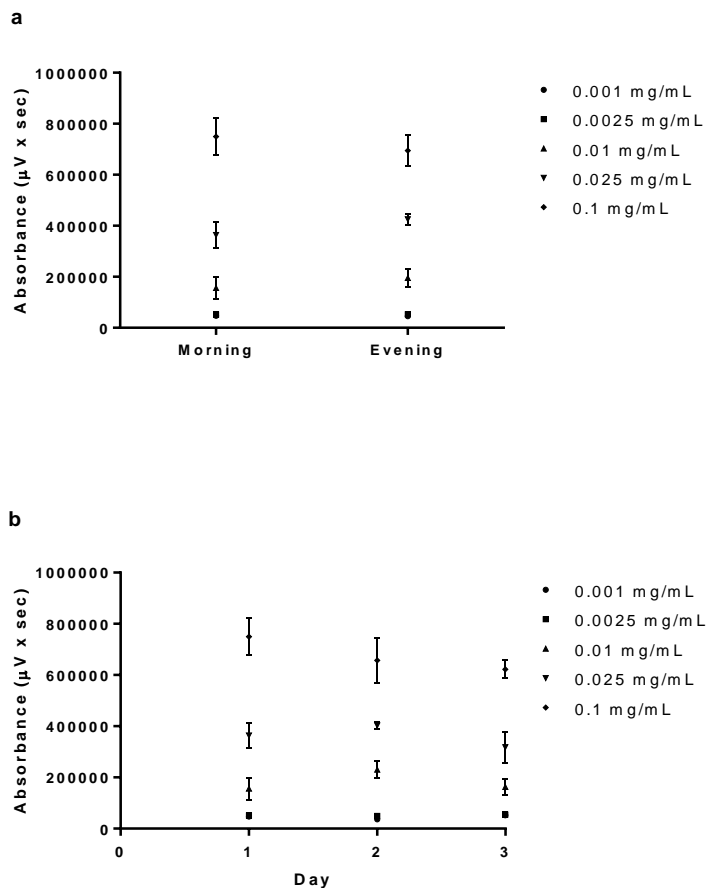


Figure 3.5: Calibration data of EGCG obtained over 3 days

Calibration data of EGCG following HPLC-UV analysis obtained over 3 days expressed as the mean of 3 repeats \pm standard deviation. The a) intraday, b) interday data is displayed. The standards of EGCG ranged from 0.5-500 $\mu\text{g/mL}$. Data represents mean \pm SD. $n=3$.

A study of the sensitivity of the method was assessed by means of the calculation of the LOD and the LOQ (Figure 3.4). Values were determined from the standard deviation of the response (σ) and the slope (S) obtained from the calibration curves carried out during the linearity assessment. According to the ICH guidelines, a signal-to-noise ratio of three was assumed for the quantification of the LOD, whereas for the LOQ, a signal-to-noise ratio of ten was set. Therefore, following Equations 3.2 and 3.3, the sensitivity of the method for EGCG was calculated; the LOD and LOQ for EGCG was 0.04 $\mu\text{g/mL}$ and 0.12 $\mu\text{g/mL}$ respectively.

3.4.3 Determination of entrapment efficiency

Drug loading is an important parameter to observe and optimise to ensure minimal drug wastage. The percentage of EGCG entrapped in the liposome in relation to how much compound was included in the lipid mix was observed. Tween 20 and EGCG are both amphiphilic therefore may compete for space within the bilayer (El Maghraby et al., 2000; Istenic et al., 2016). The change in EGCG entrapment following addition of surfactant was therefore studied.

As Tween 20 loading increased, entrapment significantly decreased from 80.0 ± 3.0 % EGCG entrapped with no surfactant to 4.3 ± 3.0 % with a 10 % w/w loading of surfactant (Figure 3.6). A significant difference was noted between liposomes loaded with no Tween 20 and up to 10 % w/w Tween 20, between 2 and 6 % w/w Tween 20, and 2 and 10 % w/w Tween 20 ($P \leq 0.0001$). A significant difference in EGCG loading was also noted between 6 and 10% w/w loading of Tween 20 ($P \leq 0.05$).

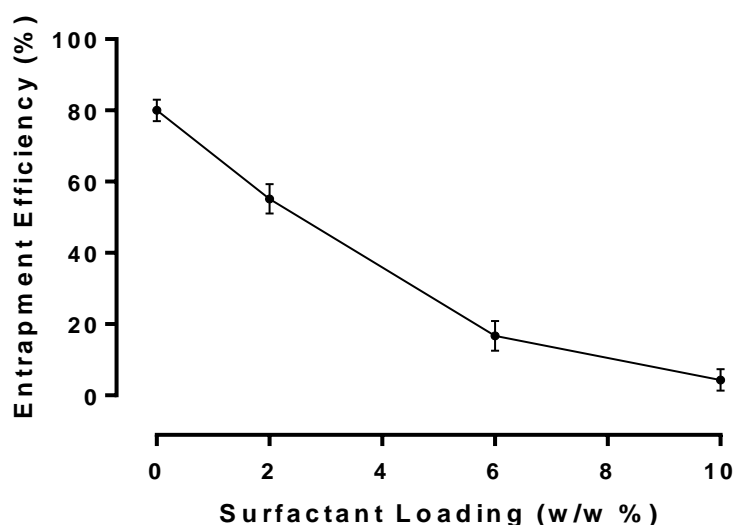


Figure 3.6: Entrapment efficiency of EGCG in liposomes formulated with up to 10% w/w Tween 20

Entrapment efficiency (%) of EGCG in liposomes formulated with varying amounts of Tween 20 (0-10% w/w) Data represents mean \pm SD. n=3 independent batches.

Blank liposomes could entrap $80\% \pm 3$ of EGCG attempted to be loaded into the bilayer. The presence of surfactant in the bilayer of the liposome allowed less drug to be incorporated in the bilayer implying the surfactant has a higher affinity to the lipids than EGCG (Casas and Baszkin, 1992; El Maghraby et al., 2000; Levy et al., 1991). Tween 20 is much larger than

EGCG (1227.54 g/mol and 386.65 g/mol respectively), thus it may be assumed it is better poised to displace EGCG from the bilayer (Figure 3.7). The hydrophobic tail of Tween 20 would have a high affinity to the chains in PC therefore it would be more poised to displace EGCG from the bilayer. Furthermore, Tween 20 is able to increase compound solubility, therefore, as not all would be entrapped within the bilayer, this may allow EGCG to solubilise within the liposomal rehydration media (Almog et al., 1986b). Therefore, as the loading of Tween 20 increased, this would increase the amount of free Tween 20 resulting in more EGCG being able to solubilise in the liposome rehydration media. An alternative explanation for the effect of surfactant decreasing entrapment efficiency could be due to the possible coexistence of vesicles and mixed micelles at high surfactant concentrations (Almog et al., 1986a), with the consequence of lower compound entrapment in mixed micelles. Furthermore, it has been observed that although drug lipophilicity doesn't affect compound loading, molecular weight does with larger molecules resulting in a lower liposomal drug loading (Ali et al., 2010).

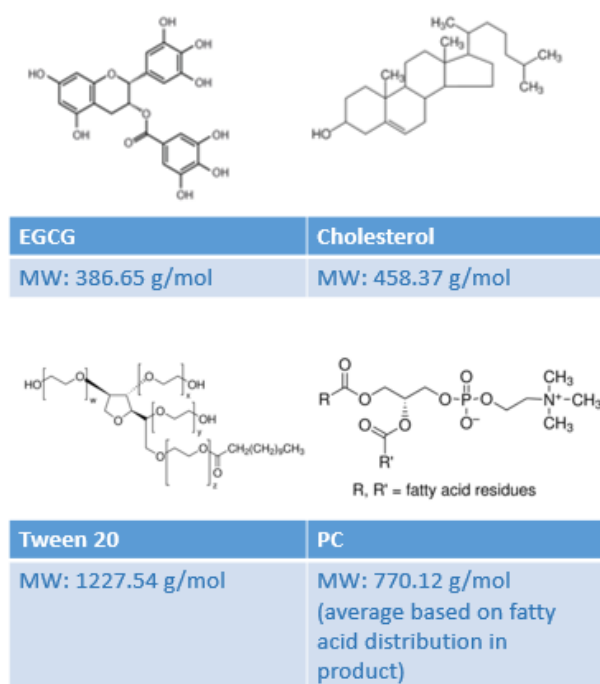


Figure 3.7: Structure and MW of EGCG, cholesterol, Tween 20 and PC

3.4.4 Assessment of liposomal deformability

The addition of surfactant to the lipid bilayer of liposomes has been found to give the liposome elastic properties (Almog et al., 1986a; Cevc, 1996; Trotta et al., 2002). This is useful in dermal drug delivery to allow the transport of molecules across the SC into the dermal layer. Liposomes loaded with up to 10% w/w of Tween 20 were formulated and the degree of deformability of each formulation was determined by extruding them through a polycarbonate filter with a pore size of 200, 100 and 50 nm (Figure 3.8).

The DI is defined as the degree the liposomes deformed. The greater the degree of deformation the less elastic the liposomes are as they were unable to regain their previous larger size.

Liposomes extruded through a membrane with a pore size of 200nm observed that as surfactant loading increased, the deformation following extrusion decreased from 73.6 ± 8.1 to 34.1 ± 7.4 % for EGCG loaded liposomes (Figure 3.8). Significant differences were found when 2, 6 and 10% w/w Tween 20 was added to the formulations ($P \leq 0.0001$). Significant differences were also found between 2 and 6% and 2 and 10% ($P \leq 0.05$). No significant differences were found between 6 and 10% w/w surfactant loadings.

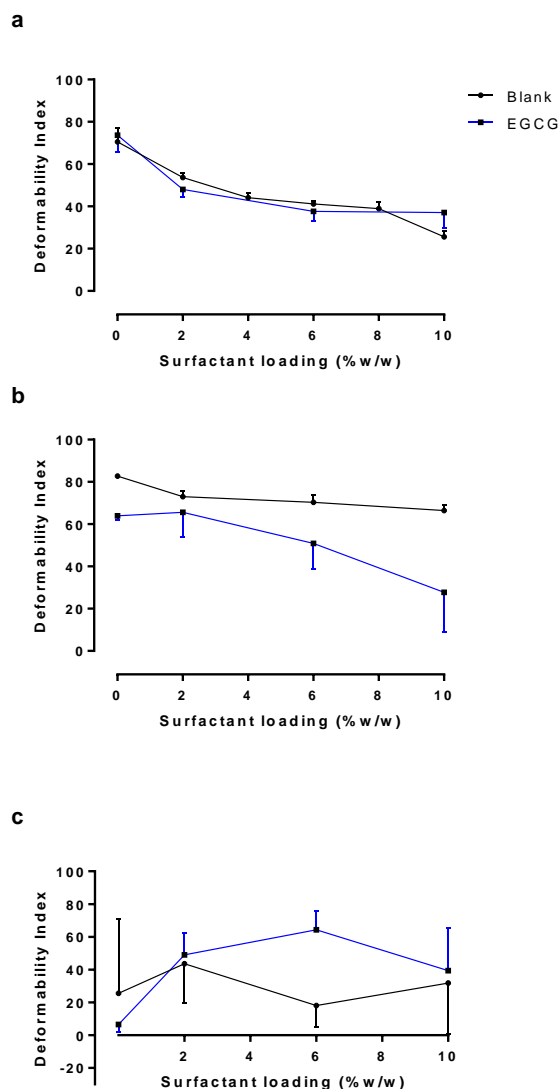


Figure 3.8: Deformability index for blank and EGCG loaded liposomes

Deformability index following extrusion through a) 200 nm, b) 100 nm, c) 50 nm membranes for blank and EGCG loaded liposomes with increasing surfactant loading up to a maximum of 10% w/w. Liposomes were prepared adapting the dry film method adding the surfactant and adding EGCG during the lipid mixing stage. The preparation was vortexed and then extruded through the membranes. Data represents mean \pm SD. n=3 independent batches.

Additionally, studies extruding liposomes through a membrane with a pore size of 100 nm observed that as the surfactant loading in the liposomes being extruded through increased, the deformation following this decreased from 64.0 ± 1.9 to 27.7 ± 18.6 % for drug loaded liposomes although no DI's were significantly different from the other. No trend however was observed for formulations forced through a 50 nm pore size. This is in comparison with studies with blank liposomes found that only liposomes forced through membranes with a pore size of 200 nm and 50 nm had a significant decrease in the DI as surfactant loading increased (section 2.4.3). Though there was a decrease in DI with increasing surfactant loading for liposomes forced through 100 nm, this was not statistically significant ($P \geq 0.05$).

These observations imply the liposomes were displaying elastic properties as they could deform to fit through a gap smaller than its diameter whilst somewhat retaining its size. A study by Goindi et al., (2013) also found the presence of surfactant to decrease the DI (52% for blank liposomes compared with 17% for liposomes formulated with surfactant). Drug loaded liposomes have a greater DI overall, however, their overall size prior to extrusion was greater than that of blank liposomes therefore they would have to deform to a greater degree to be able to pass through the filter.

Liposomes formulated with surfactant can deform as the surfactant has a propensity for highly curved structures (e.g. micelles and liposomes), thus diminishing the energy required for particle deformation. The surfactant is able to diminish the energy required for particle deformation and accommodate particle shape changes of the liposomes under stress (Trotta et al., 2004). These surfactants may have interacted with the PC with strong affinity but in reversible mode. The fast reconstruction of liposome spheres after extrusion may be due to the strong affinity between the surfactant and PC. The reversible binding mode might have provided the deformability upon physical stress (Oh et al., 2006).

Liposomes were expected to deform to a greater extent with decreasing pore size. However EGCG loaded liposomes without surfactant and blank liposomes with surfactant (to a lesser extent) were unexpectedly found to have a very low DI when forced through a 50 nm pore size. However the standard deviation for these values was extremely large demonstrating that the DI mean value is not the close representation of the actual data values obtained (Figure 3.8). Liposomes formulated with surfactant however were found to be able to retain some elasticity and reform following extrusion. Therefore, even up to 50 nm, surfactant loaded liposomes retained enough elastic energy to maintain the same size as when forced through the 200 nm membrane.

As discussed in section 2.4.3, to be able to deform, the liposomes require energy (Fresta and Puglisi, 1996; Gompper and Kroll, 1995; Trotta et al., 2002). Energy was supplied to this system in terms of pressure. The more surfactant included in the bilayer, the more energy the liposome as a whole is able to retain (Trotta et al., 2002). The energy is used to bend the lipid bilayer structure, and since all systems tend toward the lowest state of free energy, the energy stored in this structure will be expelled once the liposome has passed through the pore and there is no longer any pressure forcing the bilayer to remain in an 'unnatural state'. This energy can then be expended into reforming the liposome. Some energy will be lost during passage as heat or non-plastic deformation. Therefore, even at 10% w/w Tween 20, complete initial liposomes size was not recovered and a 0% DI was not achieved. The energy used to bend the bilayer of a liposome containing no surfactant does not benefit from the extra 'storage

space' of a surfactant, thus energy may be expended to rupture the membrane causing liposome size to decrease (Trotta et al., 2002).

In order to passage through a 50 nm pore compared to a 200 nm pore, more energy is required to deform the liposome, therefore, since the energy input was kept constant, the DI is expected to increase as pore size decreases. This was not observed within the parameters of this study. In fact, for both formulations without surfactant, the DI was lower, however, the standard deviation for these values is extremely large showing that the mean value is not the best representation of the actual data values obtained. The liposome size following extrusion for these formulations was extremely varied with some liposomes even having a larger size following extrusion compared with the original size. EGCG loaded liposomes formulated without surfactant had an original size of 1292.2 ± 33.5 nm compared with 1312.3 ± 325.2 nm following extrusion, liposomes loaded with 2% w/w surfactant had an original size of 539 ± 24.2 nm compared with 572 ± 174.6 nm following extrusion (Figure 3.7). This implies these formulations didn't retain enough elastic energy to be easily able to fit through the pores with some liposomes even rupturing and converging following extrusion (Goindi et al., 2013; Trotta et al., 2002). Surfactant loaded liposomes had slightly more reliable DI values, therefore, at 50 nm, the amount of energy stored in the liposome membrane was enough to reform the liposome to a similar extent as for when forced through a 200 nm membrane.

Despite the potential for excess energy in liposomes formulated with 10% w/w Tween 20, liposomes were not able to fully regain their pre-extrusion size. Some energy will always be lost in the friction of the particles moving through the pores as heat (Vajjha et al., 2010). An increase in surfactant loading may bring the liposomes closer to 100% reformation (Trotta et al., 2002). Further, liposomes unable to fit through the pores or lipid aggregates from ruptured liposomes may cause blockages. This may lead to an increase in pressure in the vessel causing more turbulence leading to the rupture and non-uniform reformation of liposomes.

As previously stated, the DI liposomes forced through a 50 nm pore size had a larger SD (Figure 3.8). This suggests there may have been some liposome destruction and the formulation of lipid aggregates as well as smaller liposomes that didn't reform. Liposome formulations in this study therefore were not suitable to pass through a 50 nm pore. This is not to say this is what would happen to liposomes when applied to the skin. Firstly there would not be an applied pressure, liposomes would be expected to move across the skin following the osmotic transepidermal gradient as has been found in many similar studies concerning the dermal and even transdermal delivery of drug (Cevc, 1996; Goindi et al., 2013; Gompper and Kroll, 1995; Trotta et al., 2002). Additionally such lipid carriers are miscible with the epidermal lipids present within the barrier of the stratum corneum thus would be able to penetrate into deeper layers of the skin (El Maghraby et al., 2008; Kirjavainen et al., 1996; Schäfer-Korting et al., 2007). Furthermore, the skin is warmer than room temp (35 °C compared to 20 °C).

Temperature governs the energy term of enthalpy therefore the liposomes would have more energy to be even more flexible and cross the stratum corneum. Many studies using either *in vivo* methods or *in vitro* methods with excised skin have found surfactant loaded liposomes to have better skin penetration compared with conventional liposomes as well as other formulations. (Dubey et al., 2006; El Maghraby et al., 1999; Oh et al., 2006)

3.4.5 Differential scanning calorimetry investigations of EGCG and EGCG lipid blends

Differential scanning calorimetry (DSC) has been widely used in its application in understanding the thermal characteristics of materials where an insight into a range of thermal properties including melting temperatures, phase transitions and heat capacity changes can be obtained. Figure 3.9 illustrates the DSC thermogram for EGCG.

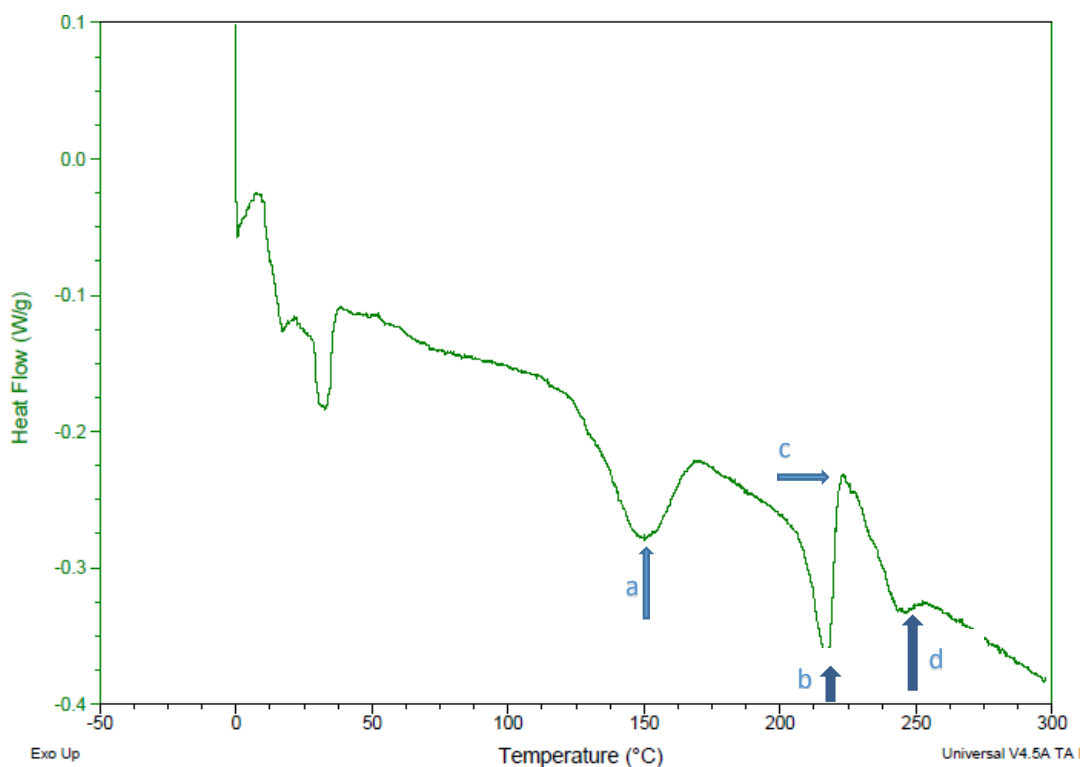


Figure 3.9: DSC scan of EGCG.

All experimental runs commenced at an initial temperature of 0 °C with a scan rate of 10 °C/min to 300 °C. Peak a and b are related to the epimer of EGCG, GCG. Peak c represents the glass transition temperature (T_c) of EGCG was at 220 °C and the melting point (T_m) of EGCG was at 245 °C.

The glass transition temperature (T_c) of EGCG was identified at 220 °C (peak c) and the melting point (T_m) of EGCG was at 245 °C (peak d) (Figure 3.9) and concurred with those reported by Cho et al (2008) where the T_m of GCG (an epimer of EGCG) was at 223 °C, the T_c of EGCG was at 235 °C and the T_m of EGCG was at 246 °C. Cho et al also observed a peak

at 97 °C and determined it to be the conversion temperature of EGCG into GCG. Therefore, the first two troughs (peak a and b) observed in the scan may be representative of the epimer GCG (Cho et al., 2008).

The DSC of the lipid (PC and cholesterol) and Tween 20 blend is illustrated in Figure 3.10a. The T_m of this mixture is 172 °C. Upon addition of EGCG to this mixture (Figure 3.10b), the melting point shifted to 191 °C (Figure 3.10b). This shows the surfactant loaded liposomes could decrease the T_m of EGCG.

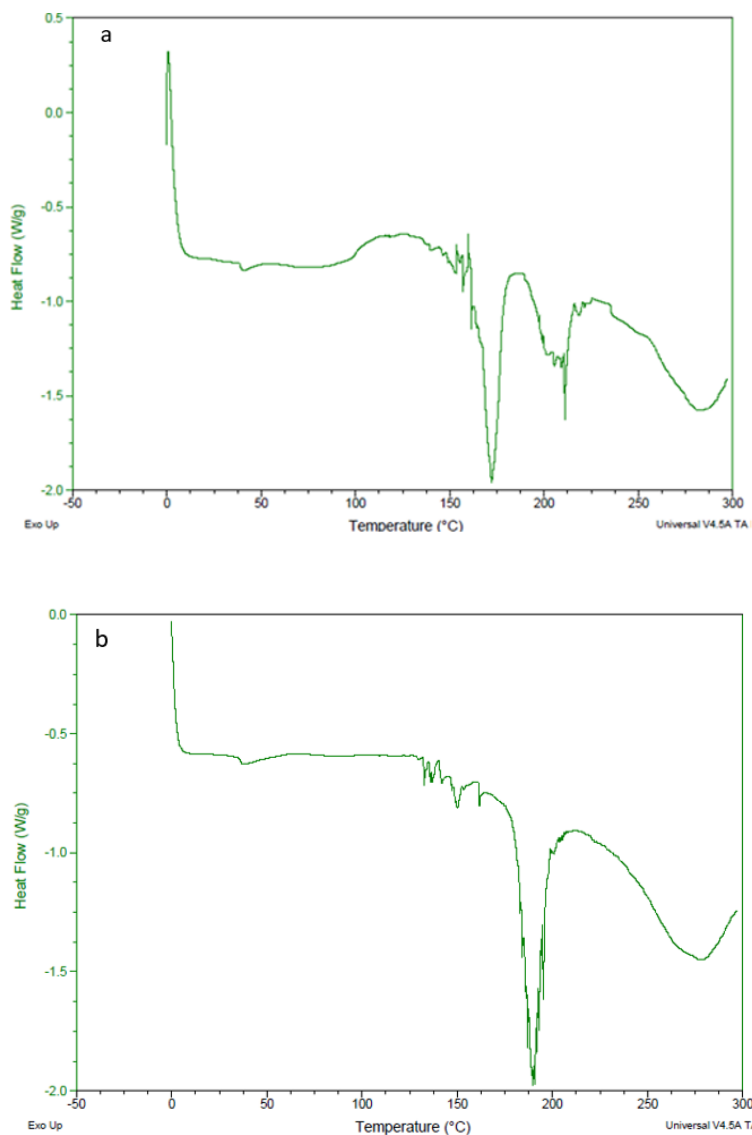


Figure 3.10: DSC analysis scans of PC, cholesterol and Tween 20 and EGCG blends.

DSC analysis scans of a) PC, cholesterol and Tween 20 blend and b) PC, cholesterol, Tween 20 and EGCG blend. The T_m of the lipid mixture is 172 °C, and upon addition of EGCG, the T_m was 191 °C. All experimental runs started at an initial temperature of 0 °C, purged under nitrogen gas, with a scan rate of 10 °C/min to 300 °C.

3.4.6 Development of a suitable dermal dissolution media

PBS is a buffer solution commonly used as a release media. The osmolarity and ion concentrations of this solution match those of the human body (isotonic) (Sigma-Aldrich(d), 2017). The HPLC methodology for each compound was established with water as the solvent, given the high water solubility of EGCG. However, method development for compounds in PBS proved problematic as, peaks either disappeared or split peaks were obtained. PBS therefore may have caused drug breakdown or ionised the drug such that it eluted out of the HPLC column straight away.

The pH of PBS is 7.4. The pH of the dermal layer however ranges from 4-7.4 (Cordero et al., 1997) and unlike, for example, gastric fluid, there are no standardised universally accepted formulas to simulate dermal fluid. The volume of dermal fluid is minimal and consists mainly of extracellular fluid (Groenendaal et al., 2010; Herting et al., 2014; van der Merwe et al., 2006; Wiig and Swartz, 2012). Studies therefore use a solution buffered to somewhere within the pH range of the dermal layer (Cordero et al., 1997; Giri et al., 2011; Hadgraft and Valenta, 2000; Herting et al., 2014; Trovatti et al., 2011).

Release into a release media buffered to pH 5.2 using sodium acetate was attempted. Again, split peaks or disappearing peaks were observed. To aid in the analysis of the EGCG release from formulations, studies were conducted in purified water buffered to a pH of 7.2. This overcame issues with HPLC coupled with UV detection. Whilst this does not mimic dermal fluid, there are no standardised formulas for such a medium. Furthermore, countless studies observing simple dermal release use a solution buffered to a pH with the aforementioned range (Bhatia et al., 2004; Bragagni et al., 2012; Cevc and Blume, 2001; Fresta and Puglisi, 1996; Trovatti et al., 2011; Tsai et al., 2015).

3.4.7 *In vitro* EGCG release studies

3.4.7.1 EGCG release studies from gel formulations

Liposomes intended to be delivered dermally are required to be delivered in a carrier due to the liquid nature of the preparation. Suitable viscosity and application properties of liposomes can be achieved by incorporating in an appropriate vehicle. It has been confirmed that liposomes are compatible with viscosity increasing agents such as cellulose based gels (Foldvari, 1996). These are known to be safe in topical, dermal and transdermal delivery (Forbes et al., 2011b; Hascicek et al., 2009; Patton et al., 2007). Therefore HEC and HPMC were selected as polymer agents to compare as carriers of liposomal preparations for dermal drug delivery.

A necessary step in the evaluation of drug delivery systems is the rate of drug release from the carrier. Dissolution/release tests are used to help predict the *in vivo* behaviour of medicinal formulations. The release of drug from a formulation is determined by many factors including diffusion, erosion of matrices followed by dissolution of drug.

Two geometric systems have been considered for EGCG release from gel systems; three-dimensional leaching from a cylinder of gel (one compartment release) and unidirectional leaching across a planar surface (two compartment release). A one compartment model can be used to study release and gel swelling behaviour whilst a two-compartment diffusion cell observes drug release across a membrane. A polycarbonate membrane with 50 nm was used to mimic the SC and the gaps in between the keratinocyte cells. The composition of both HPMC and HEC gels was varied between 1 and 5% w/v to study how gel viscosity influenced EGCG release from the gel.

3.4.7.1.1 One compartment release studies

Release from the aqueous gels HEC and HPMC gels loaded with 1% w/w EGCG using DDM as a release medium was studied over a 24-hour period (Figure 3.11 and 3.12). Both the HEC and HPMC gels displayed a similar pattern of release into the water. It is however, clear that at equal loading of polymer, HPMC was able to retard drug release. Furthermore, as the loading of polymer increased, drug release was slower. HEC gels formulated with 1% w/w of the polymer gave complete drug release by 1.5 hours, 3% w/w observed complete release by 2 hours and 5% w/w observed complete release by 3 hours.

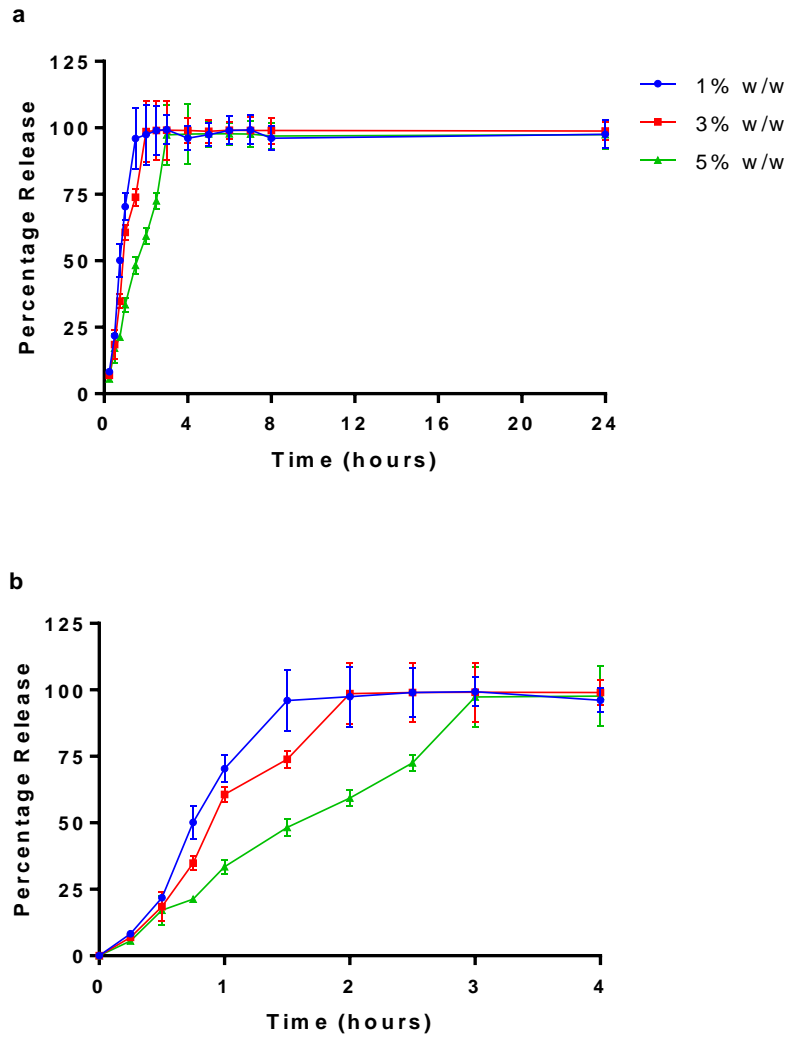


Figure 3.11: *In vitro* percentage EGCG release profiles from HEC gel.

In vitro percentage EGCG release profiles from aqueous HEC gels (1, 3 and 5% w/v) over a) 24 hours, b) 4 hours. Data represents mean \pm SD. n=3 independent batches.

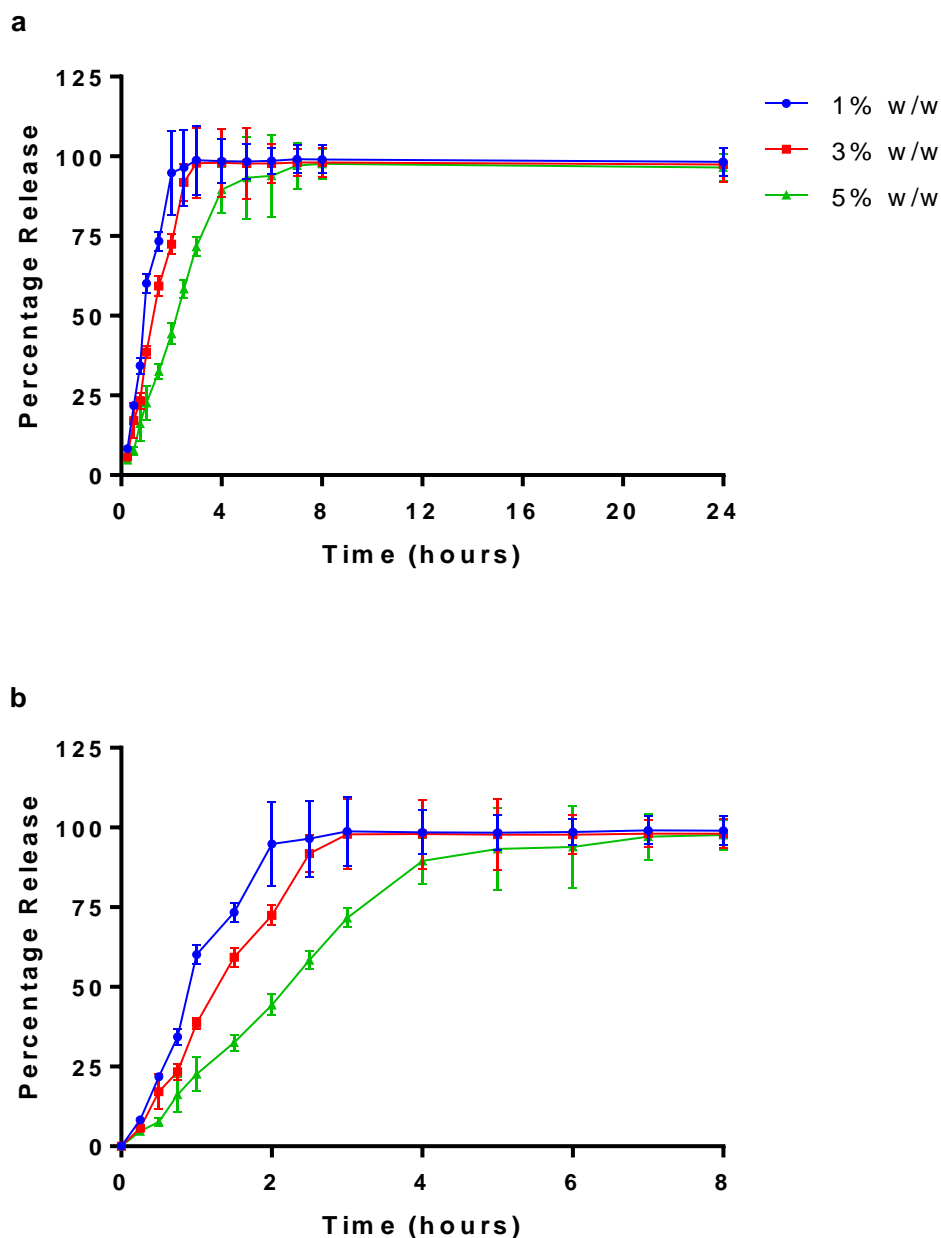


Figure 3.12: *In vitro* percentage EGCG release profiles from HPMC gels

In vitro percentage EGCG release profiles from aqueous HPMC gels (1, 3 and 5% w/v) over a) 24 hours, b) 8 hours. Data represents mean \pm SD. n=3 independent batches.

Significant differences were found between 1 and 5 % w/w and 3 and 5% w/w polymer loadings ($P < 0.05$). No significant differences were found between 1 and 3% w/w polymer loadings. HPMC gels formulated with 1% w/w of the polymer gave complete drug release by 2 hours, 3% w/w observed complete release by 3 hours and 5% w/w observed complete release by 4 hours. Significant differences were found between 1 and 3 % w/w ($P \leq 0.05$), 1 and 5% w/v, and 3 and 5% w/w polymer loadings ($P < 0.01$). At the point of complete release, the gel was observed to have completely dissipated into the release media.

Diffusion of solutes out of the polymer is known to depend on temperature, pressure, viscosity and solute size. Diffusion of solutes out of polymers is dependent upon the concentration and degree of swelling of polymers. Solvent diffusion is associated with the physical properties of the polymer network and the interactions between the polymer and solvent (Masaro and Zhu 1999). Furthermore, a study using the molecular weight of the drugs as an approximation of molecular size could not find a relation to release rates. This indicates that molecular geometry plays a role in compound release from polymer networks (Ford, Rubinstein et al. 1987, Rao, Devi et al. 1990).

The predominant molecular mechanism of drug release is a result of drug diffusion due to the concentration gradient and macromolecular relaxation of the polymer chains. This causes drug diffusion outward with a kinetic behaviour dependent on the relative ratio of diffusion and relaxation and due to the fact cellulose derivatives have limited solubility for lipophilic compounds thus the compound would diffuse out of the gel (Forbes et al., 2011b; Lee, 1985). As water penetrates the glassy hydrogel matrix containing the dispersed drug, the polymer will swell and its glass transition temperature is lowered. Concurrently, the dissolved drug diffuses through this swollen rubbery region out into the release medium (Bouwstra and Junginger, 1993; Gupta et al., 2002; Lee, 1985; Rao et al., 1990). The rate-controlling factor mediating drug release is the resistance of polymer to a change in shape due to an increase in volume (Ranga Rao and Padmalatha Devi, 1988).

It has been suggested that the addition of water-insoluble drug can increase the water uptake by the dosage form. Water influx weakens the network integrity of the polymer, as the polymer swells, the matrix experiences intra-matrix swelling force promoting disintegration and leaching of the drug leaving behind a highly porous matrix (Sai Cheong Wan et al., 1995). The drug particles in between the polymer chains therefore allow each chain to hydrate freely, which may result in weak hydrogen bonding areas around the drug molecule (Panomsuk et al., 1996). Further, the influence of drug on the swelling properties of the polymer matrix is largely dependent on the substituted groups of the polymer. The hydroxyl group in the molecules plays an important part in the matrix integrity of the swollen hydrophilic cellulose matrices. The amount and properties of the incorporated drug determine matrix integrity (Nafee et al., 2003). In this case, it appears the HEC matrix eroded/swelled quicker than HPMC giving a faster rate of release. This is in contrast with a study by Nafee *et al* (2003) comparing the release of miconazole from a 1.5% w/v HEC formulation with a 3% HPMC w/v formulation, where faster erosion was observed from the HPMC matrix. This highlights how the physiochemical properties of the drug, the polymer and the interaction between the two affect drug release from the formulation.

3.4.7.1.1.1 Kinetic assessment of drug release

A necessary step in the evaluation of drug delivery systems is the rate of drug release from the carrier. Dissolution/release tests are used to help predict *in vivo* behaviour and to study the structure of the dissolving matrix. The release of drug from a formulation is determined by many factors including diffusion, and erosion of matrices as detailed in Figure 3.13.

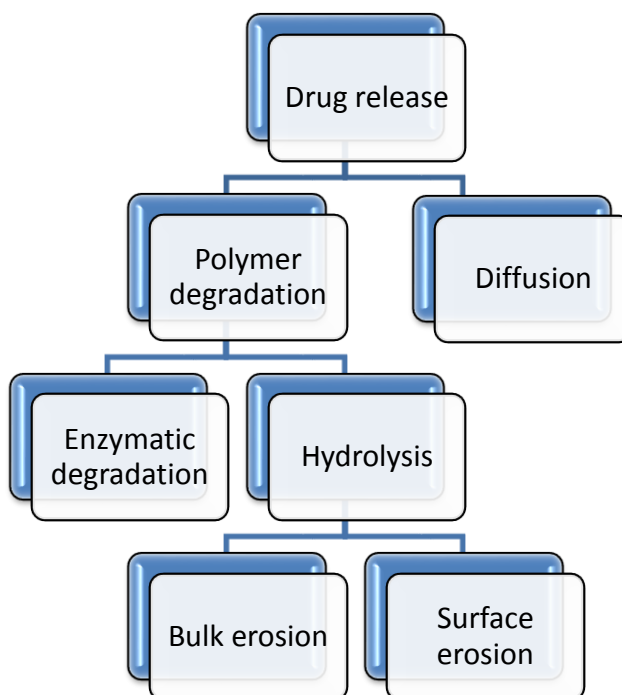


Figure 3.13: Methods of drug release from a pharmaceutical formulation

Release from modern formulations can be very complex with multiple factors driving drug release and dissolution. The relationship between formulation variables and release profiles are not entirely understood. Mathematical models may be influential in understanding drug release.

The mechanism of drug release from the carrier system is dependent upon the carrier system itself and drug interaction with it. A zero order release is observed when drug is released at a constant rate independent of the initial concentration. A first order release is observed when drug is released at a constant rate in proportion to the amount of drug available at that time. Additionally, Higuchi (Higuchi, 1961; Higuchi, 1963b) developed several theoretical models to study the release of water soluble and low soluble drugs incorporated into semi-solid and/or solid matrixes.

The release profiles were evaluated by zero-order, first-order and Higuchi kinetics (Table 3-4). Release from the gels were observed to fit the first order release model. Thus, drug was

released at a constant rate in proportion to the amount of drug available at that time. A study by Hascicek *et al.*, (2009) formulated HEC gels at 7.5% w/w with 1% w/w of drug. A kinetic analysis, observed release fitting the Higuchi model best. A study by Ford *et al* (1987) found drug release from HPMC tablets to fit the Higuchi release model. These differences may be explained by considering differences in formulation, and differences in experimental parameters for example their use of either Franz cells with only a thin film of gel spread over the membrane or dissolution chambers with large volumes of release media (Ford et al., 1987; Hascicek et al., 2009). Furthermore, release from gels formulated with a HPC cellulose polymer was found to follow first order kinetics indicating drug release depends on formulation parameters (Ranga Rao, Devi et al. 1988). A simple gel formulation was used in this study and the kinetic model of release data was not investigated further.

Table 3-4: Kinetic assessment of release data of EGCG from HEC and HPMC aqueous gels.

Kinetic model	Formulation					
	HEC (r ²)			HPMC (r ²)		
	1% w/v	3% w/v	5% w/v	1% w/v	3% w/v	5% w/v
Zero order	-3.210 ± 0.467	-2.350 ± 0.456	-1.114 ± 0.321	-2.468 ± 0.478	-1.781 ± 0.432	-0.447 ± 0.176
First order	0.868 ± 0.0256	0.971 ± 0.015	0.928 ± 0.038	0.975 ± 0.014	0.930 ± 0.036	0.938 ± 0.036
Higuchi	-0.344 ± 0.184	0.006 ± 0.150	0.462 ± 0.077	-0.004 ± 0.157	0.256 ± 0.136	0.647 ± 0.039

Results are presented as the mean ± standard deviation (n=3)

Comparison of the rate constant of each formulation shows that as the loading of both HEC or HPMC polymers was increased the rate constant decreased (Table 3-5). This implies that as polymer and thus gel consistency is increased, the rate of release is retarded. A study by Gaikwad *et al* (2012) also found that the release of drug from an aqueous gel decreased as viscosity increased. As polymer loading increase, the gel viscosity increases. Drug is released from gel by the creation of pores dues to swelling, as viscosity increases polymer chains becoming more resistant to movement as they are physically restricted thus taking longer to dissipate into the media thus slowing release drug (Bouwstra and Junginger, 1993; Forbes et

al., 2011a; Gaikwad et al., 2012). Thus as polymer loading increases, the rate constant for drug release will decrease.

Table 3-5: First order kinetics rate constant for EGCG release from formulations.

First order kinetic rate constant (min ⁻¹)					
HEC			HPMC		
1% w/v	3% w/v	5% w/v	1% w/v	3% w/v	5% w/v
0.018 ±	0.014 ±	0.009 ±	0.014 ±	0.011 ±	0.006 ±
0.002	0.002	0.001	0.002	0.001	0.001

Results are presented as the mean ± standard deviation (n=3)

Furthermore, the Korsmeyers-Peppas's model was applied to the release data and the diffusional exponent (*n*) calculated (Table 3-6). The Korsmeyer-Peppas Model is a simple, semi-empirical model that relates exponentially the drug release to the fractional release of the drug (Korsmeyer et al., 1983; Peppas, 1985). The *n* value is used to characterise release for cylindrical shaped matrices, the value of *n* can be used to describe the release mechanism as described in Table 3-2. This can be used to suggest release mechanisms from polymers.

Fickian release (case I) was observed for both polymers between 1 and 5% w/v loadings. A study by Ritger and Peppas found both Fickian and anomalous release from swellable devices (Ritger and Peppas, 1987). Additionally, a study using the polymer HPC observed both non Fickian and super case II transport (Alfrey Jr et al., 1966; Ranga Rao et al., 1988).

Table 3-6: Diffusional exponent *n* calculated from the Korsmeyer-Peppas model of drug release for EGCG release data from aqueous gels with the corresponding release mechanism.

Formulation	<i>n</i>	Transport type
HEC	1% w/v	0.206 ± 0.015
	3% w/v	0.240 ± 0.018
	5% w/v	0.312 ± 0.023
HPMC	1% w/v	0.238 ± 0.017
	3% w/v	0.272 ± 0.023
	5% w/v	0.373 ± 0.021

Results are presented as the mean ± standard deviation (n=3)

Fickian diffusion is often observed in polymer networks when the temperature is above the glass transition temperature of the polymer (T_g). When the polymer is in the rubbery state, the polymer chains have a higher mobility that allows an easier penetration of the solvent (Masaro and Zhu, 1999). This implies that, in the present studies, when Fickian transport was observed, the polymer chains could move sufficiently and that at those loadings of polymer, the gel was in a rubbery state.

Fickian diffusion and Case II solute release behaviour in swelling-controlled release systems are distinctive as each can be described in terms of a single limitation. Fickian transport is described by a diffusion coefficient (flux due to molecular diffusion and the concentration gradient), while Case-II transport is described by a characteristic relaxation constant (associated with stresses and state-transition in hydrophilic glassy polymers which swell in water or biological fluids) (Peppas and Sahlin, 1989). Non-Fickian behaviour however requires two or more parameters to describe the coupling of diffusion and relaxation phenomena (Ritger and Peppas, 1987). As previously described, the predominant molecular mechanism of drug release is a coupling of drug diffusion and macromolecular relaxation of the polymer chains because of which the drug diffuses outward. Such diffusion and swelling generally does not usually follow a Fickian diffusion mechanism however, this may depend on experimental parameters (Lee, 1985; Peppas and Sahlin, 1989; Ritger and Peppas, 1987). The existence of some molecular relaxation process in addition to diffusion is believed to be responsible for the observed non-Fickian behaviour (Lee, 1985).

3.4.7.1.2 Two compartment release

The release of EGCG from HEC and HPMC gel formulations at polymer loadings of 1, 3 and 5% w/v over a 24 hour period, across a 50 nm polycarbonate membrane in a two compartment model using a diffusion cell was also assessed. This was compared against release from solution in the donor compartment into the receiver compartment. Over 24 hours, 100% of EGCG release was observed from all formulations. HPMC and HEC gels at the compositions studied both slowed EGCG release in comparison to release from EGCG solution (Figure 3.14 and 3.15).

Release from HEC observed significant differences between release from 1 and 5 % w/v polymer ($P \leq 0.001$), solution and 3 and 5 % w/v polymer as well as 1 and 3 %, additionally 3 and 5 % w/v polymer ($P \leq 0.01$), and solution and 1 % w/v loading of polymer ($P \leq 0.05$). Release from HPMC observed significant differences between release from 1% and 5 % w/v loading of polymer ($P \leq 0.0001$), solution and 5% w/v polymer as well as 1 and 3 % w/v polymer ($P \leq 0.001$), solution and 1 and 3 % w/v polymer as well as 1 and 3% w/v polymer ($P \leq 0.01$).

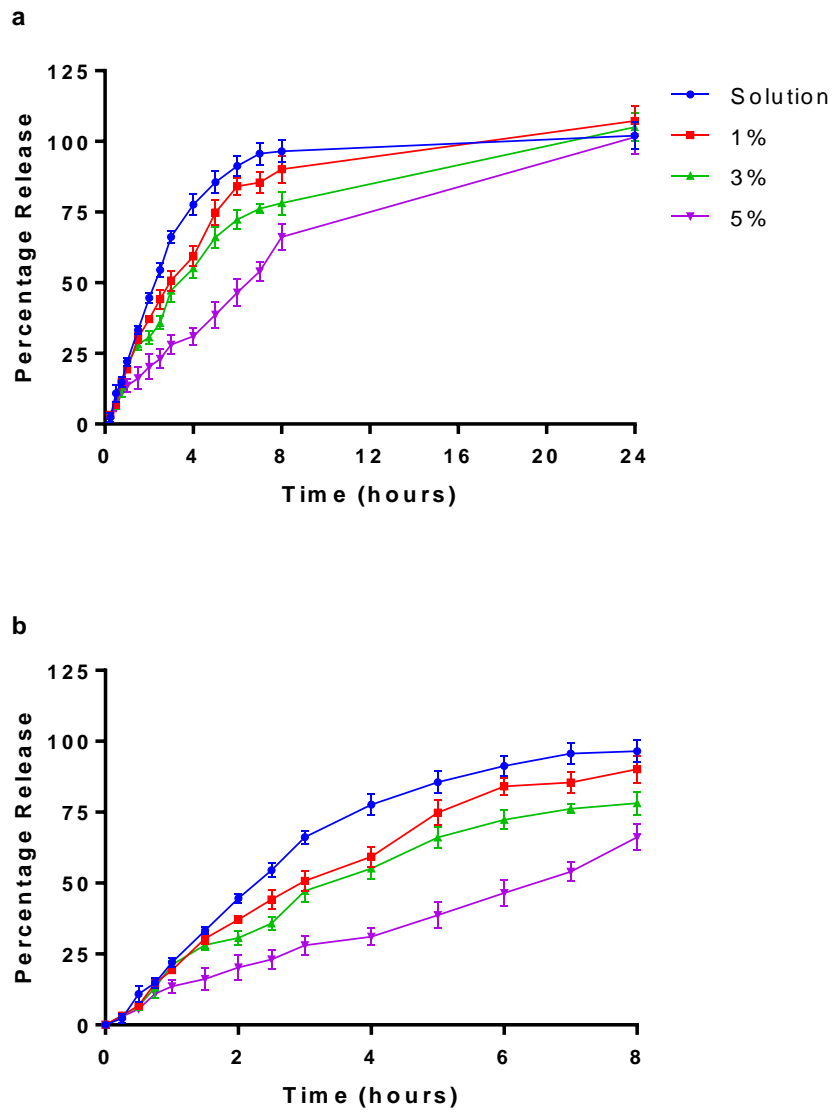


Figure 3.14: *In vitro* percentage EGCG release profiles from HEC gels and EGCG solution. Release profiles from aqueous HEC gels (1, 3 and 5% w/v) with 1% w/v EGCG and EGCG solution over a) 24 hours, B) 8 hours. Data represents mean \pm SD. n=3 independent batches.

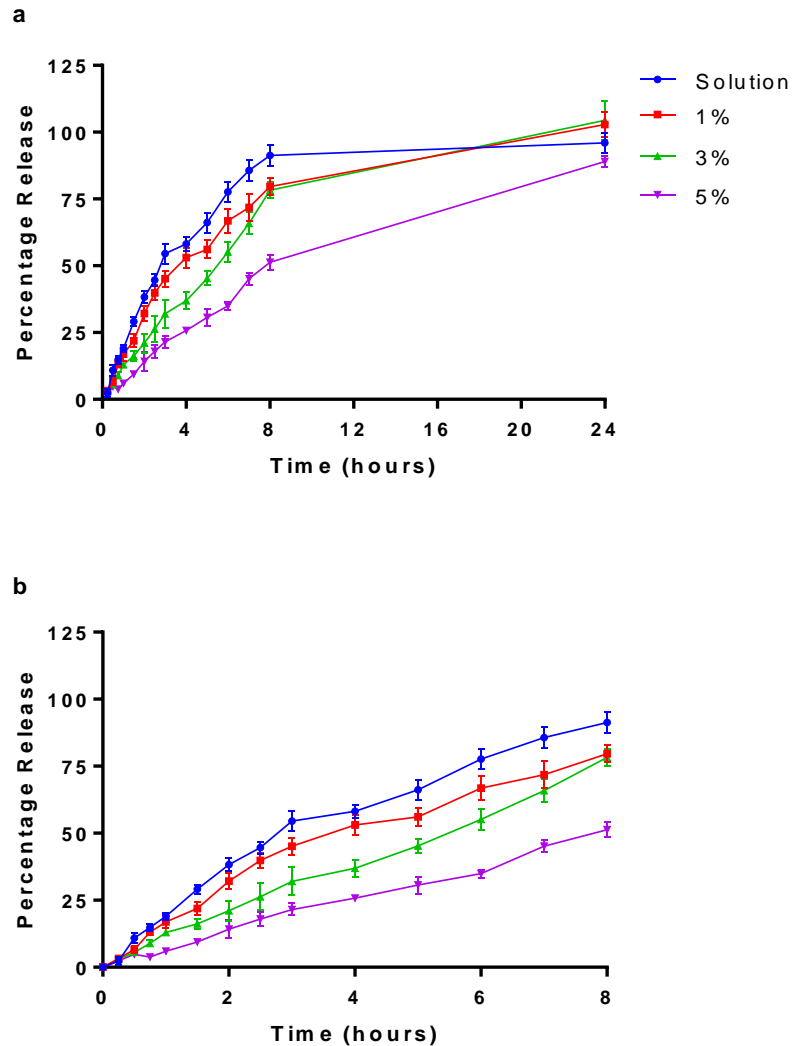


Figure 3.15: *In vitro* percentage EGCG release profiles from HPMC gels and EGCG solution. EGCG release profiles from aqueous HPMC gels (1, 3 and 5% w/v) with 1% w/v EGCG and EGCG solution over a) 24 hours, b) 8 hours. Data represents mean \pm SD. n=3 independent batches.

3.4.7.1.2.1 Kinetic assessment

Release profiles were subsequently evaluated using the Zero-order, First-order and Higuchi kinetic models. Release from the solution was observed to fit the First order release model when compared to the Zero order model and the Higuchi model (r^2 values were 0.19, 0.93 and 0.80 for the zero order, first order and Higuchi model respectively) (Table 3-7).

Furthermore, based upon the r^2 values, release from the gels was observed to fit the First order release model best upon comparison with those for the zero order model and the Higuchi model (Table 3-7). Thus drug was released at a constant rate in proportion to the amount of

drug available at that time. Following a kinetic analysis, a study formulating HEC gels at 7.5% w/w with 1% w/w of drug observed release to fit the Higuchi model (Hascicek et al., 2009).

This may be due to differences in formulation, and differences in experimental parameter including their use of Franz diffusion cells with only a thin film of gel spread over the membrane (Hascicek et al., 2009). Additionally, release from gels formulated with a HPC cellulose polymer was found to follow first order kinetics indicating drug release depends on formulation parameters (Ranga Rao, Devi et al. 1988).

Table 3-7: Kinetic assessment of release data of EGCG from solution and aqueous gels.

Kinetic model	Formulation						
	Solution (r ²)	HEC (r ²)			HPMC (r ²)		
		1% w/v	3% w/v	5% w/v	1% w/v	3% w/v	5% w/v
Zero order	0.188 ±	0.140 ±	0.169 ±	0.692 ±	0.276 ±	0.689 ±	0.850 ±
	0.0474	0.133	0.348	0.168	0.032	0.036	0.046
First order	0.929 ±	0.958 ±	0.948 ±	0.956 ±	0.960 ±	0.956 ±	0.987 ±
	0.020	0.037	0.034	0.053	0.028	0.004	0.005
Higuchi model	0.803 ±	0.859 ±	0.862 ±	0.903 ±	0.907 ±	0.908 ±	0.894 ±
	0.080	0.065	0.012	0.067	0.013	0.031	0.021

Results are presented as the mean ± standard deviation (n=3)

Comparison of the rate constant of each formulation demonstrates that as the loading of HEC or HPMC was increased the rate constant decreased (Table 3-8). This implies that as gel consistency is increased, the rate of release slows. As polymer loading increase, the gel viscosity increases. Drug is released from gel by the creation of pores due to swelling, as viscosity increases polymer chains becoming more resistant to movement as they are physically restricted thus taking longer to dissipate into the media thus slowing release drug. Furthermore, comparison between the gels found that HEC at its respective loading of polymer in the HPMC gels always gave a faster release of drug.

The water-insoluble drug incorporated in a gel matrix can increase the water uptake by the dosage form. Water influx weakens the network integrity of the polymer, as the polymer swells, the matrix experiences intra-matrix swelling force promoting disintegration and leaching of the drug leaving behind a highly porous matrix (Sai Cheong Wan, Wan Sia Heng et al. 1995).

Additionally, the influence of drug on the swelling properties of the polymer matrix is dependent on the substituted groups of the polymer (Nafee, Ismail et al. 2003). In this case, it appears the HEC matrix eroded/swelled quicker than HPMC giving a faster rate of release. This is in contrast with a similar study observing and comparing the release of miconazole from a 1.5% w/v HEC formulation with a 3% HPMC w/v formulation where faster erosion was observed from the HPMC matrix (even at double the polymer loading) (Nafee et al., 2003). This highlights how the physiochemical properties of the drug, the polymer and the interaction between the two affect drug release from the formulation.

Table 3-8: First order kinetics rate constant for EGCG release from formulations

Solution	Rate constant ($\times 10^{-3} \text{ min}^{-1}$)					
	HEC			HPMC		
	1% w/v	3% w/v	5% w/v	1% w/v	3% w/v	5% w/v
3.10 \pm	3.98 \pm	3.52 \pm	1.91 \pm	3.17 \pm	2.28 \pm	1.34 \pm
1.26	5.79	0.88	0.37	1.09	0.14	0.08

Results are presented as the mean \pm standard deviation (n=3)

Furthermore, the Korsmeyers-Peppas's model was applied to the release data and the diffusional exponent (n) calculated (Table 3-9). This can be used to suggest release mechanisms from polymers. Fickian release was observed for HEC gels at 1% w/w and 3% w/w of polymer, and HPMC gels at 1% w/w polymer. Non-fickian release was observed for the HEC gels at 5% w/w and HPMC gels at 3% and 5% w/w of polymer. It is not uncommon to observe multiple release mechanisms for gels formulated with various loading of polymers. A study by Ritger and Peppas found both Fickian and anomalous release from swellable devices (Ritger and Peppas, 1987). Additionally, a study using the polymer HPC observed both non Fickian and super case 2 transport (Alfrey Jr et al., 1966; Ranga Rao et al., 1988).

Fickian diffusion is often observed in polymer networks when the temperature is above the glass transition temperature of the polymer (T_g). When the polymer is in the rubbery state, the polymer chains have a higher mobility that allows an easier penetration of the solvent. Non-Fickian diffusion processes are mainly observed when the temperature of study is below T_g . At a specific temperature below T_g , the polymer chains are not sufficiently mobile to permit immediate penetration of the solvent in the polymer core (Masaro and Zhu, 1999). This implies that, in the present studies, when non-Fickian transport was observed, the polymer chains

were unable to move sufficiently and that at those loadings of polymer, the gel was in a glassy state.

Table 3-9: Diffusional exponent n for EGCG release data with the corresponding release mechanism.

Formulation	n	Transport type
HEC	1% w/v	0.46 ± 0.03
	3% w/v	0.48 ± 0.08
	5% w/v	0.63 ± 0.11
HPMC	1% w/v	0.48 ± 0.01
	3% w/v	0.61 ± 0.01
	5% w/v	0.70 ± 0.04

Results are presented as the mean ± standard deviation (n=3)

Diffusion of solution out of the polymer is known to depend on external parameters such as temperature and pressure as well as formulation parameters including solute size and gel viscosity. Diffusion in polymers is complex it depends strongly on the concentration and degree of swelling of polymers. Solvent diffusion is associated with the physical properties of the polymer network and the interactions between the polymer and solvent (Masaro and Zhu, 1999). The membrane would have prevented the gel from completely swelling and releasing drug, whilst water could move across it, the polymer did not have much room to swell as the donor compartment was filled to near capacity. This can be likened to the skin in the sense that the skin is a barrier, as well as the polymer chains would slow the movement of drug into the skin.

Gels formulated with 3% w/v of either HPMC or HEC were chosen for all further studies. This loading of polymer is within range of many other previous studies (Forbes et al., 2011b; Goci et al., 2014; Mahalingam et al., 2011).

3.4.7.2 Comparison of EGCG release from HEC and HPMC gels at formulated at 3% w/v of polymer

Release from EGCG loaded gels prepared from 3% w/v of either HPMC and HEC was compared. Polymer gels were observed to slow the release (Figure 3.14). HPMC demonstrated to be more pronounced than HEC in this phenomenon, for example at 6 hours, EGCG solution (in the absence of polymer gels) resulted in a 72.3 ± 4.9 % transfer of EGCG across the membrane, compared to 66.1 ± 3.4 % and 55.1 ± 1.9 % release of EGCG-

formulated from HEC and HPMC gels respectively (Figure 3.16). The solution gave 100% release by 8 hours whilst HEC and HPMC saw complete release by 24 hours. The difference in EGCG release between solution and HEC and HPMC was significant ($P \leq 0.01$ and $P \leq 0.001$ respectively). There was no significant difference between the release of EGCG from HEC and HPMC ($P \geq 0.05$).

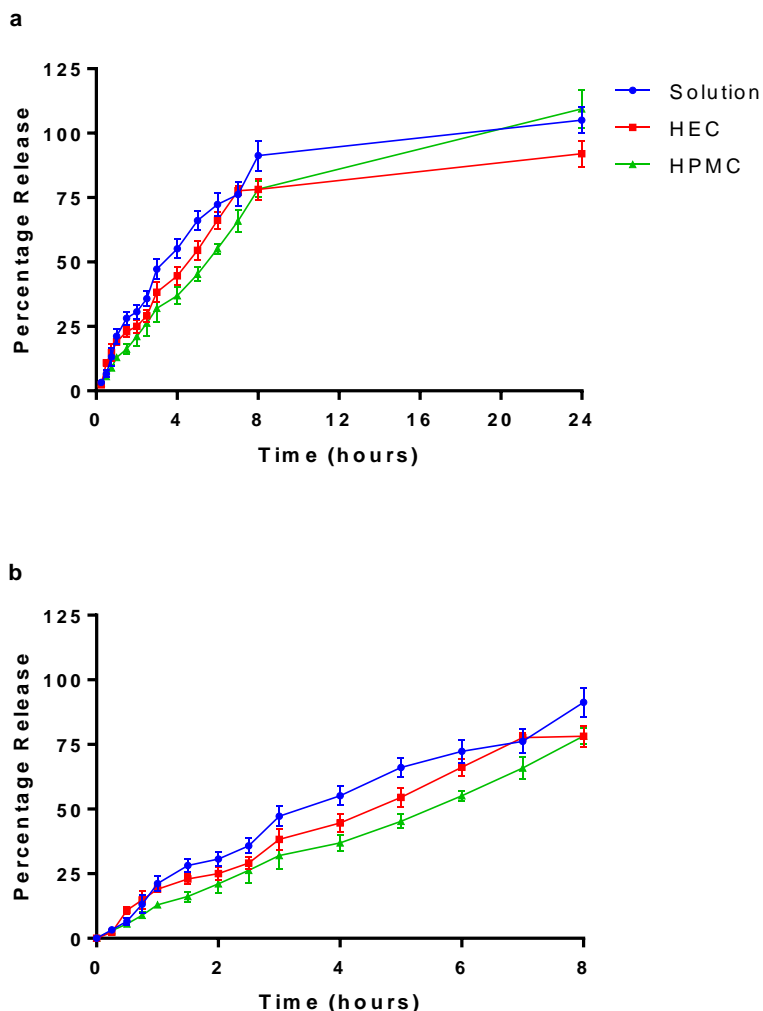


Figure 3.16: *In vitro* percentage EGCG release profiles from HEC and HPMC gel

EGCG release profiles from aqueous 3% w/v HEC and HPMC gel with 1% w/v EGCG over a) 24 hours, b) 8 hours. Data represents mean \pm SD. $n=3$ independent batches.

3.4.7.3 EGCG release from liposomes

Elastic liposomes have been reported to penetrate the skin if applied non-occlusively by virtue of the very high and self-optimizing deformability. Liposome adhesion, fusion and penetration into the stratum corneum is possible with potentially deeper penetration into the dermal layer of deformable vesicles compared with traditional liposomes (El Maghraby et al., 1999). They have been effectively employed in transdermal delivery of lipophilic and hydrophilic drugs

including anti-inflammatory agents, plasmid DNA, anti-tumour agents and hormones (Cevc and Blume, 2001; El Maghraby et al., 1999; Oh et al., 2006; Romero et al., 2013). Release of EGCG from 0.1mg/mL solution, liposomes and liposomes formulated with either 2%, 6% or 10% w/w of Tween 20 with was studied over a 24 hour period (Figure 3.17).

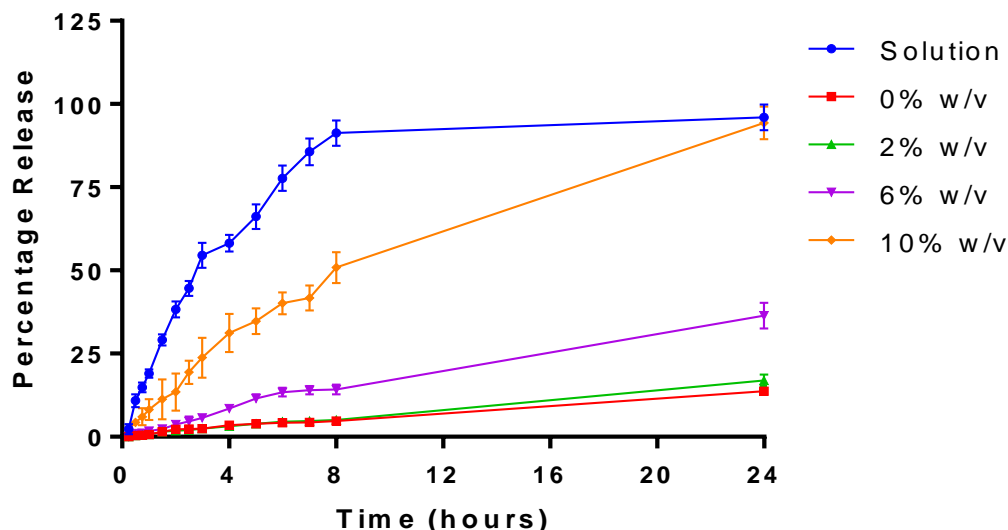


Figure 3.17: *In vitro* percentage EGCG release profiles from solution and liposomal formulations

EGCG release profiles from solution and liposomes formulated with 0-10% w/w Tween 20 over 24 hours. Liposomes were prepared adapting the dry film method adding the surfactant and EGCG during the lipid mixing stage. A diffusion cell dialysis system was used to evaluate *in vitro* drug release. Data represents mean \pm SD. n=3 independent batches.

Liposomes appeared to slow release of EGCG in comparison to release across the membrane from the EGCG solution. Over the course of 24 hours 96.0 \pm 3.9 % release of EGCG from solution was observed whilst liposomes formulated with 0%, 2%, 6% and 10% w/w of Tween 20 gave a release of 13.7 \pm 1.1 %, 17.0 \pm 1.7 %, 36.4 \pm 3.8 % and 94.4 \pm 4.9 % respectively. The cumulative percentage released after 24 hours was significant between the solution and liposomes loaded with 0%, 2% as well as 6% w/w of Tween 20 ($P \leq 0.0001$). This difference was also significant between liposomes loaded with 0% and 6% w/w as well as between liposomes loaded with 2% and 6% of Tween 20 ($P \leq 0.01$). Finally, this difference was also significant between liposomes loaded with 10% and 0, 2 and 6% w/w of Tween 20 ($P \leq 0.0001$).

Release of EGCG observed significant differences between release from solution and all loadings of Tween 20 investigated ($P \leq 0.001$). Release between Tween 20 loadings of 0 and 10% w/w, 2 and 10% w/w and 6 and 10% w/w was also significantly different ($P \leq 0.01$). Furthermore, release between 0 and 6% w/w was also significant ($P \leq 0.05$). Release between 0 and 2% w/w loading of Tween 20 was not significant.

3.4.7.3.1 Kinetic assessment of EGCG release from liposomal formulations

A higher percentage of drug was released from the EGCG solution compared with liposome formulations. Release data from the solution and deformable liposomes complied with first order release kinetics implying rate of drug release was dependent on drug concentration at that time (Table 3-10). Release data from blank liposomes however seemed to fit the zero order model of release better than first order. This implies release from blank liposomes was independent of drug concentration. This is probably due to the lack of surfactant in the formulation which would increase solubility of the drug and encourage a faster release. It is usual to see a zero order release with controlled release formulations as this model describes release independent of drug concentration (Higuchi, 1963a). Release independent of drug concentration means higher loading of drug does not affect rate of release thus a controlled, sustained release of drug is maintained as long as drug is present in abundance i.e. above saturation point (Dash et al., 2010). Blank liposomes would give the slowest release as there is no surfactant to solubilise the drug thus aiding drug release from the formulation (Almog et al., 1986b).

Table 3-10: Kinetic assessment of release data of EGCG from solution and aqueous gels.

Kinetic model	Formulation (r^2)				
	Solution	Liposome (% w/w loading of Tween 20)			
		0	2	6	10
Zero order	0.188 ±	0.988 ±	0.690 ±	0.929 ±	0.722 ±
	0.0474	0.004	0.511	0.069	0.296
First order	0.929 ±	0.961 ±	0.986 ±	0.955 ±	0.937 ±
	0.020	0.018	0.006	0.039	0.063

Results are presented as the mean ± standard deviation (n=3)

This is further reiterated as presence of surfactant appears to increase drug release. Surfactant would increase drug solubility thus explaining why an increase in drug release is observed at higher loadings of surfactant. Single chain surfactants such as Tween 20 have a high radius of curvature (Cevc, 1996; El Maghraby et al., 1999; Ita et al., 2007; Oh et al., 2006). This component of the liposome destabilizes the vesicle bilayers by reducing the amount of work required to expand the interface allowing the liposome to become more flexible (Cevc, 1996; Ita et al., 2007; Oh et al., 2006). Additionally, it has been suggested that the mechanism of the *in vitro* release seems to be the formation of transient pores in the lipid bilayer, through which drugs are released from the inner aqueous core of the liposomes to the extra-liposomal medium (Wang, Wang et al. 2016). Therefore, the presence of more surfactant in the liposome

may also encourage the formation of transient pores. Goindi et al., (2013) found elastic liposomes were able to increase drug permeation into the skin in comparison to a conventional cream (2 fold). Further studies would have to be carried out to investigate if this can be achieved with Tween 20.

Comparison of the rate constant of each formulation that fit the First order model demonstrated that EGCG solution had the highest rate of release, followed by liposomes formulated with 10% w/w, then 6% w/w and then 2% w/w of Tween 20 (Table 3-11). Complete release, $94.4 \pm 4.9 \%$, was observed within 24 hours from liposomes loaded with 10% w/w of Tween 20. In addition, $36.4 \pm 3.8 \%$ release was observed with liposomes formulated with 6% w/w of Tween 20, and $17.0 \pm 1.7 \%$ was seen both 2% w/w and $13.7 \pm 1.1 \%$, was observed with blank liposomes. As surfactant loading increased, drug entrapment decreased, therefore, drug release would be expected to be slower as there is less of a concentration gradient. Furthermore, the drug is hydrophobic therefore less inclined to diffuse out of the liposomes.

Table 3-11: First order kinetics rate constant for EGCG release from all formulations except liposomes formulated with 0% w/w Tween 20 where the zero order rate constant was observed.

Rate constant ($\times 10^{-3} \text{ min}^{-1}$)				
Solution	Liposome formulation (% w/w loading of Tween 20)			
	0	2	6	10
3.10 ± 1.26	1.07 ± 0.0005	1.27 ± 0.01	0.33 ± 0.06	1.5 ± 0.31

Results are presented as the mean \pm standard deviation (n=3)

In dynamic dialysis, the appearance of drug in the receiver compartment is the result of diffusion from liposomes followed by diffusion across the dialysis membrane, though it is generally treated as a simple first-order process (Modi and Anderson 2013). The rate constant obtained does not necessarily reflect rate of drug release from the liposomes, instead it is the net result of drug movement across two barriers in series (Figure 3.18). The driving force of drug movement, is not the total drug concentration entrapped within the liposome but the free aqueous drug concentration, a quantity of critical importance but never directly measured. Furthermore, reversible binding of the drug released from the liposome reduces the driving force for drug transport across the dialysis membrane leading to a slower overall apparent release rate (Modi and Anderson, 2013). Therefore, assessment of the reliability of rate

constants determined by dynamic dialysis require careful consideration of the pitfalls in interpreting apparent release data.

In these studies, any effect of the membrane on diffusion of the compound is a constant as it has been used to study release across all formulations including EGCG solution. Therefore, the effect of the membrane on rate of release is the same throughout studies which are to be compared. The release data observed was because of drug release from the liposome and across the membrane or movement of the liposome across the barrier and then release from this.

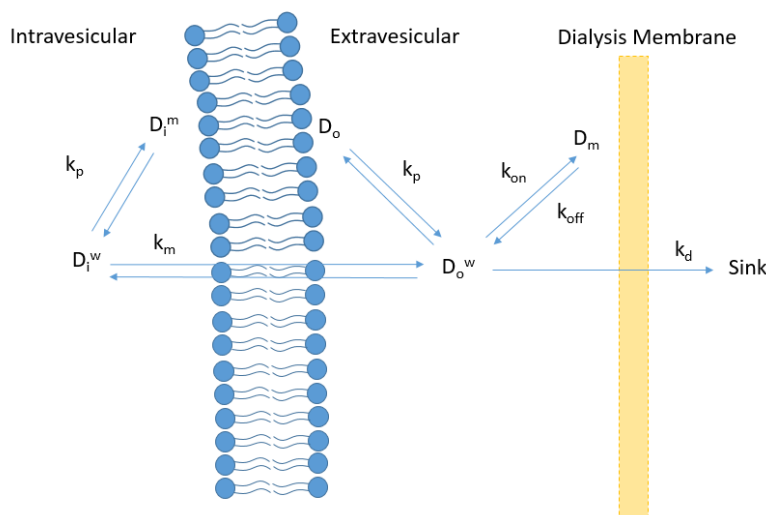


Figure 3.18: Diagram representing drug release kinetics from liposomes by dynamic dialysis.

Diagram depicting the ionization and binding equilibria along with transport pathways representing drug release kinetics from liposomes by dynamic dialysis. D_i^w and D_i^m are the intra-vesicular aqueous and membrane bound drug concentration respectively, D_o^w and D_o^m are the extravesicular aqueous and membrane bound drug concentration respectively. D_m is the dialysis membrane bound drug concentration. k_m and k_d are the rate constants for permeation across the bilayer membrane and dialysis membrane respectively. k_{on} and k_{off} are the apparent association and dissociation constants for the binding of the drug to dialysis membrane adapted from (Modi and Anderson 2013).

3.4.7.4 Liposomal gel EGCG release studies

Drug release from liposomes loaded into gels could not be measured/detected in the side-by-side diffusion chamber. Drug release in the side-by-side diffusion chamber may have been restricted by the small pore size of the membrane as well as the physical operation of the diffusion cell. Furthermore, the large receiver volume of the diffusion cell may have resulted in the drug concentration being lower than the LOD and LOQ of the HPLC-UV method. Therefore, an alternate method using 6-well plates and polyester permeable insert cups with a 400 nm pore size was employed. The purpose was to investigate if EGCG could be released from the

liposomes loaded into the gel (to ensure that only free drug samples were detected the samples were centrifuged and the supernatant analysed).

Advantages of the diffusion cell include the larger receiver volume of 100 mL thus ability to maintain sink conditions. Whilst the 6 well plate only allowed a receiver volume of 4 mL, this also results in a more concentrated drug solution which allows for HPLC-UV detection and quantification. Additionally, the membrane used in the diffusion cell had a smaller pore size of 50 nm compared with 400 nm in the inserts, which is more comparable to the gaps in the SC in the skin. A release study to observe drug release from the liposomes loaded into gels was conducted using a 6 well Thincert plate and 4 cm² cylindrical cell culture Thincert™ insert with 400 µm pore size. Drug release from solution was also observed to be able to compare any differences in release (Figure 3.19).

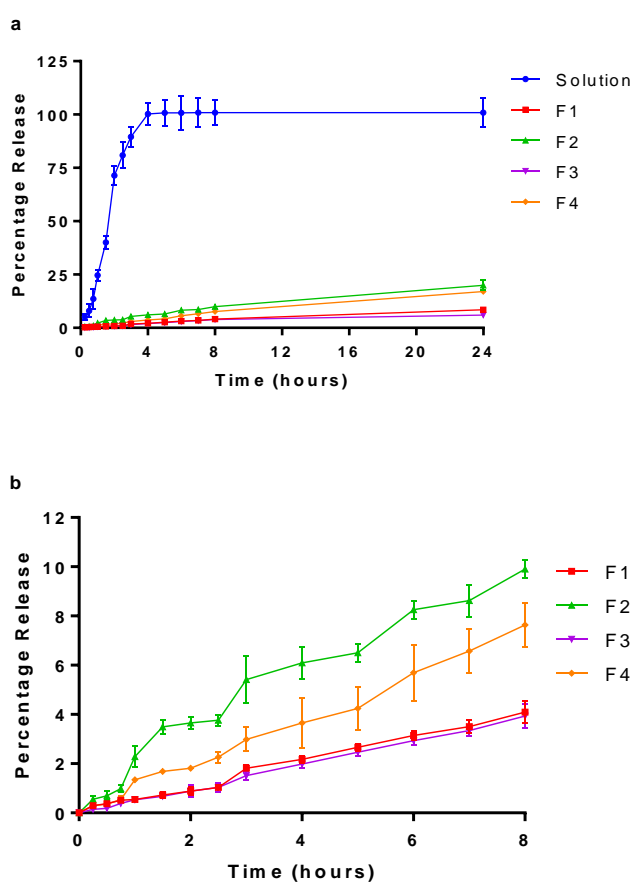


Figure 3.19: *In vitro* percentage EGCG release profiles from liposomal gels

In vitro percentage EGCG release profiles using a permeable insert of a 400 nm pore size from solution and gel loaded with either blank or elastic liposomes formulated with 2% w/w Tween 20 over a) 24 hours, b) just liposomal gels over 8 hours. F1: HEC and blank liposomes, F2: HEC and elastic liposomes, F3: HPMC and blank liposomes, F4: HPMC and elastic liposomes. Gels were prepared using 3% w/w loading of either HEC or HPMC with a 1% w/w of drug loading. Liposomes were prepared adapting the dry film method. Gels were prepared using 3% w/v loading of either HEC or HPMC. Data represents mean \pm SD. n=3 independent batches.

Complete drug release from solution was observed by 4 hours (Figure 3.19). Over the course of 24 hours solution gave a release of 100.9 ± 6.8 % whilst F1, F2, F3 and F4 gave a release of 8.5 ± 0.95 %, 20.0 ± 2.5 %, 6.0 ± 0.3 % and 17.0 ± 0.8 %, respectively. The cumulative percentage released after 24 hours was significant between the solution and all liposomal gels ($P \leq 0.0001$). The difference was also significant between F1 and F2, F2 and F3 as well as between F3 and F4 ($P \leq 0.01$). Finally, the difference was also significant between F1 and F4 ($P \leq 0.05$). F1 and F3 contained no surfactant in the liposome and F2 and F4 contained 2% w/w of Tween 20. Therefore, release in the liposomal gels appeared to be affected by presence of surfactant in liposomal gels formulated with HEC but not HPMC.

Overall the percentage of drug release from the liposome loaded gels quantified over 24 hours was slightly higher from the HEC gel (up to 19%). Furthermore, a higher percentage of drug was released from the liposomes formulated with 2% w/w Tween 20 (up to 19%). This shows elastic liposomes gave a faster rate of drug release.

The difference in release profiles was significantly different between solution and all liposomal gels ($P \leq 0.001$). A significant difference was also noted between the HEC gel loaded with blank liposomes and 2% w/w of Tween 20 as well as HEC Tween 20 2% w/w liposomal gels and HPMC gels loaded with liposomes with no Tween 20 ($P \leq 0.01$). Additionally, a significant difference was also observed between HEC and HPMC gels loaded with 2% w/w Tween 20 liposomes. No significant difference was observed between the HEC gel loaded with liposome with no Tween 20 and either HPMC liposomal gel or between the two HPMC gels.

This study observed that, unlike the side by side diffusion chamber, EGCG could diffuse into the receiver compartment. It is unclear whether liposomes and gels have an additive effect at retarding the release of EGCG as over the same time of 24 hours because of the different physical parameters. A maximum of 19% release was observed in the permeable insert system, compared with 100% release from the gels and a maximum of 16% release from the liposomes formulated with 2% w/w Tween 20. A similar pattern of results was observed in a study comparing the release of lidocaine from liposome loaded gels to hydrogels. A faster release of lidocaine from the hydrogels compared with the liposome loaded was observed. This indicates the liposomal gels had an additive retardation effect on EGCG release (Glavas-Dodov et al., 2002). It is possible liposomes diffuse through the gel and across the membrane prior to EGCG release or that EGCG diffused out of the liposomes into the gel and then across the membrane. This study was not able to determine the exact process of drug release.

In order to comment on process of drug release from the gel, whether drug released from the liposome into the gel or if the liposome diffused out of the gel first, from which drug then diffused, an ELSD HPLC method was used. This detection method was used to attempt to

detect lipid in the receiver from the diffusion cell experiment however none was detected. This may have been due to the amount of lipid in the receiver compartment being lower than the detection limit. Liposomes did diffuse across the insert as the liposomal gel could be seen in the receiver compartment at 24 hours. Regardless of this, it is yet to be determined how liposomes may or may not diffuse across the SC *in vivo* and a skin study would be needed to determine an answer.

The aim of this study was to develop a formulation that allowed liposomes to move through the gel carrier system and pass through the SC into the dermal skin layers where drug would slowly leach into the surrounding areas. The non-occlusive nature of the application should ensure the liposomes move into the skin across a hydration gradient. But that is only possible if liposomes move through the gel. Similar studies have applied a 4% HEC liposomal gel indicating the formulation at 3% should be suitable for dermal delivery of drug loaded liposomes (Mourtas et al., 2007). Furthermore, in practice, a thinner layer of gel would be applied, liposome wouldn't be moving through gel that is several millimetres thick. Additionally, the lipids in the skin would encourage liposomes to move through the skin.

Similar studies have found, calcein (hydrophilic dye) release from liposomal gels to be slower compared to control gels, and can be further retarded by using rigid-membrane liposomes (Mourtas et al., 2007). This correlates with observations in the present studies as the rate of release was observed to be faster for liposomes formulated with more surfactant in release from both liposome solution and liposomal gels. On the other hand, griseofulvin (a lipophilic drug) release from liposomal gels is released with a constant rate from liposomal gels irrespective of liposome type. Therefore it is clear, compound properties (solubility, log P) determine the system behaviour (Mourtas et al., 2007).

Further, release of EGCG from liposomal gels depends on the stability of the liposomes (membrane integrity and mechanical stability) during their dispersion in the gel formulation. This may be determined by the vesicle-membrane rigidity as well as the semisolid system physical properties (viscosity/rheological properties). Other parameters may also be concerned, as, the lipophilicity of the drug and its aqueous solubility will determine the driving force moving drug out of liposomes.

3.4.8 Impact of liposomal formulation on *In vitro* cytotoxicity on HDFa and HaCat cells

Skin is composed of the dermis, epidermis and subcutaneous layer. Each layer has a unique combination of cells, connective tissue, components and functions. Human keratinocyte and fibroblast cells were selected to test compound and formulation toxicity.

To determine the concentration of drug which was toxic to HDFa and HaCat cells, an XTT assay was performed to measure cell death after exposure of cells to different concentrations of drug for 24 hours. Results of cell viability are shown in Figure 3.20.

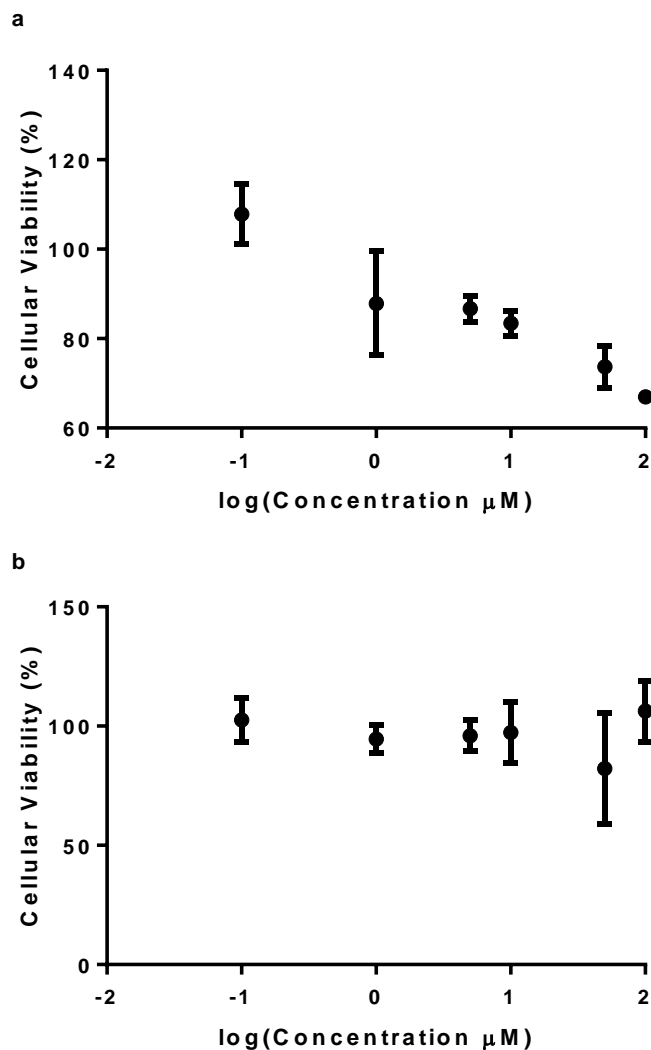


Figure 3.20: Cellular toxicity of EGCG on a) HDFa and b) HaCat cells.

Cells were grown on a 96-well plate at a density of 50×10^3 cells per well and exposed to various concentrations of EGCG (0.01 – 100 μM). After 24 hour incubation following which 25 μL of a 12.5:1 parts mixture of XTT to menadione was added each well. Plates were incubated for 3 hours at 37°C and the absorbance read at 450 nm. The control cell (without drug) corresponded to a cell viability of 100%. Data is reported as mean \pm SD with 6 replicates per compound in at 3 independent experiments.

As the concentration of EGCG was increased, there was a decrease in HDFa cell viability. This may be due to toxicity or death of damaged cells in which EGCG induced apoptosis (Bae et al., 2008; Tanigawa et al., 2014). In comparison to the control well, the viability in cells treated with 100 μ M and 50 μ M was significantly lower ($P \leq 0.0001$), as well as cells treated with 10 μ M ($P \leq 0.001$), 5 μ M ($P \leq 0.01$) and 1 μ M ($P \leq 0.05$) of EGCG. There was no significant difference in cell viability at the range of EGCG concentrations with the HaCat cells therefore within this concentration range, EGCG was safe for application on these cells ($P \geq 0.01$).

Whilst limited data exists on the cytotoxicity of EGCG towards dermal tissues, a study observing growth inhibition in a number of cell lines, observed that EGCG at 40 μ M had little or no inhibitory effect on the growth of WI38 cells, normal human fibroblast cells (Chen et al., 1998).

3.4.9 Cellular liposomal uptake assay on HDFa and HaCat cells

EGCG loaded liposomes were incubated with both HDFa and HaCat cells to assess the cellular uptake of these formulations. Following a 2-hour incubation with the cells, the labelled liposomes were identified using confocal microscopy (Figure 3.21 and 3.22). Cytoplasmic accumulation of the formulations was apparent, confirming the successful uptake into both HDFa and HaCat cells.

DilC labelled liposomes loaded with EGCG incubated for 2-hours with both HDFa and HaCat cells seeded onto collagen-coated coverslips and the cellular localisation of these liposomes was determined using confocal microscopy and z-stack image processing. Single stage confocal imaging demonstrated generalised cellular location, with the presence of liposomes within the cellular membrane and cytoplasm (Figure 3.23). However, to further discern the exact localisation within the cell, a z-stack multistage image capture was initiated to capture DilC labelled liposome fluorescence through the z-dimension of the cell (Figure 3.24).

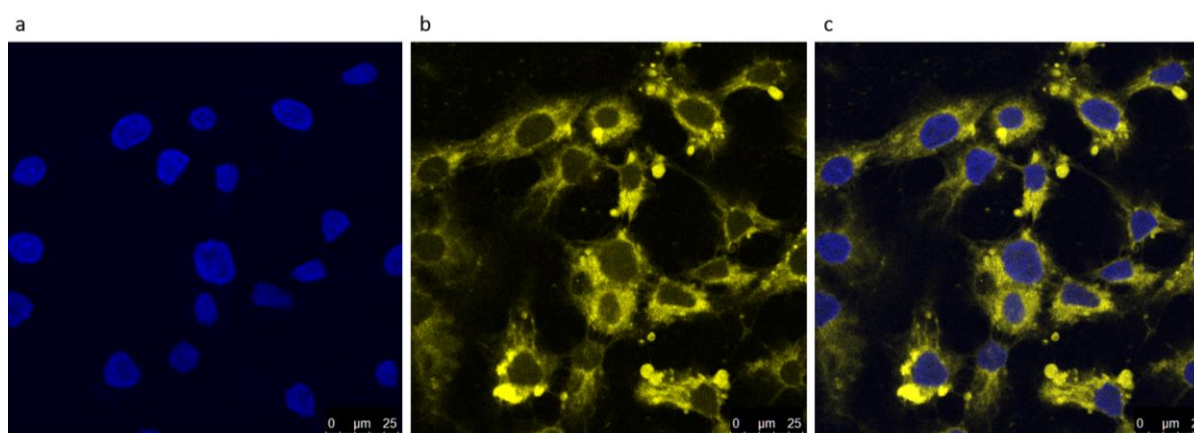


Figure 3.21: Localisation of DilC labelled liposomes loaded with EGCG and 2% w/w Tween 20 in HaCat cells.

Cells were grown on the coverslips for 2 days. Cell nuclei were visualised using a) DAPI (Blue). Liposomes were formulated with DiIc for visualisation b) (yellow). Liposome localisation within the cell is shown in the merged image c).

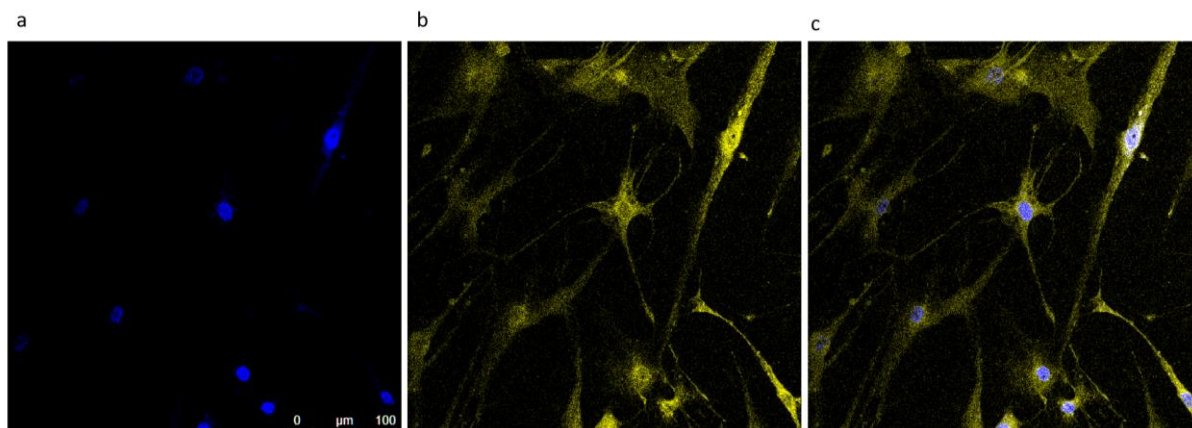


Figure 3.22: Localisation of DiIc labelled liposomes loaded with EGCG and 2% w/w Tween 20 in HDFa cells.

Cells were grown on the coverslips for 2 days. Cell nuclei were visualised using a) DAPI (Blue). Liposomes were formulated with DiIc for visualisation b) (yellow). Liposome localisation within the cell is shown in the merged image c)

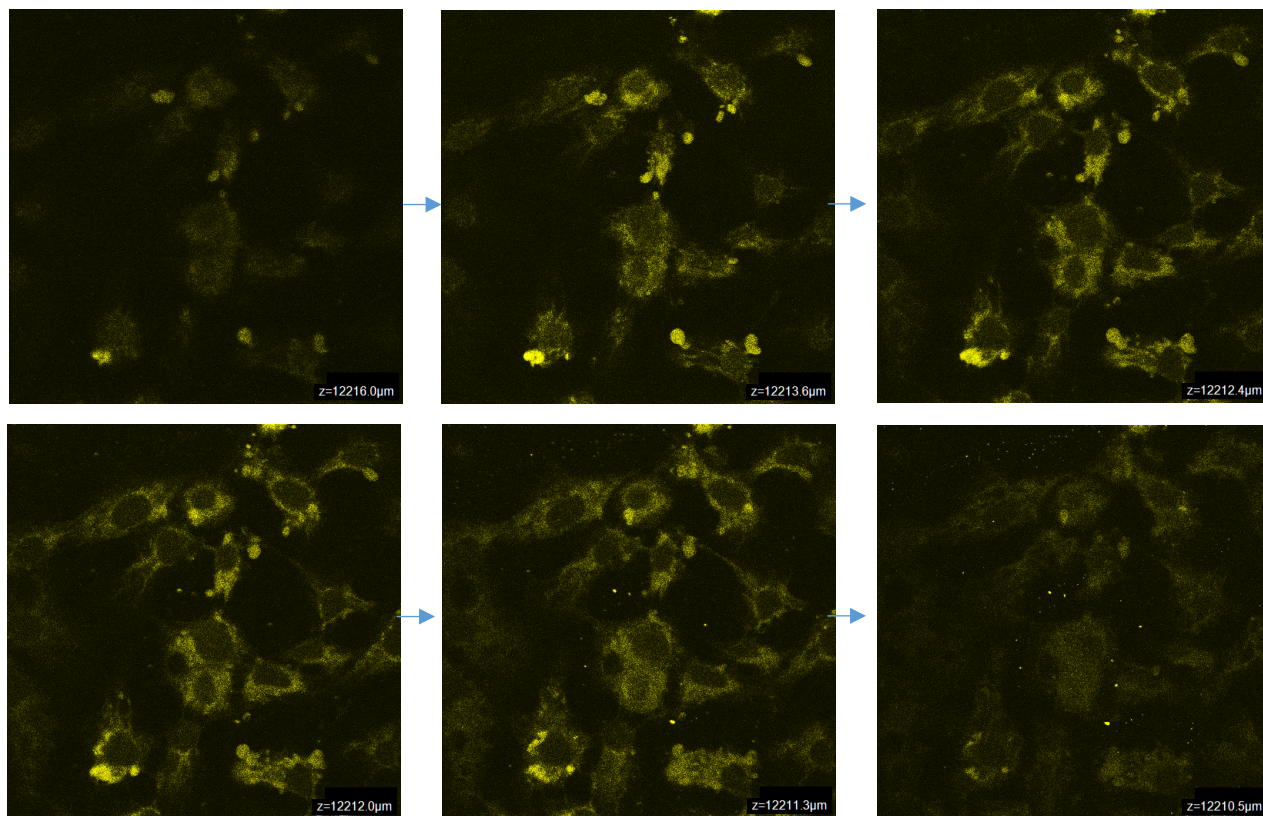


Figure 3.23: z-dimension cellular localisation of DiIC-EGCG loaded liposomes formulated with 2% w/w Tween 20 in HaCat cells.

z-dimension cellular localisation of DiIC labelled liposomes loaded with EGCG and 2% w/w Tween 20 (stage 2). DiIC labelled liposomes previously incubated with HaCat cells for 2 hours were further subjected to a z-stack analysis with the lens positioned above the cell layer (12216 μm) and lowered through the cells to the bottom of the cell layer (12210 μm). Images were captured of DiIC (green) through the z-dimension.

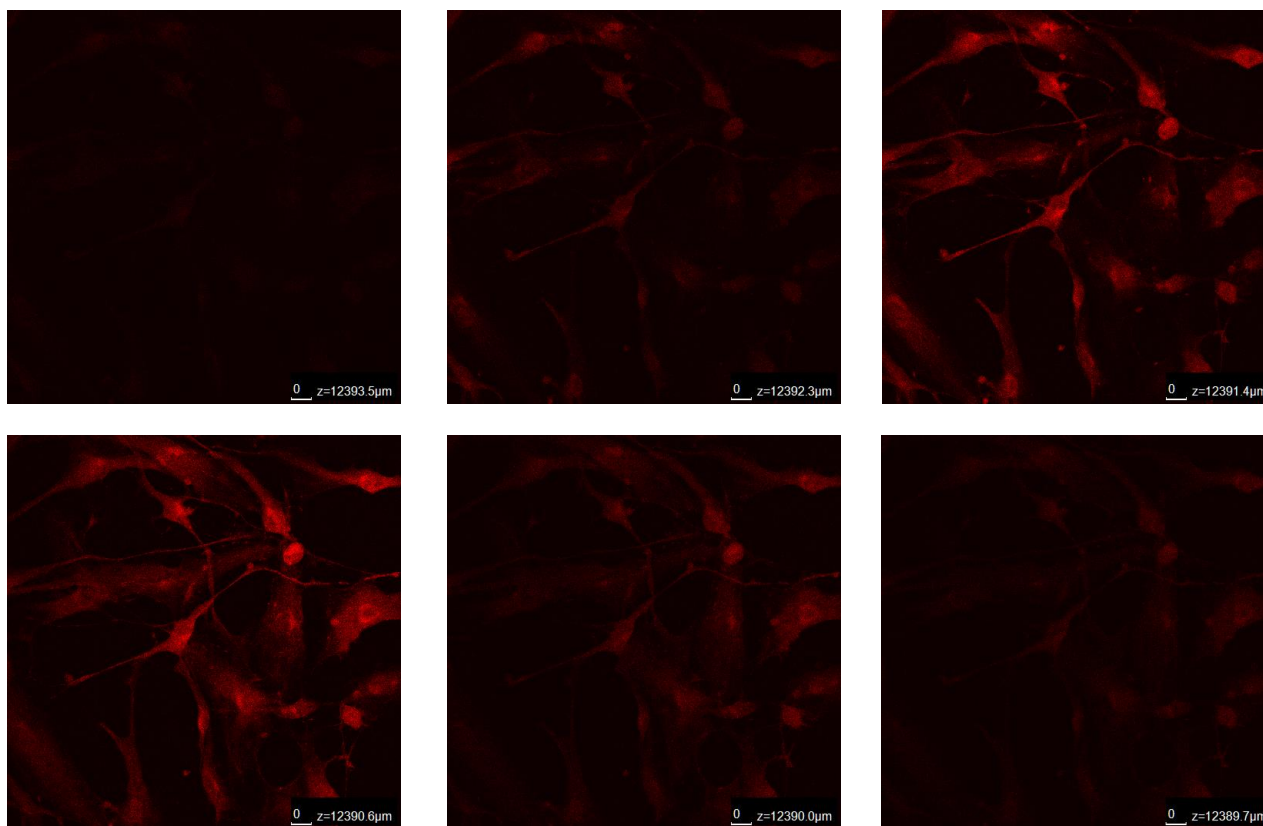


Figure 3.24: z-dimension cellular localisation of DiIC-EGCG loaded liposomes formulated with 2% w/w Tween 20 in HDFa cells

z-dimension cellular localisation of DiIC labelled liposomes loaded with EGCG and 2% w/w Tween 20 (stage 2). DiIC labelled liposomes previously incubated with HDFa cells for 2 hours were further subjected to a z-stack analysis with the lens positioned above the cell layer (12216 μm) and lowered through the cells to the bottom of the cell layer (12210 μm). Images were captured of DiIC (green) through the z-dimension

The confocal stage was set at the upper-most boundary of the HDFa/HaCat cells and the stage moved down towards the coverslip with images captured over a z-dimension of approximately 5 μm . At the onset of the z-stack analysis, liposomes are localised on the exterior of the cell boundary and potentially on the surface of the cells (12216 μm). As the stage progresses, the localisation of FITC-Fan-MSNP increases with clear demarked zones of cytoplasmic localisation near the 'mid-to-bottom' regions of the cells (Figure 3.23 and 3.24).

There are four proposed methods of liposome interaction with cells as discussed in section 2.4.5: stable adsorption, endocytosis, fusion of the lipid bilayer with the cell plasma membrane and lipid transfer (Martin and MacDonald, 1976; Pagano and Weinstein, 1978). It is unclear which of these occurred in this study, however, these methods of uptake are not mutually exclusive and any combination occur in a given experimental circumstance (Pagano and Weinstein, 1978).

This formulation is aimed to be targeting the dermal layer. It is uncertain if the liposomes would completely pass through the keratinocytes into the dermal layer or whether they would accumulate in the SC. To be able to determine this, application onto excised skin would be necessary. Nonetheless it is clear liposomes were taken up by the cells, more importantly the fibroblasts thus the liposomes were successfully able to enter the cells.

3.4.10 Stability of deformable liposomes

The stability of deformable liposomes during storage at 20°C was studied in terms of size and, for drug loaded liposomes, encapsulation efficiency. It is important to assess stability of liposomes in terms of size to assess liposome aggregation and fusion as this may affect compound encapsulation and release. Confocal images were observed on day 1 of formulation to ensure the presence of liposomes (Figure 3.25). The size of blank and surfactant loaded liposomes was measured on days 1, 2, 7, 14, 21 and 28 (Figure 3.26).

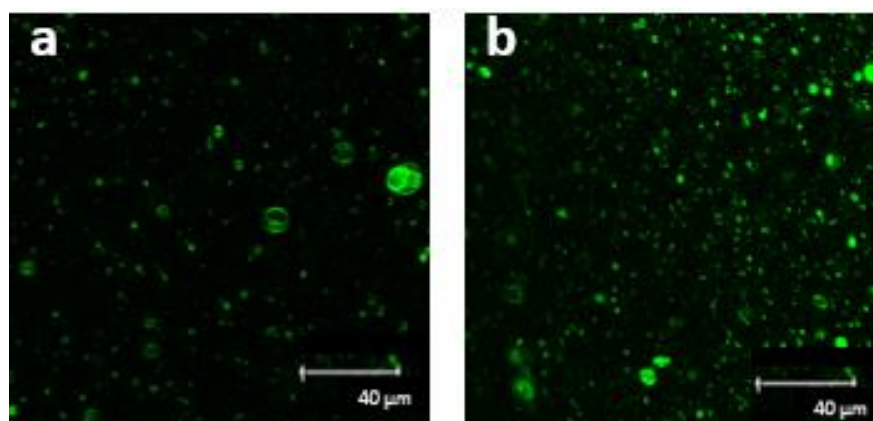


Figure 3.25: Confocal images of MLV liposomes formulated with 4% w/w of Tween 20

MLV liposomes were formulated with 4% either and were either a) blank, b) EGCG loaded. Fluorescently labelled liposomes were formulated by the addition of the fluorescent dye Dil C to the lipid mixing stage. The untrapped marker was removed by centrifuging liposomes, removing the supernatant, re-suspending in water. Liposomes were imaged using an upright confocal microscope (Leica SP5 TCS II MP) and visualised with a 40x oil immersion objective.

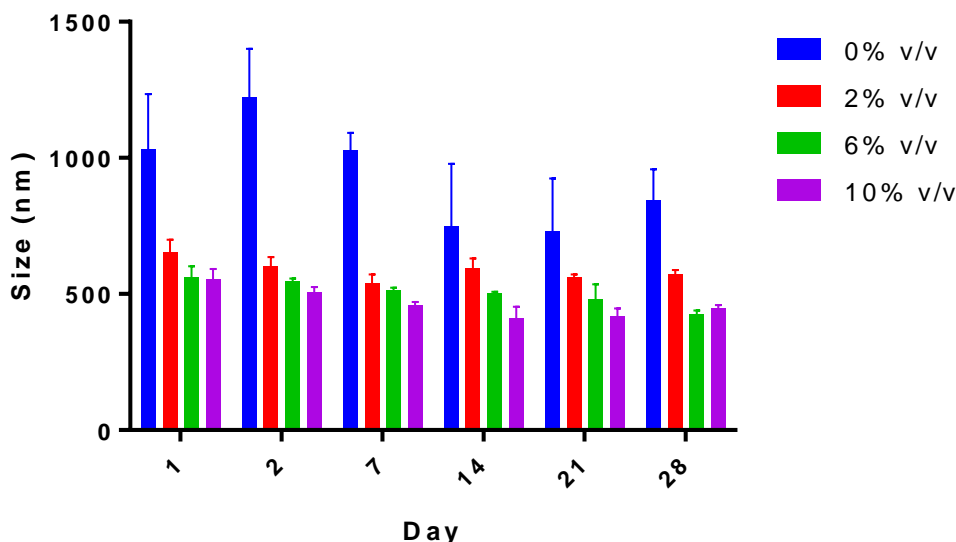


Figure 3.26: Stability of EGCG loaded liposomes as determined by size.

Size of EGCG loaded liposomes formulated with 0-10% w/w Tween 20, using DLS, formulated with up to 10% w/w Tween 20 measured on various days (1, 2, 7, 14, 21 and 28). Data represents mean \pm SD. n=6 independent batches.

EGCG loaded liposomes formulated with and without surfactant appear to decrease in size over time. This was unexpected as usually, aggregation is noted resulting in vesicle size growth (Seras et al., 1992). This is due to larger liposomes/aggregates settling as a creamy film that could be seen at the bottom of the cuvette. Formulations with 0% w/w, 2% w/w, 6% w/w and 10% w/w observed a size decrease from 1029 to 844 nm, 652 to 573 nm, 561 to 424 nm and 551 to 448 nm respectively over the course of 28 days (Figure 3.25). As liposomes formulated with surfactant have a lower polydispersity, this results in a more homogenous mix with less larger liposomes/aggregates formulated thus there would be less of these to settle out over time.

The size decrease of liposomes formulated without Tween 20 was significant between day 2 and 14 ($P \leq 0.05$), and between day 2 and 21 ($P \leq 0.001$). There was no significant difference between days 7 onwards. This may be because all lipid aggregates settled out by this time confirmed by the presence of a creamy film at the bottom of the container holding the liposomes. The size decrease between liposomes formulated with 2% w/w Tween 20 between day 1 and 7 ($P \leq 0.01$), and between day 1 and both 21 and 28 ($P \leq 0.05$). There was no

significant difference between day 2 onwards. This may be because all lipid aggregates settled out by this time. The size decrease between liposomes formulated with 6% w/w Tween 20 between day 1 and 14 ($P \leq 0.05$), and between day 1 and 21 ($P \leq 0.01$) and between day 1 and 28 ($P \leq 0.0001$). There was also a significant difference between day 2 and 21 ($P \leq 0.05$) and between day 2 and 28 ($P \leq 0.001$). There was also a significant difference between day 7 and 28 and between day 14 and 28 ($P \leq 0.05$). There was no significant difference between days 21 and 28. This may be because all lipid aggregates settled out by this time. The size decrease between liposomes formulated with 10% w/w Tween 20 between day 1 and 17 ($P \leq 0.01$), and between day 1 and both 14 and 21 ($P \leq 0.0001$) and between day 1 and 28 ($P \leq 0.01$). There was also a significant difference between day 2 and 21 ($P \leq 0.05$) and between day 2 and 28 ($P \leq 0.001$). There was also a significant difference between day 2 and 14 ($P \leq 0.01$) and between day 2 and 21 ($P \leq 0.05$). There was no significant difference between days 7 onwards. This may be because all lipid aggregates settled out by this time. There was no significant difference between day 21 onwards. This may be because all lipid aggregates settled out by this time.

Furthermore, encapsulation efficiency appears to decrease from 72% to 56%, 45% to 30%, 22% to 11% and 10% to 1% respectively for 0 % w/w, 2 % w/w, 6 % w/w, 10 % w/w loading of surfactant ($P > 0.05$) (Figure 3.27). This suggests drug leaching is independent of surfactant loading. However, Tween 20 is able to increase compound solubility, therefore, as not all would be entrapped within the bilayer, this may allow EGCG to solubilise within the liposomal media (Almog, Kushnir et al. 1986). Therefore, as the loading of Tween 20 increased, this would increase the amount of free Tween 20 resulting in more EGCG being able to solubilise in the liposome media.

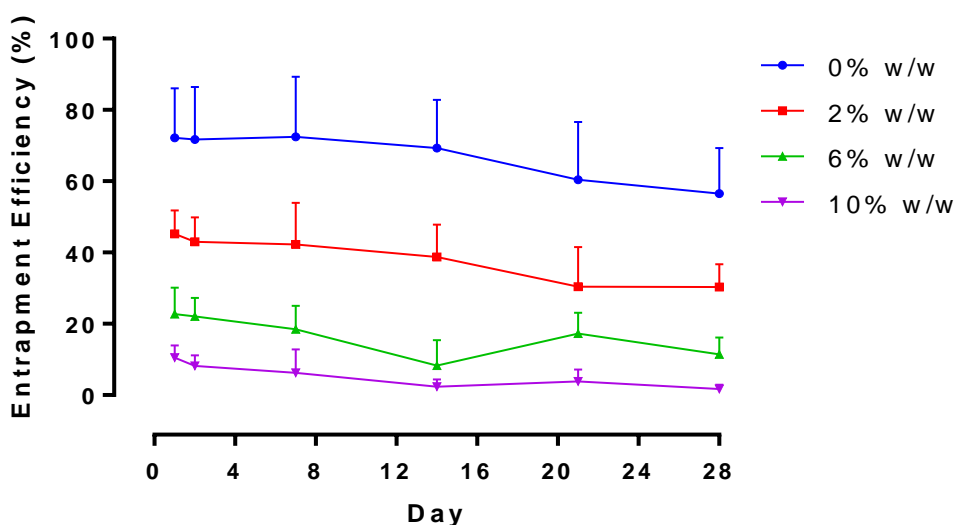


Figure 3.27: Liposome encapsulation efficiency for EGCG

Liposome encapsulation efficiency for EGCG in either 0% w/w, 2% w/w, 6% w/w or 10% w/w Tween 20 liposomes over 28 days. Liposomes were prepared adapting the dry film method adding the surfactant and drug during the lipid mixing stage. The preparation was then washed via centrifugation. The quantity of EGCG in supernatant over 28 days was then analysed by HPLC coupled with UV detection to assess liposome stability. Data represents mean \pm SD. n=6 independent batches.

Long-term stability of liposomes depends on the average elastic energy of the membrane being higher than the thermal energy. When this is no longer the case, liposomes will disintegrate (Lipowsky 1991). Therefore, temperature is an important determinate of stability and liposomes must be stored at a suitable temperature. Too high and the liposomes will break down, and, furthermore, liposomes formulated with surfactant cannot be stored in a fridge due to the freezing point of Tween 20 being 7°C (Natural-Sourcing, 2017). This suggests these liposomal formulations are not suitable for long term stability. Either additional excipients (such as a charged surfactant to reduce coalescence) are required or an additional step of freeze drying liposomes for reconstitution near the time of administration would need to be employed.

3.5 Conclusion

The use of naturally occurring compounds such as EGCG have been found to be successful as chemopreventative and chemoprotective agents. However, formulation of such compounds has been limited in success due to a limited bioavailability of promising agents and inefficient delivery systems. Liposomes could be valuable in enhancing the bioavailability of these compounds (Nishiyama, 2007; Siddiqui et al., 2009). Furthermore, elastic liposomes have been found to be advantageous in dermal delivery of drugs as they have an increase ability to cross the SC (Cevc and Blume, 2001; El Maghraby et al., 1999; Oh et al., 2006; Romero et al., 2013). EGCG is a flavonoid found in tea, and has been observed to be useful as a pharmacological anti-cancer agent in skin cancer (Casey et al., 2015). This study aimed to formulate this compound into elastic liposomes formulated with Tween 20 within an aqueous gel carrier system intended to deliver a controlled release of EGCG within the dermal layer of the skin.

As the amount of Tween 20 in the liposomal bilayer is increased, liposome size decreases. The presence of EGCG in elastic liposome increases the liposome diameter; however, the inclusion of surfactant decreases the diameter. Inclusion of surfactant in the bilayer decreases liposome DI implying liposomes retained enough elastic energy to pass through a pore size smaller than the liposome diameter which would be useful when applied to skin to pass through the SC. This was true when liposomes were forced through a 200 nm and 100 nm pore size however, liposome destruction was apparent when forced through a 50 nm pore size.

As the loading of Tween 20 in the liposome was increased the EGCG encapsulation decreased. This may have been due to Tween 20 competing for space within the bilayer or due to Tween 20 increasing the solubilisation capacity of EGCG. Further, inclusion of EGCG within the liposome bilayer was able to reduce the phase transition temperature of EGCG.

One compartment release models found HEC gels to release drug slightly faster than HPMC gels. Complete gel dissipation was observed between 3 and 4 hours. Two compartment release models found that the aqueous gels were found to hinder the release of drug compared to drug solution. Furthermore, as the polymer loading increased, the rate of release decreased. EGCG release from liposomes found liposomes were able to modify the release of drug with complete release observed within 24 hours. Liposomes added into gels may have had an additive effect in terms of retarding drug release. Release was faster from HEC gels and liposomes formulated with Tween 20.

Toxicology assay's found that between 0.1 and 100 μ M EGCG was not harmful to either keratinocytes or fibroblasts. Cell uptake of the liposomes loaded with EGCG and 2% w/w

Tween 20 was apparent into both the keratinocyte cell line and the fibroblast cell line. It appears elastic liposomes are useful in enhancing drug penetration into dermal cells and furthermore may be useful in the development of a controlled release formulation.

Liposome stability was studied in terms of size and encapsulation capacity over the course of a month. Liposomes were found to be stable regarding these two parameters over this time period.

A strategy in the development of a controlled release formulation for naturally occurring anti-cancer agents with a limited bioavailability may be the use of liposomal gels. Aqueous gels were found to hinder the release of drug compared to drug solution. Additionally EGCG release from liposomes found release was potentiated with the liposome carrier system with the presence of Tween 20 observing a faster rate of release.

4 Development of sustained release naringenin liposomal gel formulations for dermal drug delivery

4.1 Introduction

Emerging approaches for cancer management is chemoprevention and chemoprotection with the use of naturally occurring nontoxic agents (Hwang et al., 2007; Siddiqui et al., 2009; Singh, Shankar, & Srivastava, 2011). Reactive oxygen species (ROS) play a major role in many pathological conditions including photo-carcinogenesis and immune suppression. The use of anti-oxidants to prevent oxidative skin damage appears to be a promising approach (Albini and Sporn, 2007; Casey et al., 2015; Huang et al., 2011). Naringenin is the predominant flavanone in grapefruit (Figure 4.1). It is an antioxidant, free radical scavenger, anti-inflammatory agent, and immune system modulator thus may be potentially useful as a pharmacological anti-cancer agent (Casey et al., 2015; Chen et al., 2003; Huang et al., 2011).

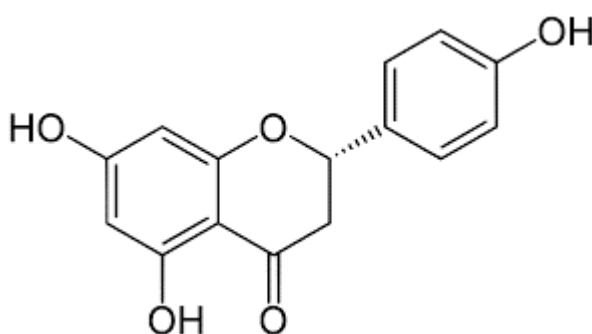


Figure 4.1: Molecular structure of naringenin

Furthermore, naringenin has been found to regulate of fibrosis. Fibroblasts and myofibroblasts play a critical role in the formation of the extra-cellular matrix and inducing fibrosis within growing tumours (Casey et al., 2015). Tissue fibrosis is frequently observed in the tumour microenvironment associated with rapid proliferation of fibroblast cells (Kerkar et al., 2012). Additionally, naringenin can increase both tyrosinase activity and melanin content, indicating naringenin can be used to prevent oxidative skin damage (Huang et al 2011, Ohguchi et al 2006, Chen et al., 2003).

In recent years, nanotechnology has been implemented and assessed in different areas of cancer management and therapeutics (Nishiyama, 2007; Siddiqui et al., 2009). Naringenin is a poorly water soluble compound ($41.76 \pm 0.51 \mu\text{g/mL}$ (Tsai et al., 2015)). A nanoparticle mediated delivery system could be valuable in enhancing the solubility of such a compound. Thus liposomes may be useful as a drug carrier for the dermal delivery of this compound thus overcoming solubility issues as well as being able to provide a controlled release of the compound (Hsiu et al., 2002; Semalty et al., 2010b; Tsai et al., 2015).

One of the primary functions of the skin is to act as a barrier to the external environment. The use of liposomal formulations as drug-delivery vehicles provide a novel approach to the delivery and targeting of the dermal layer with benefits for both delivery of existing (poorly permeable) molecules and larger (often impermeable) biologics. Elastic liposomes have been reported to penetrate the skin if applied non-occlusively by the very high and self-optimizing deformability. They have successfully been employed in the transdermal delivery of lipophilic and hydrophilic drugs including anti-inflammatory agents, plasmid DNA, anti-tumour agents and hormones (Cevc and Blume, 2001; El Maghraby et al., 1999; Oh et al., 2006; Romero et al., 2013). Liposome adhesion, fusion and penetration into the stratum corneum is possible with potentially deeper penetration into the dermal layer of deformable vesicles compared with traditional liposomes (El Maghraby et al., 1999).

Additionally, due to the liquid nature of liposomal preparations intended for application to the skin will need to be transported in a carrier. Liposomes are compatible with viscosity increasing agents such as cellulose based gels including HEC and HPMC (Foldvari, 1996) therefore these will be used as secondary carriers for EGCG.

4.2 Aims and objectives

In this body of work, a formulation aiming to deliver naringenin to the dermal layer in the management of skin cancer was developed. The effectiveness of the *in vitro* delivery of naringenin encapsulated in liposomes in an aqueous gel system to the dermal layer was assessed. The aim of this study was to formulate and characterise an aqueous gel system loaded with elastic liposomes formulated with Tween 20 for the dermal delivery of Naringenin. Liposomes were loaded with up to 10% w/w Tween 20 and 0.25 mg/mL of naringenin. They were characterised by size, zeta potential, DI and stability. naringenin release was observed from these liposomal formulations as well as from HEC and HPMC gels and from gels loaded with liposomes. Toxicity and uptake into HDFa and HaCat cells was then observed.

To achieve the aims, the overall objectives were

- Validate a HPLC method for naringenin detection
- Formulate and characterise liposomes loaded with naringenin and observe the release profiles
- Characterise naringenin loaded liposomes formulated with Tween 20 and quantify the release of naringenin delivered from these formulations.
- Formulate HEC and HPMC aqueous gels and compare the release of naringenin delivered from these formulations.

- Formulate and compare naringenin release of drug from HEC and HPMC gels loaded with naringenin loaded liposomes
- Apply formulations to fibroblast (HDFa) and keratinocyte (HaCat) cell lines to characterise toxicity of the formulations as well as cell localisation.

4.3 Materials and methods

4.3.1 Materials

The materials used to prepare liposomes, all reagents as well as materials used to grow HDFa and HaCat cells are detailed in chapter 2 (section 2.3.1) The materials used to prepare the gels are detailed in section 3.3.1. Naringenin was obtained from Sigma-Aldrich.

4.3.2 Elastic liposome preparation

Liposomes were prepared by using the film hydration method established by Bangham *et al.*, (1965) detailed in section 2.3.2. Briefly, PC, cholesterol and surfactant were dispersed in chloroform and methanol in a 9:1 ratio. Ratios of lipids are detailed in Table 3.1 rational of which has been adapted from previous studies concerning the formulation of elastic liposomes (Hiruta *et al.*, 2006; Ita *et al.*, 2007; Oh *et al.*, 2006; Tsai *et al.*, 2015). Naringenin loaded liposomes were prepared by adding the required amount of naringenin to the lipid mixing stage.

4.3.3 Liposome characterisation: particle size and polydispersity and zeta potential

Mean particle size, polydispersity index and zeta potential of liposomes was measured as detailed in section 2.3.3 using a Zetaplus (Brookhaven Instruments). Each sample was measured 3 times.

4.3.4 Assessment of liposomal deformability

The deformability index (DI) of the elastic vesicles was determined using a mini filtration technique as detailed in section 3.3.4.

4.3.5 HPLC methodology

Detection of naringenin was assessed through reverse phase HPLC methodologies. A Waters Alliance separation module HPLC with UV detection was utilised at an operating wavelength of 287 nm (Wen *et al.*, 2010a). A Waters X select column (5µm C18 4.6 x 150 mm column) was used. 10 µL of sample at room temperature was injected. The mobile phase comprised of a 50:50 ratio of 0.1% TFA in water to acetonitrile at a flow rate of 1mL/min.

Stock solutions and standard solutions of naringenin were prepared with both water and ethanol ranging from 0.05-250 µg/mL.

4.3.5.1 HPLC validation

The method was validated by assessing the linearity and range, repeatability and sensitivity in terms of the limit of detection (LOD) limit of quantification (LOQ) and precision as detailed in section 3.3.5.

For the linearity and range assessment, standard solutions ranging between 0.05 - 250 µg/mL of naringenin in water were prepared. The mean peak area ± SD was calculated and plotted against the known concentration of the standard.

4.3.6 Determination of entrapment efficiency

The entrapment percentage of naringenin loaded in elastic liposomes was determined by centrifuging samples and quantifying drug in the supernatant as detailed in section 3.3.6.

4.3.7 Differential scanning calorimetry investigations of naringenin and naringenin-lipid blends

Naringenin as well as naringenin combined with different ratio of lipid blends were analysed in the solid state using a TA Instruments Q200 Thermal Analysis DSC as described in section 3.3.7.

4.3.8 Naringenin loaded aqueous gel formulation

Aqueous gels were prepared using HEC (3% w/v) and HPMC (3% w/v) which were mixed overnight using a mechanical mixer (Polytron PT 3100 D) as detailed in section 3.3.8. Gels with a drug loading of 1% w/w was manufactured.

4.3.9 *In vitro* release studies

Drug release from gels, liposomes and liposomal gels over 24 hours was observed using multiple methods.

4.3.9.1 One compartment release model

To study the *in vitro* release and swelling behaviour of gels over 24 hours naringenin loaded gel was syringed into plastic containers with 20ml of DDM as detailed in section 3.3.9.1 and aliquots removed at set time points and analysed using HPLC quantification with UV analysis (section 4.3.5).

4.3.9.2 Two compartment release model

A diffusion cell dialysis system was used to evaluate *in vitro* drug release over 24 hours from solution (0.1 mg/mL), gels (formulated with 1% w/w of drug) and liposomes into release media as detailed in section 3.3.9.2.

4.3.9.3 Liposomal gel release study

Release from liposomal gels was observed with the use of a 6 well Thincert plate and 4 cm² cylindrical cell culture Thincert™ inserts (400 µm pore size) were filled with 1ml of formulation as detailed in section 3.3.9.3.

4.3.10 Release kinetics

Mathematical models to assess release kinetics were fit using Microsoft Excel® as detailed in section 3.3.10.

4.3.11 Growth and passage of cells

HDFa isolated from adult skin, cryopreserved at the end of the primary culture were revived in medium 106 supplemented with Low Serum Growth Supplement. HaCaT is a spontaneously transformed aneuploid immortal keratinocyte cell line from adult human skin. HDFa and HaCat cells were maintained in a humidified 37 °C incubator with 5 % CO₂, grown, fed and split for further proliferation as detailed in section 2.3.6.

4.3.12 Impact of liposomal formulation on *in vitro* cytotoxicity on HDFa and HaCat cells

To determine the concentration of naringenin which was toxic to the HDFa and HaCat cells, an XTT assay (Scudiero et al., 1988) was performed to measure cell death after exposure of cells to different concentrations of drug for 24 hours.

Cells were trypsinised, centrifuged and re-suspended in fresh media. Cells were then counted and seeded in a 96-well plate as detailed in section 2.3.7.

On day 3, media was removed. Cells were treated with 100 µL of either 100 µM, 50 µM, 10 µM, 5 µM, 1 µM or 0.1 µM of drug in DMSO (<1 %)/media. Plates were incubated for 24 hours (37 °C, 5% CO₂) following which a mixture of 12.5:1 parts of XTT to menadione (25 µL) was added each well in a 96 well plate. Plates were incubated for 3 hours at 37 °C and the absorbance read at 450 nm. Assessment of Naringenin toxicity to these cells was conducted through analysis of changes in XTT absorbance with increasing drug concentration.

4.3.13 Cellular liposomal uptake assay on HDFa and HaCat cells

Liposomes, both deformable and non-deformable, were formulated with the addition the fluorescent dye, DiIC, in DMSO as detailed in section 2.3.8. Coverslips were prepared and analysed with an upright confocal microscope (Leica SP5 TCS II MP) as detailed in section 2.3.8.

4.3.14 Liposome stability

The stability of liposomes was determined, as prepared in water, through the assessment of particle size over a 28 day period as detailed in section 2.3.4.

Furthermore, the encapsulation efficiency of naringenin loaded liposomes was assessed over 4 weeks as detailed in section 3.3.14.

4.3.15 Statistical analysis

Unless otherwise stated, all results are presented as mean +/- SD. Replicates of at least 3 were used for all studies. For multiwell plate assays replicates of 6 were used for each experimental condition with the study replicated 3 times.

A paired T test or a one way ANOVA was used to determine any statistically significant difference between means tested. A post-hoc Tukey's multiple comparisons test was then applied to assess differences between groups. Results were deemed statistically significant if $P < 0.05\%$.

4.4 Results and discussion

Naringenin is the predominant flavanone in grapefruit. It is an antioxidant, free radical scavenger, anti-inflammatory agent, and immune system modulator thus may be potentially useful as pharmacological anti-cancer agent (Casey et al., 2015; Chen et al., 2003; Huang et al., 2011).

The use of flavonoids in disease treatment is restricted in success due to inefficient delivery systems and the limited bioavailability of promising agents. Liposomes may enhancing the bioavailability of these compounds thus could prove useful as delivery agents (Nishiyama, 2007; Siddiqui et al., 2009). Elastic liposomes have been found to be useful in dermal delivery of drugs as they can increase compound solubility, protect the drug from degradation and can be formulated for targeted, sustained drug release (Benson 20016, Cevc 1996). Elastic liposomes have been reported to penetrate the skin; an efficient and effective physical barrier to the external environment. They have already been successfully employed in transdermal delivery of lipophilic and hydrophilic drugs including anti-inflammatory agents, plasmid DNA, anti-tumour agents and hormones (Cevc and Blume, 2001; El Maghraby et al., 1999; Oh et al., 2006; Romero et al., 2013). They can also improve drug deposition within the skin at the site of action where the aim is to reduce systemic absorption thereby reducing side effects (Benson 20016, Cevc 1996).

Liposomes intended for dermal delivery require an additional carrier due to the liquid nature of the preparation. Liposomes are known to be compatible with viscosity increasing agents such as cellulose based gels including HEC and HPMC (Foldvari, 1996). These are known to be safe in topical, dermal and transdermal delivery (Forbes et al., 2011b; Hascicek et al., 2009; Patton et al., 2007).

4.4.1 Liposome characterisation: particle size and polydispersity and zeta potential

A principle aim for the present studies was to increase drug loaded liposome permeation across the epidermal layer; size of drug carrier is an important element of this.

Naringenin loaded MLV liposomes were formulated using the dry film method (section 4.3.2). The bilayer included cholesterol to provide stabilising properties to the liposome bilayer by filling voids between the phospholipids as well as preventing drug from leaching out (Demel et al., 1972; Gregoriadis and Davis, 1979). Additionally, loadings of up to 10% w/w Tween 20, were added to the formulation thus adding elastic properties to the bilayer.

Similar to liposomes formulated without naringenin, as the surfactant loading in the bilayer increased size decreased significantly from 1177.7 ± 153.8 nm to 693.4 ± 37.3 nm (Figure 4.2).

The decrease in size was significant between Tween 20 loadings of 0% w/w and both 6 and 10% w/w ($P \leq 0.0001$). This was again true between 0% and 2 % w/w of surfactant ($P \leq 0.001$). The size decrease between Tween 20 loadings of 10% w/w and both 2 and 6% w/w was significant ($P \leq 0.01$). There was no significant difference between the size of liposomes formulated with 2% w/w and 6% w/w of Tween 20.

Surfactant is known to decrease liposome size in comparison to conventional liposomes (Goindi et al., 2013; Tsai et al., 2015). This is as a result of the surfactant destabilising the bilayer and its amphiphilic nature allowing a greater interaction of the phospholipid bilayer with the aqueous phase resulting in the overall formation of more liposomes of a smaller diameter thus giving a greater surface area in contact with the aqueous phase (El Zaafarany et al., 2010). Unlike liposomes formulated with EGCG, only the size decrease between 6 and 10% w/w of surfactant is not significant. This implies that either the maximum loading of Tween 20 is equal to or above 6% w/w, or that beyond this loading, there is no change in liposome size. Further studies to determine liposome composition would need to be conducted to confirm this.

Naringenin loaded liposomes had a larger diameter than blank liposomes; 1177.8 ± 153.8 nm compared with 1032.3 ± 182.5 nm for liposomes formulated with no surfactant and 693.4 ± 37.4 nm compared with 358.1 ± 57.1 nm for liposomes formulated with 10% w/w loading of surfactant. Naringenin is hydrophobic therefore was added in at the lipid mixing stage. The inclusion of drug in the bilayer may have caused an increase in liposome size by increasing bilayer hydrophobicity as it had caused the bilayer to have less interaction with the aqueous phase. Similar to blank liposomes, as the surfactant loading increased, the diameter decreased.

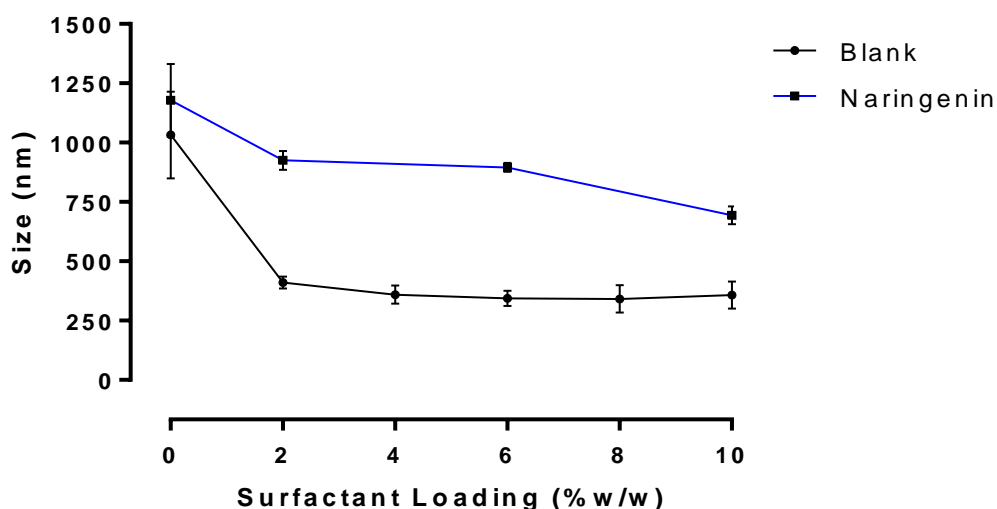


Figure 4.2: Liposome size distribution, comparing blank and naringenin loaded formulations.

Liposome size distribution, determined by DLS, comparing blank and naringenin loaded formulations with increasing loadings of Tween 20 up to a maximum of 10% w/w. Liposomes were prepared via the dry film hydration method and compound was added during the lipid mixing stage. Data represents mean \pm SD. n=3 independent batches.

A polydispersity of up to 0.3 is indicative of a homogenous formulation (Chen et al., 2012; Goindi et al., 2013; Kang et al., 2013). Liposomes formulated without surfactant were slightly out of this range (0.32 ± 0.08 and 0.31 ± 0.06 for blank and drug loaded liposomes respectively) however liposomes formulated with surfactant all had a polydispersity below 0.3 therefore can be considered homogenous (Figure 4.3). Polydispersity for naringenin loaded liposomes was lowest at 0.21 when formulated with 6% w/w Tween 20 indicating this loading of surfactant produced the most homogenous mix of liposomes. The polydispersity for 10% w/w loading of surfactant increased to 0.3 indicating homogeneity decreased. This may have been due to the surfactant having surpassed its loading capacity within the liposome and the production of some micellar structures (Casas and Baszkin, 1992; Di Marzio et al., 2011). A more homogenous mix could be obtained by using a probe sonicator in the production of liposomes. The polydispersity for drug loaded liposomes is similar to respective blank liposomes, any difference is not statistically significant ($P = 0.57$). As observed with EGCG loaded liposomes, naringenin loaded liposomes had a greater standard deviation than blank liposomes suggesting these liposomes were less homogenous than blank liposomes. This may be because of naringenin having been loaded into the bilayer membrane therefore disrupting the bilayer resulting in a wider size distribution. Additionally, as the loading of Tween 20 increased, the polydispersity decreased from 0.315 with no surfactant to 0.296 with 10% w/w of Tween 20. As discussed later on in section 4.4.4, as the loading of Tween 20 increased, the entrapment efficiency decreases. Therefore, this indicated that the presence of EGCG with the bilayer led to a wider size range of formulated liposomes.

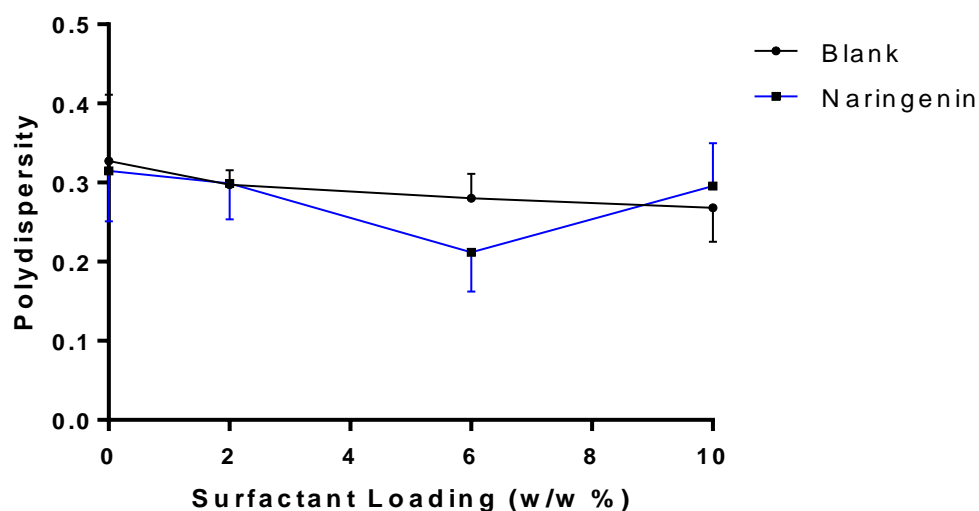


Figure 4.3: Polydispersity of blank and naringenin loaded liposomes

Polydispersity, determined with DLS, of blank and naringenin loaded liposomes formulated with increasing loadings of Tween 20 up to a maximum of 10% w/w. Liposomes were prepared via the dry film hydration method and compound was added during the lipid mixing stage. Data represents mean \pm SD. n=3 independent batches.

Comparison of the size between EGCG and naringenin observed that at 0% w/w loading of Tween 20, EGCG liposomes had a bigger diameter than naringenin (1292.2 compared with 1177.8 nm). However, in the presence of surfactant, naringenin loaded liposomes maintained a greater diameter than EGCG loaded liposomes. EGCG is a larger molecule than naringenin and the loading of the molecule decreased as the loading of Tween 20 increased. Therefore, in the absence of Tween 20, this molecule resulted in the production of larger liposome than naringenin. However, as Tween 20 displaced EGCG, liposome size decreased.

Comparison of the polydispersity between EGCG and naringenin observes at 0% w/w loading of surfactant EGCG liposomal formulations had a slight higher value than naringenin (0.322 compared with 0.315). This indicates naringenin allowed the formulation of a slightly more homogenous mix of liposomes. However, in the presence of surfactant EGCG had a lower polydispersity than naringenin (0.263 compared with 0.299 at 2% w/w loading of Tween 20). This maybe because EGCG has a slightly bigger structure than naringenin causing greater disruption in liposome shape at 0% w/w Tween 20. However, in the presence of surfactant, there was a higher loading naringenin in comparison to EGCG, therefore as surfactant loading increased, the assumed disruptive EGCG was less present to be able to cause disruption in the bilayer.

The zeta potential of both blank and naringenin liposomal formulations is detailed in Table 4-1.

Table 4-1: Zeta potential of liposomal formulations formulated with and without naringenin with up to 10% w/w loading of Tween 20

Surfactant loading (% w/w)	Zeta potential (mV)	
	Blank Liposomes	Naringenin loaded liposomes
0	5.03 ± 1.03	4.12 ± 1.14
2	4.67 ± 1.08	3.30 ± 1.09
6	3.71 ± 0.90	2.80 ± 0.60
10	-2.79 ± 0.20	-0.22 ± 0.01

Results are presented as the mean ± standard deviation (n=3)

A neutral surface charge is ideal to avoid skin irritation (Prausnitz and Langer, 2008) however, neutral liposomes have a tendency to flocculate (Weiner et al., 1992). Additionally, positively charged liposomes are known to be irritating to the skin therefore negatively charged liposomes may be advantageous (Katahira et al., 1999). This study observed the majority of formulations for both blank and naringenin loaded liposomes to have a near neutral charge (Table 4.1). Naringenin liposomal formulations formulated between 0 and 10% w/w Tween 20 were found to have general decrease in zeta potential values from of 4.12 to -0.22 mV respectively. This was similar to the trend observed with EGCG (a decrease from 2.4 to -1.9 mV). A study using Tween 80 in the liposomal formulation also found that in increase in surfactant loading did not affect liposomal charge. Although, contrasting with this study observing more positive zeta potential values, negative zeta potential values were observed (between -2.2 and -16) (Tsai et al., 2015). This may be due to differences in formulation parameters.

4.4.2 HPLC calibration and validation

Chromatographic approaches must be tested to ensure trustworthy and reliable data. Consequently, validation of the HPLC-UV method was performed according to the International Conference of Harmonization (ICH) guidelines in terms of linearity and range, limit of detection (LOD), limit of quantification (LOQ) and precision.

Stock solutions and standard solutions of naringenin were prepared in water ranging from 0.125-10 µg/mL. Calibration data using the method outlined in section 4.3.5 was then obtained (Figure 4.4).

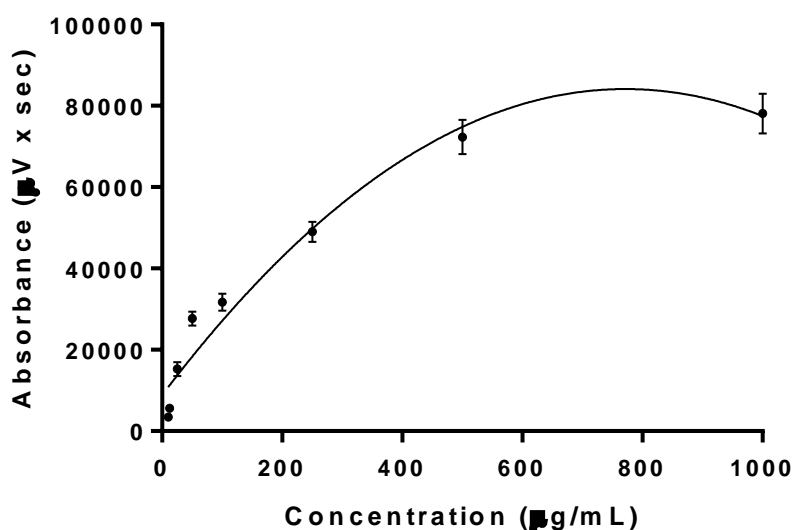


Figure 4.4: Calibration data for naringenin as determined by HPLC-UV analysis

Calibration data for naringenin over the concentration range of 12.5-1000 µg/mL in water. A proportional response was evident versus the analytical concentration over the working concentration range with an r^2 of 0.996 and polynomial equation of $y = -6 \times 10^7 x^2 + 1 \times 10^7 \cdot x$. Data represents mean \pm SD. $n=9$.

For the linearity and range assessment (Figure 4.4), standard solutions ranging between 12.5 -1000 µg/mL of naringenin in water were prepared. The method developed demonstrated a high correlation with a good linear fit, with the correlation coefficient (r^2) being greater than 0.99. Assessment of repeatability/precision of the developed method was determined by assessing the intraday (same day) and interday (over the course of three days) variability (Figure 4.5). This was done to assess variation caused by temperature fluctuations and any variation in experimental method naringenin standards from 12.5-1000 µg/mL carried out intraday and interday are plotted in Figure 4.5a and b respectively. The results show that the values have no statistically significant difference for all the calibration curves carried out at different times on the same day and also on different days, meaning the method has good precision. The results show that the values did have some overlap at extremes of the

concentration range studied. Therefore, for all further studies, it is important to ensure the concentration of naringenin is between 12.5 μg and 500 μg . Calibration data for Naringenin was obtained on 3 separate days, each with 3 repeats. No statistically significant difference in either the peak areas for any one concentration across inter- and intra-day sampling across the 3 days was found (Figure 4.5b).

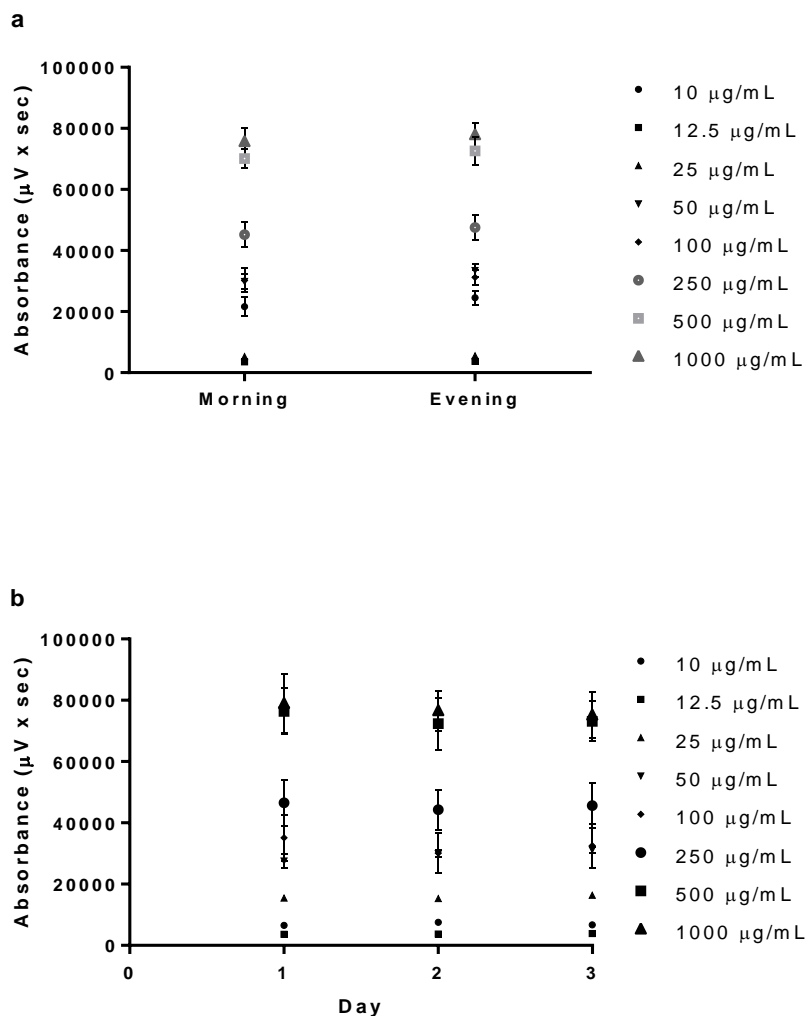


Figure 4.5: Calibration data of naringenin obtained over 3 days as determined by HPLC-UV analysis

Calibration data of naringenin displaying a) intraday, b) interday data. The standards of naringenin ranged from 0.1-10 $\mu\text{g}/\text{mL}$. Data represents mean \pm SD. $n=3$.

Study of the sensitivity of this method was assessed by means of the calculation of the LOD and the LOQ. Values were determined from the standard deviation of the response (σ) and the slope (S) obtained from the calibration curves carried out during the linearity assessment (Figure 4.4). According to the ICH guidelines, a signal-to-noise ratio of three was assumed for the quantification of the LOD, whereas for the LOQ, a signal-to-noise ratio of ten was set.

Therefore, the sensitivity of the method for naringenin was calculated; the LOD and LOQ was 1 µg/mL and 5 µg/mL respectively.

4.4.3 Determination of entrapment efficiency

The fraction of naringenin entrapped in the liposome compared with how much compound was added into the lipid mix was observed; the impact of surfactant addition on the amount of naringenin entrapped was therefore studied. As surfactant loading increased from 0% w/w to 10% w/w, drug entrapment decreased from an efficiency of 90.8 ± 4.6 % to 64.3 ± 5.6 % (Figure 4.6). A significant difference in naringenin entrapment was observed between surfactant loadings of 0% and 2% w/w ($P \leq 0.0001$). There was also a significant difference in naringenin entrapment between surfactant loadings of 0% and 6% w/w as well as between 2% and 10% w/w ($P \leq 0.01$). There was no significant difference in compound entrapment between other loadings of surfactant.

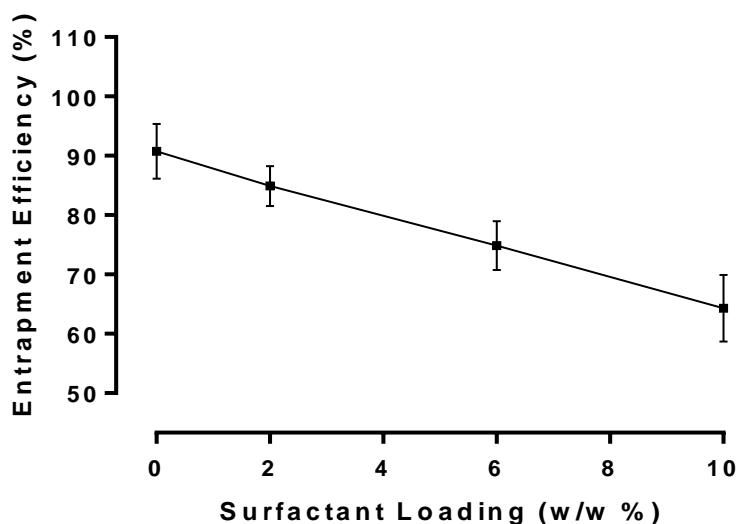


Figure 4.6: Entrapment efficiency of naringenin in liposomes formulated with up to 10% w/w Tween 20

Entrapment efficiency (%) of naringenin in liposomes formulated with varying amounts of Tween 20 (0-10% w/w) Data represents mean \pm SD. n=3 independent batches.

Inclusion of surfactant in the bilayer of the liposome may have prevented drug inclusion within the bilayer implying the surfactant has a higher affinity to the lipids (Casas and Baszkin, 1992; Levy et al., 1991). Tween 20 is much larger than naringenin, thus it may be assumed it is better poised to displace naringenin from the bilayer (Figure 4.7). The hydrophobic tail of Tween 20 would have a high affinity to the chains in PC therefore giving Tween 20 a better rooting in the bilayer than naringenin. Furthermore, Tween 20 is able to increase compound solubility, therefore, as not all would be entrapped within the bilayer, this may allow naringenin to solubilise within the liposomal rehydration media. Furthermore, studies using Tween 80

instead of Tween 20 were able to achieve a 99% entrapment efficiency (Tsai et al 2015). This may be due to the difference in the surfactant chains. Tween 80 has one more unsaturated bond causing a kink in the chain. This may then allow for the accommodation of more naringenin.

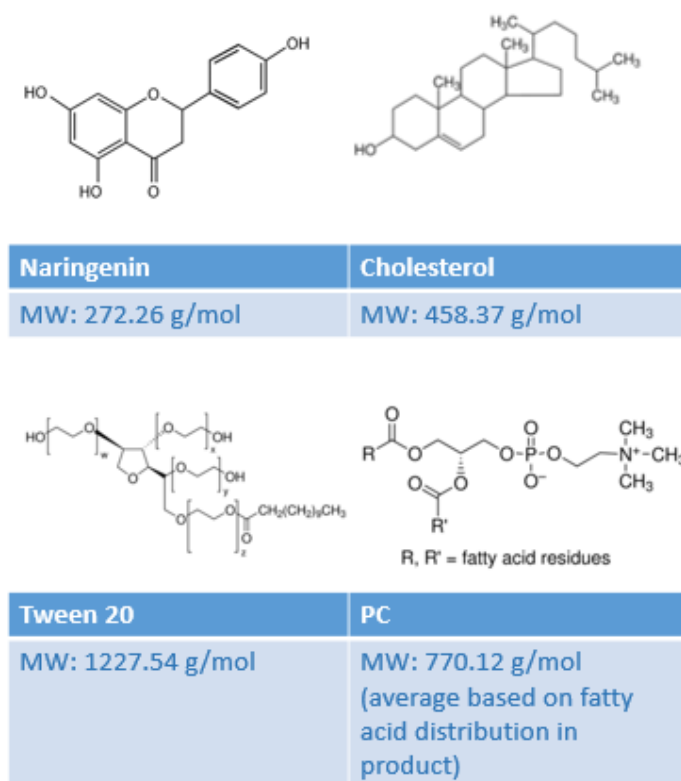


Figure 4.7: Structure and MW of naringenin, cholesterol, Tween 20 and PC

The entrapment efficiency of naringenin when compared to EGCG at increasing loadings of Tween 20 observed that naringenin always had a higher entrapment efficiency than EGCG (90.8 compared with 80.0% and 64.3 compared with 4.3% at 0 and 10% w/w loading of Tween 20 respectively). EGCG is amphiphilic (Istenic et al., 2016) whereas naringenin is hydrophobic (Tsai et al., 2015) therefore naringenin would have a stronger affinity to the lipids in the bilayer. Therefore, as the loading of Tween 20 increased, EGCG was more liable to displacement out of the bilayer than naringenin.

4.4.4 Assessment of liposomal deformability

The addition of surfactant to the lipid bilayer of liposomes allows the liposome to display elastic properties (Almog et al., 1986a; Cevc, 1996; Trotta et al., 2002). This is advantageous when considering the design of a drug delivery system to deliver molecules across the SC into the dermal layer. Liposomes loaded with up to 10% w/w of Tween 20 were formulated and the extent of deformation of each formulation was determined by extruding them through a polycarbonate filter with a pore size of 200, 100 and 50 nm (Figure 4.8). The DI is the degree

the liposomes deformed. The greater the degree of deformation the less elastic the liposomes are as they were unable to regain their previous larger size.

When liposomes were forced through the 200 nm pores the DI for naringenin loaded liposomes decreased significantly from 80.7 ± 2.0 to 59.2 ± 4.4 %. The decrease in deformation was significant between 0% w/w of surfactant and both 6 and 10% w/w of surfactant ($P \leq 0.0001$). There was also a significant difference between the DI of liposomes formulated with 2% w/w of surfactant and both 0 and 10% w/w of surfactant ($P \leq 0.001$). Additionally, there was a significant difference in the DI of liposomes formulated with 6% w/w of surfactant and 10% w/w. There was no significant difference between the DI of the other formulations.

When liposomes were forced through the 100 nm pores, the deformability index for naringenin loaded liposomes decreased from 82.7 ± 0.7 to 66.4 ± 2.6 %. The decrease in deformation was not statistically significant between any of the loadings.

No trend however was observed for formulations forced through a 50 nm pore size. Any differences in deformation between surfactant loadings was not significant between any of the formulations.

The observed decrease in DI imply the liposomes were displaying elastic properties as they could deform to fit through a gap smaller than its diameter whilst somewhat regaining its size following extrusion. A study formulating liposomes with Phosphonlipon 90 G, stearylamine, Span 80 and cholesterol subjected liposomes to a similar mini-filtration technique used in this study observed the presence of surfactant added elastic properties to the liposome as the DI of these liposomes decreased (52% for blank liposomes compared with 17% for liposomes formulated with surfactant) (Goindi et al., 2013).

Furthermore, the DI of the naringenin loaded liposomes forced through 200 and 100 nm was greater than blank loaded liposomes ($P \leq 0.05$). Naringenin loaded liposomes have a greater deformability index overall, however, their overall size prior to extrusion was greater than that of blank liposomes therefore they would have to deform to a greater degree to be able to pass through the filter. This trend was not observed for liposomes forced through the 50 nm pores but this may be due to liposome destruction (discussed later in this section).

Liposomes formulated with surfactant are able to deform as the surfactant has a tendency toward curved structures, thus diminishing the energy required for particle deformation. The surfactant can diminish the energy required for particle deformation and accommodate particle shape changes of the liposomes under stress (Trotta et al., 2004).

Tween 20 may have interacted with the PC with strong affinity but in reversible mode. The fast reconstruction of liposome spheres after extrusion may be due to the strong affinity between

the surfactant and PC. The reversible binding mode might have provided the deformability upon physical stress (Oh, Y. K. et al., 2006).

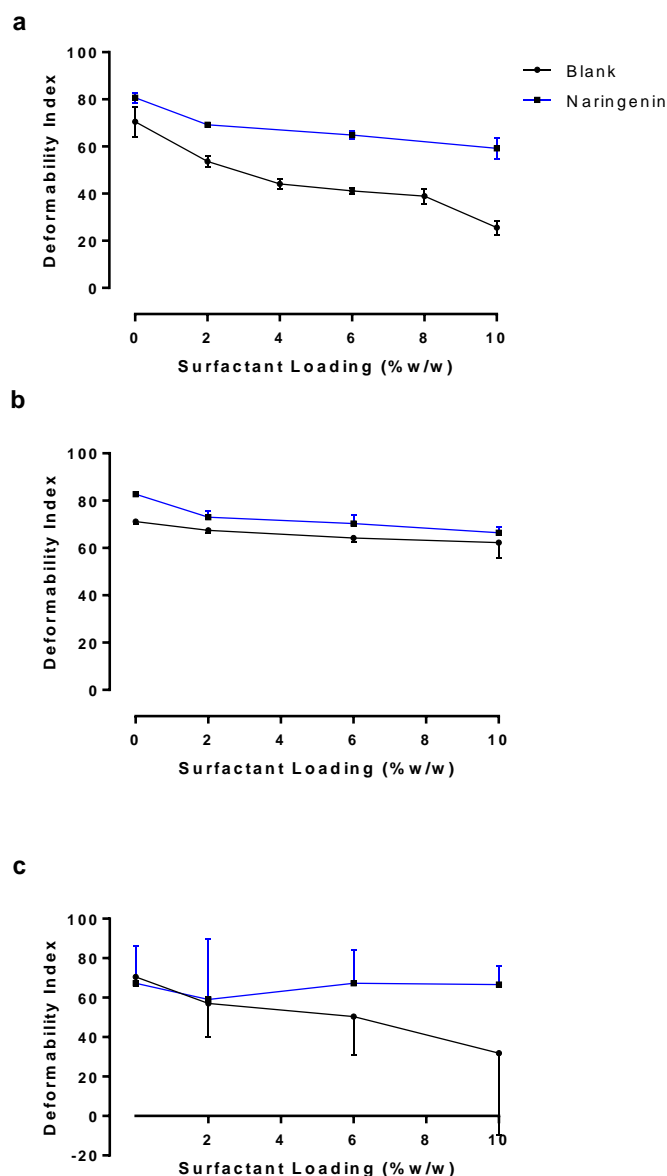


Figure 4.8: Deformability index following extrusion for blank and naringenin loaded liposomes

Deformability index following extrusion through a) 200 nm, b) 100 nm, c) 50 nm membranes for blank and naringenin loaded liposomes with increasing surfactant loading up to a maximum of 10% w/w. Liposomes were prepared adapting the dry film method adding the surfactant and adding naringenin during the lipid mixing stage. The preparation was vortexed and then extruded through the membranes. Data represents mean \pm SD. n=3 independent batches.

Deformability for both blank and drug loaded liposomes was not significantly affected by the different pore sizes investigated. Liposomes were expected to deform more so as pore size

decreased. This demonstrates that even up to 50 nm, liposomes retained enough elastic energy to maintain the same size as when forced through the 200 nm membrane.

In order to deform liposomes require energy (Fresta and Puglisi, 1996; Gompper and Kroll, 1995; Trotta et al., 2002). As detailed in section 3.4.4, in this system energy was supplied as pressure. The more surfactant included in the bilayer, the more energy the liposome will be able to retain (Trotta et al., 2002). This energy would be employed in bending the lipid bilayer structure, which will be expelled once the liposome has passed through the pore. This energy can then be used in reforming the liposome. Some energy is lost as heat or non-plastic deformation. Therefore, even at 10% w/w of Tween 20, 100% size was not recovered and a 0% deformability index was not achieved. Liposome containing no surfactant does not benefit from the extra 'storage space' of a surfactant, thus energy may be spent in rupturing the membrane causing liposome size to decrease (Trotta et al., 2002).

To fit through a 50 nm pore in comparison to a 200 nm pore, more energy is necessary to deform the liposome, therefore the deformability index is expected to increase as pore size decreases. This was not observed within the bounds of this study. The standard deviation of the DI for liposomes forced through a 50 nm pore size was extremely large (for liposomes formulated with 2% Tween 20 an SD of 30 was observed) therefore the mean value is not the best representation of the actual data values obtained. Liposome size following extrusion for these formulations was extremely varied with some liposomes coming through the pores larger than the original size. Naringenin loaded liposomes formulated without surfactant had an original size of 1012 nm compared with 1354 nm following extrusion, liposomes loaded with 2% w/w surfactant had an original size of 694 nm compared with 737 nm following extrusion (Figure 4.8). This indicates these formulations didn't retain enough elastic energy to be easily able to fit through the pores with some liposomes even converging following extrusion (Goindi et al., 2013; Trotta et al., 2002). However, even when forced through the 50 nm pores, the amount of energy stored in the liposome membrane was enough to reform at least a fraction of the liposomes to the same extent as for when forced through 200 nm pores.

The larger standard deviations suggest there may have been smaller liposomes that didn't reform alongside some destroyed liposomes clumping together as lipid aggregates. Liposome formulations in this study therefore were not suitable to pass through a 50 nm pore. As detailed in section 2.4.3 this does not imply this is what would happen to liposomes when applied to the skin. The liposomes would instead be expected to move across the skin following the hydrogen based transepidermal gradient (Cevc, 1996; Goindi et al., 2013; Gompper and Kroll, 1995; Trotta et al., 2002). Additionally, the skin temperature is warmer than room temperature (35°C compared to 20°C) which will supply more energy to be even more flexible and cross the stratum corneum.

As discussed in section 2.4.3 even in an excess of energy, the liposomes did not fully regain their pre-extrusion size. Some energy is lost in the friction of the particles moving through the pores as heat. Increasing surfactant loading may result in an increase in liposome reformation (Trotta et al., 2002). Additionally, lipids may block membrane pores resulting in an increase in pressure in the vessel causing more turmoil leading to the rupture and non-uniform reformation of liposomes.

Comparison of the DI between EGCG and naringenin loaded liposomes forced through 200, 100 and 50 nm pore sized membranes observed that at 0, 2, 6 and 10% w/w loading of Tween 20, naringenin loaded liposomes maintained a greater DI. This implies that these liposomes were less able to regain their pre-extrusion size thus were less elastic than EGCG loaded liposomes. This does not however imply that EGCG can add elastic properties to the liposome bilayer. Naringenin loaded liposomes also observed a greater liposomal size than their EGCG counterparts therefore would have to deform more to be able to fit through the pore size. This deformation will require more energy and if this requirement is not met, the liposome will rupture and form smaller vesicles thus not regain its original size (Fresta and Puglisi, 1996; Gompper and Kroll, 1995; Trotta et al., 2002). Furthermore, neither EGCG nor naringenin is known to be an elastic molecule. This was observed in this study; in comparison to their respective blank, Tween 20 loaded liposomes, as discussed earlier, when forced through 200 nm, there was no difference in the DI EGCG loaded liposomes, however, naringenin loaded liposomes deformed more. However, as the loading of Tween 20 increased, the loading of EGCG decreased at a greater rate than the decrease observed with the loading of naringenin. Therefore, EGCG loaded liposomes may appear more elastic however, they contain less EGCG than their respective naringenin loaded liposomes thus allowing them to be more elastic at a loading of Tween 20.

4.4.5 Differential scanning calorimetry investigations of naringenin and naringenin lipid blends

Differential scanning calorimetry (DSC) is extensively used in its application in understanding the thermal characteristics of materials where an insight into a range of thermal properties including melting temperatures, phase transitions and heat capacity changes can be obtained. The investigations were carried out over the temperature range 0–300 °C with a heating rate of 10°C min⁻¹. The thermogram of naringenin is displayed in Figure 4.9. Naringenin showed a sharp endothermic peak (T_m) at 253 °C.

To substantiate the association of naringenin with the lipid/surfactant complex, DSC analysis was performed on, the lipid blend, and the naringenin-lipid/surfactant blend. In the lipid/surfactant mix a very small peak at 40 °C is noticeable, a larger peak at 172 °C and a medium peak at 212 °C. On the other hand naringenin–lipid/surfactant complex showed a

small peak at 40 °C and a large peak at 152 °C, differing from the peaks of the individual components of the complex (Figure 4.9). It is evident that the original peaks of naringenin and phospholipids disappear from the thermogram of complex and the phase transition temperature is lower than that of naringenin as there is no sharp peak around 253 °C.

The T_m of Naringenin corresponds with similar studies (Khan et al., 2015; Semalty et al., 2010b). Furthermore, Semalty *et al.*, observed the association of naringenin with soy phosphatidylcholine. PC showed a smaller peak at 64.45 °C and major peaks at 83.21 °C and 107.90 °C. They suggested the first peak was probably due to the hot movement of the phospholipids polar head group. The second peak was assumed to be due to phase transition from gel to liquid crystalline state. The non-polar hydrocarbon tail of phospholipids may be melted during this phase, yielding a sharp peak. This melting might have occurred in two phases which subsequently gave the next peak. The naringenin–PC complex showed two peaks at 51.23 °C and 62.21 °C, which is different from the peaks of the individual components of the complex. Therefore Semalty *et al.*, also found that the original peaks of naringenin and PC disappear from the thermogram of the blend and the phase transition temperature is lower than that of naringenin alone.

This interaction may be a result of hydrophobic interaction and/or hydrogen bonding (Semalty et al., 2010a). The –OH groups of the phenol rings of naringenin may be involved in hydrogen bonding and the aromatic rings may be involved in any hydrophobic interaction. Consequently, the major sharp peaks of phospholipids disappear and decrease the phase transition temperature.

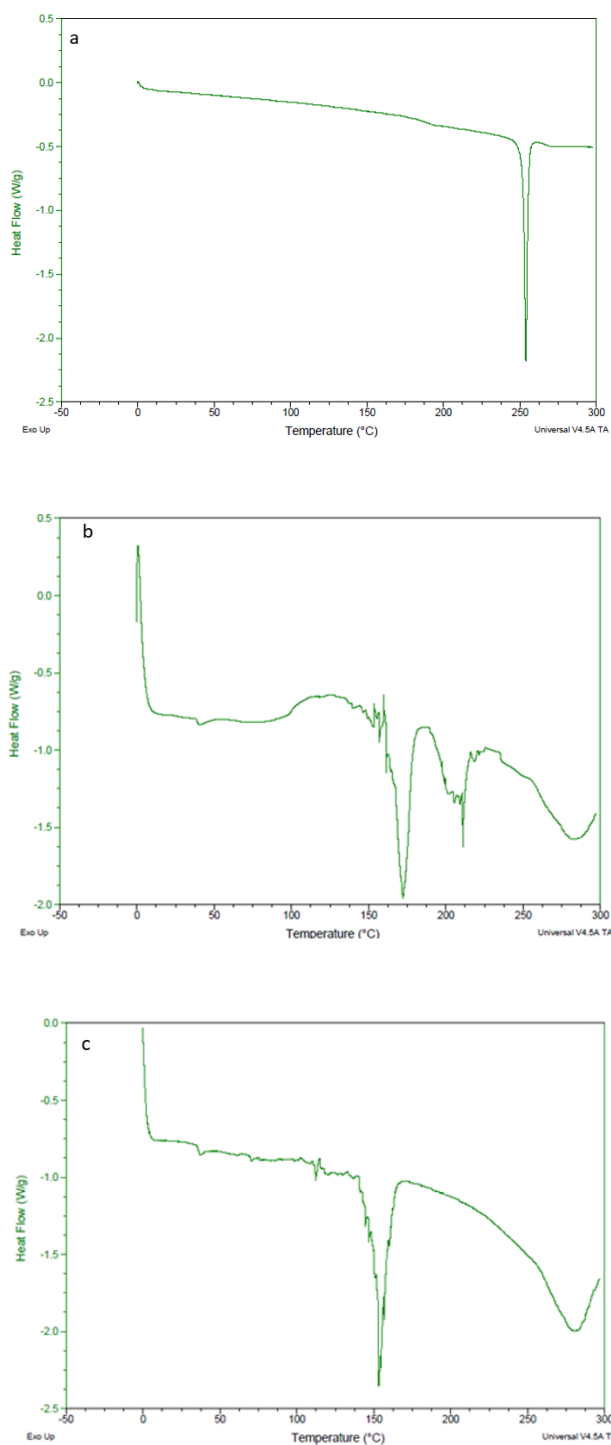


Figure 4.9: DSC scan of naringenin and lipid blends.

DSC scan of a) naringenin b) PC, cholesterol and Tween 20 blend and c) PC, cholesterol, Tween 20 and naringenin blend. All experimental runs commenced at an initial temperature of 0°C with a scan rate of 10 °C/min to 300 °C. The peak in a) shows the melting point (T_m) of naringenin was at 253 °C. The T_m of the lipid mixture is 172 °C, and upon addition of naringenin, the T_m was 152 °C.

These DSC data are supported with the results of DSC thermograms of the phospholipid complexes of some phytoconstituents including silybin, puerarin and curcumin in which the thermogram of the complex also exhibited a single peak which was different from the peak of phytoconstituents and the phospholipids (Kumar et al., 2008; Li et al., 2008; Maiti et al., 2007; Yanyu et al., 2006).

4.4.6 Naringenin release studies

4.4.6.1 Naringenin release studies from gel formulations

Liposomes employed in dermal drug delivery systems must be delivered in a carrier due to the liquid nature of the preparation. The viscosity and application properties can be adjusted by incorporating in an appropriate vehicle. Liposomes are known to be compatible with viscosity increasing agents such as cellulose based gels (Foldvari, 1996). These are established as safe in topical, dermal and transdermal delivery (Forbes et al., 2011b; Hascicek et al., 2009; Patton et al., 2007). Simple HEC and HPMC gel formulations were employed to compare as carriers of liposomal preparations.

As with release studies for EGCG detailed in section 3.4.7.1, two geometric systems have been considered for naringenin release from gel systems; three-dimensional leaching from a cylinder of gel (one compartment release) and unidirectional leaching across a planar surface (two compartment release). A one compartment model was used to study release and gel swelling behaviour whilst a two compartment diffusion cell observed drug release across a membrane. A polycarbonate membrane with 50 nm was used to mimic the stratum corneum and the gaps in between the keratinocyte cells. The composition of both HPMC and HEC gels was kept at 3% w/v. The release of drug from a formulation is determined by many factors including diffusion, and erosion of matrices followed by dissolution of drug. Such dissolution/release tests are required to help predict *in vivo* behaviour and to study the structure of the dissolving matrix.

4.4.6.1.1 One compartment release studies

Naringenin release from the aqueous HEC and HPMC gels loaded with 1% w/w naringenin into DDM was studied over a 24-hour period (section 4.3.9.1) (Figure 4.10).

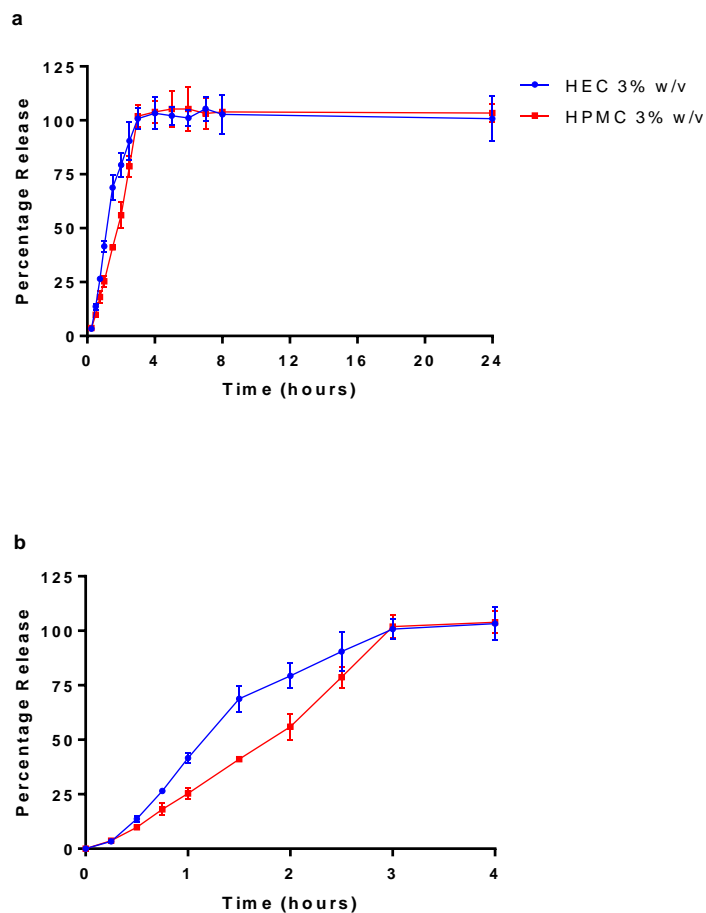


Figure 4.10: Naringenin release profiles from aqueous gels

Naringenin release profiles from aqueous HEC and HPMC gels (3% w/v) over a) 24 hours, b) 4 hours was observed. Data represents mean \pm SD. n=3 independent batches.

HEC and HPMC gels displayed a similar pattern of release into the DDM. It is clear however that at 3% w/v loading of polymer, HPMC could retard drug release to a greater degree up until 3 hours at which time 100% of compound was released, HEC consistently had a higher cumulative percentage of drug released (at 1.5 hours HEC released 68% of Naringenin compared with 41% from HPMC). Similar trends were observed with EGCG. At the point of complete release, the gel was observed to have completely dissipated into the release media.

As discussed in section 3.4.7.1.1, the diffusion of solution out of the polymer depends on temperature, pressure, viscosity and solute size. Diffusion in polymers is complex and the diffusion rates should lie between those in liquids and in solids. Solvent diffusion is associated with the physical properties of the polymer network and the interactions between the polymer and solvent (Masaro and Zhu 1999). Furthermore, molecular geometry has been observed to influence compound release from polymer networks (Ford, Rubinstein et al. 1987, Rao, Devi et al. 1990).

The principal mechanism of compound release is the net consequence of drug diffusion due to the concentration gradient, macromolecular relaxation of the polymer chains which causes drug diffusion outward with a kinetic behaviour dependent on the relative ratio of diffusion and relaxation and due to the fact cellulose derivatives have limited solubility for lipophilic compounds thus the compound would diffuse out of the gel (Forbes et al., 2011b; Lee, 1985). As water penetrates the glassy hydrogel matrix containing the dispersed drug, the polymer will swell thus its glass transition temperature is lowered. Simultaneously, dissolved drug diffuses through this swollen network into the release medium (Bouwstra and Junginger, 1993; Gupta et al., 2002; Lee, 1985; Rao et al., 1990). The rate-controlling factor mediating drug release is the resistance of the polymer to a change in shape owing to an increase in volume (Ranga Rao and Padmalatha Devi, 1988).

Further, the addition of water-insoluble drug can increase the water uptake by the dosage form thus weakening the network integrity of the polymer, causing drug leaching (Sai Cheong Wan et al., 1995). The compound particles between polymer chains allow each chain to hydrate freely, which may result in weak hydrogen bonding areas around the drug molecule (Panomsuk et al., 1996). Additionally, the influence of drug on the swelling properties of the polymer matrix is largely dependent on the substituted groups of the polymer. The hydroxyl group in the molecules plays an important role in the matrix integrity of the swollen hydrophilic cellulose matrices. The amount and properties of the incorporated drug determine matrix integrity (Nafee et al., 2003). In this case, similar to release observed with EGCG, it appears the HEC matrix eroded/swelled quicker than HPMC giving a faster rate of release.

4.4.6.1.1.1 Kinetic assessment

Release profiles were evaluated by zero-order, first-order and Higuchi kinetics model (Table 4-2). As with EGCG, release from the gels were observed to fit the first order release model best as the r^2 values were highest upon comparison with those for the zero order model and the Higuchi model (for example for 3% w/v HEC the r^2 values were -1.4, 0.92 and 0.33 for the zero order, first order and Higuchi model respectively). Thus, drug was released at a constant rate in proportion to the amount of drug available at that time. As discussed in section 3.4.7.1.1, other studies have found the other models better at describing release from polymer gel systems but this was dependent on formulation parameters. This was a simple gel formulation and no further investigation into kinetic release model was carried out.

Table 4-2: Kinetic assessment of release data of naringenin from HEC and HPMC aqueous gels.

Kinetic model	Formulation r^2	
	HEC (3% w/w)	HPMC (3% w/w)
Zero order	-1.434 ± 0.170	-0.686 ± 0.071
First order	0.923 ± 0.007	0.896 ± 0.013
Higuchi model	0.330 ± 0.095	0.539 ± 0.021

Results are presented as the mean ± standard deviation (n=3)

Comparison of the rate constant between formulations found HEC to have a larger rate constant than HPMC (Table 4-3). This shows HEC gave a faster release of naringenin per unit time. Drug is released from gel by the creation of pores due to swelling, as viscosity increases polymer chains becoming more resistant to movement as they are physically restricted thus taking longer to dissipate into the media thus slowing release drug. This implies HPMC had a greater viscosity than HEC.

Table 4-3: First order kinetics rate constant for naringenin release from formulations

Rate constant (min ⁻¹)	
HEC 3% w/v	HPMC 3% w/v
0.011 ± 0.001	0.009 ± 0.000

Results are presented as the mean ± standard deviation (n=3)

The Korsmeyers-Peppas model was applied to the release data and the diffusional exponent (I) calculated (Table 4-4). Fickian release (case I) was observed for both polymers at 3% w/v. A study by Ritger and Peppas found both Fickian and anomalous release from swellable devices (Ritger and Peppas, 1987). Additionally, a study using the polymer HPC observed both Non-Fickian and Super Case II transport (Alfrey Jr et al., 1966; Ranga Rao et al., 1988).

Table 4-4: Diffusional exponent n calculated from the Korsmeyer-Peppas model of drug release for naringenin release data from aqueous gels with the corresponding release mechanism.

Formulation	n	Transport type
HEC 3% w/v	0.285 ± 0.015	Fickian
HPMC 3% w/v	0.341 ± 0.007	Fickian

Results are presented as the mean \pm standard deviation (n=3)

Fickian diffusion from polymer networks is regularly observed when the temperature is above the glass transition temperature of the polymer (T_g). In this state, the polymer chains have a higher mobility allowing easier penetration of the solvent (Masaro and Zhu, 1999). Thus in this study it may be deduced that the polymer chains were able to move sufficiently, the gel was in a rubbery state.

4.4.6.1.2 Two compartment release

Release of naringenin from HEC and HPMC gel formulations at polymer loading of 3% w/v in a two-compartment model using a diffusion cell was also observed. Release across a 50 nm polycarbonate membrane was observed. This was compared against release from solution in the donor compartment into the receiver compartment. Naringenin loaded gels were prepared (section 4.3.8) and release over 24 hours observed.

Gels appeared to slow the release of naringenin with HPMC proving to be more pronounced than HEC in this phenomenon (Figure 4.11). Over 24 hours, the solution gave 54.5 ± 4.2 % release whilst HEC and HPMC saw a 33.1 ± 2.0 and 31.1 ± 1.0 % release respectively. The release profile was significantly different between HPMC and both solution and HEC ($P \leq 0.001$). There was no significant difference in the release profile of naringenin from solution and the HEC gel implying HPMC is better at compound retardation in this case. Comparison between the gels found that HEC at its respective loading of polymer in the HPMC gels, consistently resulted in a faster release of drug (at the time point of 3 hours, 9.8 ± 0.5 % was released in comparison to 5.6 ± 0.2 %). Therefore, drug release was faster from the HEC gel compared to the HPMC gel.

The addition of water-insoluble drug can increase the water uptake by the dosage form thus weakening network integrity thus drug loading will influence network integrity (Nafee et al., 2003; Panomsuk et al., 1996). In this case, it appears the HEC matrix eroded/swelled quicker than HPMC giving a faster rate of release. This is in contrast with a study comparing the release of miconazole from a 1.5% w/v HEC formulation with a 3% HPMC w/v formulation

where a faster erosion was observed from the HPMC matrix (even at double the polymer loading) (Nafee et al., 2003). This highlights how the physiochemical properties of the drug, the polymer and the interaction between the two affect drug release from the formulation.

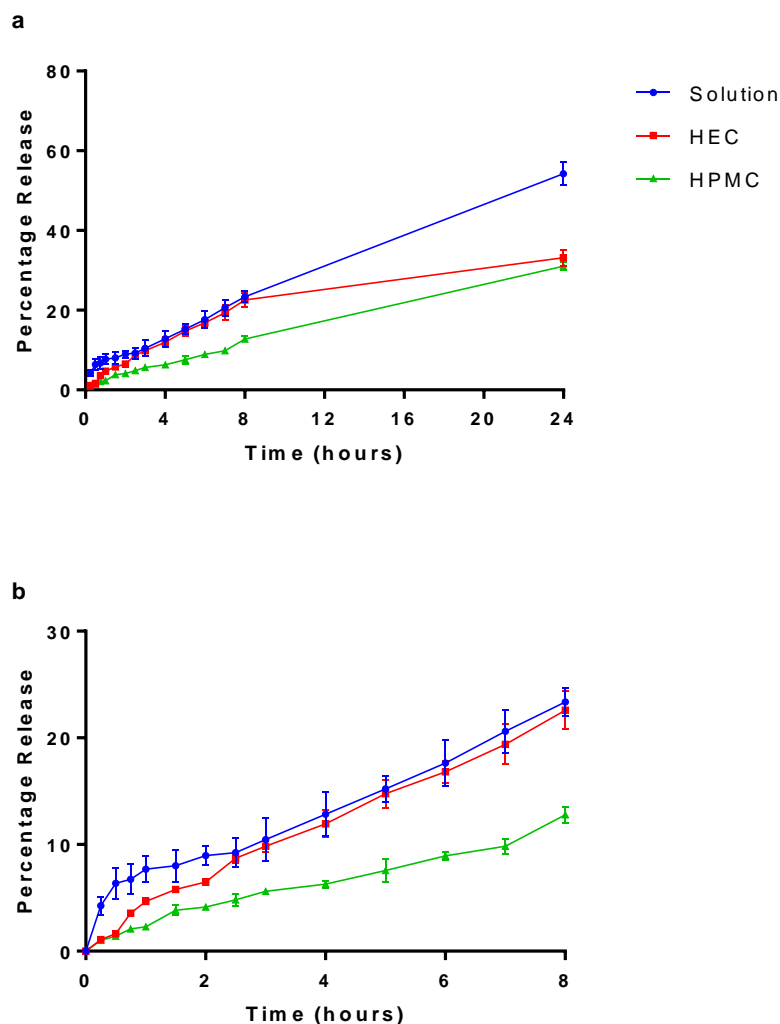


Figure 4.11: *In vitro* percentage naringenin release profiles from aqueous gels

Naringenin release profiles from HEC and HPMC (3% w/v) aqueous gels with 1% w/v naringenin and naringenin solution over a) 24 hours, B) 8 hours. Data represents mean \pm SD. n=3 independent batches.

Comparison of the release of naringenin to the release of EGCG from aqueous solution, HEC and HPMC observed a greater EGCG to have a greater rate of release from all formulations. After 24 hours, a release of 105 ± 4.9 , 92 ± 4.9 and 109 ± 7.3 % EGCG from aqueous solution, HEC and HPMC was observed compared with 54.5 ± 4.2 , 33.1 ± 2.0 and 31.1 ± 1.0 % release of naringenin. This may be due to the amphiphilic nature of EGCG, this compound has a solubility of ≥ 5 mg/mL (Sigma-Aldrich(e), 2017) compared with naringenin which is insoluble

in water at room temperature (Wen et al., 2010b). This would mean that EGCG would solubilise in water and diffusion would allow this compound to move across the polycarbonate membrane. Naringenin however may solubilise at a slower rate (due to the experimental conditions maintaining the environment at 35°C) therefore have a slower rate of release from any formulation.

4.4.6.1.2.1 Kinetic assessment

The release profiles were evaluated by the zero-order, first-order and Higuchi kinetic models. Release from the solution was observed to fit the first order release model best as the r^2 values were highest upon comparison with those for the zero order model and the Higuchi model (the r^2 values were 0.91 and 0.96 for the zero order and first order model respectively) (Table 4-5). This indicates rate of release was dependent on the amount of drug present at that time point. Release from the HEC gel fit the Higuchi model release model whereas release from the HPMC gel followed the first order release model (r^2 values of 0.93 and 0.99 respectively).

Following a kinetic analysis, a study formulating HEC gels at 7.5% w/w with 1% w/w of drug observed release to fit the Higuchi model. This may be due to differences in formulation, and differences in experimental parameter including their use of Franz diffusion cells with only a thin film of gel spread over the membrane (Hascicek et al., 2009).

Table 4-5: Kinetic assessment of release data of naringenin from solution and aqueous gels.

Kinetic model	Formulation r^2		
	Solution	HEC (3% w/w)	HPMC (3% w/w)
Zero order	0.917 ± 0.022	0.645 ± 0.116	0.970 ± 0.012
First order	0.964 ± 0.021	0.789 ± 0.085	0.985 ± 0.004
Higuchi model		0.933 ± 0.012	0.822 ± 0.023

Results are presented as the mean ± standard deviation (n=3)

Comparison of the rate constant of each formulation shows that HEC had a higher rate constant than HPMC (Table 4-6). This implies that HPMC had a higher gel consistency thus slowing naringenin release. Naringenin is released from gel by the creation of pores due to swelling, as viscosity increases polymer chains becoming more resistant to movement as they are physically restricted consequently taking longer to dissipate into the media thus slowing drug release. This data is consistent with that of EGCG.

Table 4-6: First order kinetics rate constant for naringenin release from formulations

Rate constant (min ⁻¹)		
Solution	HEC (3% w/w)	HPMC (3% w/w)
$5.9 \times 10^{-4} \pm 1.3 \times 10^{-4}$	0.852 ± 0.018	$2.7 \times 10^{-4} \pm 7.1 \times 10^{-6}$

Results are presented as the mean \pm standard deviation (n=3)

The Korsmeyers-Peppas model was applied to the release data and the diffusional exponent (n) calculated (Table 4-7). Non-Fickian release was observed for both HEC and HPMC gels at 3% w/w polymer. A study by Ritger and Peppas found both Fickian and anomalous release from swellable devices (Ritger and Peppas, 1987). Additionally, a study using the polymer HPC observed both Non-Fickian and super case 11 transport (Alfrey Jr et al., 1966; Ranga Rao et al., 1988).

At temperatures below the T_g , the polymer chains are not sufficiently able to move to permit immediate penetration of the solvent in the polymer core (Masaro and Zhu, 1999). This implies that, in our studies, when Non-Fickian transport was observed, the polymer chains were unable to move sufficiently and that at those particular loadings of polymer, the gel was in a glassy state.

Table 4-7: Diffusional exponent n for naringenin release data with the corresponding release mechanism.

Formulation	n	Transport type
HEC (3% w/v)	0.590 ± 0.041	Non-Fickian
HPMC (3% w/v)	0.851 ± 0.036	Non-Fickian

Results are presented as the mean \pm standard deviation (n=3)

Diffusion of solution out of the polymer is known to depend on temperature, pressure, solute size and viscosity. Diffusion in polymers is complex and the diffusion rates should lie between those in liquids and in solids. It depends strongly on the concentration and degree of swelling of polymers. Solvent diffusion is associated with the physical properties of the polymer network and the interactions between the polymer and solvent (Masaro and Zhu 1999). Furthermore, a study using the molecular weight of the drugs as an approximation of molecular size could not find a relation to release rates. This indicates that molecular geometry plays a role in compound release from polymer networks (Ford, Rubinstein et al. 1987, Rao, Devi et al. 1990).

It has been suggested that drug release from aqueous gels is governed by a swelling-controlled mechanism in which the drug releases into the media due to the simultaneous absorption of water by the gel causing the gel to dissipate into the media thus releasing drug and due to desorption of drug from the gel (Bouwstra and Junginger, 1993; Nafee et al., 2003; Ranga Rao and Padmalatha Devi, 1988; Sinha Roy and Rohera, 2002). The rate-controlling factor mediating drug release is the resistance of the polymer to a change in shape owing to an increase in volume (Ranga Rao and Padmalatha Devi, 1988). The membrane would have prevented the gel from completely swelling and releasing drug, whilst water could move across it, the polymer did not have much room to swell as the donor compartment was filled to near capacity. This can be likened to the skin in the sense that the skin is a barrier, as well as the polymer chains would slow the movement of drug into the skin.

4.4.6.2 Naringenin release from liposomes

Deformable liposomes have been successfully used in transdermal delivery of lipophilic and hydrophilic drugs (Cevc and Blume, 2001; El Maghraby et al., 1999; Oh et al., 2006; Romero et al., 2013). The use of elastic liposomes as drug carriers across the stratum corneum for dermal drug delivery is advantageous as they can penetrate the skin if applied non-occlusively by virtue of the very high and self-optimizing deformability. Liposomes can penetrate the stratum corneum with potentially deeper penetration into the dermal layer of deformable vesicles compared with traditional liposomes (El Maghraby et al., 1999). Release of naringenin from 0.1mg /10mL solution, liposomes and liposomes formulated with either 2%, 6% or 10% w/w of Tween 20 with was studied over a 24 hour period (Figure 4.12).

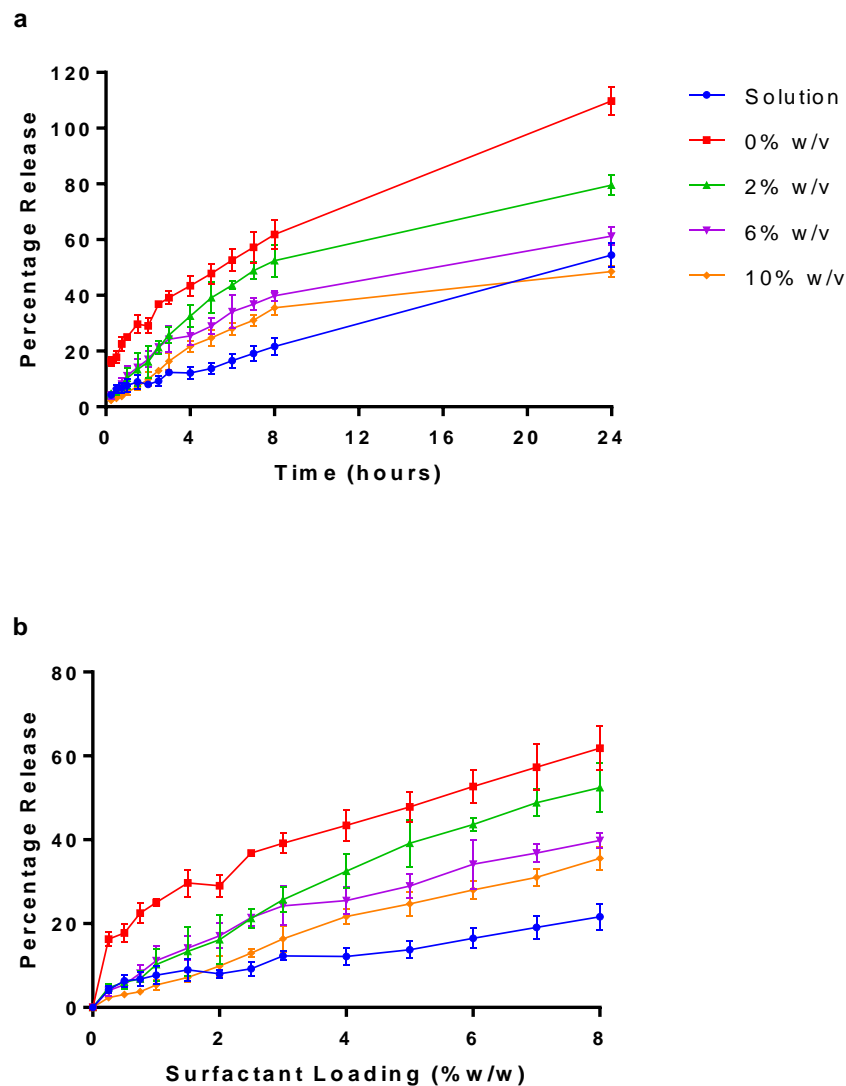


Figure 4.12: *In vitro* percentage naringenin release profiles from solution and liposomes

Liposomes were formulated with 0-10 % w/w Tween 20 and release was observed over a) 8 hours, b) 24 hours. Liposomes were prepared adapting the dry film method adding the surfactant and naringenin during the lipid mixing stage. A diffusion cell dialysis system was used to evaluate *in vitro* drug release. Data represents mean \pm SD. n=3 independent batches.

A higher percentage of naringenin was released from liposomes compared with drug solution. Over the course of 24 hours solution gave a release of 54.5 ± 4.2 % whilst liposomes formulated with 0%, 2%, 6% and 10% w/w of Tween 20 gave a release of 109.7 ± 5.0 %, 79.5 ± 3.7 %, 61.3 ± 3.4 % and 48.5 ± 2.1 % respectively. The cumulative percentage released after 24 hours was significant between the solution and liposomes loaded with 0 and 2% w/w of Tween 20 as well as between all liposomal formulations ($P \leq 0.0001$ and $P \leq 0.01$ between liposomes loaded with 6 and 10% Tween 20).

As the loading of Tween 20 increased, the release from the liposomes slowed. This is in contrast with release of EGCG from the same formulations in which solution gave the fastest

release of drug and EGCG release increased with increased surfactant loading. This may be because at higher loadings of surfactant, less EGCG was loaded into the liposomes therefore the amount of surfactant available may have been able to solubilise EGCG thus aid the release of it from the liposomes. Release of naringenin observed significant differences over 24 hours between release from solution and 0% w/w Tween 20 ($P \leq 0.0001$) as well as, 2 and 6% w/w Tween 20 ($P \leq 0.01$). Release between 0 and 2, 6 and 10% w/w Tween 20 liposomes was significantly different ($P \leq 0.0001$). The release profile was between 10% w/w Tween 20 and 2 and 6% w/w was also significantly different ($P \leq 0.01$ and $P \leq 0.0001$ respectively).

As surfactant loading increased, drug entrapment decreased, therefore, drug release would be expected to be slower as there is less of a concentration gradient. Furthermore, the drug is hydrophobic therefore less inclined to diffuse out of the hydrophobic liposome bilayer into the media. At higher concentrations of drug, if the bilayer becomes saturated with the drug, more would diffuse out of the liposome.

4.4.6.2.1 Kinetic assessment of naringenin release from liposomal formulations

Release data from the solution and all liposomal formulations complied with first order release kinetics implying rate of drug release was dependent on drug concentration at that time (Table 4-8).

A study comparing the deposition of naringenin in the skin from elastic liposomes and saturated solution found elastic liposomes (zero-order release) formulated with Tween 80 increased the deposition of naringenin in the skin significantly (by about 7.3~11.8-fold) compared with the saturated aqueous solution. Another study also found elastic liposomes were able to increase drug permeation into the skin in comparison to a conventional cream (2 fold) (Goindi et al., 2013). Our studies do imply liposomal carriers would be able to increase permeation however, further studies with excised skin would have to be carried out to see if the same results can be achieved with Tween 20. It has been suggested that the mechanism of the *in vitro* release seems to be the formation of transient pores in the lipid bilayer, through which drugs are released from the inner aqueous core of the liposomes to the extra-liposomal medium (Wang et al., 2016).

Table 4-8: Kinetic assessment of release data of naringenin from solution and liposomal formulations.

Kinetic model	Formulation (r^2)				
	Solution	Liposome (% w/w loading of Tween 20)			
		0	2	6	10
Zero order	0.917 ± 0.022	0.327 ± 0.362	0.600 ± 0.150	0.385 ± 0.292	0.558 ± 0.079
First order	0.964 ± 0.021	0.855 ± 0.095	0.981 ± 0.015	0.815 ± 0.125	0.828 ± 0.027

Results are presented as the mean ± standard deviation (n=3)

Comparison of the rate constant of each formulation shows liposomes formulated with 0% w/w Tween 20 had the highest rate of release, followed by liposomes formulated with 2% w/w Tween 20, then 6% w/w Tween 20, naringenin solution and then liposomes formulated with 10% w/w of Tween 20 (Table 4-9).

Table 4-9: First order kinetics rate constant for naringenin release from formulations

Rate constant ($\times 10^{-3} \text{ min}^{-1}$)				
Solution	Liposome formulation (% w/w loading of Tween 20)			
	0% w/w	2% w/w	6% w/w	10% w/w
5.85 ± 1.29	2.69 ± 1.4	1.59 ± 0.57	1.07 ± 0.22	0.74 ± 0.12

Results are presented as the mean ± standard deviation (n=3)

As discussed in section 3.4.7.2.1 in dynamic dialysis drug appearance in the receiver compartment is the result of diffusion from liposomes followed by diffusion across the membrane, though it is generally treated as a simple first-order process (Modi and Anderson 2013). The driving force of drug movement is dependent on free aqueous drug concentration. Therefore, the reliability of rate constants determined by dynamic dialysis must be carefully considered (Modi and Anderson, 2013). The release data observed will be either as a consequence of drug release from the liposome and then the membrane or movement of the liposome across the barrier and then release from this. The diffusion cell system will see

release from the liposome first owing to the physical set up of the cell and the smaller pore size of 50 nm.

Furthermore, reversible binding of the drug released from the liposome reduces the driving force for drug transport across the dialysis membrane leading to a slower overall apparent release rate (Modi and Anderson, 2013). In this case, this reversible binding was greater as surfactant loading increased resulting in a slower rate of release for liposome formulated with 10% w/w Tween 20 in comparison to liposomes formulated with no Tween 20.

4.4.6.3 Liposomal gel naringenin release studies

Drug release from liposomal gels could not be measured/detected in the side by side diffusion chamber therefore a different method using 6- well Thincert plate and 4 cm² cylindrical cell culture Thincert™ insert with 400 µm pore size was employed. Neither the diffusion cell nor the insert mimic what would happen following formulation application on the skin. The diffusion cell observed how drug diffused across a membrane with a pore size similar to that of the gaps in the SC whilst maintaining sink conditions. The plate with inserts was used simply to observe ability of drug release from a liposomal gel. To ensure we were only detecting free drug samples were centrifuged and supernatant analysed. Naringenin release from liposomal gels is displayed in Figure 4.13.

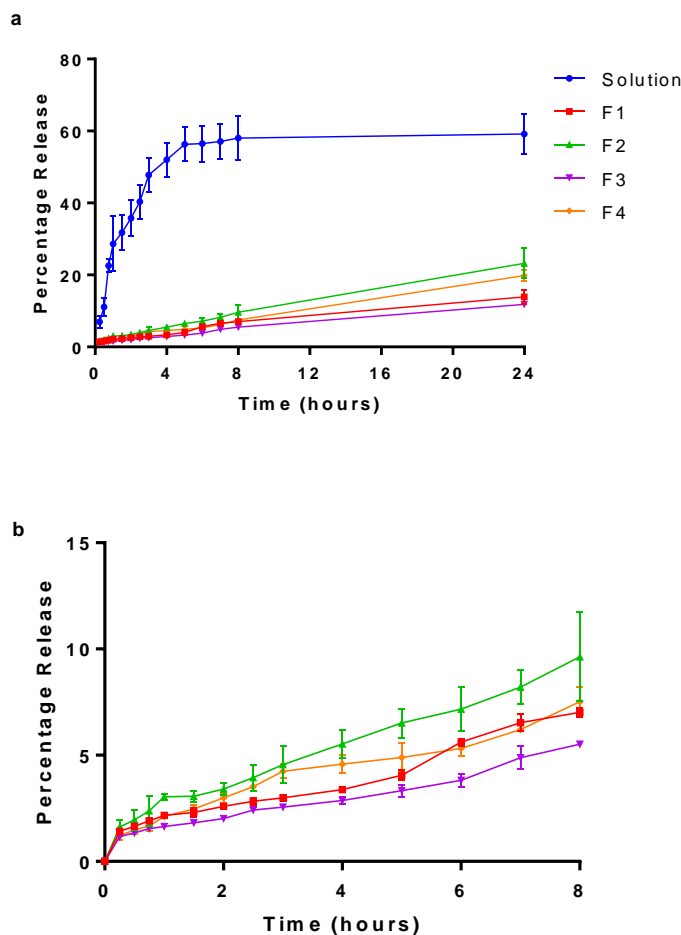


Figure 4.13: *In vitro* percentage naringenin release profiles from liposomal gels

Naringenin release profiles using a transwell system with permeable inserts of a 400nm pore size from solution and gel loaded with either blank or elastic liposomes formulated with 2% w/w Tween 20 over a) 24 hours, b) just liposomal gel formulations. F1: HEC and blank liposomes, F2: HEC and elastic liposomes, F3: HPMC and blank liposomes, F4: HPMC and elastic liposomes. Gels were prepared using 3% w/v loading of either HEC or HPMC with a 1% w/w of drug loading. Liposomes were prepared adapting the dry film method. Data represents mean \pm SD. n=3 independent batches.

Drug release from solution seemed to reach a maximum between the 4th and 5th hour (~55%). Solution saturation may have been reached beyond this point thus appearing as though 100% release was not achieved. Over all the percentage of drug release from the liposome loaded gels quantified over 24 hours was slightly higher from the HEC gel (up to 23%). Furthermore, a higher percentage of drug was released from the elastic liposome (up to 23%). This followed the same trend as seen with EGCG liposomal gels.

Over the course of 24 hours solution gave a release of 59.2 ± 5.6 % whilst F1, F2, F3 and F4 gave a release of 13.9 ± 2.0 %, 23.2 ± 4.1 %, 11.8 ± 0.4 % and 19.8 ± 1.5 %, respectively. The cumulative percentage released after 24 hours was significant between the solution and all liposomal gels ($P \leq 0.0001$). The difference was also significant between F1 and F2 as well as

between F2 and F3. F1 and F3 contained no surfactant in the liposome and F2 and F4 contained 2% w/w of Tween 20. Therefore, release in the liposomal gels appeared to be affected by presence of surfactant in liposomal gels formulated with HEC but not HPMC.

This indicated that either elastic liposomes were more able to move through the HEC gel compared with blank liposomes (movement based on weight of liposomes, being denser hence sedimenting within the gel) or that the presence of surfactant increased the solubility of drug thus encouraging release from the liposome bilayer. (Some gel could possibly have seeped through the inserts which could result in false higher drug detection toward the end of this study). A study observing lidocaine HCL release from liposome loaded gels had similar results with hydrogel formulations having a faster release rate of lidocaine HCl compared to liposomal gel formulations (Glavas-Dodov et al., 2002).

As discussed in section 3.4.8.3, drug properties (solubility, log P) as well as liposome stability when formulated as part of a gel system determines the entire system behaviour and thus drug release (Mourtas et al., 2007).

4.4.7 Impact of liposomal formulation on *In vitro* cytotoxicity on HDFa and HaCat cells

To assess the toxicity of naringenin on HDFa and HaCat cells, an XTT assay was performed to measure cell death after exposure of cells to different concentrations of drug for 24 hours. Results of cell viability are shown in Figure 4.14.

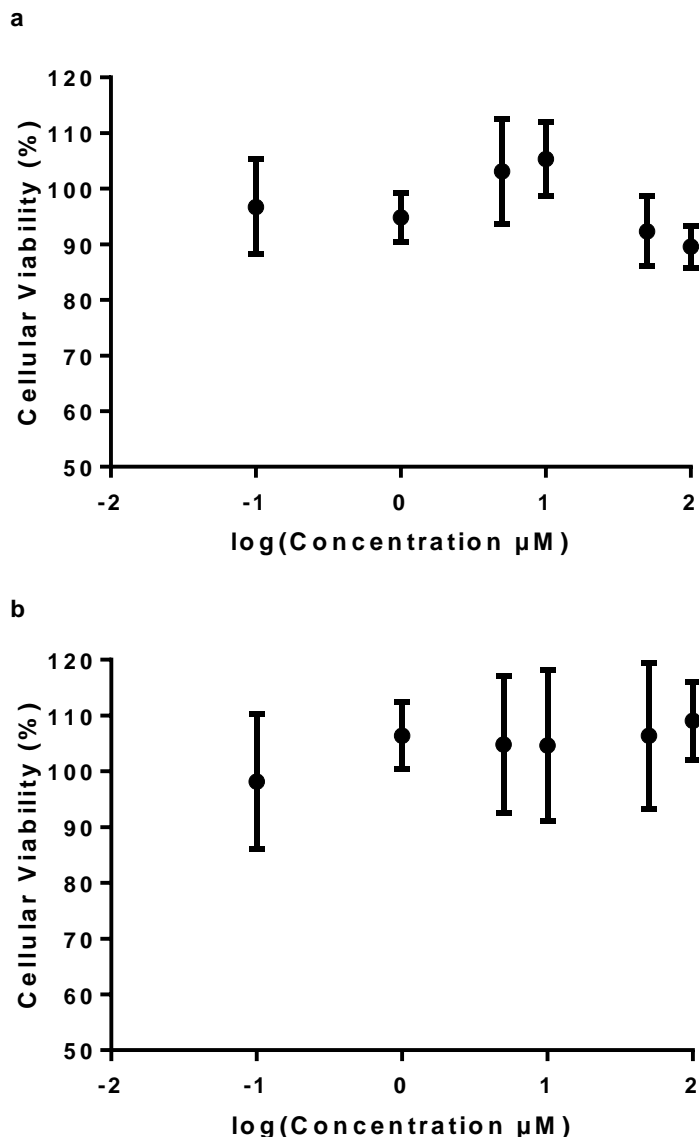


Figure 4.14: Cellular toxicity of naringenin towards HDFa and HaCat cells.

Cellular toxicity of naringenin a), HDFa b), HaCat cells. Cells were grown on a 96-well plate at a density of 50×10^3 cells per well and exposed to various concentrations of naringenin (0.1 – 100 μM). After 24 hour incubation following which 25 μL of a 12.5:1 parts mixture of XTT to menadione was added each well. Plates were incubated for 3 hours at 37°C and the absorbance read at 450 nm. The control cell (without drug) corresponded to a cell viability of 100%. Data is reported as mean \pm SD with 6 replicates per compound in at 3 independent experiments.

As the concentration of naringenin was increased, no decrease in HDFa cell viability when compared with the control well was observed. As the concentration of naringenin was increased on the keratinocytes, no change in cell viability was observed. Any differences in these percentages was not significant ($P = 0.4246$) therefore, at these concentrations naringenin was not toxic to this line of keratinocytes.

4.4.8 Cellular uptake assay on HDFa and HaCat cells

Fluorescently labelled liposomes loaded with naringenin were incubated with both HDFa and HaCat cells to assess the cellular uptake of these formulations. Following a 2-hour incubation with the cells, the labelled liposomes were identified using confocal microscopy (Figure 4.15, 4.16, 4.17 and 4.18). Cytoplasmic accumulation of the formulations was apparent, confirming the successful uptake into both HDFa and HaCat cells.

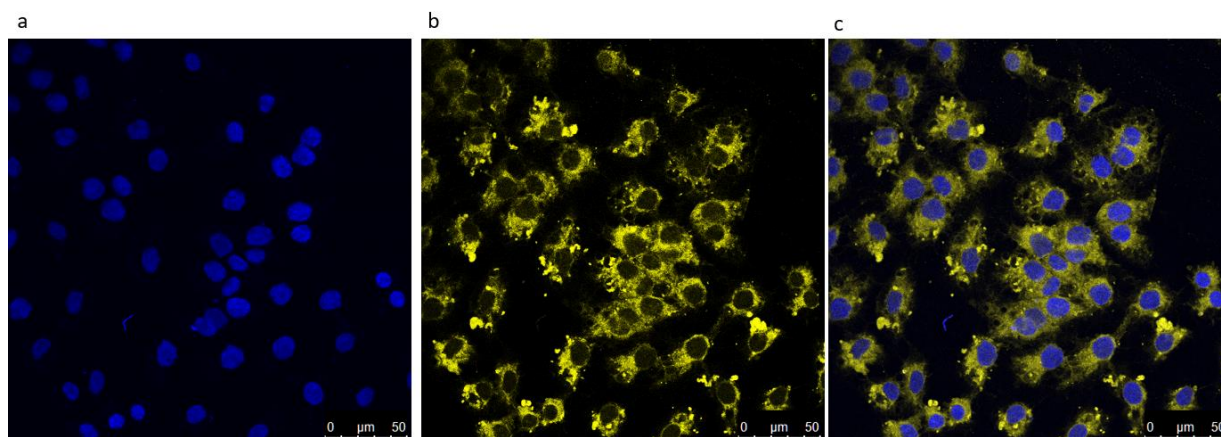


Figure 4.15: Localisation of DilC-naringenin loaded liposomes in HaCat cells

Localisation of DilC labelled liposomes loaded with naringenin and 2% w/w Tween 20 in HaCat cells. Cells were grown on the coverslips for 2 days. Cell nuclei were visualised using a) DAPI (Blue). Liposomes were formulated with DilC for visualisation b) (yellow). Liposome localisation within the cell is shown in the merged image c).

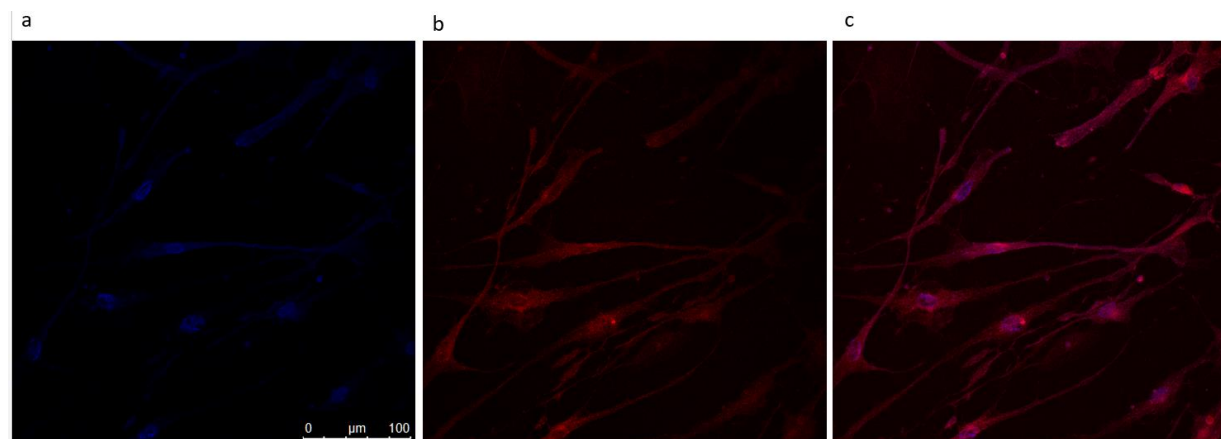


Figure 4.16: Localisation of DilC-naringenin loaded liposomes in HDFa cells

Localisation of DilC labelled liposomes loaded with naringenin and 2% w/w Tween 20 in HDFa cells. Cells were grown on the coverslips for 2 days. Cell nuclei were visualised using a) DAPI (Blue). Liposomes were formulated with b) DilC for visualisation (red). Liposome localisation within the cell is shown in the merged image c).

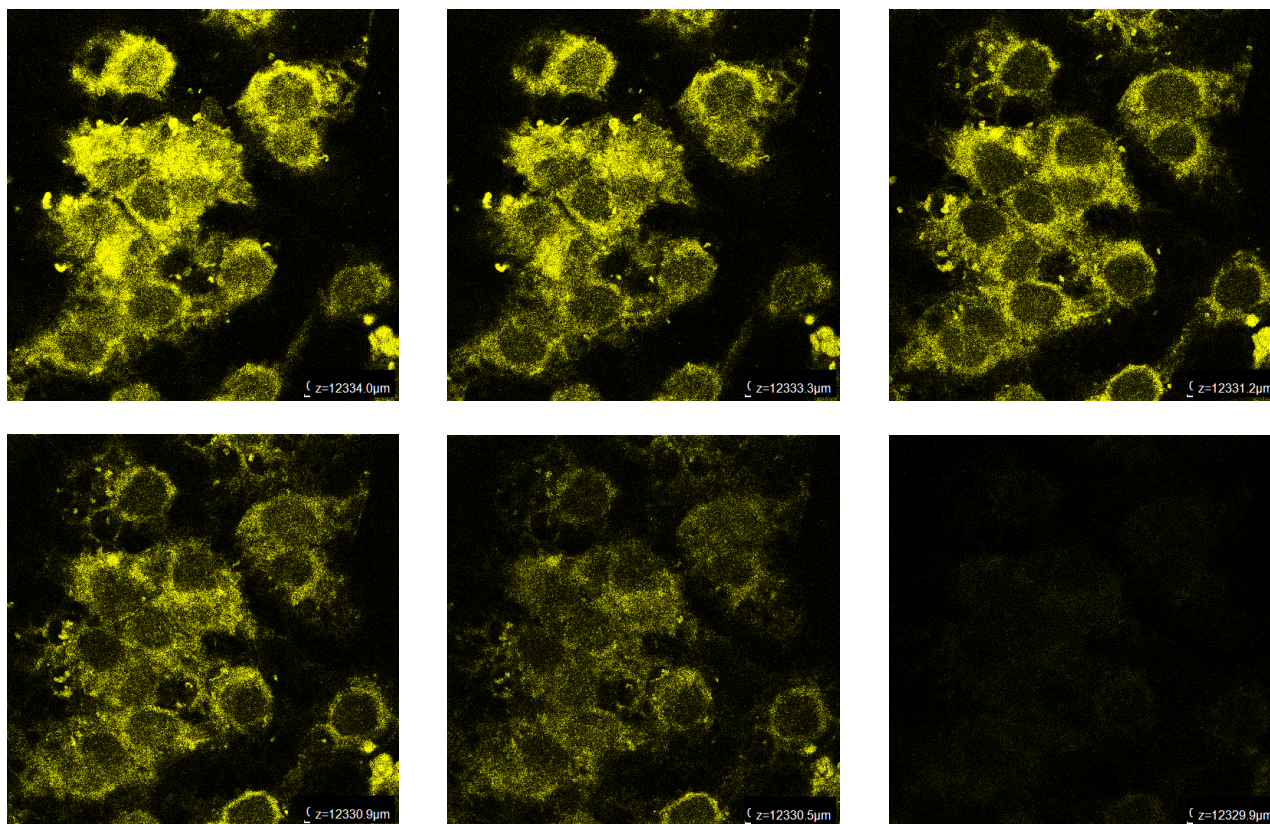


Figure 4.17: z-dimension cellular localisation of DiIC-naringenin loaded liposomes formulated with 2% w/w Tween 20 in HaCat cells

z-dimension cellular localisation of DiIC labelled liposomes loaded with naringenin and 2% w/w Tween 20 (stage 2). DiIC labelled liposomes previously incubated with HaCaT cells for 2 hours were further subjected to a z-stack analysis with the lens positioned above the cell layer (12216 μm) and lowered through the cells to the bottom of the cell layer (12210 μm). Images were captured of DiIC (green) through the z-dimension.

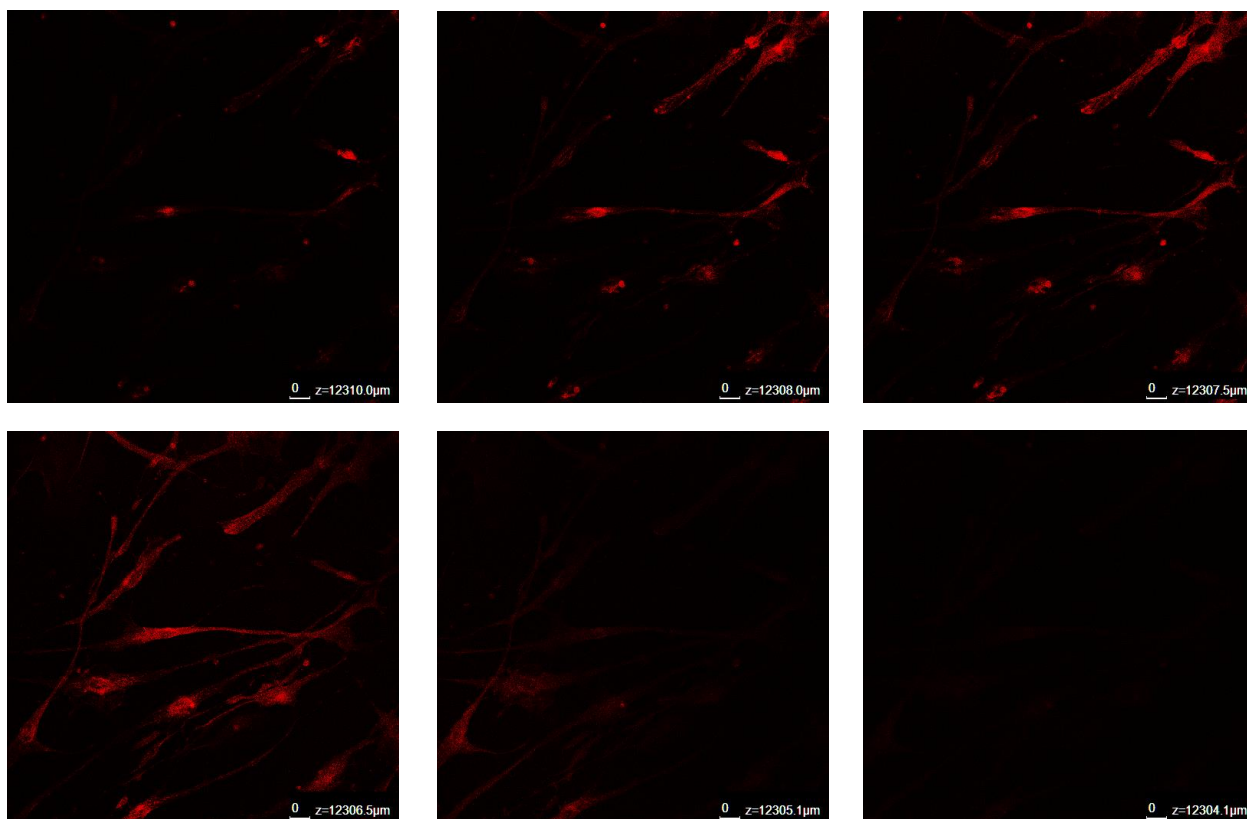


Figure 4.18: z-dimension cellular localisation of DiIC-naringenin loaded liposomes formulated with 2% w/w Tween 20 in HDFa cells

z-dimension cellular localisation of DiIC labelled liposomes loaded with naringenin and 2% w/w Tween 20 (stage 2). DiIC labelled liposomes previously incubated with HDFa cells for 2 hours were further subjected to a z-stack analysis with the lens positioned above the cell layer (12216 μm) and lowered through the cells to the bottom of the cell layer (12210 μm). Images were captured of DiIC (green) through the z-dimension.

The confocal stage was set at the upper-most boundary of the HDFa/HaCat cells and the stage moved down towards the coverslip with images captured over a z-dimension of approximately 5 μm . At the onset of the z-stack analysis, liposomes are localised on the exterior of the cell boundary and potentially on the surface of the cells (12334 μm). As the stage progresses, the localisation of FITC-Fan-MSNP increases with clear demarked zones of cytoplasmic localisation near the 'mid-to-bottom' regions of the cells (Figure 4.17 and 4.18).

There are four proposed methods of liposome interaction with cells as discussed in section 2.4.5: stable adsorption, endocytosis, fusion of the lipid bilayer with the cell plasma membrane and lipid transfer (Martin and MacDonald, 1976; Pagano and Weinstein, 1978). It is unclear which of these occurred in this study, however, these methods of uptake are not mutually exclusive and any combination occur in a given experimental circumstance (Pagano and Weinstein, 1978).

This formulation is aimed to be targeting the dermal layer. It is uncertain if the liposomes would completely pass through the keratinocytes into the dermal layer or whether they would accumulate in the SC. To be able to determine this, application onto excised skin would be necessary. Nonetheless it is clear liposomes were taken up by the cells, more importantly the fibroblasts thus the liposomes were successfully able to enter the cells.

4.4.9 Stability of deformable liposomes

The stability of deformable liposomes during storage at 20°C was studied in terms of size and, for drug loaded liposomes, encapsulation efficiency. Confocal images were observed on day 1 of formulation to ensure the presence of liposomes (Figure 4.19). The size of blank and surfactant loaded liposomes was measured on day 1, 2, 7, 14, 21 and 28 (Figure 4.20).

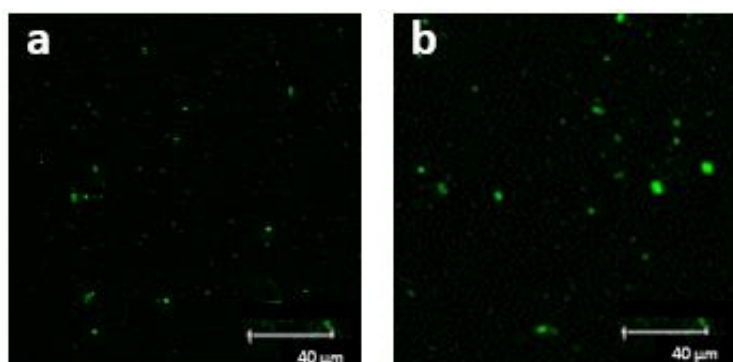


Figure 4.19: Confocal images of MLV liposomes formulated with 4% w/w Tween 20

Confocal images of MLV liposomes formulated with 4% w/w Tween 20 either a) blank, b) drug loaded. Fluorescently labelled liposomes were formulated by the addition of the fluorescent dye Dil C to the lipid mixing stage. The untrapped marker was removed by centrifuging liposomes, removing the supernatant, re-suspending in water. Liposomes were imaged using

an upright confocal microscope (Leica SP5 TCS II MP) and visualised with a 40× oil immersion objective.

Drug loaded liposomes formulated with no surfactant appear to decrease in size from 1217 nm to 556 nm over time. This was unexpected as usually, aggregation is noted resulting in vesicle size growth (Seras et al., 1992). This may be a result of larger, denser liposomes/aggregates settling as a creamy film which could be observed at the bottom of the cuvette.

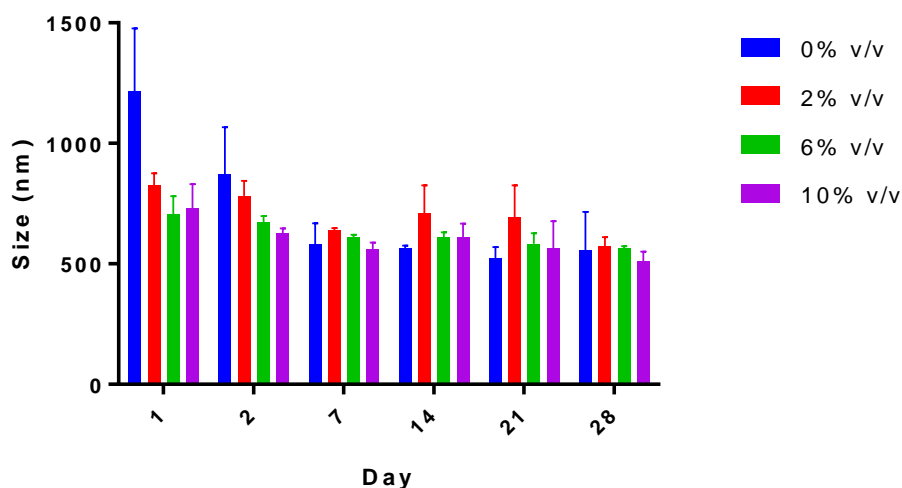


Figure 4.20: Stability of naringenin loaded liposomes as determined by size

Size of naringenin loaded liposomes formulated with 0-10% w/w Tween 20, using DLS, formulated with up to 10% w/w Tween 20 measured on various days (1, 2, 7, 14, 21 and 28). Liposomes were prepared adapting the dry film method. Liposome size was assessed via DLS. Data represents mean \pm SD. n=6 independent batches.

The inclusion of surfactant seemed to decrease this phenomenon to a degree. Formulations with 2% w/w, 6% w/w and 10% w/w observed a size decrease from 825 to 572 nm, 705 to 565 nm and 731 to 511 nm respectively over the course of 28 days. Liposomes formulated without surfactant have a lower polydispersity, thus inclusion of surfactant provides a more homogenous mix with less larger liposomes/aggregates formulated thus there would be less of these to settle out over time.

The size decrease of liposomes formulated without Tween 20 was significant between day 1 and 2 ($P \leq 0.01$) and between 1 and all other days ($P \leq 0.0001$), as well as between day 2 and 7, 14 and 28 ($P \leq 0.05$), and between day 2 and 21 ($P \leq 0.01$). There was no significant difference between days 7 onwards. This may be because all lipid aggregates settled out by this time. The size decrease between liposomes formulated with 2% w/w Tween 20 between day 1 and 7 ($P \leq 0.05$), as well as between day 1 and 28 ($P \leq 0.001$), as well as between day 2 and 28

($P \leq 0.05$). There was no significant difference between day 7 onwards. This may be because all lipid aggregates settled out by this time. The size decrease between liposomes formulated with 6% w/w Tween 20 between day 1 and 14 ($P \leq 0.05$), as well as between day 1 and both 21 and 28 ($P \leq 0.01$). There was no significant difference between day 2 onwards. This may be because all lipid aggregates settled out by this time. The size decrease between liposomes formulated with 10% w/w Tween 20 between day 1 and both 7 and 21 ($P \leq 0.05$), as well as between day 1 and and 28 ($P \leq 0.001$). There was no significant difference between day 2 onwards. This may be because all lipid aggregates settled out by this time.

Additionally, encapsulation efficiency appears to decrease from 93% to 87%, 85% to 81%, 75% to 67% and 64% to 59% respectively for 0 % w/w, 2 % w/w, 6 % w/w, 10 % w/w loading of surfactant (Figure 4.21). All of these decreases were however non-significant. Liposome aggregation may have led to drug leaching or *vice versa*. This suggests a lower loading of surfactant is best to ensure stability.

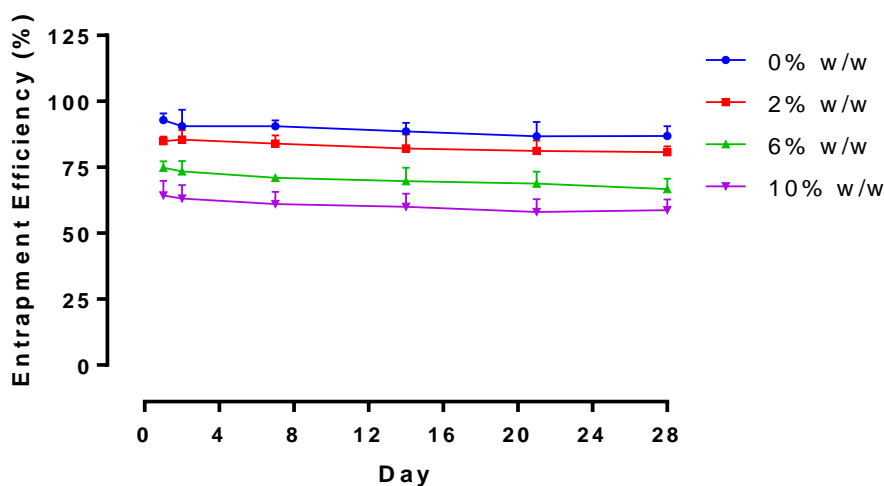


Figure 4.21: Liposome encapsulation efficiency for naringenin over 28 days.

Liposome encapsulation efficiency for naringenin in either 0% w/w, 2% w/w, 6% w/w or 10% w/w Tween 20 liposomes over 28 days. Liposomes were prepared adapting the dry film method adding the surfactant and drug during the lipid mixing stage. The preparation was then washed via centrifugation. The quantity of naringenin in supernatant over 28 days was then analysed by HPLC coupled with UV detection to assess liposome stability. Data represents mean \pm SD. n=6 independent batches.

Long-term stability of liposomes depends on the average elastic energy of the membrane being higher than the thermal energy. When this is no longer the case, liposomes will disintegrate (Lipowsky 1991). Therefore, temperature is an important determinate of stability and liposomes must be stored at a suitable temperature. Too high and the liposomes will break down, and, furthermore, liposomes formulated with surfactant cannot be stored in a fridge due

to the freezing point being at 7°C (Natural-Sourcing, 2017). This suggests these liposomal formulations are not suitable for long term stability. Either additional excipients (such as a charged surfactant to reduce coalescence) are required or an additional step of freeze drying liposomes for reconstitution near the time of administration. Formulations including Tween 20 appeared the most stable over the 4-week period. A study by Tsai et al., (2015) found deformable liposomes formulated with Tween 80 loaded with Naringenin were stable over a 3-month period with no significant size difference noted. Similar to observations in this study however, creaming was noted.

4.5 Conclusion

Developing strategies in cancer management is chemoprevention and chemoprotection with the use of naturally occurring agents (Hwang et al., 2007; Siddiqui et al., 2009; Singh, Shankar, & Srivastava, 2011). The use of anti-oxidants to prevent oxidative skin damage appears to be a favourable strategy (Albini & Sporn, 2007; Casey et al., 2015; Huang et al., 2011). Naringenin is a major flavanone in found in grapefruit. It is an antioxidant, free radical scavenger, anti-inflammatory agent, and immune system modulator thus may be potentially useful as pharmacological anti-cancer agent (Casey et al., 2015; Chen et al., 2003; Huang et al., 2011).

The use of such flavonoids in disease management is limited due to poor bioavailability of promising agents. Liposomes are able to improve the bioavailability profile of these compounds thus could prove useful as compound carriers (Nishiyama, 2007; Siddiqui et al., 2009). In particular, elastic liposomes have been observed to be useful in dermal drug delivery as they can increase compound solubility and can be formulated for targeted, sustained drug release (Benson 20016, Cevc 1996). Furthermore, elastic liposomes have been reported to penetrate the SC barrier layer of the skin. This study aimed to formulate this naringenin into elastic liposomes formulated with Tween 20 within an aqueous gel carrier system intended to deliver a controlled release of this compound within the dermal layer of the skin.

As the amount of Tween 20 in the bilayer of the liposome is increased, liposome size decreases. The presence of naringenin in elastic liposome increases the liposome diameter; however, the inclusion of surfactant decreases the diameter. Inclusion of surfactant in the bilayer decreases liposome DI implying liposomes retained enough elastic energy to pass through a pore size smaller than the liposome diameter thus may be useful in being able to pass through the gaps in the SC. This was true when liposomes where forced through a 200 nm and 100 nm pore size however, liposome destruction was apparent when forced through a 50 nm pore size.

As the loading of Tween 20 in the liposome was increased naringenin encapsulation decreased. This may have been due to Tween 20 competing for space within the bilayer or due to Tween 20 increasing the solubilisation capacity of naringenin. Further, inclusion of naringenin within the liposome bilayer was able to reduce the phase transition temperature of naringenin.

One compartment release models found HEC gels to release drug slightly faster than HPMC gels. Complete gel dissipation was observed between 3 and 4 hours. Two compartment release models found that the aqueous gels were found to slow the release of drug compared to drug solution. Naringenin release from liposomes found liposomes were able to modify the

release of drug with complete release observed within 24 hours. Over the course of 24 hours solution gave a release of 54.5 ± 4.2 % whilst liposomes formulated with 0%, and 10% w/w of Tween 20 gave a release of 109.7 ± 5.0 %, and 48.5 ± 2.1 % respectively. Therefore, the loading of Tween 20 influenced compound release. Liposomes added into gels seemed to have an additive effect in terms of retarding drug release. Release was faster from HEC gels and liposomes formulated with Tween 20.

Toxicology assay's found that between 0.1 and 100 μ M naringenin was not harmful to either keratinocytes or fibroblasts. Cell uptake of the liposomes loaded with naringenin and 2% w/w Tween 20 was apparent into both the keratinocyte cell line and the fibroblast cell line. It appears elastic liposomes are useful in enhancing drug penetration into dermal cells and furthermore may be useful in the development of a controlled release formulation.

Liposome stability was studied in terms of size and encapsulation capacity over the course of a month. Liposomes were found to be stable regarding these two parameters over this time period.

Liposomal gels appear to be useful in the development of a controlled release formulation of anti-cancer agents with a limited bioavailability. Aqueous gels were found to hinder the release of naringenin compared to naringenin solution. Additionally release of naringenin from the liposomes was influenced by Tween 20 loading in the bilayer.

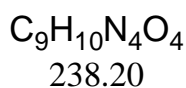
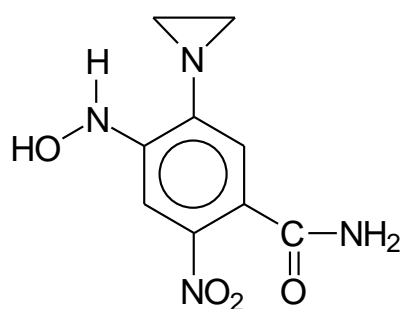
**5 Development of sustained
release MTL-004
liposomal gel
formulations for dermal
drug delivery**

5.1 Introduction

Skin cancer is emerging as an increasing public health problem especially in developed countries. Poor treatment results in 2,500 deaths annually in the UK. The most common treatment is surgical excision of the tumour. However this may not be suitable for all patients thus development of alternative treatments is necessary.

MTL-004 (Figure 5.1) is a potent cytotoxic agent proposed for use in the local treatment of non-melanoma skin cancer and pre-cancerous lesions. MTL-004 is the active form of the prodrug, Tretazicar. Tretazicar is reduced to the cytotoxic bifunctional alkylating agent MTL-004 when in the presence of an endogenous enzyme (NQO1 or NQO2). When originally discovered and tested in rats, tretazicar seemed to be the ideal compound for cancer chemotherapy a simple, selective, low molecular weight compound able to treat tumours with minimal side-effects. However, it was not found to be active against human cancers as human NQO1 is not as efficient at metabolising Tretazicar.

MTL-004 forms DNA interstrand crosslinks and these are poorly repaired resulting in cell death. A significant advantage is the lack of systemic toxicity due to the high reactivity of MTL-004 with serum proteins. Furthermore MTL-004 has been found to have no effect on normal cells as it only works in rapidly dividing cells (Knox et al., 1991).



C 45.4% H 4.2% N 23.5% O 26.9%

Figure 5.1: Molecular structure and relative molecular weight of MTL-004

The chief function of the skin is to form a barrier against the external environment. Liposomal formulations may prove useful as dermal drug-delivery vehicles with benefits for delivery of poorly permeable molecules and larger biologics. Liposome adhesion, fusion and penetration into the SC is possible with potentially deeper penetration into the dermal layer of deformable vesicles compared with traditional liposomes (El Maghraby et al., 1999).

Furthermore, chemotherapy agents are notoriously difficult to formulate with one of the principle concerns being solubility. Formulations must overcome this limitation with the use of

appropriate excipients all the while limiting adverse effects. Liposomes would offer this benefit and have already been employed in the transdermal delivery of lipophilic and hydrophilic drugs including anti-inflammatory agents , anti-tumour agents and hormones (Cevc and Blume, 2001; El Maghraby et al., 1999; Oh et al., 2006; Romero et al., 2013).

Due to the liquid nature of liposomal formulations, an additional excipient to increase the viscosity is required to allow for topical application. Liposomes are compatible with viscosity increasing agents such as cellulose based gels including HEC and HPMC (Foldvari, 1996) therefore these will be employed in this study.

5.2 Aims and objectives

In this body of work, a formulation aiming to deliver MTL-004 to the dermal layer in the management of skin cancer was developed. The effectiveness of the *in vitro* delivery of MTL-004 encapsulated in liposomes in an aqueous gel system to the dermal layer was assessed. The aim of this study was to formulate and characterise an aqueous gel system loaded with elastic liposomes formulated with Tween 20 for the dermal delivery of MTL-004. Liposomes were loaded with up to 10% w/w Tween 20 and 0.25 mg/mL of MTL-004. They were characterised by size, zeta potential, DI and stability. MTL-004 release was observed from these liposomal formulations as well as from HEC and HPMC gels and from gels loaded with liposomes. Toxicity and uptake into HDFa and HaCat cells was then observed.

To achieve the aims, the overall objectives were

- Formulate and characterise liposomes loaded with MTL-004 and observe the release profiles
- Develop, optimise and validate a HPLC coupled with either UV or fluorescent detection
- Characterise MTL-004 loaded liposomes formulated with Tween 20 and quantify the release of MTL-004 from these
- Formulate HEC and HPMC aqueous gels loaded with and MTL-004 compare release of drug from these
- Formulate and compare MTL-004 release of drug from HEC and HPMC gels loaded MTL-004 loaded liposomes
- Apply formulations to fibroblast (HDFa) and keratinocyte (HaCat) cell lines to characterise toxicity

5.3 Materials and methods

5.3.1 Materials

The materials used to prepare liposomes, all reagents as well as materials used to grow HDFa and HaCat cells are detailed in chapter 2 (section 2.3.1) The materials used to prepare the gels are detailed in chapter 3 (section 3.3.1). MTL-004 was acquired from Morvus (Morvus Technology Ltd © 2013, Llanvetherine Court, Llanvetherine, Monmouthshire, NP7 8NL).

5.3.2 Elastic liposome preparation

Liposomes were prepared by using the film hydration method established by Bangham *et al.*, (1965) detailed in section 2.3.2. Briefly, PC, cholesterol and surfactant were dispersed in chloroform and methanol in a 9:1 ratio. Ratios of lipids are detailed in Table 3.1 rational of which has been adapted from previous studies concerning the formulation of elastic liposomes (Hiruta *et al.*, 2006; Ita *et al.*, 2007; Oh *et al.*, 2006; Tsai *et al.*, 2015). MTL-004 loaded liposomes were prepared by adding the required amount of MTL-004 to the lipid mixing stage.

5.3.3 Liposome characterisation: particle size and polydispersity and zeta potential

Mean particle size, polydispersity index and zeta potential of liposomes was measured as detailed in section 2.3.3 using a Zetaplus (Brookhaven Instruments). Each sample was measured 3 times.

5.3.4 Assessment of liposomal deformability

The deformability index (DI) of the elastic vesicles was determined using a mini filtration technique as detailed in section 2.3.5.

5.3.5 HPLC methodology

Detection of MTL-004 was assessed through reverse phase HPLC methodologies. A Waters Alliance separation module HPLC with UV detection was utilised at an operating wavelength of 263 nm. A Waters X select column (5 µm C18 4.6 x 150 mm column) was used. 10 µL of sample at room temperature was injected. The mobile phase comprised of a 50:50 ratio of 0.1% TFA in water to acetonitrile at a flow rate of 1mL/min.

Stock solutions and standard solutions of MTL-004 in water were prepared with ranging from 2.5-100 µg/mL.

5.3.5.1 HPLC method establishment

5.3.5.2 UV spectrometry

A UV scan was run on MTL-004 in water in a quartz crystal cuvette to determine the λ max using Thermo Scientific Genesys 10S UV-vis Spectroscopy between the wavelengths 100 – 600 nm.

5.3.5.3 Chromatographic separation

Mobile phase ratios using 0.1% TFA in water with either methanol or acetonitrile were varied for optimal peak shape of a 5 μ g/mL of MTL-004 in water.

5.3.5.4 Fluorescence detection

In an attempt to improve the detection limits of MTL-004, a method using HPLC coupled with fluorescence detection was attempted to be optimised. Detection of MTL-004 was again assessed through reverse phase HPLC methodologies. A Waters Alliance separation module HPLC with a fluorescence detector running Empower software was utilised at an operating wavelength of 263 nm. A Waters X select column (5 μ m C18 4.6 x 150 mm column) was used. 10 μ l of sample at room temperature was injected. The mobile phase comprised of a 50:50 ratio of 0.1% TFA in water to acetonitrile at a flow rate of 1ml/min.

The emission and excitation wavelengths were varied to find the optimum combination. The excitation wavelength was set at 20 nm higher than the λ max (263 nm) and an emission scan was then run. After obtaining a 3D image of the scan, the optimum emission was selected against which the excitation wavelength was varied.

5.3.5.5 HPLC validation

The method was validated by assessing the linearity and range, repeatability and sensitivity in terms of the limit of detection (LOD) limit of quantification (LOQ) and precision as detailed in section 3.3.5.1.

For the linearity and range assessment, standard solutions ranging between 2.5 - 100 μ g/mL of MTL-004 in water were prepared. The mean peak area \pm SD was calculated and plotted against the known concentration of the standard.

5.3.6 Physicochemical properties

5.3.6.1 Solubility determination

The solubility of MTL-004 in water was determined by removing the supernatant of a saturated solution and quantifying by HPLC separation with UV analysis (section 5.3.6).

5.3.6.2 Log P determination

The log P of MTL-004 across octanol and water (pH 7) was determined by adding drug to a vial containing both solvents and shaking. The sample was then left to sit to allow the drug to partition over 24 hours (Cordero *et al.*, 1996). Samples were then withdrawn from both phases and quantified by HPLC analysis with UV detection (section 5.3.6). Data was then put into Equation 5.1

Equation 5.1:

$$\text{Log } P = \log\left(\frac{C_o}{C_w}\right)$$

Where C_o is the concentration in octanol and C_w is the concentration in water

5.3.7 Determination of entrapment efficiency

The entrapment percentage of MTL-004 loaded in elastic liposomes was determined by centrifuging samples and quantifying drug in the supernatant as detailed in section 3.3.6.

5.3.8 Differential scanning calorimetry investigations of MTL-004 and MTL-004 lipid blends

MTL-004 as well as MTL-004 combined with different ratio of lipid blends were analysed in the solid state using a TA Instruments Q200 Thermal Analysis DSC as described in section 3.3.7.

5.3.9 MTL-004 loaded aqueous gel formulation

Aqueous gels were prepared using HEC (3% w/v) and HPMC (3% w/v) which were mixed overnight using a mechanical mixer (Polytron PT 3100 D) as detailed in section 3.3.8. Gels with a drug loading of 1% w/w was manufactured.

5.3.10 *In vitro* release studies

Drug release from gels, liposomes and liposomal gels over 24 hours was observed using multiple methods.

5.3.10.1 One compartment release model

To study the *in vitro* release and swelling behaviour of gels over 24 hours naringenin loaded gel was syringed into plastic containers with 20ml of DDM as detailed in section 3.3.9.1 and aliquots removed at set time points and analysed using HPLC quantification with UV analysis (section 5.3.6).

5.3.10.2 Two compartment release model

A diffusion cell dialysis system was used to evaluate *in vitro* drug release over 24 hours from solution (0.1mg/mL), gels (formulated with 1% w/w of drug) and liposomes into release media as detailed in section 3.3.9.2.

5.3.11 Liposomal gel release study

Release from liposomal gels was observed with the use of a 6 well Thincert plate and 4 cm² cylindrical cell culture Thincert™ inserts (400 µm pore size) were filled with 1ml of formulation as detailed in section 3.3.9.3.

5.3.12 Release kinetics

Mathematical models to assess release kinetics were fit using Microsoft Excel® as detailed in section 3.3.10.

5.3.13 Growth and passage of cells

HDFa isolated from adult skin, cryopreserved at the end of the primary culture were revived in medium 106 supplemented with Low Serum Growth Supplement. HaCaT is a spontaneously transformed aneuploid immortal keratinocyte cell line from adult human skin. HDFa and HaCat cells were maintained in a humidified 37 °C incubator with 5 % CO₂, grown, fed and split for further proliferation as detailed in section 2.3.6.

5.3.14 Impact of liposomal formulation on *In vitro* cytotoxicity on HDFa and HaCat cells

To determine the concentration of MTL-004 which was toxic to the HDFa and HaCat cells, an XTT assay (Scudiero et al., 1988) was performed to measure cell death after exposure of cells to different concentrations of drug for 24 hours. Cells were trypsinised, centrifuged and re-suspended in fresh media. Cells were then counted and seeded in a 96-well plate as detailed in section 2.3.9. On day 3, media was removed. Cells were treated with 100 µL of either 100 µM, 50 µM, 10 µM, 5 µM, 1 µM or 0.1 µM of drug in DMSO (<1%)/media. Plates were incubated for 24 hours (37°C, 5% CO₂) following which a mixture of 12.5:1 parts of XTT to menadione (25µL) was added each well in a 96 well plate. Plates were incubated for 3 hours at 37°C and the absorbance read at 450 nm. Assessment of MTL-004 toxicity to these cells was conducted through analysis of changes in XTT absorbance with increasing drug concentration.

5.3.15 Cellular liposomal uptake assay on HDFa and HaCat cells

Liposomes, both deformable and non-deformable, were formulated with the addition the fluorescent dye, DiIC, in DMSO as detailed in section 2.3.10. Coverslips were prepared and

analysed with an upright confocal microscope (Leica SP5 TCS II MP) as detailed in section 2.3.8.

5.3.16 Liposome stability

The stability of liposomes was determined, as prepared in water, through the assessment of particle size over a 28 day period as detailed in section 2.3.4.

Furthermore, the encapsulation efficiency of MTL-004 loaded liposomes was assessed over 4 weeks as detailed in section 3.3.6.

5.3.17 Statistical analysis

Unless otherwise stated, all results are presented as mean \pm SD. Replicates of at least 3 were used for all studies. For multiwell plate assays replicates of 6 were used for each experimental condition with the study replicated 3 times

A paired T test or a one way ANOVA was used to determine any statistically significant difference between means tested. A post-hoc Tukey's multiple comparisons test was then applied to assess differences between groups. Results were deemed statistically significant if $P < 0.05$ %.

5.4 Results and discussion

MTL-004 is a potent cytotoxic agent proposed for use in the local treatment of non-melanoma skin cancer. MTL-004 forms DNA interstrand crosslinks and these are poorly repaired resulting in cell death. A significant advantage is the lack of systemic toxicity due to the high reactivity of MTL-004 with serum proteins. Furthermore MTL-004 has been found to have no effect on normal cells as it only works in rapidly dividing cells.

Chemotherapeutic agents are notoriously difficult to formulate particularly due to compounds having a low solubility. Liposomes may enhance the bioavailability of these agents thus could prove useful as delivery agents. Elastic liposomes have been found to be useful in dermal delivery of drugs as they can increase compound solubility, protect the drug from degradation and can be formulated for targeted, sustained drug release (Benson 20016, Cevc 1996). Elastic liposomes have been reported to penetrate the skin; an efficient and effective physical barrier to the external environment. They have already been used in the topical, dermal and transdermal delivery of chemotherapeutic agents (Fang et al., 2008; Lau et al., 2005; Trotta et al., 2004).

Liposomes proposed for dermal delivery require an additional carrier due to the liquid nature of the preparation. Liposomes are known to be compatible with viscosity increasing agents such as cellulose based gels including HEC and HPMC (Foldvari, 1996). Furthermore, these are established as safe in skin application (Forbes et al., 2011b; Hascicek et al., 2009; Patton et al., 2007).

5.4.1 MTL-004 concerns and supply issues

Due to a very limited supply from the manufacturers alongside batch to batch inconsistencies (Figure 5.2), it was not possible to repeat studies showing anomalous results. This has been noted throughout the discussion and points of future work highlighted.

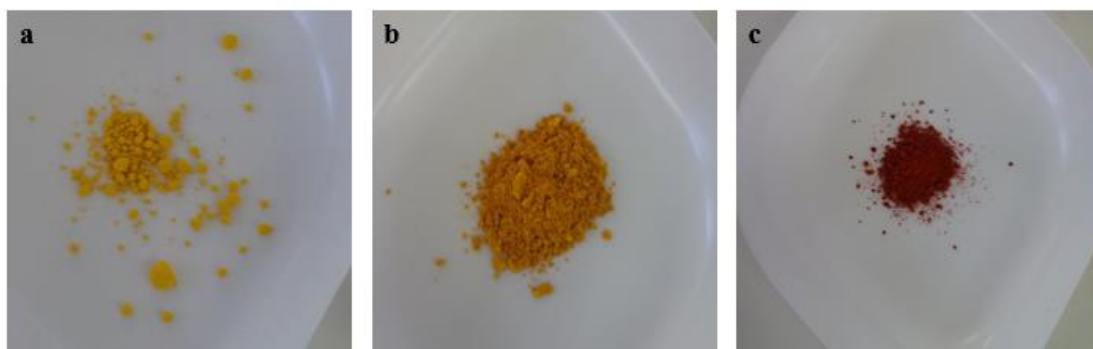


Figure 5.2: Images of MTL-004 batches

Images of three MTL-004 batches received from Morvus over the course of this study

5.4.2 Liposome characterisation: particle size and polydispersity and zeta potential

Liposome size is a key determinant in liposome permeation across the SC thus the effect of surfactant loading on size was investigated. Loadings of up to 10 % w/w Tween 20, were added to the formulation thus adding elastic properties to the bilayer. MTL-004 loaded MLV liposomes were formulated using the dry film method. The bilayer included cholesterol to provide stabilising properties to the liposome bilayer as well as limiting drug leaching (Demel et al., 1972; Gregoriadis and Davis, 1979).

Similar to liposomes formulated without drug, as the surfactant loading in the bilayer increased size decreased significantly from 1362.1 ± 75.9 nm to 800.1 ± 69.5 nm (Figure 5.3). The decrease in size was significant between Tween 20 loadings of 0% w/w and all other loadings of surfactant ($P \leq 0.0001$). There was no significant difference between the sizes of liposomes formulated with any loading of Tween 20 investigated. This implies either surfactant loading reached a maximum at 2% w/w, or, that between 4 and 10% w/w there is not enough surfactant to decrease the size any further.

As discussed in section 3.4.1 surfactant decreases liposome size in comparison to conventional liposomes (Goindi et al., 2013; Tsai et al., 2015). This is due to the amphiphilic nature of Tween 20 allowing a greater interaction of the phospholipid bilayer with the aqueous

phase resulting in the overall formation of more liposomes of a smaller diameter thus giving a greater surface area in contact with the aqueous phase (El Zaafarany et al., 2010).

Drug loaded liposomes had a larger than blank liposomes; 1032.3 ± 182.5 nm compared with 1362.1 ± 75.9 nm for liposomes formulated with no surfactant and 358.1 ± 57.1 nm compared with 800.1 ± 69.5 nm for liposomes formulated with 10% w/w loading of surfactant. The inclusion of drug in the bilayer may have caused an increase in liposome size by increasing bilayer hydrophobicity as it had caused the bilayer to have less interaction with the aqueous phase. Similar to blank liposomes, as the surfactant loading increased in drug loaded liposomes, the diameter decreased.

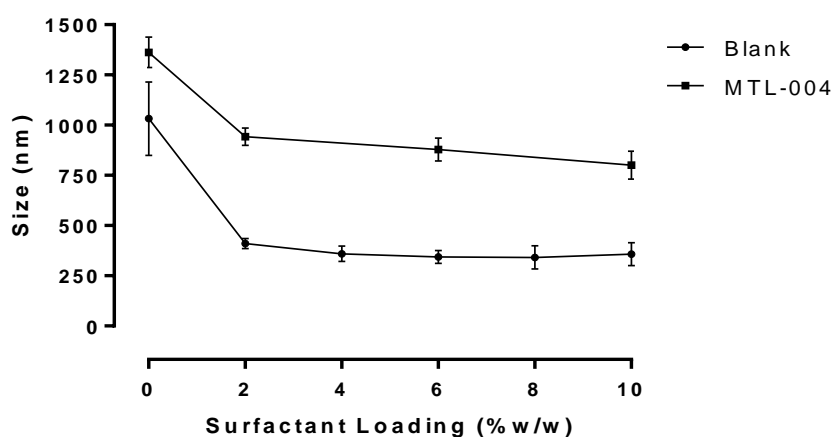


Figure 5.3: Liposome size distribution comparing blank and MTL-004 loaded formulations

Figure 5.3: Liposome size distribution, determined by DLS, comparing blank and MTL-004 loaded formulations with increasing loadings of Tween 20 up to a maximum of 10% w/w. Liposomes were prepared via the dry film hydration method and compound was added during the lipid mixing stage. Data represents mean \pm SD. n=3 independent batches.

A homogenous liposome preparation in terms of size is essential to ensure uniform liposome distribution *in vivo* as well as influence drug release kinetics. A polydispersity of up to 0.3 indicates a homogenous formulation (Chen et al., 2012; Goindi et al., 2013; Kang et al., 2013). Blank liposomes formulated without surfactant were slightly out of this range at 0.32 however blank liposomes formulated with surfactant and all drug loaded liposomes had a polydispersity below 0.3 therefore can be considered homogenous (Figure 5.4). Polydispersity for MTL-004 loaded liposomes was lowest at 0.24 when formulated with 10% w/w Tween 20 indicating this loading of surfactant produced the most homogenous mix of liposomes.

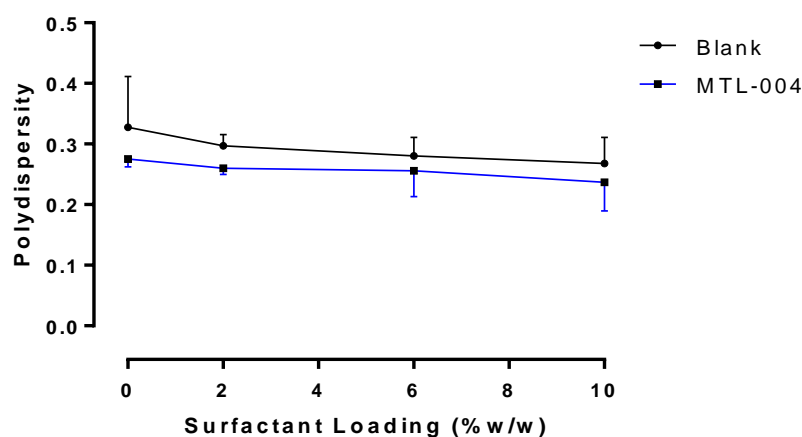


Figure 5.4: Polydispersity of blank and MTL-004 loaded liposomes

Polydispersity of blank and MTL-004 loaded liposomes formulated with increasing loadings of Tween 20 up to a maximum of 10% w/w was determined with DLS. Liposomes were prepared via the dry film hydration method and compound was added during the lipid mixing stage. Data represents mean \pm SD. n=3 independent batches.

The zeta potential is the potential difference between the dispersion medium and the stationary layer of fluid directly surrounding the dispersed particle. The scale of the zeta potential illustrates the degree of electrostatic repulsion between adjacent, similarly charged particles in a dispersion. Thus, it is one of the fundamental factors influencing stability. The zeta potential of blank and MTL-004 liposomal formulations is displayed in Table 5-1.

Table 5-1: Zeta potential of liposomal formulations formulated with and without drug with up to 10% w/w loading of Tween 20

Surfactant loading (% w/w)	Zeta potential (mV)	
	Blank Liposomes	MTL-004 loaded liposomes
0	5.03 \pm 1.03	-23.11 \pm 6.08
2	4.67 \pm 1.08	-18.94 \pm 2.73
6	3.71 \pm 0.90	-5.4 \pm 0.9
10	-2.79 \pm 0.20	-9.6 \pm 2.16

Results are presented as the mean \pm standard deviation (n=3)

Liposomes are miscible with the lipids in the skin thus are advantageous when employed as dermal drug delivery carriers as they can penetrate into deeper layers. Thus a neutral surface charge is ideal (Prausnitz and Langer, 2008). Positively charged liposomes are known to be irritating to the skin, whilst neutral liposomes have a tendency to flocculate (Weiner et al., 1992). Negatively charged liposomes have been observed to provide better skin retention for

drugs intended for topical use (Katahira et al., 1999). This study observed the majority of formulations for MTL-004 loaded liposomes to have a slight negative charge (Table 5-1). MTL-004 liposomal formulations formulated with 0 %, 2 %, 6 % and 10 % w/w Tween 20 were found to have zeta potential values of -23.1 ± 6.1 , -18.9 ± 2.7 , -5.4 ± 0.9 , -9.6 ± 2.2 mV respectively. Such charges appear optimal for dermal drug delivery as these particles will not flocculate whilst they will not irritate the skin.

Additionally charged bilayers repel each other, thereby increasing the trapped volume of encapsulated aqueous medium within MLV (Schroeder et al., 2009; Zuidam and Barenholz, 1997). Furthermore, introducing molecules of the same charge into the membrane causes more repulsion within the bilayer, thereby increasing the permeability of the liposome (Crommelin, 1984; Lichtenberg and Barenholz, 1988).

5.4.3 HPLC methodology establishment

Prior to any formulation and release studies, a HPLC method for the detection of MTL-004 was developed and optimised. Reversed phase HPLC is an effective and sensitive technique able to separate and detect a range of molecules including charged and non-polar compounds. A range of variables such as organic solvent type, concentration, pH, temperature all influence compound elution. Chromatographic approaches must be tested to ensure trustworthy and reliable data. Consequently, validation of the HPLC-UV method was performed according to the International Conference of Harmonization (ICH) guidelines in terms of linearity and range, limit of detection (LOD), limit of quantification (LOQ) and precision.

5.4.3.1 UV spectroscopy

To establish the UV wavelength at which to detect the drug on the HPLC apparatus, a UV scan was run on MTL-004 in water. UV absorption spectroscopy is the measurement of the attenuation of a beam of light after it passes through a sample and is dependent on electrons able to absorb this energy. Absorption measurements may be at a single wavelength or over a range. The optimal wavelength at which to detect the drug was determined to be 263 ± 2.03 nm.

5.4.3.2 HPLC method optimisation

Mobile phase ratios using 0.1 % TFA in water with either methanol or acetonitrile were varied for optimal peak shape of a 5 µg/mL of MTL-004 in water (Table 5-2 and 5-3).

Table 5-2: Effect of variations in the mobile phase ratio of the elution of MTL-004 in water where A is 0.1% TFA in water and B in acetonitrile

Acetonitrile				
Mobile Phase Ratio (A:B)	Retention time (min)	Standard deviation	Peak area ($\mu\text{V} \cdot \text{s}$)	Standard deviation
00:100	1.99	0.01	53021.11	60.55
10:90	1.98	0.06	53034.11	45.23
20:80	2.06	0.07	53052.07	72.43
30:70	2.09	0.11	53023.13	93.78
40:60	2.07	0.03	52821.89	131.22
50:50	2.09	0.04	52927.78	47.14
60:40	1.8	0.01	52530.32	36.21
70:30	1.67	0.04	52567.28	75.29

Table 5-3: Effect of variations in the mobile phase ratio of the elution of MTL-004 in water where A is 0.1% TFA in water and B in methanol

Methanol				
Mobile Phase Ratio (A:B)	Retention time (min)	Standard deviation	Peak area ($\mu\text{V} \cdot \text{s}$)	Standard deviation
00:100	2.03	0.03	53345.24	124.76
10:90	2.04	0.1	53265.42	91.63
20:80	2.11	0.11	53332.36	204.85
30:70	2.14	0.13	53148.68	56.84
40:60	2.16	0.15	53459.55	306.86
50:50	2.18	0.05	53859.38	118.59
60:40	2.09	0.14	53343.25	205.86
70:30	2.07	0.08	53750.63	121.23
80:20	2.23	0.05	53676.47	63.27
90:10	2.17	0.03	53232.65	137.75
100:00	2.17	0.05	53223.84	144.53

The compound eluted around 2 minutes regardless of mobile phase composition. It was noted that the drug eluted a fraction later when methanol was used as the mobile phase. Acetonitrile

is more polar than methanol. Methanol would therefore be faster at eluting hydrophobic compounds. Variations in the mobile phase ratio only very slightly affected peak shape. 0.1% TFA in water/methanol at 50:50 appeared to give the sharpest peak at 2.17 ± 0.05 minutes. The calibration curve for MTL-004 with this mobile phase is shown in Figure 5.5.

5.4.3.3 HPLC calibration

Stock solutions and standard solutions of MTL-004 were prepared in water ranging from 2.5 $\mu\text{g/mL}$ – 100 $\mu\text{g/mL}$. Calibration data using the method outlined in section 5.3.5 was then obtained (Figure 5.5).

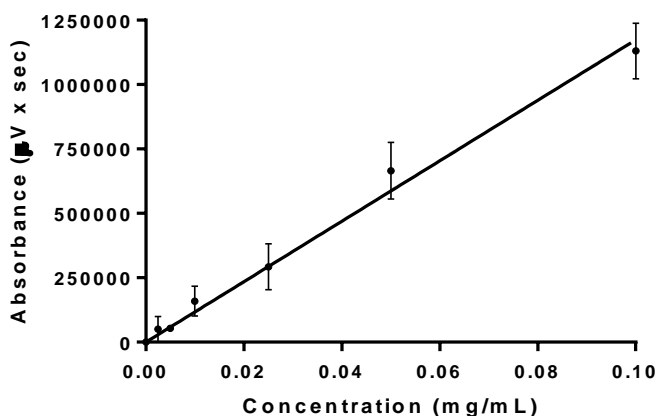


Figure 5.5: Calibration data for MTL-004 as determined by HPLC-UV analysis.

Calibration data for MTL-004 over the concentration range of 0.125-10 $\mu\text{g/mL}$ in water. A proportional response was evident versus the analytical concentration over the working concentration range with an r^2 of 0.99 and linear equation of $y = 1 \times 10^7 \cdot x$. Data represents mean \pm SD. $n=9$.

5.4.3.4 HPLC Validation

To assess the linearity and range MTL-004 concentrations ranging from 2.5 - 100 $\mu\text{g/mL}$ in water were prepared. The method developed demonstrated a high correlation with a good linear fit, with the correlation coefficient (r^2) being greater than 0.99 (Figure 5.5).

Assessment of repeatability/precision of the developed method was determined by assessing the intraday (same day) and interday (over the course of three days) variability (Figure 5.6a and 5.6b). This was done to assess variation caused by temperature fluctuations and any variation in experimental method. MTL-004 standards from 2.5 - 100 $\mu\text{g/mL}$ carried out within the intraday and interday are plotted in Figure 5.6a and b respectively. The results show that the values have no statistically significant difference for all the calibration curves carried out at different times on the same day and also on different days, meaning the method has good precision. Calibration data for MTL-004 was obtained on 3 separate days, each with 3 repeats.

No statistically significant difference in either the peak areas for any one particular concentration across inter- and intra-day sampling across the 3 days was found.

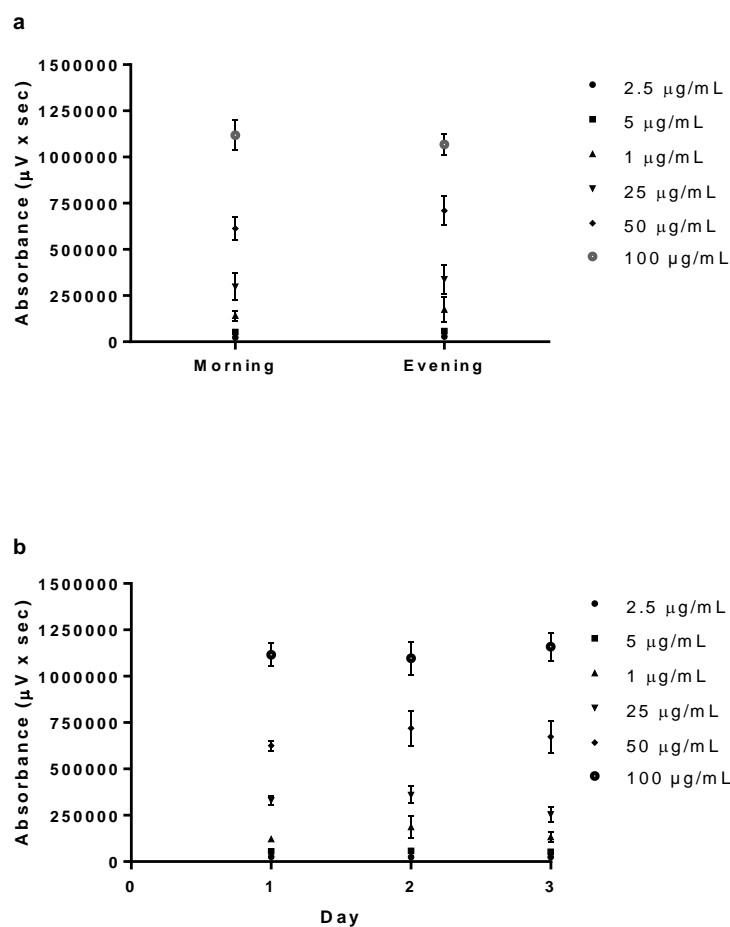


Figure 5.6: Calibration data of MTL-004 as determined by HPLC-UV analysis obtained over 3 days.

The a) intraday, b) interday data is displayed. The standards of MTL-004 ranged from 2.5-100 µg/mL. Data represents mean ± SD. n=3.

Study of the sensitivity of this method was assessed by means of the calculation of the LOD and the LOQ. Values were determined from the standard deviation of the response (σ) and the slope (S) obtained from the calibration curves carried out during the linearity assessment. According to the ICH guidelines, a signal-to-noise ratio of three was assumed for the quantification of the LOD, whereas for the LOQ, a signal-to-noise ratio of ten was set. Therefore, following Equations 3.2 and 3.3, the sensitivity of the method for MTL-004 was calculated; the LOD and LOQ was 2.5×10^{-5} µg/mL and 8.1×10^{-4} µg/mL respectively.

5.4.3.5 Fluorescence detection

Fluorescence spectroscopy is the most sensitive optical detection technique used with HPLC therefore, to develop a more sensitive MTL-004 detection method, optimisation of such detection was attempted. The λ max of MTL-004 in water (263 nm) was selected as the excitation wavelength and the emission scan run from 273-600 nm. A 3D image was obtained from which the peak emission wavelength was selected from which to run an excitation scan to optimise fluorescent detection. As the images shown in Figure 5.7 shows, peak emission and excitation wavelengths could not be clearly ascertained, and due to MTL-004 supply issues, this method was not optimised and HPLC detection with UV detection was used.

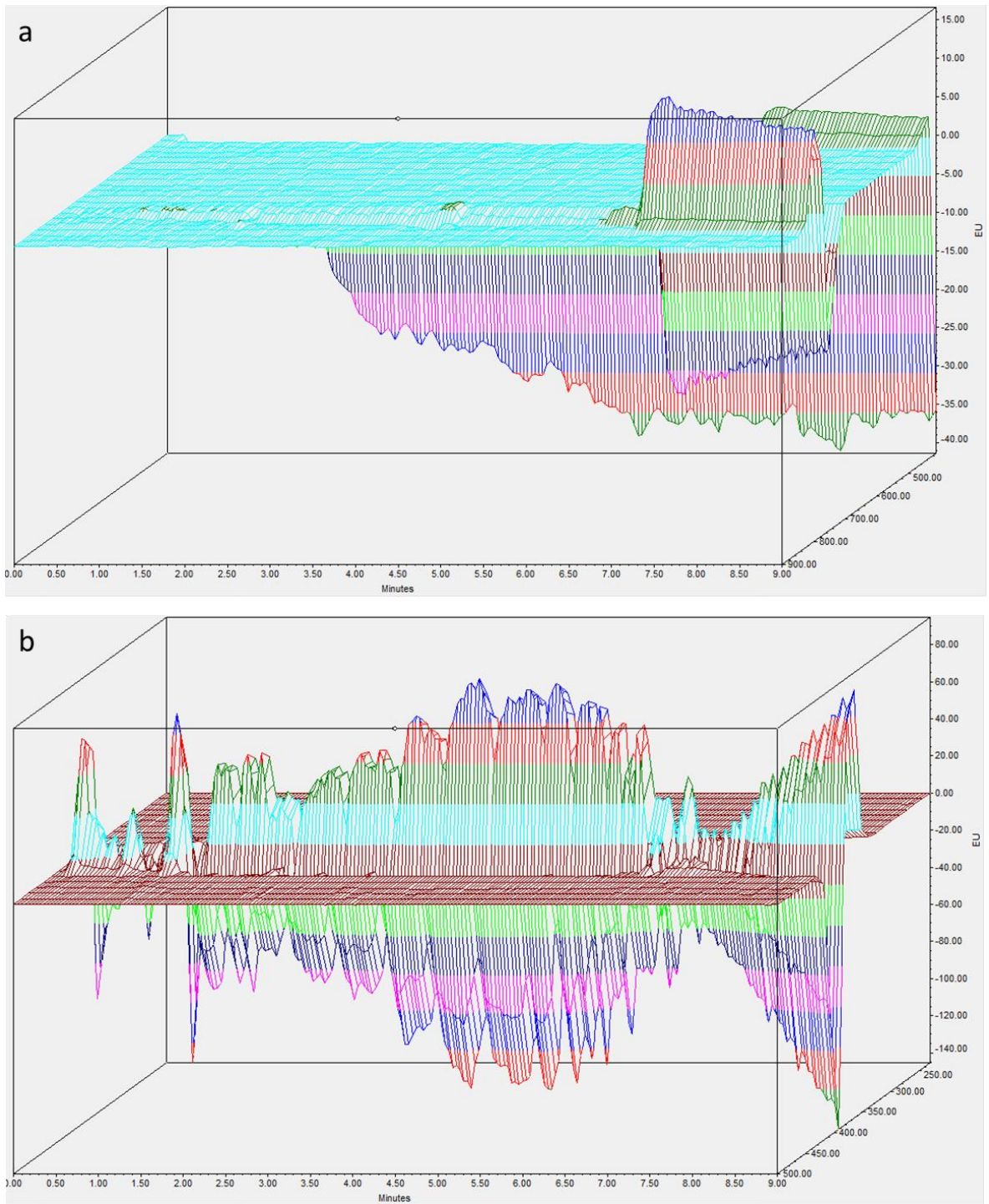


Figure 5.7: Fluorescence scans of MTL-004

a) 3D emission scan, b) 3D excitation scan. The λ max of MTL-004 in water (263 nm) was selected as the excitation wavelength and the emission scan run from 273-600 nm. A 3D image was obtained from which the peak emission wavelength was selected from which to run an excitation scan to optimise fluorescent detection.

5.4.4 Physiochemical properties

5.4.4.1 Solubility

The solubility of MTL-004 in water was determined to be 1.41 ± 0.2 mg/mL. Stability studies of MTL-004 in a range of solvents needs to be determined; detection of MTL-004 degradation products may then be optimised. Due to supply limitations as well as batch to batch inconsistencies, this was unable to be completed in this body of work.

5.4.4.2 Log P determination

The partition characteristics of compounds into the lipids of the SC can be approximated using octanol as the solvent (Hadgraft and Valenta, 2000). The Log P between octanol and water was determined to be -0.82 ± 0.077 . This implies the drug is more hydrophilic and would be contained in the aqueous core contradicting the information provided by Morvus. Due to supply limitations as well as batch to batch inconsistencies this value cannot be considered reliable. Further studies would need to be carried out to confirm the log P value. Regardless, it is known drugs with a log P < 5 are better at permeating the skin therefore this is a beneficial characteristic.

5.4.5 Determination of entrapment efficiency

The fraction of MTL-004 entrapped in the liposome in comparison to how much compound was added into the lipid mix was assessed. Surfactant and MTL-004 may compete for space within the bilayer. The impact of surfactant addition on the amount of compound entrapped was therefore studied. As surfactant loading increased from 0 % w/w to 10 % w/w, drug entrapment decreased from an efficiency of 44.0 ± 4.8 % to 20.7 ± 2.6 % (Figure 5.8). A significant difference in MTL-004 entrapment was observed between surfactant loadings of 0 % w/w and both 6 and 10 % w/w as well as between 2 % w/w and 10 % w/w ($P \leq 0.0001$). There was a significant difference in entrapment between surfactant loadings of 0 % and 2 % w/w ($P \leq 0.001$). There was a significant difference in entrapment between surfactant loadings of 6 % w/w and 10 % w/w ($P \leq 0.01$). There was a significant difference in entrapment between surfactant loadings of 2 % w/w and 6 % w/w ($P \leq 0.05$).

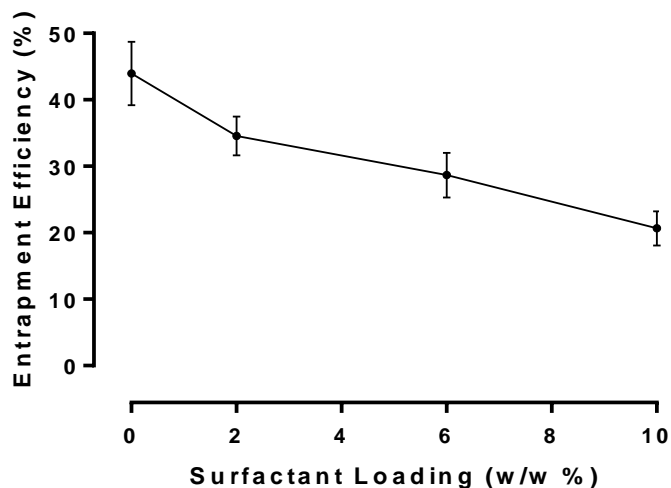


Figure 5.8: Entrapment efficiency of MTL-004 in liposomes formulated with up to 10% w/w Tween 20

Liposomes were formulated with varying amounts of Tween 20 (0-10 % w/w) Data represents mean \pm SD. n=3 independent batches.

As with both previously reported flavonoids, addition of surfactant in the liposomal bilayer may have limited drug inclusion within the bilayer implying the surfactant has a higher affinity to the lipids (Casas and Baszkin, 1992; Levy et al., 1991). Tween 20 is much larger than MTL-004, thus it may be assumed it is better poised to displace MTL-004 from the bilayer (Figure 5.9). The hydrophobic tail of Tween 20 would have a high affinity to the chains in PC therefore giving Tween 20 a better rooting in the bilayer than MTL-004. Furthermore, Tween 20 is able to increase compound solubility, therefore, as not all would be entrapped within the bilayer, this may allow MTL-004 to solubilise within the liposomal rehydration media.

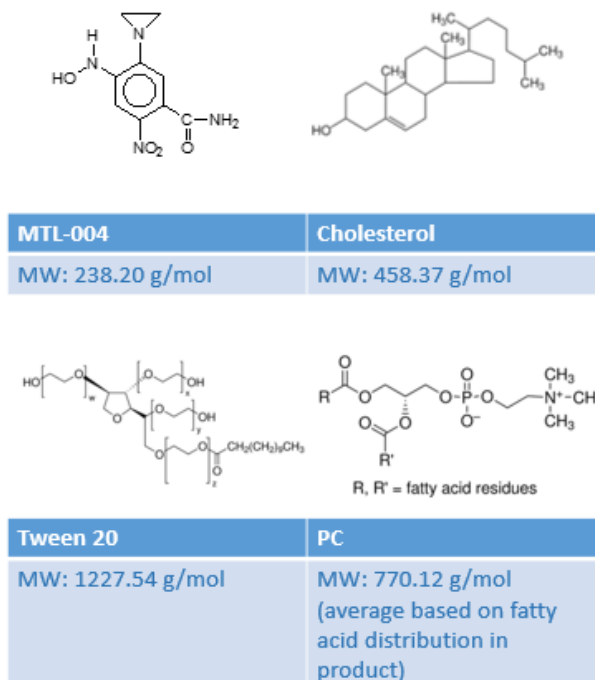


Figure 5.9: Structure and MW of MTL-004, cholesterol, Tween 20 and PC

5.4.6 Assessment of liposomal deformability

Inclusion of surfactant within the liposomal bilayer allows the liposome to display elastic properties (Almog et al., 1986a; Cevc, 1996; Trotta et al., 2002). This attribute may be useful when employing such carriers in topical formulations intended for dermal delivery. Liposomes loaded with up to 10 % w/w of Tween 20 were formulated and deformation following extrusion was determined by extruding through a polycarbonate filter with a pore size of 200, 100 and 50 nm (Figure 5.10). The DI is defined as the degree the liposomes deformed following extrusion. The greater the degree of deformation the less elastic the liposomes are as they were unable to regain their previous larger size.

When liposomes were forced through 200 nm the DI for MTL-004 loaded liposomes decreased significantly from 84.3 ± 1.1 to 35.7 ± 5.1 %. The decrease in deformation was significant between 0% w/w of surfactant and 10% w/w of surfactant ($P \leq 0.001$). There was also a significant difference between the DI of liposomes formulated with 0 % w/w and 6 % w/w of surfactant as well as 2 % w/w and 10 % w/w of surfactant ($P \leq 0.05$). There was no significant difference between the DI of the other formulations.

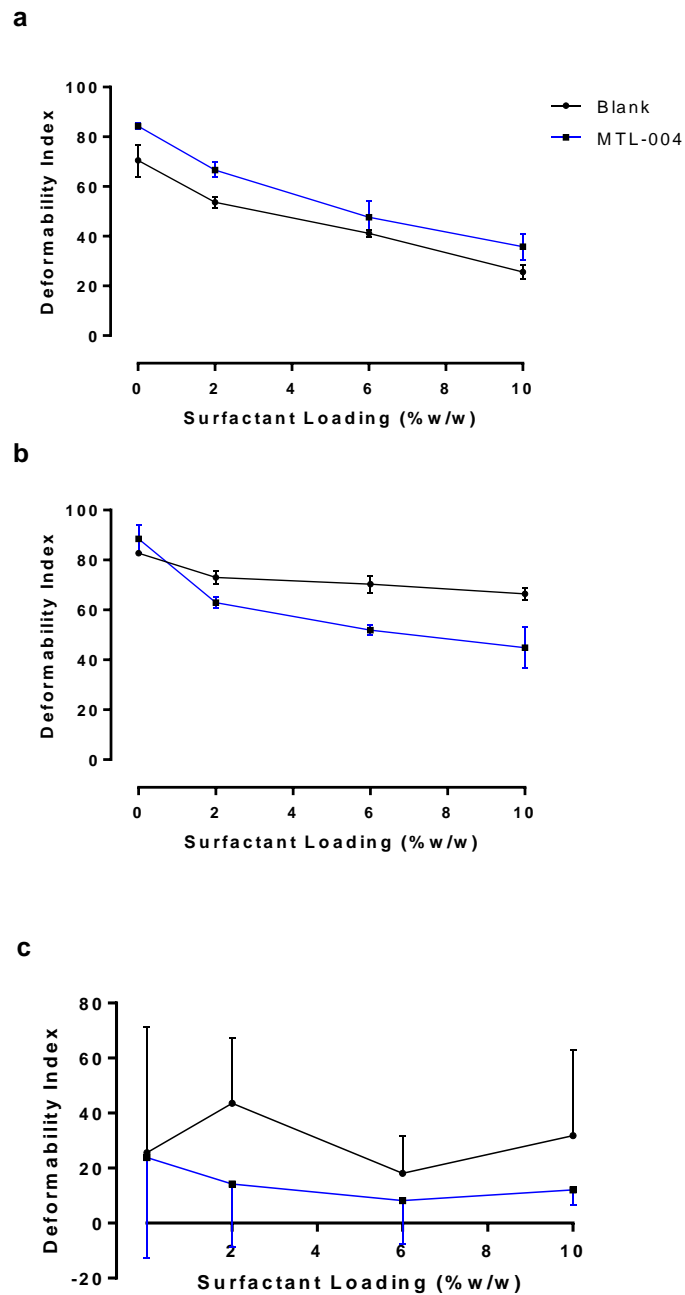


Figure 5.10: Deformability index of liposomes following extrusion

Liposomes were extruded through a) 200 nm, b) 100 nm, c) 50 nm membranes for blank and MTL-004 loaded liposomes with increasing surfactant loading up to a maximum of 10 % w/w. Liposomes were prepared adapting the dry film method adding the surfactant and adding MTL-004 during the lipid mixing stage. The preparation was vortexed and then extruded through the membranes. Data represents mean \pm SD. n=3 independent batches.

When liposomes were forced through 100 nm pores, the deformability index for MTL-004 loaded liposomes decreased from 88.4 ± 5.6 to 44.9 ± 8.1 %. The decrease in deformation was significant between 0 % w/w of surfactant and 2, 6 and 10 % w/w of surfactant ($P \leq 0.0001$). The decrease in deformation was significant between 2 % w/w of surfactant and 10 % w/w of surfactant ($P \leq 0.001$). The decrease in deformation was also significant between 2 % w/w of surfactant and 6 % w/w of surfactant ($P \leq 0.01$). There was no significant difference between the DI of the other formulations.

As with the flavonoids, no trend was observed for formulations forced through a 50nm pore size. Any differences in deformation between surfactant loadings was not significant between any of the formulations. The decrease in DI observed suggest liposomes were displaying elastic properties as they deformed to fit through a gap smaller than its diameter whilst to some extent regaining its size following extrusion. As noted in previous works, the presence the presence of surfactant added elastic properties to the liposome as the DI of these liposomes decreased (section 3.4.4)

Furthermore, the deformability index of the MTL-004 loaded liposomes forced through 200 and 100 nm was greater than blank loaded liposomes ($P \leq 0.05$). MTL-004 loaded liposomes have a greater deformability index overall, however, their overall size prior to extrusion was greater than that of blank liposomes therefore they would have to deform to a greater degree to be able to pass through the filter. This trend was not observed for liposomes forced through 50 nm pores but this may be due to liposome destruction (see section 3.4.4).

As discussed in section 3.4.4, surfactant has a tendency toward curved structures, thus liposomes formulated with surfactant can deform thus lessening the energy required for particle deformation and permit liposomes shape change whilst under stress (Trotta et al., 2004). Further, the fast reconstruction of liposome spheres after extrusion may be due to the strong affinity between the surfactant and PC. This phenomenon might have provided the deformability upon physical stress (Oh, Y. K. et al., 2006).

Deformability for both blank and drug loaded liposomes was not significantly between extrusions though 200 nm and 100 nm. Liposomes were expected to deform more so as pore size decreased. This shows that even up to extrusion through a 50 nm pore size, liposomes retained enough elastic energy to maintain the same size as when forced through the 200 nm membrane.

Deformation and the subsequent reformation liposomes require energy (Fresta and Puglisi, 1996; Gompper and Kroll, 1995; Trotta et al., 2002). As detailed in section 3.4.4, in this system energy was supplied as pressure. The more surfactant included in the bilayer, the more energy the liposome was able to retain (Trotta et al., 2002). This energy was used in bending the

liposomal bilayer, and was expelled once the liposome passed through the pore. This energy was then being used in reforming the liposome. Some energy was lost as heat or non-plastic deformation. Consequently, even at 10 % w/w of Tween 20, 100 % size was not recovered. Liposome formulated with no surfactant does not have the extra 'storage space' of a surfactant, thus energy may be spent in rupturing the membrane causing liposome size to decrease (Trotta et al., 2002).

As with liposomes loaded with flavonoid, the deformability index did not increase as membrane pore size decreased. The standard deviation of the DI for liposomes extruded through a 50 nm pore size was extremely large (for liposomes formulated with 2 % Tween 20 a standard deviation of 14 was observed) therefore the mean value perhaps is not the best representation of the actual data values. The liposome size following extrusion for these formulations was extremely varied with some liposomes coming out larger than the original size. Drug loaded liposomes formulated without surfactant had an original size of 1451.2 ± 256.1 nm compared with 1636.6 ± 512.5 nm following extrusion, liposomes loaded with 2 % w/w surfactant had an original size of 1015.7 ± 247.1 nm compared with 1178.5 ± 298.4 nm following extrusion. This implies these formulations were not able to maintain enough elastic energy to be easily able to fit through the pores with some liposomes even converging following extrusion (Goindi et al., 2013; Trotta et al., 2002).

Whilst even when forced through 50 nm, the amount of energy retained in the liposome was enough to reform at least a portion of the liposomes, it can be concluded that in this study liposome formulations were not suitable to pass through a 50 nm pore. As detailed in section 2.4.3 this is not necessarily what would happen to liposomes when applied to the skin. Liposomes would instead move across the skin following the hydrogen based transepidermal gradient (Cevc, 1996; Goindi et al., 2013; Gompper and Kroll, 1995; Trotta et al., 2002). Moreover, the warmer skin temperature will supply more energy to be even more flexible and cross the stratum corneum.

As with liposomes loaded with flavonoids, even in an excess of energy, liposomes were not able fully return to their pre-extrusion size. This is because energy was lost through other means (friction of the particles moving through the pores as heat). Increasing surfactant loading may result in an increase in liposome reformation (Trotta et al., 2002). However, this must be balanced with drug loading capacity.

5.4.7 Differential scanning calorimetry investigations of MTL-004 and MTL-004 lipid blends

Differential scanning calorimetry (DSC) is used to understanding the thermal characteristics of materials where an insight into a range of thermal properties including melting temperatures, phase transitions and heat capacity changes can be obtained. The investigations were carried

out over the temperature range 0 – 300 °C with a heating rate of 10 °C min⁻¹. The DSC plot of MTL-004 is displayed in Figure 5.11. MTL-004 showed a sharp endothermic peak signifying crystallisation (T_c) at 201 °C (Figure 5.11). The T_m was not able to be determined due to short sample supply but it may be assumed it would be after 300 °C as no exothermic peak was observed within this temperature range.

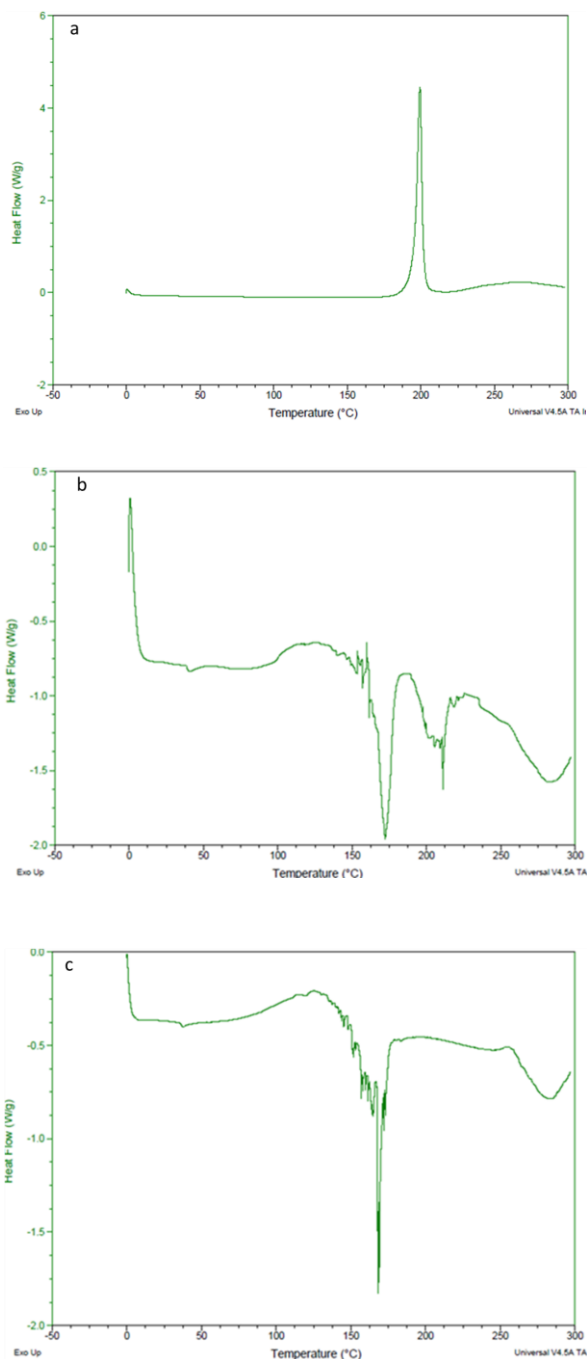


Figure 5.11: DSC scan of MTL-004 and lipid blends

DSC scan of a) MTL-004 b) PC, cholesterol and Tween 20 blend and c) PC, cholesterol, Tween 20 and MTL-004 blend. All experimental runs commenced at an initial temperature of 0 °C with a scan rate of 10 °C/min to 300 °C. The peak in a) shows the T_c of MTL-004 was at 201 °C. The T_m of the lipid mixture is 172 °C, and upon addition of MTL-004, the T_m was 169 °C.

To demonstrate the association of MTL-004 with the lipid/surfactant complex, DSC analysis was performed on, the lipid blend, and the MTL-004, lipid/surfactant blend. In the lipid/surfactant mix we see a very small peak at 40 °C and then a large peak at 172 °C a medium peak at 212 °C.

On the other hand, MTL-004, lipid/surfactant complex showed a small peak at 40 °C and a large peak at 169 °C which is different from the peaks of the individual components of the complex. (Figure 5.11). It is evident that the original peaks of MTL-004 and phospholipids disappear from the thermogram of complex and the phase transition temperature can be assumed to be lower than that of MTL-004. This disappearance of peaks may be a result of hydrophobic interaction and/or hydrogen bonding determined by the functional groups on MTL-004 (Semalty et al., 2010b).

5.4.8 MTL-004 release studies

5.4.8.1 MTL-004 release studies from gel formulations

Due to the liquid nature of liposomal preparations a carrier is required if they are to be employed in dermal drug delivery systems. Liposomes are known to be compatible with viscosity increasing agents such as cellulose based gels (Foldvari, 1996). Furthermore, such gels are established as safe in topical, dermal and transdermal delivery (Forbes et al., 2011b; Hascicek et al., 2009; Patton et al., 2007). HEC and HPMC were employed to compare as carriers of liposomal preparations.

The drug release from a gel is determined by many factors including diffusion, and erosion of matrices followed by dissolution of drug. As with release studies for both flavonoids, two geometric systems have been considered for MTL-004 release from gel systems. A one compartment model was employed to study release and gel swelling behaviour whilst a two-compartment diffusion cell observed drug release across a membrane. A polycarbonate membrane with 50 nm was used to mimic the stratum corneum and the gaps in between the keratinocyte cells. The composition of both HPMC and HEC gels was kept at 3% w/v. Such dissolution/release tests are required to help predict *in vivo* behaviour and to study the structure of the dissolving matrix.

5.4.8.2 One compartment release studies

MTL-004 release from the aqueous gels HEC and HPMC gels loaded with 1 % w/w MTL-004 using water as a release medium was studied over a 24-hour period (Figure 5.12).

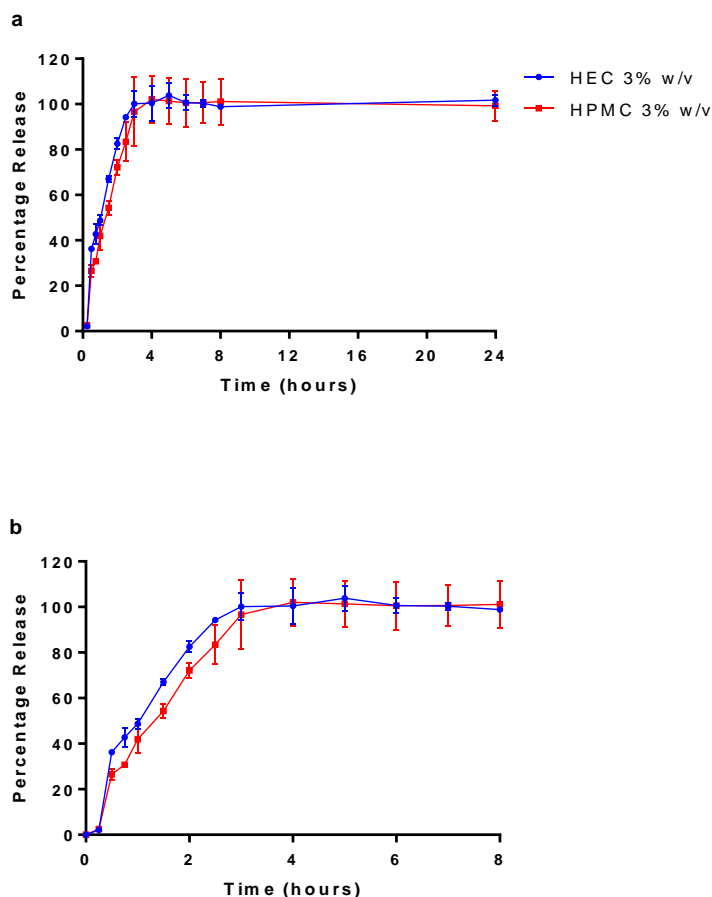


Figure 5.12: *In vitro* percentage MTL-004 release profiles from HEC and HPMC gels

MTL-004 release profiles from aqueous HEC and HPMC gels (3 % w/v) over a) 24 hours, b) 8 hours. Data represents mean \pm SD. n=3 independent batches.

MTL-004 release from both HEC and HPMC gels displayed a similar pattern of release into the DDM (Figure 5.12). As with flavonoids, at 3 % w/v loading of polymer, HPMC could retard drug release to a greater degree. Up until 3 hours at which time 100 % of compound was released, HEC consistently had a higher cumulative percentage of drug released. At the point of complete release, the gel was observed to have completely dissipated into the release media.

As discussed previously (section 3.4.7.1.1), diffusion of solution out of the polymer depends on a range of factors including temperature, pressure, viscosity, solute size and interactions between the polymer and solvent (Masaro and Zhu 1999). Furthermore, molecular geometry

can influence drug release from the gel matrix (Ford, Rubinstein et al. 1987, Rao, Devi et al. 1990).

5.4.8.2.1 Kinetic assessment

Release profiles were evaluated by zero-order, first-order and Higuchi kinetics model (Table 5-4). As with the flavonoids, release from the gels were observed to fit the first order release model. This indicates drug was released at a constant rate in proportion to the amount of drug available at that time. As discussed in section 3.4.7.1.1.1, other studies have found the other models better at describing release from polymer gel systems but is dependent on particular formulations parameters.

Table 5-4: Kinetic assessment of release data of MTL-004 from HEC and HPMC aqueous gels.

Kinetic model	Formulation r^2	
	HEC (3 % w/w)	HPMC (3 % w/w)
Zero order	-2.332 ± 0.077	-1.571 ± 0.083
First order	0.954 ± 0.009	0.945 ± 0.050
Higuchi model	0.112 ± 0.022	0.351 ± 0.011

Results are presented as the mean \pm standard deviation (n=3)

Comparison of the rate constant between formulations found HEC to have a larger rate constant (Table 5-5). This shows HEC gave a faster release of MTL-004 per unit time. Drug is released from gel by the creation of pores due to the uptake of water, as viscosity increases polymer chains becoming more resistant to movement as they are physically restricted thus taking longer to dissipate into the media thus slowing release drug. This implies HPMC had a greater viscosity than HEC.

Table 5-5: First order kinetics rate constant for MTL-004 release from formulations

Rate constant (min ⁻¹)	
HEC 3% w/v	HPMC 3% w/v
0.013 ± 4.075 × 10 ⁻⁴	0.010 ± 0.002

Results are presented as the mean ± standard deviation (n=3)

The Korsmeyers-Peppas's model was then applied to the release data and the diffusional exponent (*n*) calculated (Table 5-6). Fickian release (case I) was observed for both polymers at 3% w/v. As discussed with both flavonoids, both Fickian and anomalous release is possible from swellable matrixes (Ritger and Peppas, 1987).

Table 5-6: Diffusional exponent *n* calculated from the Korsmeyer-Peppas model of drug release for MTL-004 release data from aqueous gels with the corresponding release mechanism.

Formulation	<i>n</i>	Transport type
HEC 3% w/v	0.250 ± 0.002	Fickian
HPMC 3% w/v	0.284 ± 0.001	Fickian

Results are presented as the mean ± standard deviation (n=3)

Fickian diffusion from polymer networks is observed when the temperature is above the polymers glass transition temperature (*T_g*). In this study, it may be deduced that the polymer chains were able to move sufficiently, thus the gel was in a rubbery state.

5.4.8.3 Two compartment release

Release of MTL-004 from HEC and HPMC gel formulations at polymer loading of 3 % w/v in a two-compartment model using a diffusion cell with a 50 nm pore polycarbonate membrane was also observed. This was compared against release from solution in the donor compartment into the receiver compartment. MTL-004 loaded gels were prepared and release over 24 hours was observed.

The gel formulations did appear to slow the release of MTL-004. As with both flavonoids, HPMC proved to be more pronounced than HEC in this phenomenon (Figure 5.13).

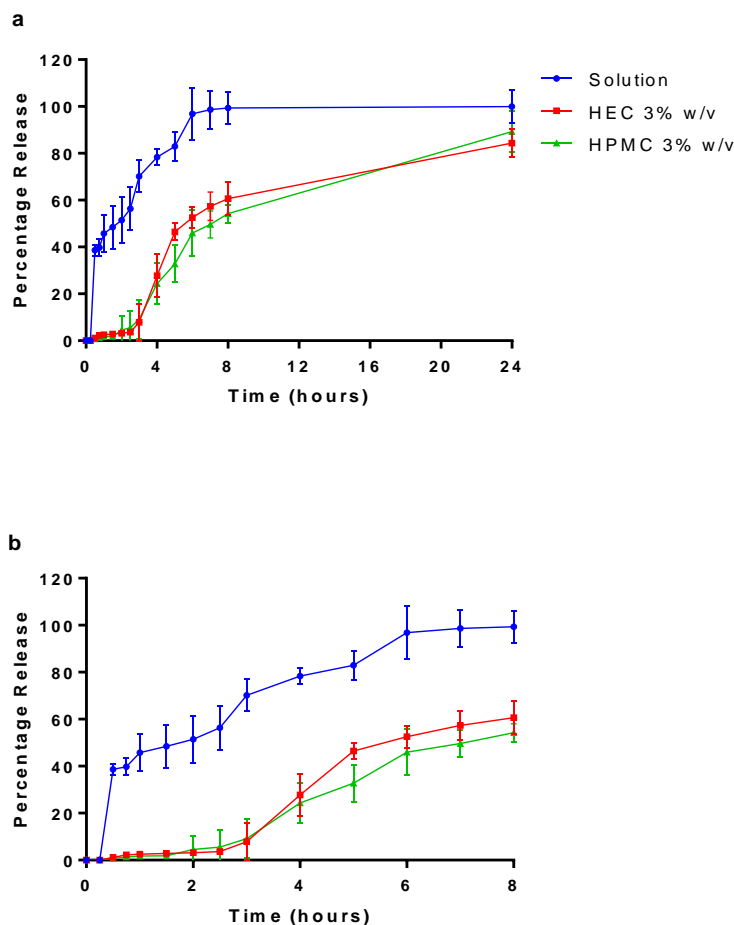


Figure 5.13: *In vitro* percentage MTL-004 release profiles from HEC and HPMC

MTL-004 release profiles from HEC and HPMC (3 % w/v) aqueous gels with 1 % w/v MTL-004 and MTL-004 solution over a) 8 hours, B) 24 hours. Data represents mean \pm SD. n=3 independent batches.

Complete release of solution across the membrane was observed between the 6th and 7th hour whilst HEC and HPMC saw 84.4 ± 6.0 % and 89.2 ± 8.7 % release respectively at the 24th hour. The release profile was significantly different between the solution and both gels but not between the gels ($P \leq 0.0001$). However, comparison between the gels found that HEC at its respective loading of polymer in the HPMC gels, always gave a faster release of drug (at the time point of 5 hours, 46.5 ± 3.6 % was released in comparison to 32.7 ± 7.9 %). Additionally, within the first couple of hours of this study, no drug release was observed, this may have been due to the amount of drug being lower than that of the limit of detection.

As discussed in section 3.4.7.1.1, the addition of water-insoluble drug can increase the water uptake by the gel thus weakening network integrity thus drug loading will influence network integrity (Nafee et al., 2003; Panomsuk et al., 1996). In this case, it appears the HEC matrix

eroded/swelled quicker than HPMC giving a faster rate of release. The physiochemical properties of the drug, the polymer and the interaction between the two affect drug release from the formulation.

5.4.8.3.1 Kinetic assessment

The release profiles were evaluated by the zero-order, first-order and Higuchi kinetic models. Release from the solution, HEC and HPMC gels was observed to fit the first order release model with r^2 values of 0.885, 0.861 and 0.884 respectively, (Table 5-7). This indicates rate of release was dependent on the amount of drug present at that time point.

Table 5-7: Kinetic assessment of release data of MTL-004 from solution and aqueous gels.

Kinetic model	Formulation r^2		
	Solution	HEC (3% w/w)	HPMC (3% w/w)
Zero order	-1.442 ± 0.763	0.684 ± 0.081	0.809 ± 0.070
First order	0.885 ± 0.025	0.884 ± 0.047	0.861 ± 0.050
Higuchi model		0.727 ± 0.052	0.741 ± 0.041

Results are presented as the mean ± standard deviation (n=3)

Comparison of the rate constant of each formulation shows that HEC had a higher rate constant than HPMC (Table 5-8). This implies that HPMC had a higher gel consistency thus slowing MTL-004 release. MTL-004 is released from gel following swelling which allows for the creation of pores, as viscosity increases polymer chains become more resistant to movement taking longer to dissipate into the media thus slowing release drug. This data is consistent with that of both flavonoids.

Table 5-8: First order kinetics rate constant for MTL-004 release from formulations.

Rate constant (min^{-1})		
Solution	HEC (3% w/w)	HPMC (3% w/w)
0.007 ± 0.001	2.0 ± 1.355 × 10 ⁻³	1.01 ± 1.638 × 10 ⁻³

Results are presented as the mean ± standard deviation (n=3)

The Korsmeyers-Peppas model was applied to the releases data and the diffusional exponent (n) calculated (Table 5-9). Non-Fickian release was observed for both HEC and HPMC gels at

3 % w/w polymer. At temperatures below the T_g , the polymer chains are not sufficiently able to move to permit immediate penetration of the solvent in the polymer core (Masaro and Zhu, 1999). This implies that, in our studies, when Non-Fickian transport was observed, the polymer chains were unable to move sufficiently and that at those particular loadings of polymer, the gel was in a glassy state.

Table 5-9: Diffusional exponent n for MTL-004 release data with the corresponding release mechanism.

Formulation (3 % w/w)	n	Transport type
HEC	0.698 ± 0.037	Non-Fickian
HPMC	0.781 ± 0.036	Non-Fickian

Results are presented as the mean \pm standard deviation (n=3)

As discussed in section 3.4.7, diffusion of solution out of the polymer depends upon temperature, pressure, solute size, molecular geometry and on the concentration and degree of swelling of polymers. Solvent diffusion is associated with the physical properties of the polymer network and the interactions between the polymer and solvent (Ford et al., 1987; Masaro and Zhu, 1999; Rao et al., 1990). Drug release from aqueous gels is governed by a swelling- controlled mechanism in which the drug releases into the media due to the simultaneous absorption of water by the gel causing the gel to dissipate into the media thus releasing drug and due to desorption of drug from the gel (Bouwstra and Honeywell-Nguyen, 2002; Nafee et al., 2003; Ranga Rao and Padmalatha Devi, 1988; Sinha Roy and Rohera, 2002). The membrane would have prevented the gel from completely swelling and releasing drug.

5.4.9 MTL-004 release from liposomes

Elastic liposomes employed to carry drugs across the SC for dermal drug delivery are advantageous as they can penetrate the skin if applied non-occlusively by virtue of the very high and self-optimizing deformability. Liposomes can penetrate the SC with potentially deeper penetration into the dermal layer of deformable vesicles compared with traditional liposomes (El Maghraby et al., 1999). Deformable liposomes have been effectively employed in transdermal delivery of lipophilic and hydrophilic drugs including anti-inflammatory agents, plasmid DNA, anti-tumour agents and hormones (Cevc and Blume, 2001; El Maghraby et al., 1999; Oh et al., 2006; Romero et al., 2013). Release of MTL-004 from a 0.01 mg/ mL solution, liposomes and liposomes formulated with either 2 %, 6 % or 10 % w/w of Tween 20 with was studied over a 24-hour period (Figure 5.14).

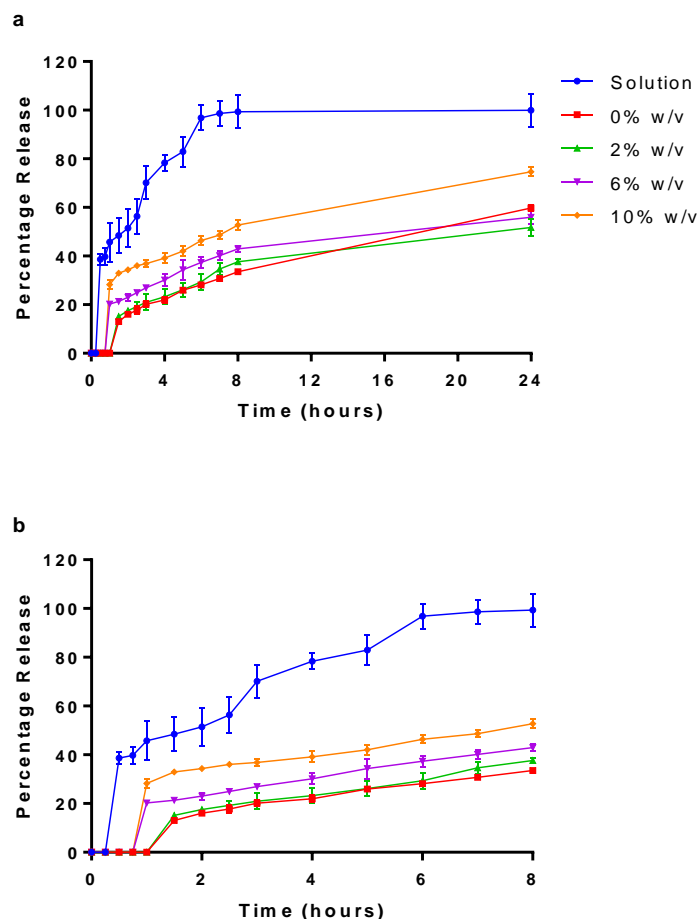


Figure 5.14: *In vitro* percentage MTL-004 release profiles from solution and liposomes

MTL-004 release profiles from solution and liposomes formulated with 0-10 % w/w Tween 20 over a) 24 hours, b) 8 hours. Liposomes were prepared adapting the dry film method adding the surfactant and MTL-004 during the lipid mixing stage. A diffusion cell dialysis system was used to evaluate *in vitro* drug release. Data represents mean \pm SD. n=6 independent batches.

Liposomes appeared to slow release of MTL-004 in comparison to release across the membrane from the MTL-004 solution. As the loading of surfactant increased, drug release also increased. This was similar to the release pattern seen with EGCG. Within 1 hour of the release study, drug release was not detected from any of the formulations. This does not necessarily suggest there was no release from the formulation, instead, this is perhaps more likely concerning detection issues. The drug release into the donor compartment must have been lower than the LOD thus was not detected by the HPLC-UV apparatus.

Over the course of 24 hours' solution gave a release of 100.0 ± 6.8 % whilst liposomes formulated with 0 %, 2 %, 6 % and 10 % w/w of Tween 20 gave a release of 59.8 ± 1.2 %, 51.8 ± 3.6 %, 56.0 ± 2.7 % and 74.0 ± 1.8 % respectively. The cumulative percentage released after 24 hours was significant between the solution and all liposomal formulations as well as between 2 % and 10 % w/w of Tween 20 ($P \leq 0.0001$). This difference was also significant

between liposomes loaded with 0 % and 10 % w/w Tween 20 ($P \leq 0.01$). Finally, this difference was also significant between liposomes loaded with 6 % and 10 % w/w of Tween 20 ($P \leq 0.001$).

Release of MTL-004 observed significant differences between release from solution and all loadings of surfactant was significant ($P \leq 0.0001$). Release between 10 % w/w and 0 and 2 and 6 % of surfactant was significantly different ($P \leq 0.001$). The release profile between 2 % w/w and 6 % w/w Tween 20 was significantly different ($P \leq 0.01$). The release profile between 0 % w/w and 6 % w/w Tween 20 was significantly different ($P \leq 0.05$). The release profile between 0 % w/w and 2 % w/w of surfactant was not significantly different. Complete release of the solution was observed between the 6th and 7th hour. Liposomes formulated with 0, 2, 6 and 10 % w/w Tween 20 gave 60 %, 52 %, 56 %, and 74 % release respectively.

5.4.9.1 Kinetic assessment of MTL-004 release from liposomal formulations

MTL-004 release data from the solution and all liposomal formulations complied with first order release kinetics implying rate of drug release was dependent on drug concentration at that time (Table 5-10 and 5-11).

Presence of surfactant appears to decrease drug release between 0 % and 2 % w/w loading of Tween 20, after which drug release increased and at 10 % cumulative percentage release surpassed that of liposome containing no surfactant. At lower loadings of surfactant, compared with liposomes containing no surfactant there is less entrapped drug thus less of a concentration gradient for the drug to diffuse across. However, surfactant would increase drug solubility thus explaining why an increase in drug release is observed at higher loadings of surfactant. Furthermore, the mechanism of the *in vitro* release from liposomes may be due to be the formation of transient pores in the lipid bilayer, through which drugs are released from the inner aqueous core of the liposomes to the extra-liposomal medium (Wang, Wang et al. 2016). Therefore, the presence of more surfactant in the liposome may also encourage the formation of transient pores.

Table 5-10: Kinetic assessment of release data of MTL-004 from solution and liposomal formulations.

Kinetic model	Formulation (r^2)				
	Solution	Liposome (% w/w loading of Tween 20)			
		0	2	6	10
Zero order	-1.442 ± 0.763	0.706 ± 0.019	0.474 ± 0.145	0.642 ± 0.062	0.004 ± 0.017
First order	0.885 ± 0.025	0.907 ± 0.011	0.776 ± 0.079	0.076 ± 0.064	0.740 ± 0.017

Results are presented as the mean ± standard deviation (n=3)

Comparison of the rate constant of each formulation shows MTL-004 solution had the highest rate of release liposomes followed by liposomes formulated with 10% w/w Tween 20, followed by liposomes formulated with 0% w/w Tween 20, then 6% w/w Tween 20 and then liposomes formulated with 2% w/w of Tween 20 (Table 5-11).

Table 5-11: First order kinetics rate constant for MTL-004 release from formulations.

Formulation ($\times 10^{-3} \text{ min}^{-1}$)				
Solution	Liposome formulation (% w/w loading of tween 20)			
	0	2	6	10
7.10 \pm 1.02	0.45 \pm 0.04	0.08 \pm 0.04	0.91 \pm 0.004	1.963 \pm 0.2

Results are presented as the mean \pm standard deviation (n=3)

As discussed in section 3.4.7.3 the release data observed will be either because of drug release from the liposome and then the membrane or movement of the liposome across the barrier and then release from this. The diffusion cell system will see release from the liposome first owing to the physical set up of the cell and the smaller pore size of 50 nm. Additionally, reversible binding of the drug released from the liposome reduces the driving force for drug transport across the dialysis membrane leading to a slower overall apparent release rate (Modi and Anderson, 2013). In this case, this reversible binding was greater with lower loadings of surfactant loading resulting in a slower rate of release for liposome formulated with 2 % and 6 % Tween 20 in comparison to liposomes formulated with no Tween 20 or 10 % w/w Tween 20.

5.4.10 Liposomal gel MTL-004 release studies

Similar to both flavonoids, drug release from liposomal gels could not be measured/detected in the side by side diffusion chamber therefore a cell culture Thincert™ insert (400 μm pore size) was filled with 1 mL of formulation and release into 4 mL of DDM in a 6-well Thincert™ plate was quantified. Neither the diffusion cell nor the Thincert™ system mimic what would happen following formulation application on the skin. The diffusion cell was used to see how drug diffused across a membrane with a pore size similar to that of the gaps in the stratum corneum whilst maintaining sink conditions. The Thincert™ plate with inserts was used simply to overcome detection/experimental limitations of the diffusion cell and see if drug was able to come out from the liposomes loaded into the gel and then the release media. To ensure we were only detecting free drug samples were centrifuged and supernatant analysed.

Both HEC and HPMC gels were loaded with either drug loaded liposomes or drug loaded elastic liposomes formulated with 2 % Tween 20. Only liposomes loaded with 2 % of Tween

20 were investigated since an increase in surfactant results in a decrease of drug loading of which would make drug detection even harder. Within the first 2 hours of the study, drug release was not detected from any of the formulations, suggesting there was no release (Figure 5.15). This is perhaps more likely concerning detection issues. The drug release into the donor compartment must have been lower than the LOD thus was not detected by the HPLC-UV apparatus.

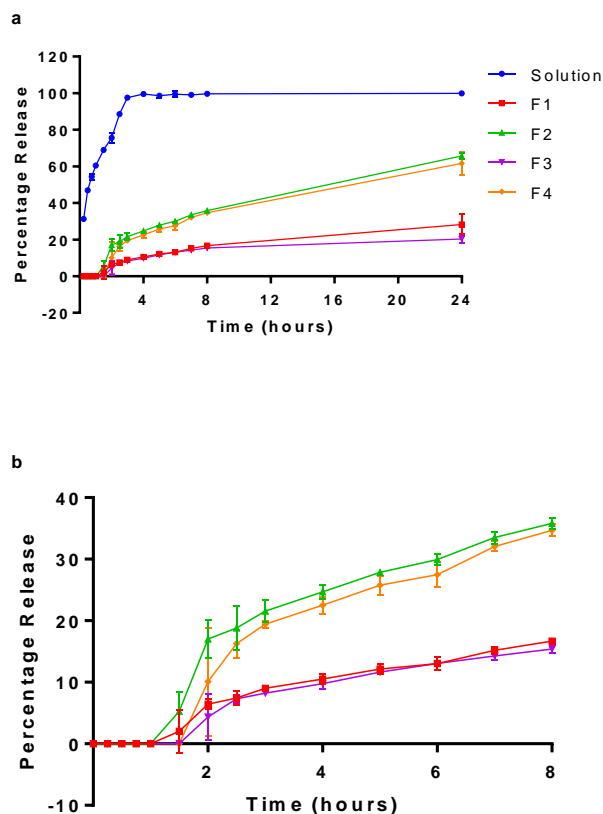


Figure 5.15: *In vitro* percentage MTL-004 release profiles from liposomal gels

In vitro percentage MTL-004 release profiles using a transwell system with permeable inserts of a 400 nm pore size from solution and gel loaded with either blank or elastic liposomes formulated with 2 % w/w Tween 20 over a) 24 hours, b) 8 hours. F1: HEC and blank liposomes, F2: HEC and elastic liposomes, F3: HPMC and blank liposomes, F4: HPMC and elastic liposomes. Liposomes were prepared adapting the dry film method. Gels were prepared using 3 % w/w loading of either HEC or HPMC. Data represents mean \pm SD. n=3 independent batches.

Complete drug release from solution seemed to reach a maximum occur between the 3rd and 4th hour (Figure 5.15). As with both flavonoids, over all, the percentage of drug release from the liposome loaded gels quantified over 24 hours was slightly higher from the HEC gel (up to 66 %). Furthermore, a higher percentage of drug was released from the elastic liposome (up to 66 %).

Over the course of 24-hours solution gave a release of 99.9 ± 0.9 % whilst F1, F2, F3 and F4 gave a release of 28.3 ± 5.4 %, 65.7 ± 1.5 %, 20.3 ± 1.9 % and 61.6 ± 6.1 %, respectively. The cumulative percentage released after 24 hours was significant between the solution and all liposomal gels as well as between all liposomal gels except between formulation 1 and 3 as well as 2 and 4 ($P \leq 0.0001$). F1 and F3 contained no surfactant in the liposome and F2 and F4 contained 2 % w/w of Tween 20. Therefore, release in the liposomal gels appeared to be affected by presence on surfactant rather than the type of aqueous gel used.

This implies that either elastic liposomes were more able to move through the gel compared with blank liposomes or that the presence of surfactant increased the solubility of drug thus encouraging release from the liposome bilayer. As discussed in section 3.4.7.4, drug properties (solubility, log P), liposome stability during their dispersion in the gel formulation determine the system behaviour and thus drug release (Mourtas et al., 2007).

5.4.11 Impact of liposomal formulation on *In vitro* cytotoxicity on HDFa and HaCat cells

To assess the toxicity of MTL-004 on HDFa and HaCat cells, an XTT assay was performed to measure cell death after exposure of cells to different concentrations of drug for 24 hours. Results of cell viability are shown in Figure 5.16.

As the concentration of MTL-004 was increased, there was a decrease in HDFa cell viability. In comparison to the control well, the viability in cells treated with 100, 50, 10, 5 and 0.1 μM was significantly lower ($P \leq 0.0001$), as well as cells treated with 1 μM ($P \leq 0.05$) of MTL-004. At 100 μM MTL-004 concentration cell viability decreased to 46.1 ± 3.9 %. An IC_{50} value of 191.1 μM was observed. This may be due to toxicity or death of damaged cells in which MTL-004 induced apoptosis (Bae et al., 2008; Tanigawa et al., 2014).

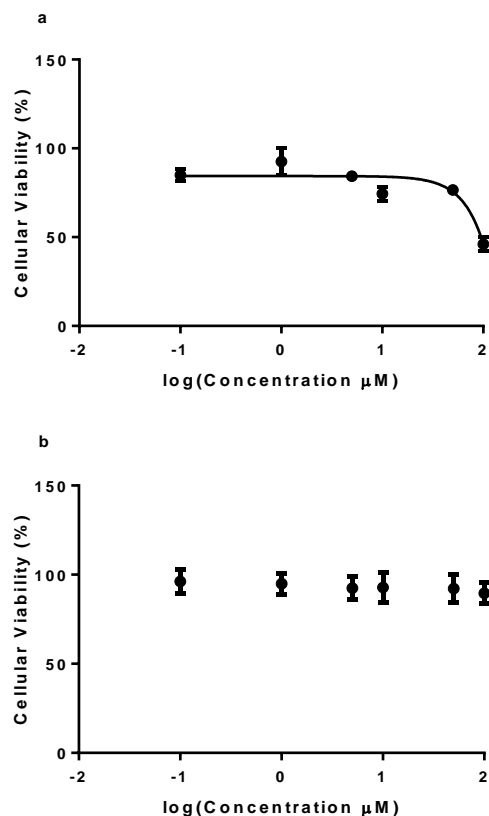


Figure 5.16: Cellular toxicity of MTL-004 on HDFa and HaCat cells.

Cellular toxicity of MTL-004 (A), HDFa (B), HaCat cells. Cells were grown on a 96-well plate at a density of 50×10^3 cells per well and exposed to various concentrations of MTL-004 (0.1 – 100 μM). After 24 hour incubation following which 25 μL of a 12.5:1 parts mixture of XTT to menadione was added each well. Plates were incubated for 3 hours at 37°C and the absorbance read at 450 nm. The control cell (without drug) corresponded to a cell viability of 100 %. Data is reported as mean \pm SD with 6 replicates per compound in 3 independent experiments.

There was no significant difference in cell viability at the range of MTL-004 concentrations studied with the HaCat cells therefore within this concentration range, MTL-004 was safe for application on these cells ($P \geq 0.01$). This was also observed with both flavonoid and is not unexpected as keratinocytes are by nature more resilient cells owing to their barrier function property. Any differences in these percentages was not significant therefore, at these concentrations MTL-004 was not toxic to this line of keratinocytes.

5.4.12 Cellular liposomal uptake assay on HDFa and HaCat cells

Fluorescently labelled liposomes loaded with MTL-004 were incubated with both HDFa and HaCat cells to assess the cellular uptake of these formulations. Following a 2-hour incubation with the cells, the labelled liposomes were identified using confocal microscopy (Figure 5.17 and 5.18). Cytoplasmic accumulation of the formulations was apparent, confirming the successful uptake into both HDFa and HaCat cells.

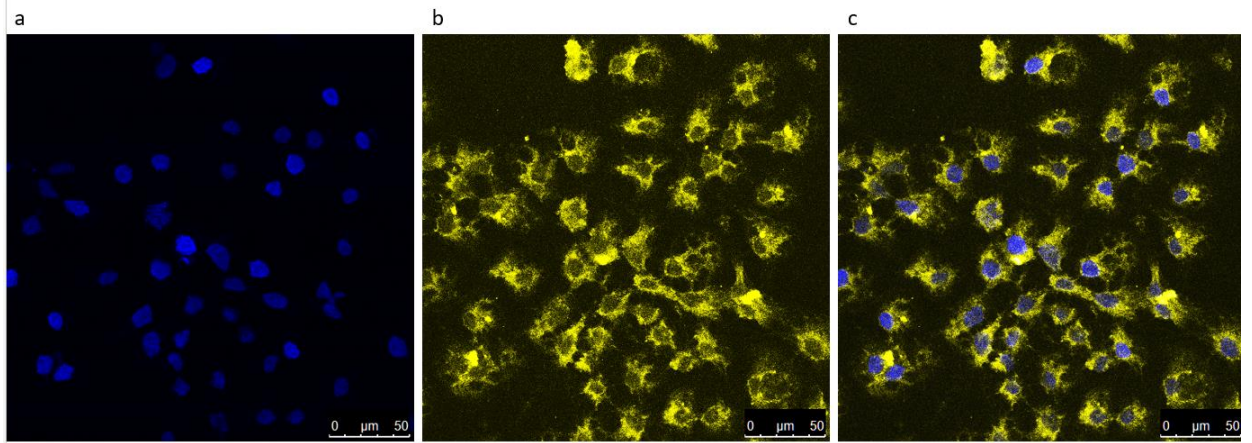


Figure 5.17: Localisation DilC-liposomes loaded with MTL-004 and 2% w/w Tween 20 in HaCat cells

Localisation of DilC labelled liposomes loaded with MTL-004 and 2% w/w Tween 20 in HaCat cells. Cells were grown on the coverslips for 2 days. Cell nuclei were visualised using a) DAPI (Blue). Liposomes were formulated with DilC for visualisation b) (yellow). Liposome localisation within the cell is shown in the merged image c).

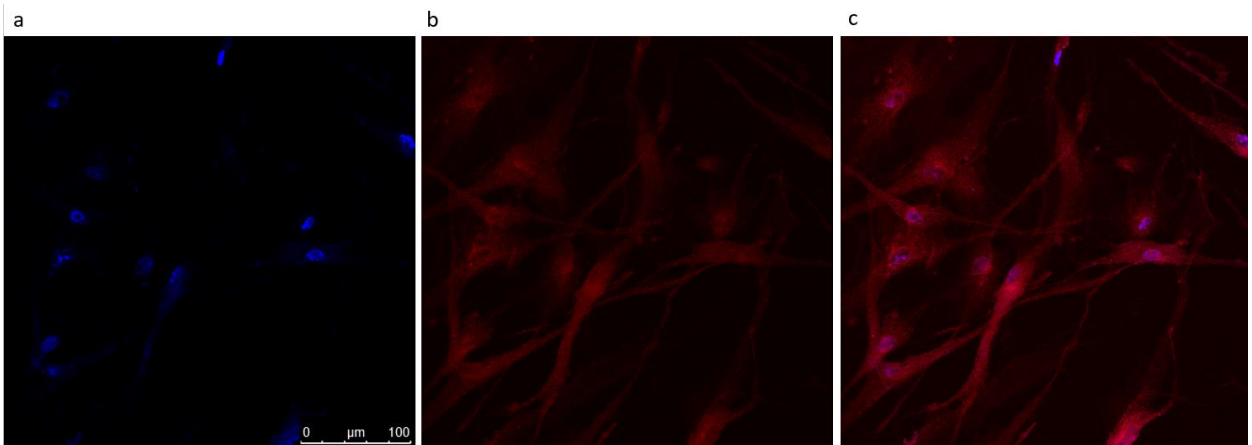


Figure 5.18: Localisation of DilC-liposomes loaded with MTL-004 and 2% w/w Tween 20 in HDFa cells.

Localisation of DilC labelled liposomes loaded with MTL-004 and 2% w/w Tween 20 in HDFa cells. Cells were grown on the coverslips for 2 days. Cell nuclei were visualised using a) DAPI (Blue). Liposomes were formulated with b) DilC for visualisation (red). Liposome localisation within the cell is shown in the merged image c).

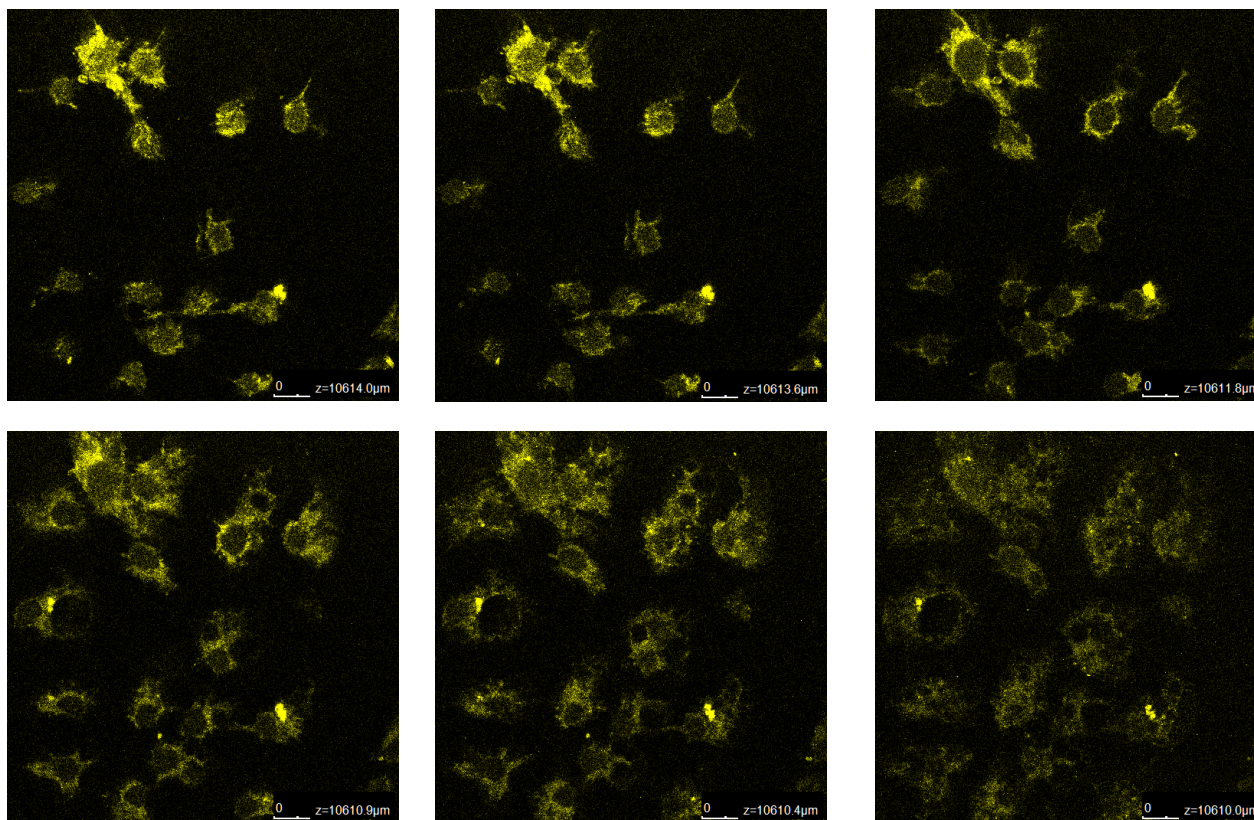


Figure 5.19: z-dimension cellular localisation of DiIC-MTL-004 loaded liposomes formulated with 2% w/w Tween 20 in HaCat cells

z-dimension cellular localisation of DiIC labelled liposomes loaded with MTL-004 and 2 % w/w Tween 20 (stage 2). DiIC labelled liposomes previously incubated with HaCat cells for 2 hours were further subjected to a z-stack analysis with the lens positioned above the cell layer (12216 μm) and lowered through the cells to the bottom of the cell layer (12210 μm). Images were captured of DiIC (green) through the z-dimension.

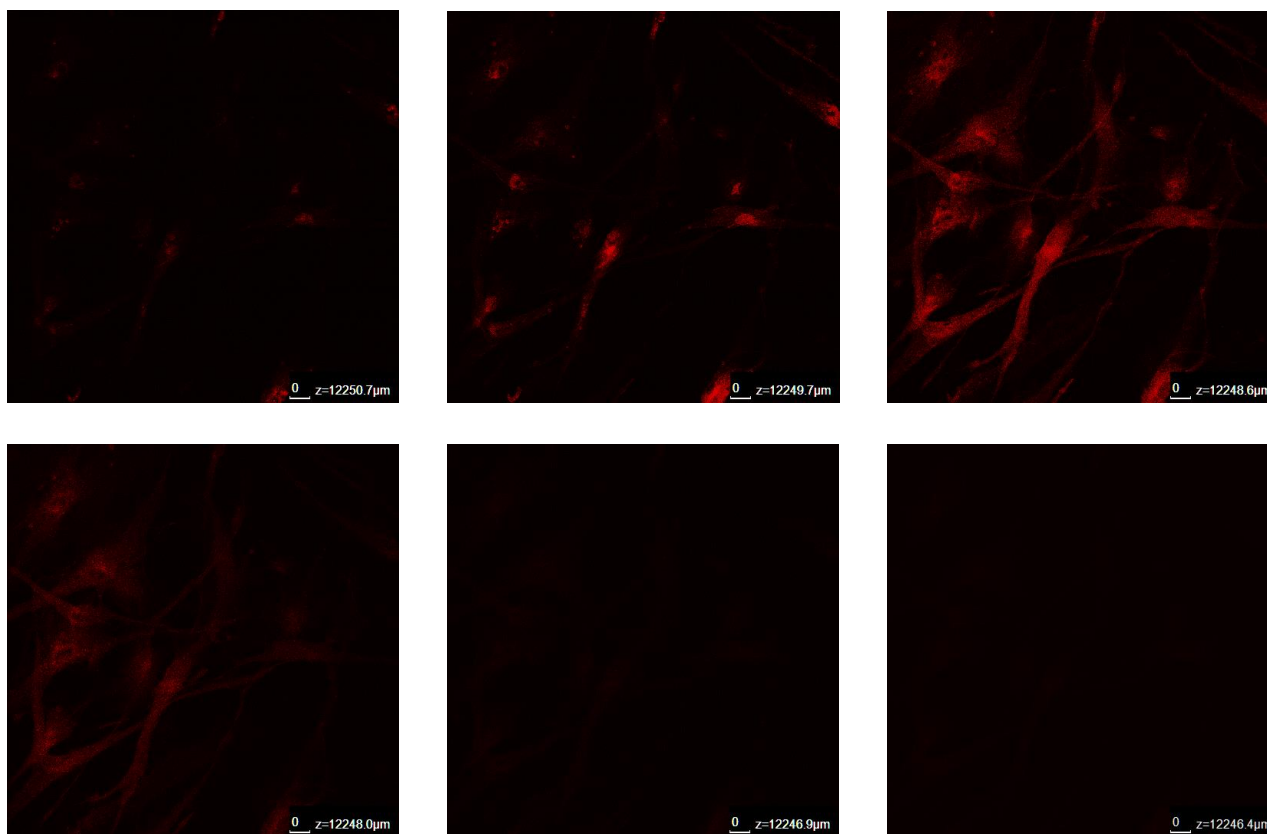


Figure 5.20: z-dimension cellular localisation of DiIC-MTL-004 loaded liposomes formulated with 2% w/w Tween 20 in HDFa cells

z-dimension cellular localisation of DiIC labelled liposomes loaded with MTL-004 and 2 % w/w Tween 20 (stage 2). DiIC labelled liposomes previously incubated with HDFa cells for 2 hours were further subjected to a z-stack analysis with the lens positioned above the cell layer (12216 μm) and lowered through the cells to the bottom of the cell layer (12210 μm). Images were captured of DiIC (green) through the z-dimension.

The confocal stage was set at the upper-most boundary of the HDFa/HaCat cells and the stage moved down towards the coverslip with images captured over a z-dimension of approximately 5 μm (Figure 5.19 and 5.20). At the onset of the z-stack analysis, liposomes are localised on the exterior of the cell boundary and potentially on the surface of the cells (10614 μm). As the stage progresses, the localisation of FITC-Fan-MSNP increases with clear demarked zones of cytoplasmic localisation near the 'mid-to-bottom' regions of the cells.

There are four methods of liposome interaction with cells as discussed in section 2.4.5: stable adsorption, endocytosis, fusion of the lipid bilayer with the cell plasma membrane and lipid transfer (Martin and MacDonald, 1976; Pagano and Weinstein, 1978). It is unclear which of these occurred in this study, however, these methods of uptake are not mutually exclusive and any given amalgamation could have occurred in these circumstances (Pagano and Weinstein, 1978).

This formulation is aimed to be targeting the dermal layer. Liposomes may completely pass through the keratinocytes into the dermal layer or they may accumulate in the stratum corneum. To be able to determine this, application onto excised skin would be necessary. Nonetheless it is clear liposomes were taken up by the cells, more importantly the fibroblasts thus the liposomes were successfully able to enter the cells.

5.4.13 Stability of deformable liposomes

The stability of deformable liposomes during storage at 20°C was studied in terms of size and, for drug loaded liposomes, encapsulation efficiency. Confocal images were observed on day 1 of formulation to ensure the presence of liposomes (Figure 5.21). The size of blank and surfactant loaded liposomes was measured on day 1, 2, 7, 14, 21 and 28 (Figure 5.22).

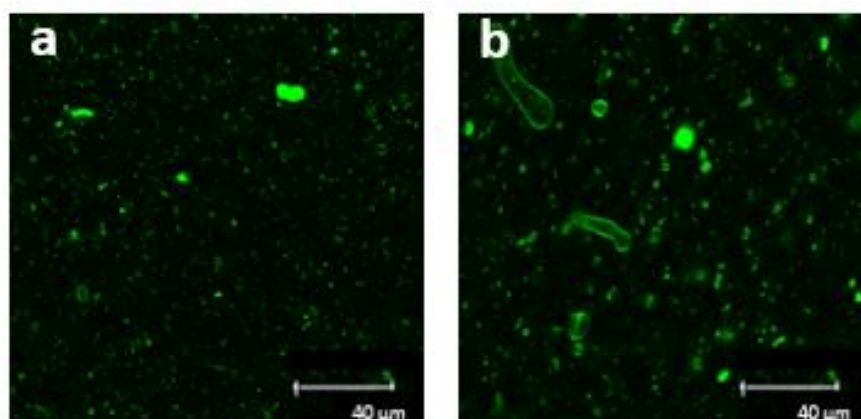


Figure 5.21: Confocal images of MLV liposomes formulated with MTL-004

MLV liposomes formulated with MTL-004 were loaded with either a) 0 % w/w Tween 20, b) 2 % w/w Tween 20. Fluorescently labelled liposomes were formulated by the addition of the fluorescent dye DiIc to the lipid mixing stage. The untrapped marker was removed by

centrifuging liposomes, removing the supernatant, re-suspending in water. Liposomes were imaged using an upright confocal microscope (Leica SP5 TCS II MP) and visualised with a 40x oil immersion objective.

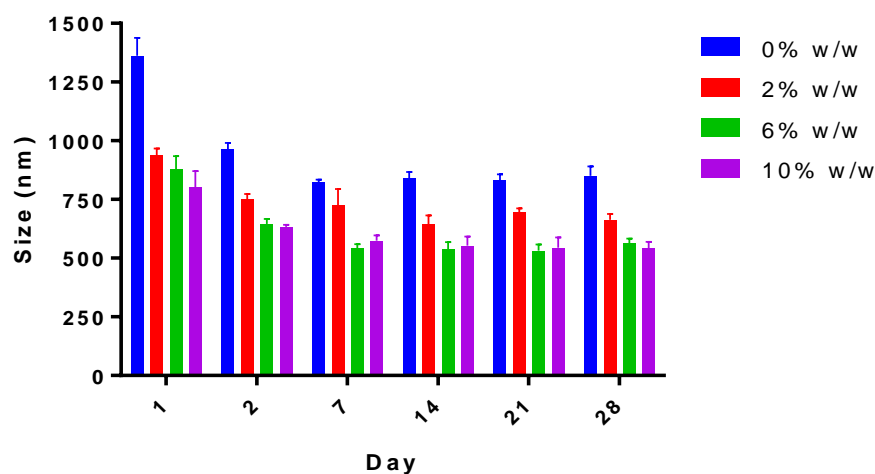


Figure 5.22: Stability of MTL-004 loaded liposomes as determined by size

Size of MTL-004 loaded liposomes formulated with 0-10% w/w Tween 20 was determined using DLS, formulated with up to 10 % w/w Tween 20 measured on various days (1, 2, 7, 14, 21 and 28). Liposomes were prepared adapting the dry film method. Liposome size was assessed via DLS. Data represents mean \pm SD. n=6 independent batches.

Drug loaded liposomes formulated with no surfactant appear to decrease in size from 1362 nm to 850 nm over time. This was unexpected as usually, aggregation is noted resulting in vesicle size growth (Seras et al., 1992). This may be a result of to larger, more dense liposomes/aggregates settling as a creamy film could be seen at the bottom of the cuvette. This trend was however also spotted with both flavonoid loaded liposomes.

The inclusion of surfactant seemed to decrease this phenomenon to a degree. Formulations with 2 % w/w, 6 % w/w and 10 % w/w observed a size decrease from 937 to 663 nm, 878 to 562 nm and 801 to 543 nm respectively over the course of 28 days. Liposomes formulated without surfactant have a lower polydispersity, thus inclusion of surfactant provides a more homogenous mix with less larger liposomes/aggregates formulated thus there would be less of these to settle out over time.

The size decrease of liposomes formulated without Tween 20 was significant between day 1 and all other days ($P \leq 0.0001$), as well as between day 2 and 7 ($P \leq 0.01$), and between day 2 and 14, 21, and 28 ($P \leq 0.05$). There was no significant difference between days 7 onwards. This may be because all lipid aggregates settled out by this time. The size decrease between liposomes formulated with 2 % w/w Tween 20 between day 1 and all other days ($P \leq 0.0001$), as well as between day 2 and 14 ($P \leq 0.01$), and between day 2 and 28 ($P \leq 0.05$). There was

no significant difference between days 7 onwards. This may be because all lipid aggregates settled out by this time. The size decrease of liposomes formulated with 6 % w/w Tween 20 was significant between day 1 and all other days ($P \leq 0.0001$), as well as between day 2 and both 7 and 14 ($P \leq 0.01$), and between day 2 and 28 ($P \leq 0.05$). There was no significant difference between days 7 onwards. This may be because all lipid aggregates settled out by this time. The size decrease of liposomes formulated with 10 % w/w Tween 20 was significant between day 1 and 2 ($P \leq 0.01$), 1 and 7 ($P \leq 0.001$) and between day 1 and 14, 21 and 28 ($P \leq 0.0001$), There was no significant difference between day 2 onwards. This may be because all lipid aggregates settled out by this time. There may have been less large lipid aggregates to settle out of this formulation because the presence of more surfactant would solubilise the lipids leading to less aggregation.

Additionally, encapsulation efficiency appears to decrease from 44 % to 39 %, 35 % to 25 %, 29 % to 20 % and 21 % to 13 % respectively for 0 % w/w, 2 % w/w, 6 % w/w, 10 % w/w loading of surfactant (Figure 5.23). This drug leaching phenomenon was non-significant in liposomes loaded with no surfactant. The decrease in encapsulation efficiency was significant for liposomes loaded with 2 % w/w Tween 20 between days 1 and 28 ($P \leq 0.0001$), 2 and 28, 7 and 21 ($P \leq 0.001$), 1 and 21, 14 and 28 ($P \leq 0.01$) and finally, 7 and 21 ($P \leq 0.05$). For liposomes loaded with 6 % w/w Tween 20, the decrease in encapsulation efficiency was significant between days 1 and 28 ($P \leq 0.001$), 1 and 21, 2 and 28 ($P \leq 0.01$) and finally between days 1 and 14 as well as 7 and 28 ($P \leq 0.05$). For liposomes loaded with 10 % w/w Tween 20, the decrease in encapsulation efficiency was significant between days 1 and 28 ($P \leq 0.0001$), between days 1 and 21, 2 and 28 ($P \leq 0.001$), between days 1 and 14 as well as 2 and 21 ($P \leq 0.01$), and finally between days 2 and 14 as well as 7 and 28 ($P \leq 0.05$). Liposome aggregation may have led to drug leaching or visa versa. This suggests a lower loading of surfactant is best to ensure stability.

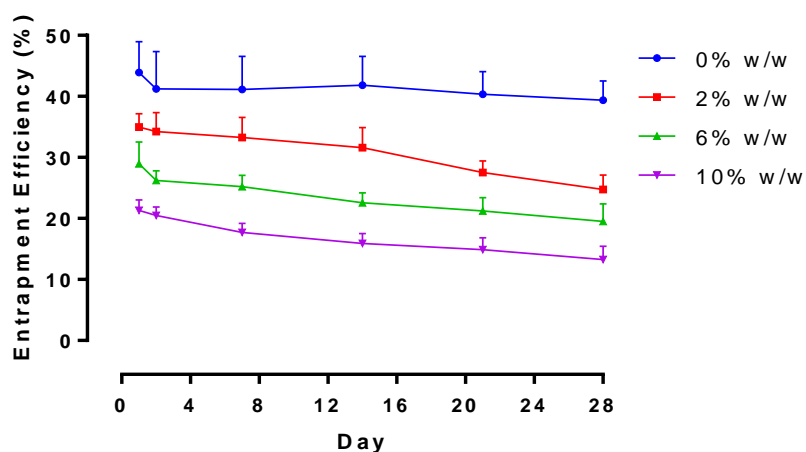


Figure 5.23: Liposome encapsulation efficiency for MTL-004 over 28 days

Liposome encapsulation efficiency for MTL-004 in either 0 % w/w, 2 % w/w, 6 % w/w or 10 % w/w Tween 20 liposomes over 28 days. Liposomes were prepared adapting the dry film method adding the surfactant and drug during the lipid mixing stage. The preparation was then washed via centrifugation. The quantity of MTL-004 in supernatant over 28 days was then analysed by HPLC coupled with UV detection to assess liposome stability. Data represents mean \pm SD. n=6 independent batches.

As discussed in section 3.4.10 the long-term stability of liposomes depends on the average elastic energy of the membrane being higher than the thermal energy (Lipowsky 1991). Therefore, temperature is an important determinate of stability and liposomes must be stored at a suitable temperature. This suggests these liposomal formulations may not be suitable for long term stability. Either additional excipients are required or an additional step of freeze drying liposomes for reconstitution near the time of administration.

5.5 Conclusion

MTL-004 is a novel potent cytotoxic agent suggested for use in the local treatment of NMSC. This drug elicits an effect by forming DNA interstrand crosslinks which are poorly repaired resulting in cell death. An additional advantage is the lack of systemic toxicity due to the high reactivity of MTL-004 with serum proteins. Moreover MTL-004 has been found to have no effect on normal cells as it only works in rapidly dividing cells.

Chemotherapeutic agents are infamously problematic when considering formulation options due to compounds having a low solubility. Liposomes can improve the bioavailability of these agents and are therefore useful as delivery agents. Furthermore, elastic liposomes have been found to be useful in dermal drug delivery as they increase compound solubility, protect the drug from degradation, can be formulated for targeted, controlled drug release (Benson 20016, Cevc 1996) and are able to penetrate the SC (Fang et al., 2008; Lau et al., 2005; Trotta et al., 2004).

As the loading of Tween 20 in the liposomal bilayer increased, liposome size decreased. The presence of MTL-004 in elastic liposome increases the liposome diameter; however, the inclusion of surfactant decreases the diameter. Inclusion of surfactant in the bilayer decreases liposome deformability index implying such elastic carriers may be useful in dermal drug delivery as they would be able to pass through the gaps in the SC.

As the loading of Tween 20 in the liposome increased MTL-004 encapsulation decreased. This may have been due to Tween 20 competing for space within the bilayer or due to Tween 20 increasing the solubilisation capacity of MTL-004.

Aqueous gels were found to slow the release of drug compared to drug solution. MTL-004 release from liposomes found liposomes were able to modify the release of drug and complete release was not observed within 24 hours. Furthermore, as surfactant loading in the bilayer increased, the rate of release per unit time also increased. Liposomes added into gels seemed to have an additive effect in terms of retarding drug release. Release was faster from HEC gels and liposomes formulated with Tween 20.

Toxicology assay's found that between 0.1 and 100 μM MTL-004 did decrease fibroblast cell viability but not keratinocytes viability. Cell uptake of the liposomes loaded with EGCG and 2 % w/w Tween 20 was apparent into both the keratinocyte cell line and the fibroblast cell line. It appears elastic liposomes are useful in enhancing drug penetration into dermal cells and furthermore may be useful in the development of a controlled release formulation.

Deformable liposomes appear to be a useful carrier in the development of a controlled release formulation for novel chemotherapeutic agents. Aqueous gels were found to hinder the release

of MTL-004 compared to MTL-004 solution. Furthermore, MTL-004 release from liposomes observed rate of release was influenced by the liposome carrier system with the presence of Tween 20 observing a faster rate of release.

6 General conclusions

6.1 General conclusions

The overall aim of this work was to formulate and develop formulations for the dermal delivery of potential anti-cancer agents following topical application to NMSC tumours. Skin cancer is emerging as an increasing public health problem especially in developed countries. The most common treatment is surgical excision of the tumour. However this may not be suitable for all patients thus development of alternative treatments is necessary.

The use of anti-oxidants to prevent oxidative skin damage appears to be a promising approach. EGCG and naringenin have been found to affect specific biological processes that could be exploited as targets for the prevention and treatment of cancer. MTL-004 is a new compound developed by Morvus to target NMSC tumours unique in its ability to detect and target cancer cells only.

Liposomes were investigated as the primary drug carriers as they can protect compounds from degradation as well as provide sustained release of drug. Current topical treatments for NMSC suffer with a multi dosing regimen that is met with poor patient compliance. A sustained release drug delivery system would overcome this. Elastic liposomes were developed with the aim to be able to pass through the gaps in the SC into the dermal layer where they would provide a slow release of compound. Liposome elasticity was modified with the use of the surfactants Tween 80, Tween 20 or sodium cholate. Furthermore, the aqueous gels HEC and HPMC were investigated as carriers for the liposomes to be applied topically.

Chapter 2 concerned the formulation and characterisation of liposomes formulated with either Tween 80, Tween 20 or sodium cholate. As the loading of Tween 80, Tween 20 or sodium cholate in the bilayer was increased, liposome size decreased. Furthermore, the inclusion of surfactant within the bilayer seemed to produce a more homogenous formulation as defined by the polydispersity index.

Stability studies concerning liposome size for liposomes formulated with either Tween 80, Tween 20 or sodium cholate found that over the first 2 days, liposome size decreased although this may have been due to lipid aggregates settling out (as confirmed by creaming at the bottom of the liposome container). Beyond this, over 28 days, the liposome size was maintained for liposomes formulated with Tween 20 and sodium cholate, a slight decrease in size was observed for liposomes formulated with Tween 80.

Inclusion of either Tween 80, Tween 20 or sodium cholate in the bilayer decreased the liposome DI and increased the amount of lipid able to pass through a membrane. Increasing the loading of the surfactant decreased the DI across all three surfactants. Sodium cholate appeared to increase deformability the greatest, however, at the loadings investigated, Tween

80 and Tween 20 appeared the most stable. Therefore, only Tween 20 was selected for all further studies.

Increasing loadings of Tween 20 within the liposomal bilayer appeared to increase the amount of energy stored within the bilayer which allowed the liposome to reform following extrusion rather than deforming permanently into smaller liposomal structures/aggregates. This suggests that liposomes loaded with Tween 20 may be better poised than conventional liposomes to pass through gaps in the SC and reach the dermal layer of the skin.

As the loading of Tween 20 increased, the difference in pre- and post- extrusion lipid concentration decreased as detected by the HPLC-ELSD equipment. This was due to the Tween 20 increasing fluidity of the liposome, thus decreasing liposome destruction, therefore less constituents become stuck within the pores. This implies that increasing loadings of Tween 20 allow the liposome, closer to its original composition, to pass through the pore.

Following application of liposomes onto dermal cell lines, 50% of the liposome solution containing 16:8 mM of PC:cholesterol and up to 10% w/w of Tween 20 decreased fibroblast cell viability. This was only true for liposomes formulated with 10% w/w Tween 20 on the keratinocytes; these cells were not affected by blank liposomes or those formulated with 2% w/w of Tween 20. This highlights fibroblast cells are more sensitive therefore further formulation development must consider this phenomenon.

Chapters 3, 4 and 5 concerned the formulation of liposomes loaded with EGCG, naringenin and MTL-004 respectively as well as 16:8 mM of PC:cholesterol and varying ratios of Tween 20. As with blank liposomes, as the amount of surfactant in the bilayer is increased, liposome size decreases. The presence of EGCG, naringenin and MTL-004 in elastic liposome increased the liposome diameter; however, the inclusion of surfactant decreased the diameter. Inclusion of surfactant in the bilayer decreases liposome DI implying liposomes retained enough elastic energy to pass through a pore size smaller than the liposome diameter. This suggests that compound loaded liposomes formulated with Tween 20 may be better able to pass through gaps in the SC and reach the dermal layer of the skin than conventional liposomes. This was true when liposomes were forced through a 200 nm and 100 nm pore size however, liposome destruction was apparent when forced through a 50 nm pore size.

As the loading of Tween 20 in the liposome was increased the EGCG, naringenin and MTL-004 encapsulation decreased. This may have been due to Tween 20 competing for space within the bilayer or due to Tween 20 increasing the solubilisation capacity of the compound. Further, inclusion of all three compounds within the liposome bilayer could reduce the phase transition temperature of the individual compound.

Across all three compounds, the one compartment release models found HEC gels to release drug slightly faster than HPMC gels. Complete gel dissipation was observed between 3 and 4

hours. Two compartment release models found that the aqueous gels were found to hinder the release of all three compounds compared to compound solutions. Furthermore, as the polymer loading increased, the rate of release decreased.

EGCG release from liposomes found they could modify the release of drug with complete release observed within 24 hours. Comparison of the rate constant of each EGCG liposomal formulation that fit the first order model shows that the EGCG solution had the highest rate of release, followed by liposomes formulated with 10% w/w, then 6% w/w and then 2% w/w of Tween 20. Complete release, $94.4 \pm 4.9 \%$, was observed within 24 hours from liposomes loaded with 10% w/w of Tween 20. In addition, $36.4 \pm 3.8 \%$ release was observed with liposomes formulated with 6% w/w of Tween 20, and $17.0 \pm 1.7 \%$ was seen both 2% w/w and $13.7 \pm 1.1 \%$, was observed with blank liposomes. As surfactant loading increased, drug entrapment decreased, therefore, drug release would be expected to be slower as there is less of a concentration gradient. Furthermore, the drug is hydrophobic therefore less inclined to diffuse out of the liposomes.

Comparison of the rate constant of each naringenin liposomal formulation showed liposomes formulated with 0% w/w Tween 20 had the highest rate of release, followed by liposomes formulated with 2% w/w Tween 20, then 6% w/w Tween 20, naringenin solution and then liposomes formulated with 10% w/w of Tween 20. Surfactant appeared to have the opposite effect on naringenin release when compared with EGCG where surfactant increased the rate of drug release. This indicates that compounds individual physiochemical properties influences the release of compound from liposomes. EGCG is amphiphilic in nature and naringenin is not, EGCG may therefore have been more inclined to diffuse out of the liposomal bilayer. A higher percentage of naringenin was released from liposomes compared with drug solution. Over the course of 24 hours the EGCG solution gave a release of $54.5 \pm 4.2 \%$ whilst liposomes formulated with 0%, 2%, 6% and 10% w/w of Tween 20 gave a release of $109.7 \pm 5.0 \%$, $79.5 \pm 3.7 \%$, $61.3 \pm 3.4 \%$ and $48.5 \pm 2.1 \%$ respectively.

As with EGCG, comparison of the rate constant of each MTL-004 formulation showed MTL-004 solution had the highest rate of release followed by liposomes formulated with 10% w/w Tween 20, followed by liposomes formulated with 0% w/w Tween 20, then 6% w/w Tween 20 and then liposomes formulated with 2% w/w of Tween 20. Over the course of 24 hours the MTL-004 solution gave a release of $100.0 \pm 6.8 \%$ whilst liposomes formulated with 0 %, 2 %, 6 % and 10 % w/w of Tween 20 gave a release of $59.8 \pm 1.2 \%$, $51.8 \pm 3.6 \%$, $56.0 \pm 2.7 \%$ and $74.0 \pm 1.8 \%$ respectively.

EGCG, naringenin and MTL-004 loaded liposomes added into the aqueous HEC or HPMC gels may have had an additive effect in terms of retarding drug release. Release was faster from HEC gels and liposomes formulated with Tween 20.

Toxicology assays used to assay compound toxicology on both HDFa and HaCat cells found that 0.1-100 μM EGCG was not harmful to either HDFa or HaCat cells. Additionally, between 0.1 and 100 μM naringenin was not harmful to either HDFa or HaCat cells.

Cell uptake of the liposomes loaded with either EGCG, naringenin and MTL-004 and 2% w/w Tween 20 was apparent into both the keratinocyte cell line and the fibroblast cell line. It appears elastic liposomes are useful in enhancing drug penetration into dermal cells and furthermore may be useful in the development of a controlled release formulation.

A clear challenge in targeting the dermal layer via the topical route is the ability of drug carriers to penetrate the SC. Elastic liposomes may not only be able to overcome this challenge but provide a controlled release of drug. The main aim of the study was to develop a dermal drug delivery system for the controlled release of anti-cancer agents and it appears, elastic liposomal gels may be useful in achieving this objective.

6.2 Future studies

Application of formulations to excised skin is necessary to determine how the formulations will interact with the different skin components and how compound will move out of the carrier across the stratum corneum and into the dermal layer. Confocal microscopy on the different layers of skin separated by the skin stripping method will be useful to view this interaction and determine how the liposome moves through the gel and into the skin. Further studies surrounding *in vivo* work will need to consider how the increased solubilisation of the active compound will affect the pharmacokinetic and pharmacodynamic profile of the drug thus careful monitoring is required to assess clinically adverse effects caused by this phenomenon or by the excipients themselves.

Further work surrounding MTL-004 and its characteristics and stability will need to be carried out. MTL-004 is acid labile and the dermal layer is acidic. When release studies into a release media buffered at pH 5.2 were carried out split peaks or disappearing peaks were observed. In fact MTL-004 is known to be acid labile therefore, release into media buffered at this pH was problematic. In fact one of the aims of the liposomes is to protect the MTL-004 whilst it is being delivered to cells.

Additionally, gel characterisation work that contribute to patient acceptability and clinical efficacy including optimal mechanical properties, good bioadhesion and appropriate viscosity need to be investigated for the various gel formulations loaded with liposomes in order to optimise the formulation. Rheology studies could be carried out to assess how the gels respond to applied forces to deduce information on the viscosity and spreadability of the gel. Ease of product removal from a tube may be determined using a Texture Analyser fitted with the texture profile analysis probe in compression mode.

7 References

- Al-Khalili, M., Meidan, V.M., Michniak, B.B., 2003. Iontophoretic transdermal delivery of buspirone hydrochloride in hairless mouse skin. *AAPS PharmSci* 5, E14.
- Albini, A., Sporn, M.B., 2007. The tumour microenvironment as a target for chemoprevention. *Nature Reviews Cancer* 7, 139-147.
- Alexander, A., Dwivedi, S., Giri, T.K., Saraf, S., Saraf, S., Tripathi, D.K., 2012. Approaches for breaking the barriers of drug permeation through transdermal drug delivery. *J Control Release* 164, 26-40.
- Alfrey Jr, T., Gurnee, E., Lloyd, W., 1966. *Sci. Part C* 12, 249.
- Ali, M.H., Kirby, D.J., Mohammed, A.R., Perrie, Y., 2010. Solubilisation of drugs within liposomal bilayers: alternatives to cholesterol as a membrane stabilising agent. *J Pharm Pharmacol* 62, 1646-1655.
- Ali, M.H., Moghaddam, B., Kirby, D.J., Mohammed, A.R., Perrie, Y., 2013. The role of lipid geometry in designing liposomes for the solubilisation of poorly water soluble drugs. *Int J Pharmaceut* 453, 225-232.
- Almog, S., Kushnir, T., Nir, S., Lichtenberg, D., 1986a. Kinetic and structural aspects of reconstitution of phosphatidylcholine vesicles by dilution of phosphatidylcholine-sodium cholate mixed micelles. *Biochemistry* 25, 2597-2605.
- Almog, S., Kushnir, T., Nir, S., Lichtenberg, D., 1986b. Kinetic and structural aspects of reconstitution of phosphatidylcholine vesicles by dilution of phosphatidylcholine-sodium cholate mixed micelles. *Biochemistry* 25, 2597-2605.
- Anlezark, G.M., Melton, R.G., Sherwood, R.F., Coles, B., Friedlos, F., Knox, R.J., 1992. The bioactivation of 5-(aziridin-1-yl)-2, 4-dinitrobenzamide (CB1954)—I: purification and properties of a nitroreductase enzyme from *Escherichia coli*—a potential enzyme for antibody-directed enzyme prodrug therapy (ADEPT). *Biochemical pharmacology* 44, 2289-2295.
- Armstrong, B.K., Kricker, A., 1993. Cutaneous melanoma. *Cancer surveys* 19, 219-240.
- Aungst, B.J., 1989. Structure/Effect Studies of Fatty Acid Isomers as Skin Penetration Enhancers and Skin Irritants. *Pharm Res-Dord* 6, 244-247.
- Bae, J.Y., Choi, J.S., Choi, Y.J., Shin, S.Y., Kang, S.W., Han, S.J., Kang, Y.H., 2008. (-)Epigallocatechin gallate hampers collagen destruction and collagenase activation in ultraviolet-B-irradiated human dermal fibroblasts: involvement of mitogen-activated protein kinase. *Food and chemical toxicology : an international journal published for the British Industrial Biological Research Association* 46, 1298-1307.
- Baier, G., Cavallaro, A., Friedemann, K., Müller, B., Glasser, G., Vasilev, K., Landfester, K., 2014. Enzymatic degradation of poly(l-lactide) nanoparticles followed by the release of octenidine and their bactericidal effects. *Nanomedicine: Nanotechnology, Biology and Medicine* 10, 131-139.
- Bangham, A.D., Standish, M.M., Watkins, J.C., 1965. Diffusion of univalent ions across the lamellae of swollen phospholipids. *Journal of molecular biology* 13, 238-252.
- Barry, B.W., 2001. Novel mechanisms and devices to enable successful transdermal drug delivery. *Eur J Pharm Sci* 14, 101-114.
- Berger, N., Sachse, A., Bender, J., Schubert, R., Brandl, M., 2001. Filter extrusion of liposomes using different devices: comparison of liposome size, encapsulation efficiency, and process characteristics. *Int J Pharmaceut* 223, 55-68.
- Berman, B., 2002. Imiquimod: a new immune response modifier for the treatment of external genital warts and other diseases in dermatology. *Int J Dermatol* 41 Suppl 1, 7-11.
- Bernoulli, D., 1738. Danielis Bernoulli Joh. fil. med. prof. Basil. ... *Hydrodynamica, sive De viribus et motibus fluidorum commentarii. Opus academicum ab auctore, dum Petropoli ageret, congestum. Sumptibus J.R. Dulseckeri, Argentorati.*
- Bhaskar, K., Anbu, J., Ravichandiran, V., Venkateswarlu, V., Rao, Y.M., 2009. Lipid nanoparticles for transdermal delivery of flurbiprofen: formulation, in vitro, ex vivo and in vivo studies. *Lipids Health Dis* 8, 6.

Bhatia, A., Kumar, R., Katare, O.P., 2004. Tamoxifen in topical liposomes: development, characterization and in-vitro evaluation. *J Pharm Pharm Sci* 7, 252-259.

Boland, M.P., Knox, R.J., Roberts, J.J., 1991. The differences in kinetics of rat and human DT diaphorase result in a differential sensitivity of derived cell lines to CB 1954 (5-(aziridin-1-yl)-2,4-dinitrobenzamide). *Biochemical pharmacology* 41, 867-875.

Bommaman, D., Potts, R.O., Guy, R.H., 1991. Examination of the effect of ethanol on human stratum corneum in vivo using infrared spectroscopy. *J Control Release* 16, 299-304.

Bos, J.D., Meinardi, M.M., 2000. The 500 Dalton rule for the skin penetration of chemical compounds and drugs. *Experimental dermatology* 9, 165-169.

Bouwstra, J., Junginger, H., 1993. Hydrogels. *Encyclopaedia of Pharmaceutical Technology*, 441-465.

Bouwstra, J.A., Honeywell-Nguyen, P.L., 2002. Skin structure and mode of action of vesicles. *Adv Drug Deliv Rev* 54 Suppl 1, S41-55.

Bradfield, A., Penney, M., 1948. 456. The catechins of green tea. Part II. *Journal of the Chemical Society (Resumed)*, 2249-2254.

Bragagni, M., Mennini, N., Maestrelli, F., Cirri, M., Mura, P., 2012. Comparative study of liposomes, transfersomes and ethosomes as carriers for improving topical delivery of celecoxib. *Drug Deliv* 19, 354-361.

Brandner, J.M., Zorn-Kruppa, M., Yoshida, T., Moll, I., Beck, L.A., De Benedetto, A., 2015. Epidermal tight junctions in health and disease. *Tissue barriers* 3, e974451.

Brooks, G., Idson, B., 1991. Skin lipids. *International journal of cosmetic science* 13, 103-113.

CancerResearchUK, 2014. CancerResearchUK, Skin cancer incidence. CancerResearchUK.

Casas, M., Baszkin, A., 1992. Interactions of a non-ionic surfactant with mixed phospholipid—oleic acid monolayers. Surface potential and surface pressure studies at constant area. *Colloid Surface* 63, 301-309.

Casey, S.C., Amedei, A., Aquilano, K., Azmi, A.S., Benencia, F., Bhakta, D., Bilisland, A.E., Boosani, C.S., Chen, S., Ciriolo, M.R., Crawford, S., Fujii, H., Georgakilas, A.G., Guha, G., Halicka, D., Helferich, W.G., Heneberg, P., Honoki, K., Keith, W.N., Kerkar, S.P., Mohammed, S.I., Niccolai, E., Newsheen, S., Vasantha Rupasinghe, H.P., Samadi, A., Singh, N., Talib, W.H., Venkateswaran, V., Whelan, R.L., Yang, X., Felsher, D.W., 2015. Cancer prevention and therapy through the modulation of the tumor microenvironment. *Seminars in cancer biology*.

Cevc, G., 1996. Transfersomes, liposomes and other lipid suspensions on the skin: permeation enhancement, vesicle penetration, and transdermal drug delivery. *Crit Rev Ther Drug Carrier Syst* 13, 257-388.

Cevc, G., Blume, G., 2001. New, highly efficient formulation of diclofenac for the topical, transdermal administration in ultradeformable drug carriers, Transfersomes. *Biochimica et Biophysica Acta (BBA) - Biomembranes* 1514, 191-205.

Cevc, G., Gebauer, D., Stieber, J., Schätzlein, A., Blume, G., 1998. Ultraflexible vesicles, Transfersomes, have an extremely low pore penetration resistance and transport therapeutic amounts of insulin across the intact mammalian skin. *Biochimica et Biophysica Acta (BBA) - Biomembranes* 1368, 201-215.

Cevc, G., Schätzlein, A., Blume, G., 1995. Transdermal drug carriers: Basic properties, optimization and transfer efficiency in the case of epicutaneously applied peptides. *J Control Release* 36, 3-16.

Cevc, G., Vierl, U., 2010. Nanotechnology and the transdermal route: A state of the art review and critical appraisal. *J Control Release* 141, 277-299.

Chakrabarty, A., Geisse, J.K., 2004. Medical therapies for non-melanoma skin cancer. *Clin Dermatol* 22, 183-188.

Chapman, D., 1975. Phase transitions and fluidity characteristics of lipids and cell membranes. *Quarterly reviews of biophysics* 8, 185-235.

Chaudhary, H., Rohilla, A., Rathee, P., Kumar, V., 2013. Optimization and formulation design of carbopol loaded Piroxicam gel using novel penetration enhancers. *International journal of biological macromolecules* 55, 246-253.

Chen, C., Shen, G., Hebbar, V., Hu, R., Owuor, E.D., Kong, A.N., 2003. Epigallocatechin-3-gallate-induced stress signals in HT-29 human colon adenocarcinoma cells. *Carcinogenesis* 24, 1369-1378.

Chen, Y., Wu, Q., Zhang, Z., Yuan, L., Liu, X., Zhou, L., 2012. Preparation of curcumin-loaded liposomes and evaluation of their skin permeation and pharmacodynamics. *Molecules* 17, 5972-5987.

Chen, Z.P., Schell, J.B., Ho, C.-T., Chen, K.Y., 1998. Green tea epigallocatechin gallate shows a pronounced growth inhibitory effect on cancerous cells but not on their normal counterparts. *Cancer letters* 129, 173-179.

Chitwood, K., Etkorn, J., Cohen, G., 2013. Topical and intralesional treatment of nonmelanoma skin cancer: efficacy and cost comparisons. *Dermatol Surg* 39, 1306-1316.

Cho, H.H., Han, D.-W., Matsumura, K., Tsutsumi, S., Hyon, S.-H., 2008. The behavior of vascular smooth muscle cells and platelets onto epigallocatechin gallate-releasing poly(l-lactide-co-ε-caprolactone) as stent-coating materials. *Biomaterials* 29, 884-893.

Chtourou, Y., Fetoui, H., Jemai, R., Slima, A.B., Makni, M., Gdoura, R., 2015. Naringenin reduces cholesterol-induced hepatic inflammation in rats by modulating matrix metalloproteinases-2, 9 via inhibition of nuclear factor κB pathway. *Eur J Pharmacol* 746, 96-105.

Chung, H., Caffrey, M., 1994. The curvature elastic-energy function of the lipid-water cubic mesophase. *Nature* 368, 224-226.

Coates, A., Abraham, S., Kaye, S.B., Sowerbutts, T., Frewin, C., Fox, R.M., Tattersall, M.H., 1983. On the receiving end--patient perception of the side-effects of cancer chemotherapy. *European journal of cancer & clinical oncology* 19, 203-208.

Cockcroft, M., Latham, D., 1968. Ductility and the workability of metals. *J Inst Metals* 96, 33-39.

Conklin, K.A., 2000. Dietary antioxidants during cancer chemotherapy: impact on chemotherapeutic effectiveness and development of side effects. *Nutrition and cancer* 37, 1-18.

Cordero, J.A., Alarcon, L., Escribano, E., Obach, R., Domenech, J., 1997. A comparative study of the transdermal penetration of a series of nonsteroidal antiinflammatory drugs. *J Pharm Sci* 86, 503-508.

Cornwell, P.A., Barry, B.W., Bouwstra, J.A., Gooris, G.S., 1996. Modes of action of terpene penetration enhancers in human skin; Differential scanning calorimetry, small-angle X-ray diffraction and enhancer uptake studies. *Int J Pharmaceut* 127, 9-26.

Crommelin, D.J., 1984. Influence of lipid composition and ionic strength on the physical stability of liposomes. *J Pharm Sci* 73, 1559-1563.

Cui, J., Li, C., Deng, Y., Wang, Y., Wang, W., 2006. Freeze-drying of liposomes using tertiary butyl alcohol/water cosolvent systems. *Int J Pharm* 312, 131-136.

Cullis, P.R., Hope, M.J., Tilcock, C.P., 1986. Lipid polymorphism and the roles of lipids in membranes. *Chem Phys Lipids* 40, 127-144.

Dash, S., Murthy, P.N., Nath, L., Chowdhury, P., 2010. Kinetic modeling on drug release from controlled drug delivery systems. *Acta poloniae pharmaceutica* 67, 217-223.

Dayan, N., Touitou, E., 2000. Carriers for skin delivery of trihexyphenidyl HCl: ethosomes vs. liposomes. *Biomaterials* 21, 1879-1885.

de Visser, K.E., Eichten, A., Coussens, L.M., 2006. Paradoxical roles of the immune system during cancer development. *Nature reviews. Cancer* 6, 24-37.

Demel, R.A., Geurts van Kessel, W.S.M., van Deenen, L.L.M., 1972. The properties of polyunsaturated lecithins in monolayers and liposomes and the interactions of these lecithins with cholesterol. *Biochimica et Biophysica Acta (BBA) - Biomembranes* 266, 26-40.

Di Marzio, L., Marianecchi, C., Petrone, M., Rinaldi, F., Carafa, M., 2011. Novel pH-sensitive non-ionic surfactant vesicles: comparison between Tween 21 and Tween 20. *Colloids and Surfaces B: Biointerfaces* 82, 18-24.

Diepgen, T.L., Mahler, V., 2002. The epidemiology of skin cancer. *The British journal of dermatology* 146 Suppl 61, 1-6.

Dillaha, C.J., Jansen, G.T., Honeycutt, W.M., Bradford, A.C., 1963. Selective Cytotoxic Effect of Topical 5-Fluorouracil. *Archives of dermatology* 88, 247-256.

Donaldson, M.R., Coldiron, B.M., 2011. No end in sight: the skin cancer epidemic continues, *Seminars in cutaneous medicine and surgery*. Frontline Medical Communications, pp. 3-5.

Doolittle, G.M., Chang, T.Y., 1982. Solubilization, partial purification, and reconstitution in phosphatidylcholine-cholesterol liposomes of acyl-CoA: cholesterol acyltransferase. *Biochemistry* 21, 674-679.

- Dragicevic-Curic, N., Fahr, A., 2012. Liposomes in topical photodynamic therapy. *Expert Opin Drug Del* 9, 1015-1032.
- Dreher, F., Fouchard, F., Patouillet, C., Andrian, M., Simonnet, J.T., Benech-Kieffer, F., 2002. Comparison of cutaneous bioavailability of cosmetic preparations containing caffeine or alpha-tocopherol applied on human skin models or human skin ex vivo at finite doses. *Skin Pharmacol Appl* 15, 40-58.
- Drobits, B., Holcman, M., Amberg, N., Swiecki, M., Grundtner, R., Hammer, M., Colonna, M., Sibia, M., 2012. Imiquimod clears tumors in mice independent of adaptive immunity by converting pDCs into tumor-killing effector cells. *The Journal of clinical investigation* 122, 575.
- Du, G., Jin, L., Han, X., Song, Z., Zhang, H., Liang, W., 2009. Naringenin: a potential immunomodulator for inhibiting lung fibrosis and metastasis. *Cancer research* 69, 3205-3212.
- du Plessis, J., Weiner, N., Müller, D., 1994a. The influence of in vivo treatment of skin with liposomes on the topical absorption of a hydrophilic and a hydrophobic drug in vitro. *Int J Pharmaceut* 103, R1-R5.
- du Plessis, J., Weiner, N., Müller, D.G., 1994b. The influence of in vivo treatment of skin with liposomes on the topical absorption of a hydrophilic and a hydrophobic drug in vitro. *Int J Pharmaceut* 103, R1-R5.
- Dubey, V., Mishra, D., Asthana, A., Jain, N.K., 2006. Transdermal delivery of a pineal hormone: melatonin via elastic liposomes. *Biomaterials* 27, 3491-3496.
- Dummer, R., Becker, J.C., Boser, B., Hartmann, A.A., Burg, G., 1992. Successful therapy of metastatic eccrine poroma using perilesional interferon alfa and interleukin 2. *Archives of dermatology* 128, 1127-1128.
- Egbaria, K., Weiner, N., 1990. Liposomes as a topical drug delivery system. *Adv Drug Deliver Rev* 5, 287-300.
- Ehrenstrom Reiz, G.M., Reiz, S.L., 1982. EMLA--a eutectic mixture of local anaesthetics for topical anaesthesia. *Acta Anaesthesiol Scand* 26, 596-598.
- El-Kattan, A., Asbill, C.S., Haidar, S., 2000. Transdermal testing: practical aspects and methods. *Pharmaceutical science & technology today* 3, 426-430.
- El Maghraby, G., Williams, A.C., Barry, B., 2004. Interactions of surfactants (edge activators) and skin penetration enhancers with liposomes. *Int J Pharmaceut* 276, 143-161.
- El Maghraby, G.M., Barry, B.W., Williams, A.C., 2008. Liposomes and skin: From drug delivery to model membranes. *Eur J Pharm Sci* 34, 203-222.
- El Maghraby, G.M., Williams, A.C., Barry, B.W., 1999. Skin delivery of oestradiol from deformable and traditional liposomes: mechanistic studies. *J Pharm Pharmacol* 51, 1123-1134.
- El Maghraby, G.M.M., Williams, A.C., Barry, B.W., 2000. Oestradiol skin delivery from ultradeformable liposomes: refinement of surfactant concentration. *Int J Pharmaceut* 196, 63-74.
- El Zaafarany, G.M., Awad, G.A., Holayel, S.M., Mortada, N.D., 2010. Role of edge activators and surface charge in developing ultradeformable vesicles with enhanced skin delivery. *Int J Pharm* 397, 164-172.
- Essa, E.A., Bonner, M.C., Barry, B.W., 2002. Ionophoretic estradiol skin delivery and tritium exchange in ultradeformable liposomes. *Int J Pharm* 240, 55-66.
- Fahy, E., Cotter, D., Sud, M., Subramaniam, S., 2011. Lipid classification, structures and tools. *Biochimica et Biophysica Acta (BBA)-Molecular and Cell Biology of Lipids* 1811, 637-647.
- Fang, J.Y., Liu, P.F., Huang, C.M., 2008. Decreasing systemic toxicity via transdermal delivery of anticancer drugs. *Current drug metabolism* 9, 592-597.
- Felicio, L., Ferreira, J., Kurachi, C., Bentley, M., Tedesco, A., Bagnato, V., 2009. Long-term follow-up of topical 5-aminolaevulinic acid photodynamic therapy diode laser single session for non-melanoma skin cancer. *Photodiagnosis and photodynamic therapy* 6, 207-213.
- Feng, L., Yang, X., Shi, X., Tan, X., Peng, R., Wang, J., Liu, Z., 2013. Polyethylene Glycol and Polyethylenimine Dual-Functionalized Nano-Graphene Oxide for Photothermally Enhanced Gene Delivery. *Small* 9, 1989-1997.
- Ferderber, K., Hook, S., Rades, T., 2009. Phosphatidyl choline-based colloidal systems for dermal and transdermal drug delivery. *J Liposome Res* 19, 267-277.
- Ferry, J.D., 1980. *Viscoelastic properties of polymers*. John Wiley & Sons.

Foldvari, M., 1996. Effect of vehicle on topical liposomal drug delivery: petrolatum bases. *J Microencapsul* 13, 589-600.

Forbes, C.J., Lowry, D., Geer, L., Veazey, R.S., Shattock, R.J., Klasse, P.J., Mitchnick, M., Goldman, L., Doyle, L.A., Muldoon, B.C., 2011a. Non-aqueous silicone elastomer gels as a vaginal microbicide delivery system for the HIV-1 entry inhibitor maraviroc. *J Control Release* 156, 161-169.

Forbes, C.J., Lowry, D., Geer, L., Veazey, R.S., Shattock, R.J., Klasse, P.J., Mitchnick, M., Goldman, L., Doyle, L.A., Muldoon, B.C., Woolfson, A.D., Moore, J.P., Malcolm, R.K., 2011b. Non-aqueous silicone elastomer gels as a vaginal microbicide delivery system for the HIV-1 entry inhibitor maraviroc. *J Control Release* 156, 161-169.

Ford, J.L., Rubinstein, M.H., McCaul, F., Hogan, J.E., Edgar, P.J., 1987. Importance of drug type, tablet shape and added diluents on drug release kinetics from hydroxypropylmethylcellulose matrix tablets. *Int J Pharmaceut* 40, 223-234.

Fresta, M., Puglisi, G., 1996. Application of liposomes as potential cutaneous drug delivery systems. In vitro and in vivo investigation with radioactively labelled vesicles. *J Drug Target* 4, 95-101.

Friedlos, F., Quinn, J., Knox, R.J., Roberts, J.J., 1992. The properties of total adducts and interstrand crosslinks in the DNA of cells treated with CB 1954: Exceptional frequency and stability of the crosslink. *Biochemical pharmacology* 43, 1249-1254.

Gaikwad, V.L., Yadav, V.D., Dhavale, R.P., Choudhari, P.B., Jadhav, S.D., 2012. Effect of carbopol 934 and 940 on fluconazole release from topical gel formulation: a factorial approach. *Current Pharma Research* 2, 487-493.

Ganesan, M.G., Weiner, N.D., Flynn, G.L., Ho, N., 1984. Influence of liposomal drug entrapment on percutaneous absorption. *Int J Pharmaceut* 20, 139-154.

Garrison, M.D., Doh, L.M., Potts, R.O., Abraham, W., 1994. Effect of oleic acid on human epidermis: Fluorescence spectroscopic investigation. *J Control Release* 31, 263-269.

Gaspari, A.A., Sauder, D.N., 2003. Immunotherapy of basal cell carcinoma: evolving approaches. *Dermatol Surg* 29, 1027-1034.

Gay, C., Murphy, T., Hadgraft, J., Kellaway, I., Evans, J., Rowlands, C., 1989. An electron spin resonance study of skin penetration enhancers. *Int J Pharmaceut* 49, 39-45.

Ghosal, K., Nanda, A., 2013. Development of diclofenac potassium gel from hydrophobically modified HPMC. *Iranian Polymer Journal* 22, 457-464.

Giles, G.G., Marks, R., Foley, P., 1988. Incidence of non-melanocytic skin cancer treated in Australia. *Br Med J (Clin Res Ed)* 296, 13-17.

Giri, A., Bhowmick, M., Pal, S., Bandyopadhyay, A., 2011. Polymer hydrogel from carboxymethyl guar gum and carbon nanotube for sustained trans-dermal release of diclofenac sodium. *International journal of biological macromolecules* 49, 885-893.

Glass, A.G., Hoover, R.N., 1989. The emerging epidemic of melanoma and squamous cell skin cancer. *Jama* 262, 2097-2100.

Glavas-Dodov, M., Goracinova, K., Mladenovska, K., Fredro-Kumbaradzi, E., 2002. Release profile of lidocaine HCl from topical liposomal gel formulation. *Int J Pharm* 242, 381-384.

Gloster, H.M., Jr., Brodland, D.G., 1996. The epidemiology of skin cancer. *Dermatol Surg* 22, 217-226.

Goci, E., Haloci, E., Xhulaj, S., Malaj, L., 2014. Formulation and in vitro evaluation of diclofenac sodium gel. *Int J Pharm Pharm Sci* 6, 259-261.

Godin, B., Touitou, E., 2007. Transdermal skin delivery: predictions for humans from in vivo, ex vivo and animal models. *Adv Drug Deliver Rev* 59, 1152-1161.

Goindi, S., Kumar, G., Kumar, N., Kaur, A., 2013. Development of novel elastic vesicle-based topical formulation of cetirizine dihydrochloride for treatment of atopic dermatitis. *Aaps Pharmscitech* 14, 1284-1293.

Golden, G.M., Guzek, D.B., Harris, R.R., McKie, J.E., Potts, R.O., 1986. Lipid thermotropic transitions in human stratum corneum. *J Invest Dermatol* 86, 255-259.

Gompper, G., Kroll, D.M., 1995. Driven transport of fluid vesicles through narrow pores. *Physical review. E, Statistical physics, plasmas, fluids, and related interdisciplinary topics* 52, 4198-4208.

Good, L.M., Miller, M.D., High, W.A., 2011. Intralesional agents in the management of cutaneous malignancy: a review. *Journal of the American Academy of Dermatology* 64, 413-422.

Green, A., 1992. Changing patterns in incidence of non-melanoma skin cancer. *Epithelial cell biology* 1, 47-51.

Gregoriadis, G., 1973. Drug entrapment in liposomes. *Febs Lett* 36, 292-296.

Gregoriadis, G., Davis, C., 1979. Stability of liposomes in vivo and in vitro is promoted by their cholesterol content and the presence of blood cells. *Biochemical and biophysical research communications* 89, 1287-1293.

Groenendaal, W., von Basum, G., Schmidt, K.A., Hilbers, P.A., van Riel, N.A., 2010. Quantifying the composition of human skin for glucose sensor development. *Journal of diabetes science and technology* 4, 1032-1040.

Grossman, D., Mcniff, J.M., Li, F., Altieri, D.C., 1999. Expression of the apoptosis inhibitor, survivin, in nonmelanoma skin cancer and gene targeting in a keratinocyte cell line. *Laboratory investigation; a journal of technical methods and pathology* 79, 1121-1126.

Guideline, I.H.T., 2005. Validation of analytical procedures: text and methodology. Q2 (R1) 1.

Gupta, P., Vermani, K., Garg, S., 2002. Hydrogels: from controlled release to pH-responsive drug delivery. *Drug discovery today* 7, 569-579.

Gupta, S., Hastak, K., Afaq, F., Ahmad, N., Mukhtar, H., 2004. Essential role of caspases in epigallocatechin-3-gallate-mediated inhibition of nuclear factor kappa B and induction of apoptosis. *Oncogene* 23, 2507-2522.

Gusterson, B., Cui, W., Iwobi, M., Crompton, M., Harold, G., Hobbs, S., Kamalati, T., Knox, R., Neil, C., Yull, F., 1997. Selective cell ablation in the mammary gland of transgenic mice. *Endocrine-Related Cancer* 4, 67-74.

Guy, R.H., Hadgraft, J., 1985. Transdermal drug delivery: a simplified pharmacokinetic approach. *Int J Pharmaceut* 24, 267-274.

Hadgraft, J., 1999. Passive enhancement strategies in topical and transdermal drug delivery. *Int J Pharmaceut* 184, 1-6.

Hadgraft, J., Valenta, C., 2000. pH, pKa and dermal delivery. *Int J Pharmaceut* 200, 243-247.

Hascicek, C., Bediz-Ölçer, A., Gönül, N., 2009. Preparation and evaluation of different gel formulations for transdermal delivery of meloxicam. *Turk J. Pharm. Sci* 6, 177-186.

Herting, G., Jiang, T., Sjostedt, C., Odnevall Wallinder, I., 2014. Release of Si from silicon, a ferrosilicon (FeSi) alloy and a synthetic silicate mineral in simulated biological media. *PloS one* 9, e107668.

Heurtault, B., Saulnier, P., Pech, B., Proust, J.-E., Benoit, J.-P., 2003. Physico-chemical stability of colloidal lipid particles. *Biomaterials* 24, 4283-4300.

Higuchi, T., 1961. Rate of release of medicaments from ointment bases containing drugs in suspension. *J Pharm Sci* 50, 874-875.

Higuchi, T., 1963a. Mechanism of sustained-action medication. Theoretical analysis of rate of release of solid drugs dispersed in solid matrices. *J Pharm Sci* 52, 1145-1149.

Higuchi, T., 1963b. Mechanism of sustained - action medication. Theoretical analysis of rate of release of solid drugs dispersed in solid matrices. *J Pharm Sci* 52, 1145-1149.

Hiruta, Y., Hattori, Y., Kawano, K., Obata, Y., Maitani, Y., 2006. Novel ultra-deformable vesicles entrapped with bleomycin and enhanced to penetrate rat skin. *J Control Release* 113, 146-154.

Holme, S.A., Malinowszky, K., Roberts, D.L., 2000. Changing trends in non-melanoma skin cancer in South Wales, 1988-98. *The British journal of dermatology* 143, 1224-1229.

Honeywell-Nguyen, P.L., Bouwstra, J.A., 2003. The in vitro transport of pergolide from surfactant-based elastic vesicles through human skin: a suggested mechanism of action. *J Control Release* 86, 145-156.

Honeywell-Nguyen, P.L., de Graaff, A.M., Groenink, H.W., Bouwstra, J.A., 2002. The in vivo and in vitro interactions of elastic and rigid vesicles with human skin. *Biochimica et Biophysica Acta (BBA)-General Subjects* 1573, 130-140.

Hsiu, S.L., Huang, T.Y., Hou, Y.C., Chin, D.H., Chao, P.D., 2002. Comparison of metabolic pharmacokinetics of naringin and naringenin in rabbits. *Life Sci* 70, 1481-1489.

Huang, Y.C., Yang, C.H., Chiou, Y.L., 2011. Citrus flavanone naringenin enhances melanogenesis through the activation of Wnt/beta-catenin signalling in mouse melanoma cells. *Phytomedicine : international journal of phytotherapy and phytopharmacology* 18, 1244-1249.

Hwang, J.-T., Ha, J., Park, I.-J., Lee, S.-K., Baik, H.W., Kim, Y.M., Park, O.J., 2007. Apoptotic effect of EGCG in HT-29 colon cancer cells via AMPK signal pathway. *Cancer letters* 247, 115-121.

Istemic, K., Cerc Korosec, R., Poklar Ulrih, N., 2016. Encapsulation of (-)-epigallocatechin gallate into liposomes and into alginate or chitosan microparticles reinforced with liposomes. *Journal of the science of food and agriculture* 96, 4623-4632.

Ita, K.B., Du Preez, J., Lane, M.E., Hadgraft, J., du Plessis, J., 2007. Dermal delivery of selected hydrophilic drugs from elastic liposomes: effect of phospholipid formulation and surfactants. *J Pharm Pharmacol* 59, 1215-1222.

Jaeger, A., Walti, M., Neftel, K., 1988. Side effects of flavonoids in medical practice. *Progress in clinical and biological research* 280, 379-394.

Jain, S.K., Jain, R.K., Chourasia, M.K., Jain, A.K., Chalasani, K.B., Soni, V., Jain, A., 2005. Design and development of multivesicular liposomal depot delivery system for controlled systemic delivery of acyclovir sodium. *Aaps Pharmscitech* 6, E35-E41.

Jiang, A.J., Jiang, G., Li, L.T., Zheng, J.N., 2015. Curcumin induces apoptosis through mitochondrial pathway and caspases activation in human melanoma cells. *Molecular biology reports* 42, 267-275.

Jousma, H., Talsma, H., Spies, F., Joosten, J.G.H., Junginger, H.E., Crommelin, D.J.A., 1987. Characterization of liposomes. The influence of extrusion of multilamellar vesicles through polycarbonate membranes on particle size, particle size distribution and number of bilayers. *Int J Pharmaceut* 35, 263-274.

Kajihara, M., Sugie, T., Hojo, T., Maeda, H., Sano, A., Fujioka, K., Sugawara, S., Urabe, Y., 2001. Development of a new drug delivery system for protein drugs using silicone (II). *J Control Release* 73, 279-291.

Kakkar, S., Pal Kaur, I., 2013. A novel nanovesicular carrier system to deliver drug topically. *Pharm Dev Technol* 18, 673-685.

Kalluri, R., Zeisberg, M., 2006. Fibroblasts in cancer. *Nature Reviews Cancer* 6, 392-401.

Kang, S.N., Hong, S.-S., Kim, S.-Y., Oh, H., Lee, M.-K., Lim, S.-J., 2013. Enhancement of liposomal stability and cellular drug uptake by incorporating tributyrin into celecoxib-loaded liposomes. *Asian Journal of Pharmaceutical Sciences* 8, 128-133.

Kaplan, B., Moy, R.L., 2000. Effect of perilesional injections of PEG-interleukin-2 on basal cell carcinoma. *Dermatol Surg* 26, 1037-1040.

Katahira, N., Murakami, T., Kugai, S., Yata, N., Takano, M., 1999. Enhancement of topical delivery of a lipophilic drug from charged multilamellar liposomes. *J Drug Target* 6, 405-414.

Katalinic, A., Kunze, U., Schäfer, T., 2003. Epidemiology of cutaneous melanoma and non - melanoma skin cancer in Schleswig - Holstein, Germany: incidence, clinical subtypes, tumour stages and localization (epidemiology of skin cancer). *Brit J Dermatol* 149, 1200-1206.

Katiyar, S.K., 2011. Green tea prevents non-melanoma skin cancer by enhancing DNA repair. *Arch Biochem Biophys* 508, 152-158.

Keith, A.D., 1983. Polymer matrix considerations for transdermal devices. *Drug Dev Ind Pharm* 9, 605-625.

Kerkar, S.P., Restifo, N.P., 2012. Cellular constituents of immune escape within the tumor microenvironment. *Cancer research* 72, 3125-3130.

Khan, A.W., Kotta, S., Ansari, S.H., Sharma, R.K., Ali, J., 2015. Enhanced dissolution and bioavailability of grapefruit flavonoid Naringenin by solid dispersion utilizing fourth generation carrier. *Drug Dev Ind Pharm* 41, 772-779.

Kirjavainen, M., Urtti, A., Jääskeläinen, I., Marjukka Suhonen, T., Paronen, P., Valjakka-Koskela, R., Kiesvaara, J., Mönkkönen, J., 1996. Interaction of liposomes with human skin in vitro — The influence of lipid composition and structure. *Biochimica et Biophysica Acta (BBA) - Lipids and Lipid Metabolism* 1304, 179-189.

Knox, R., 2012. MTL-004 - A contact anti-tumour agent for skin cancers.

Knox, R.J., Friedlos, F., Biggs, P.J., Flitter, W.D., Gaskell, M., Goddard, P., Davies, L., Jarman, M., 1993. Identification, synthesis and properties of 5-(aziridin-1-yl)-2-nitro-4-nitrosobenzamide, a novel DNA crosslinking agent derived from CB1954. *Biochemical pharmacology* 46, 797-803.

Knox, R.J., Friedlos, F., Jarman, M., Roberts, J.J., 1988. A new cytotoxic, DNA interstrand crosslinking agent, 5-(aziridin-1-yl)-4-hydroxylamino-2-nitrobenzamide, is formed from 5-(aziridin-1-yl)-2,4-

dinitrobenzamide (CB 1954) by a nitroreductase enzyme in Walker carcinoma cells. *Biochemical pharmacology* 37, 4661-4669.

Knox, R.J., Friedlos, F., Lydall, D.A., Roberts, J.J., 1986. Mechanism of cytotoxicity of anticancer platinum drugs: evidence that cis-diamminedichloroplatinum (II) and cis-diammine-(1, 1-cyclobutanedicarboxylato) platinum (II) differ only in the kinetics of their interaction with DNA. *Cancer research* 46, 1972-1979.

Knox, R.J., Friedlos, F., Marchbank, T., Roberts, J.J., 1991. Bioactivation of CB 1954: reaction of the active 4-hydroxylamino derivative with thioesters to form the ultimate DNA-DNA interstrand crosslinking species. *Biochemical pharmacology* 42, 1691-1697.

Ko, C.B., Walton, S., Kecskes, K., Bury, H.P., Nicholson, C., 1994. The emerging epidemic of skin cancer. *The British journal of dermatology* 130, 269-272.

Kootstra, A., 1994. Protection from UV-B-induced DNA damage by flavonoids. *Plant Molecular Biology* 26, 771-774.

Korsmeyer, R.W., Gurny, R., Doelker, E., Buri, P., Peppas, N.A., 1983. Mechanisms of solute release from porous hydrophilic polymers. *Int J Pharmaceut* 15, 25-35.

Küchler, S., Radowski, M.R., Blaschke, T., Dathe, M., Plendl, J., Haag, R., Schäfer-Korting, M., Kramer, K.D., 2009. Nanoparticles for skin penetration enhancement—a comparison of a dendritic core-multishell-nanotransporter and solid lipid nanoparticles. *Eur J Pharm Biopharm* 71, 243-250.

Kuflik, E.G., 1994. Cryosurgery updated. *Journal of the American Academy of Dermatology* 31, 925-944.

Kumar, M., Ahuja, M., Sharma, S.K., 2008. Hepatoprotective study of curcumin-soya lecithin complex. *Scientia pharmaceutica* 76, 761.

Kunnumakkara, A.B., Anand, P., Aggarwal, B.B., 2008. Curcumin inhibits proliferation, invasion, angiogenesis and metastasis of different cancers through interaction with multiple cell signaling proteins. *Cancer letters* 269, 199-225.

Kuntsche, J., Bunjes, H., Fahr, A., Pappinen, S., Ronkko, S., Suhonen, M., Urtti, A., 2008. Interaction of lipid nanoparticles with human epidermis and an organotypic cell culture model. *Int J Pharm* 354, 180-195.

Laouini, A., Jaafar-Maalej, C., Limayem-Blouza, I., Sfar, S., Charcosset, C., Fessi, H., 2012. Preparation, characterization and applications of liposomes: state of the art. *Journal of colloid Science and Biotechnology* 1, 147-168.

Lapinski, M.M., Castro-Forero, A., Greiner, A.J., Ofoli, R.Y., Blanchard, G.J., 2007. Comparison of liposomes formed by sonication and extrusion: rotational and translational diffusion of an embedded chromophore. *Langmuir* 23, 11677-11683.

Lasic, D.D., Barenholz, Y., 1996. *Handbook of nonmedical applications of liposomes: Theory and basic sciences*. CRC Press.

Lau, K.G., Hattori, Y., Chopra, S., O'Toole, E.A., Storey, A., Nagai, T., Maitani, Y., 2005. Ultra-deformable liposomes containing bleomycin: In vitro stability and toxicity on human cutaneous keratinocyte cell lines. *Int J Pharmaceut* 300, 4-12.

Lee, A., 1975. Fluorescence studies of chlorophyll α incorporated into lipid mixtures, and the interpretation of "phase" diagrams. *Biochimica et Biophysica Acta (BBA)-Biomembranes* 413, 11-23.

Lee, E.H., Kim, A., Oh, Y.-K., Kim, C.-K., 2005. Effect of edge activators on the formation and transfection efficiency of ultradeformable liposomes. *Biomaterials* 26, 205-210.

Lee, M.-H., Yoon, S., Moon, J.-O., 2004. The flavonoid naringenin inhibits dimethylnitrosamine-induced liver damage in rats. *Biological and Pharmaceutical Bulletin* 27, 72-76.

Lee, P.I., 1985. Kinetics of drug release from hydrogel matrices. *J Control Release* 2, 277-288.

Lee, R.W., Shenoy, D.B., Sheel, R., 2010. Micellar nanoparticles: applications for topical and passive transdermal drug delivery. *Handbook of Non-Invasive Drug Delivery Systems*. Burlington, MA: Elsevier Inc, 37-58.

Lentz, B.R., Carpenter, T.J., Alford, D.R., 1987. Spontaneous fusion of phosphatidylcholine small unilamellar vesicles in the fluid phase. *Biochemistry* 26, 5389-5397.

Levy, M.Y., Benita, S., Baszkin, A., 1991. Interactions of a non-ionic surfactant with mixed phospholipid—oleic acid monolayers. *Studies under dynamic conditions. Colloid Surface* 59, 225-241.

Li, Y., Yang, D.-J., Chen, S.-L., Chen, S.-B., Chan, A.S.-C., 2008. Comparative physicochemical characterization of phospholipids complex of puerarin formulated by conventional and supercritical methods. *Pharm Res-Dord* 25, 563-577.

Lichtenberg, D., Barenholz, Y., 1988. Liposomes: preparation, characterization, and preservation. *Methods of biochemical analysis* 33, 337-462.

Lindley, C., McCune, J.S., Thomason, T.E., Lauder, D., Sauls, A., Adkins, S., Sawyer, W.T., 1999. Perception of Chemotherapy Side Effects Cancer versus Noncancer Patients. *Cancer Practice* 7, 59-65.

Liu, B., Krieger, M., 2002. Highly purified scavenger receptor class B, type I reconstituted into phosphatidylcholine/cholesterol liposomes mediates high affinity high density lipoprotein binding and selective lipid uptake. *Journal of Biological Chemistry* 277, 34125-34135.

Liu, Y., Steiniger, S.C., Kim, Y., Kaufmann, G.F., Felding-Habermann, B., Janda, K.D., 2007. Mechanistic studies of a peptidic GRP78 ligand for cancer cell-specific drug delivery. *Molecular pharmaceutics* 4, 435-447.

Lomas, A., Leonardi-Bee, J., Bath-Hextall, F., 2012. A systematic review of worldwide incidence of nonmelanoma skin cancer. *The British journal of dermatology* 166, 1069-1080.

Lorenz, W., Schmal, A., Schult, H., Lang, S., Ohmann, C., Weber, D., Kapp, B., Luben, L., Doenicke, A., 1982. Histamine release and hypotensive reactions in dogs by solubilizing agents and fatty acids: analysis of various components in cremophor El and development of a compound with reduced toxicity. *Agents and actions* 12, 64-80.

MacLennan, R., Green, A.C., McLeod, G.R., Martin, N.G., 1992. Increasing incidence of cutaneous melanoma in Queensland, Australia. *Journal of the National Cancer Institute* 84, 1427-1432.

Madan, V., Lear, J.T., Szeimies, R.-M., Non-melanoma skin cancer. *The Lancet* 375, 673-685.

Mahalingam, A., Simmons, A.P., Ugaonkar, S.R., Watson, K.M., Dezzutti, C.S., Rohan, L.C., Buckheit, R.W., Kiser, P.F., 2011. Vaginal microbicide gel for delivery of IQP-0528, a pyrimidinedione analog with a dual mechanism of action against HIV-1. *Antimicrob Agents Ch* 55, 1650-1660.

Maiti, K., Mukherjee, K., Gantait, A., Saha, B.P., Mukherjee, P.K., 2007. Curcumin–phospholipid complex: preparation, therapeutic evaluation and pharmacokinetic study in rats. *Int J Pharmaceut* 330, 155-163.

Marcil, I., Stern, R.S., 2000. Risk of developing a subsequent nonmelanoma skin cancer in patients with a history of nonmelanoma skin cancer: a critical review of the literature and meta-analysis. *Archives of dermatology* 136, 1524-1530.

Marks, R., 1996. Squamous cell carcinoma. *The Lancet* 347, 735-738.

Marks, R., Gebauer, K., Shumack, S., Amies, M., Bryden, J., Fox, T.L., Owens, M.L., Group, T.A.M.T., 2001. Imiquimod 5% cream in the treatment of superficial basal cell carcinoma: results of a multicenter 6-week dose-response trial. *Journal of the American Academy of Dermatology* 44, 807-813.

Martin, F.J., MacDonald, R.C., 1976. Lipid vesicle-cell interactions. I. Hemagglutination and hemolysis. *The Journal of cell biology* 70, 494-505.

Masaro, L., Zhu, X.X., 1999. Physical models of diffusion for polymer solutions, gels and solids. *Progress in Polymer Science* 24, 731-775.

Mashghi, A., Partovi-Azar, P., Jadidi, T., Nafari, N., Maass, P., Tabar, M.R., Bonn, M., Bakker, H.J., 2012. Hydration strongly affects the molecular and electronic structure of membrane phospholipids. *The Journal of chemical physics* 136, 114709.

Mashak, A., Rahimi, A., 2009. Silicone polymers in controlled drug delivery systems: a review. *Iranian Polymer Journal* 18, 279-295.

McGraw-HillCompanies, 2003. *Skin Structure and Function*.

McLoughlin, P., Roengvoraphoj, M., Gissel, C., Hescheler, J., Certa, U., Sachinidis, A., 2004. Transcriptional responses to epigallocatechin-3 gallate in HT 29 colon carcinoma spheroids. *Genes to cells : devoted to molecular & cellular mechanisms* 9, 661-669.

Melchior, D.L., Steim, J.M., 1976. Thermotropic transitions in biomembranes. *Annual review of biophysics and bioengineering* 5, 205-238.

Meyer, T., Nindl, I., Schmook, T., Ulrich, C., Sterry, W., Stockfleth, E., 2003. Induction of apoptosis by Toll - like receptor - 7 agonist in tissue cultures. *Brit J Dermatol* 149, 9-13.

Middleton Jr, E., 1998. Effect of plant flavonoids on immune and inflammatory cell function, *Flavonoids in the Living System*. Springer, pp. 175-182.

Mignet, N., Seguin, J., Chabot, G.G., 2013. Bioavailability of polyphenol liposomes: a challenge ahead. *Pharmaceutics* 5, 457-471.

Mihara, M., Nakayama, H., Nakamura, K., Morimura, T., Hagari, Y., Shima, S., 1990. Histologic changes in superficial basal cell epithelioma and Bowen's disease by intralesional injection of recombinant interleukin 2: recombinant interleukin 2 may induce redifferentiation of malignant tumor cells in vivo. *Archives of dermatology* 126, 1107.

Modi, S., Anderson, B.D., 2013. Determination of drug release kinetics from nanoparticles: overcoming pitfalls of the dynamic dialysis method. *Molecular pharmaceutics* 10, 3076-3089.

Mogensen, M., Joergensen, T.M., N rnberg, B.M., Morsy, H.A., Thomsen, J.B., Thrane, L., Jemec, G.B.E., 2009. Assessment of Optical Coherence Tomography Imaging in the Diagnosis of Non-Melanoma Skin Cancer and Benign Lesions Versus Normal Skin: Observer-Blinded Evaluation by Dermatologists and Pathologists. *Dermatol Surg* 35, 965-972.

Mohammed, A.R., Weston, N., Coombes, A.G., Fitzgerald, M., Perrie, Y., 2004. Liposome formulation of poorly water soluble drugs: optimisation of drug loading and ESEM analysis of stability. *Int J Pharm* 285, 23-34.

Mourtas, S., Fotopoulou, S., Duraj, S., Sfika, V., Tsakiroglou, C., Antimisiaris, S.G., 2007. Liposomal drugs dispersed in hydrogels. Effect of liposome, drug and gel properties on drug release kinetics. *Colloids and surfaces. B, Biointerfaces* 55, 212-221.

Mukhtar, H., Ahmad, N., 2000. Tea polyphenols: prevention of cancer and optimizing health. *The American journal of clinical nutrition* 71, 1698s-1702s.

Nafee, N.A., Ismail, F.A., Boraie, N.A., Mortada, L.M., 2003. Mucoadhesive buccal patches of miconazole nitrate: in vitro/in vivo performance and effect of ageing. *Int J Pharmaceut* 264, 1-14.

Nagarajan, R., 2002. Molecular packing parameter and surfactant self-assembly: the neglected role of the surfactant tail. *Langmuir* 18, 31-38.

Naik, A., Kalia, Y.N., Guy, R.H., 2000. Transdermal drug delivery: overcoming the skin's barrier function. *Pharmaceutical science & technology today* 3, 318-326.

Natural-Sourcing, 2017. Material safety data sheet, Polysorbate 20. Natural Sourcing 341 Christian Street, Oxford, CT 06478, USA.

Neville, J.A., Welch, E., Leffell, D.J., 2007. Management of nonmelanoma skin cancer in 2007. *Nat Clin Prac Oncol* 4, 462-469.

Nguyen, T.H., Ho, D.Q., 2002. Nonmelanoma skin cancer. *Current treatment options in oncology* 3, 193-203.

Nishiyama, N., 2007. Nanomedicine: Nanocarriers shape up for long life. *Nat Nano* 2, 203-204.

Oguz Acart rk, T., Edington, H., 2005. Nonmelanoma Skin Cancer. *Clinics in plastic surgery* 32, 237-248.

Oh, Y.K., Kim, M.Y., Shin, J.Y., Kim, T.W., Yun, M.O., Yang, S.J., Choi, S.S., Jung, W.W., Kim, J.A., Choi, H.G., 2006. Skin permeation of retinol in Tween 20-based deformable liposomes: in-vitro evaluation in human skin and keratinocyte models. *J Pharm Pharmacol* 58, 161-166.

Pagano, R.E., Weinstein, J.N., 1978. Interactions of liposomes with mammalian cells. *Annual review of biophysics and bioengineering* 7, 435-468.

Panomsuk, S.P., Hatanaka, T., Aiba, T., Katayama, K., Koizumi, T., 1996. A Study of the Hydrophilic Cellulose Matrix : Effect of Drugs on Swelling Properties. *Chemical & pharmaceutical bulletin* 44, 1039-1042.

Paolino, D., Cosco, D., Muzzalupo, R., Trapasso, E., Picci, N., Fresta, M., 2008. Innovative bola-surfactant niosomes as topical delivery systems of 5-fluorouracil for the treatment of skin cancer. *Int J Pharm* 353, 233-242.

Papahadjopoulos, D., Kimelberg, H.K., 1974. Phospholipid vesicles (liposomes) as models for biological membranes: their properties and interactions with cholesterol and proteins. *Progress in surface science* 4, 141N9145-144232.

Papahadjopoulos, D., 1976. The role of cholesterol as a membrane component: effects on lipid-protein interactions. *Lipids*. (R. Paoletti, G. Porcelatti, and G. Lacini, editors. Raven Press, New York. 1: 187-196.

Pappinen, S., Hermansson, M., Kuntsche, J., Somerharju, P., Wertz, P., Urtti, A., Suhonen, M., 2008. Comparison of rat epidermal keratinocyte organotypic culture (ROC) with intact human skin: lipid composition and thermal phase behavior of the stratum corneum. *Biochim Biophys Acta* 1778, 824-834.

Park, S.-I., Lee, E.-O., Yang, H.-M., Park, C.W., Kim, J.-D., 2013. Polymer-hybridized liposomes of poly (amino acid) derivatives as transepidermal carriers. *Colloids and Surfaces B: Biointerfaces* 110, 333-338.

Patton, D., Sweeney, Y.C., Balkus, J., Rohan, L., Moncla, B., Parniak, M., Hillier, S., 2007. Preclinical safety assessments of UC781 anti-human immunodeficiency virus topical microbicide formulations. *Antimicrob Agents Ch* 51, 1608-1615.

Peng, P.-L., Hsieh, Y.-S., Wang, C.-J., Hsu, J.-L., Chou, F.-P., 2006. Inhibitory effect of berberine on the invasion of human lung cancer cells via decreased productions of urokinase-plasminogen activator and matrix metalloproteinase-2. *Toxicology and applied pharmacology* 214, 8-15.

Peppas, N.A., 1985. Analysis of Fickian and non-Fickian drug release from polymers. *Pharmaceutica acta Helvetiae* 60, 110-111.

Peppas, N.A., Sahlin, J.J., 1989. A simple equation for the description of solute release. III. Coupling of diffusion and relaxation. *Int J Pharmaceut* 57, 169-172.

Phan, C.T., Tso, P., 2001. Intestinal lipid absorption and transport. *Frontiers in bioscience : a journal and virtual library* 6, D299-319.

Prausnitz, M.R., Langer, R., 2008. Transdermal drug delivery. *Nat Biotech* 26, 1261-1268.

Proceedings of the National Academy of Sciences of the United States of America, 2014. Role of lipid polymorphism in G protein-membrane interactions: Nonlamellar-prone phospholipids and peripheral protein binding to membranes.

Prow, T.W., Grice, J.E., Lin, L.L., Faye, R., Butler, M., Becker, W., Wurm, E.M., Yoong, C., Robertson, T.A., Soyer, H.P., 2011. Nanoparticles and microparticles for skin drug delivery. *Adv Drug Deliver Rev* 63, 470-491.

Puri, R., Jain, S., 2012. Ethogel topical formulation for increasing the local bioavailability of 5-fluorouracil: a mechanistic study. *Anti-Cancer Drug* 23, 923-934.

Ranga Rao, K.V., Devi, K.P., Buri, P., 1988. Cellulose Matrices for Zero-Order Release of Soluble Drugs. *Drug Dev Ind Pharm* 14, 2299-2320.

Ranga Rao, K.V., Padmalatha Devi, K., 1988. Swelling controlled-release systems: recent developments and applications. *Int J Pharmaceut* 48, 1-13.

Rao, K.V.R., Devi, K.P., Buri, P., 1990. Influence of molecular size and water solubility of the solute on its release from swelling and erosion controlled polymeric matrices. *J Control Release* 12, 133-141.

Rashidinejad, A., Birch, E.J., Sun-Waterhouse, D., Everett, D.W., 2014. Delivery of green tea catechin and epigallocatechin gallate in liposomes incorporated into low-fat hard cheese. *Food chemistry* 156, 176-183.

Ritger, P.L., Peppas, N.A., 1987. A simple equation for description of solute release II. Fickian and anomalous release from swellable devices. *J Control Release* 5, 37-42.

Rogalski, C., Dummer, R., Burg, G., 1999. Immunomodulators in the treatment of cutaneous lymphoma. *Journal of the European Academy of Dermatology and Venereology* 13, 83-90.

Romero, E.L., Morilla, M.J., 2013a. Highly deformable and highly fluid vesicles as potential drug delivery systems: theoretical and practical considerations. *Int J Nanomedicine* 8, 3171-3186.

Romero, E.L., Morilla, M.J., 2013b. Highly deformable and highly fluid vesicles as potential drug delivery systems: theoretical and practical considerations. *Int J Nanomedicine* 8, 86.

Romero, H.L., Dellaert, N.P., van der Geer, S., Frunt, M., Jansen-Vullers, M.H., Krekels, G.A., 2013. Admission and capacity planning for the implementation of one-stop-shop in skin cancer treatment using simulation-based optimization. *Health care management science* 16, 75-86.

Rubin, A.I., Chen, E.H., Ratner, D., 2005. Basal-cell carcinoma. *The New England journal of medicine* 353, 2262-2269.

Salko, N., Ajkovic, M., Jalenjak, I., 1998. Liposomes with metronidazole for topical use: the choice of preparation method and vehicle. *J Liposome Res* 8, 283-293.

Sabin, J., Prieto, G., Ruso, J., Hidalgo-Alvarez, R., Sarmiento, F., 2006. Size and stability of liposomes: a possible role of hydration and osmotic forces. *The European Physical Journal E: Soft Matter and Biological Physics* 20, 401-408.

Sackmann, E., 1994. The seventh Datta Lecture. Membrane bending energy concept of vesicle- and cell-shapes and shape-transitions. *Febs Lett* 346, 3-16.

Sai Cheong Wan, L., Wan Sia Heng, P., Fun Wong, L., 1995. Matrix swelling: A simple model describing extent of swelling of HPMC matrices. *Int J Pharmaceut* 116, 159-168.

Sato, K., Oda, T., Sugibayashi, K., Morimoto, Y., 1988. Estimation of blood concentration of drugs after topical application from in vitro skin permeation data. I. Prediction by convolution and confirmation by deconvolution. *Chemical & pharmaceutical bulletin* 36, 2232-2238.

Sauder, D., 2003. Imiquimod: modes of action. *Brit J Dermatol* 149, 5-8.

Schäfer-Korting, M., Mehnert, W., Korting, H.-C., 2007. Lipid nanoparticles for improved topical application of drugs for skin diseases. *Adv Drug Deliver Rev* 59, 427-443.

Schmuth, M., Blunder, S., Dubrac, S., Gruber, R., Moosbrugger-Martinz, V., 2015. Epidermal barrier in hereditary ichthyoses, atopic dermatitis, and psoriasis. *Journal der Deutschen Dermatologischen Gesellschaft = Journal of the German Society of Dermatology : JDDG* 13, 1119-1123.

Schreier, H., Bouwstra, J., 1994. Liposomes and niosomes as topical drug carriers: dermal and transdermal drug delivery. *J Control Release* 30, 1-15.

Schroeder, A., Kost, J., Barenholz, Y., 2009. Ultrasound, liposomes, and drug delivery: principles for using ultrasound to control the release of drugs from liposomes. *Chem Phys Lipids* 162, 1-16.

Schubert, M., Müller-Goymann, C., 2003. Solvent injection as a new approach for manufacturing lipid nanoparticles—evaluation of the method and process parameters. *Eur J Pharm Biopharm* 55, 125-131.

Scudiero, D.A., Shoemaker, R.H., Paull, K.D., Monks, A., Tierney, S., Nofziger, T.H., Currens, M.J., Seniff, D., Boyd, M.R., 1988. Evaluation of a soluble tetrazolium/formazan assay for cell growth and drug sensitivity in culture using human and other tumor cell lines. *Cancer research* 48, 4827-4833.

Semalty, A., Semalty, M., Singh, D., Rawat, M.S.M., 2010a. Preparation and characterization of phospholipid complexes of naringenin for effective drug delivery. *J Incl Phenom Macro* 67, 253-260.

Semalty, A., Semalty, M., Singh, D., Rawat, M.S.M., 2010b. Preparation and characterization of phospholipid complexes of naringenin for effective drug delivery. *J Incl Phenom Macro* 67, 253-260.

Seras, M., Handjani-Vila, R.-M., Ollivon, M., Lesieur, S., 1992. Kinetic aspects of the solubilization of non-ionic monoalkyl amphiphile-cholesterol vesicles by octylglucoside. *Chem Phys Lipids* 63, 1-14.

Shakeel, F., Ramadan, W., Faisal, M.S., Rizwan, M., Faiyazuddin, M., Mustafa, G., Shafiq, S., 2010. Transdermal and topical delivery of anti-inflammatory agents using nanoemulsion/microemulsion: an updated review. *Current nanoscience* 6, 184-198.

Shankar, S., Ganapathy, S., Hingorani, S.R., Srivastava, R.K., 2008. EGCG inhibits growth, invasion, angiogenesis and metastasis of pancreatic cancer. *Frontiers in bioscience : a journal and virtual library* 13, 440-452.

Siddiqui, I.A., Adhami, V.M., Bharali, D.J., Hafeez, B.B., Asim, M., Khwaja, S.I., Ahmad, N., Cui, H., Mousa, S.A., Mukhtar, H., 2009. Introducing Nanochemoprevention as a Novel Approach for Cancer Control: Proof of Principle with Green Tea Polyphenol Epigallocatechin-3-Gallate. *Cancer research* 69, 1712-1716.

Siepmann, J., Peppas, N., 2012. Modeling of drug release from delivery systems based on hydroxypropyl methylcellulose (HPMC). *Adv Drug Deliver Rev* 64, 163-174.

Sigler, K., Ruch, R.J., 1993. Enhancement of gap junctional intercellular communication in tumor promoter-treated cells by components of green tea. *Cancer letters* 69, 15-19.

Sigma-Aldrich(a), 2017. Tween 80.

Sigma-Aldrich(b), 2017. Tween 20.

Sigma-Aldrich(c), 2017. Sodium cholate.

Sigma-Aldrich(d), 2017. Phosphate buffered saline.

Sigma-Aldrich(e), 2017. Epigallocatechin gallate. Sigma Aldrich.

Singh, B.N., Shankar, S., Srivastava, R.K., 2011a. Green tea catechin, epigallocatechin-3-gallate (EGCG): Mechanisms, perspectives and clinical applications. *Biochemical pharmacology* 82, 1807-1821.

Singh, T., Vaid, M., Katiyar, N., Sharma, S., Katiyar, S.K., 2011b. Berberine, an isoquinoline alkaloid, inhibits melanoma cancer cell migration by reducing the expressions of cyclooxygenase-2, prostaglandin E(2) and prostaglandin E(2) receptors. *Carcinogenesis* 32, 86-92.

Sinha Roy, D., Rohera, B.D., 2002. Comparative evaluation of rate of hydration and matrix erosion of HEC and HPC and study of drug release from their matrices. *Eur J Pharm Sci* 16, 193-199.

Sitzia, J., Huggins, L., 1998. Side effects of cyclophosphamide, methotrexate, and 5-fluorouracil (CMF) chemotherapy for breast cancer. *Cancer Practice* 6, 13-21.

Soltani-Arabshahi, R., Tristani-Firouzi, P., 2013. Chemoprevention of nonmelanoma skin cancer. *Facial Plastic Surgery* 29, 373-383.

Sou, K., 2011. Electrostatics of carboxylated anionic vesicles for improving entrapment capacity. *Chem Phys Lipids* 164, 211-215.

Specht, C., Stoye, I., Muller-Goymann, C.C., 1998. Comparative investigations to evaluate the use of organotypic cultures of transformed and native dermal and epidermal cells for permeation studies. *Eur J Pharm Biopharm* 46, 273-278.

Sternberg, B., Sorgi, F.L., Huang, L., 1994. New structures in complex formation between DNA and cationic liposomes visualized by freeze—fracture electron microscopy. *Febs Lett* 356, 361-366.

Stott, P.W., Williams, A.C., Barry, B.W., 1998. Transdermal delivery from eutectic systems: enhanced permeation of a model drug, ibuprofen. *J Control Release* 50, 297-308.

Sullivan, T.P., Dearaujo, T., Vincek, V., Berman, B., 2003. Evaluation of superficial basal cell carcinomas after treatment with imiquimod 5% cream or vehicle for apoptosis and lymphocyte phenotyping. *Dermatol Surg* 29, 1181-1186.

Sun Spot Melanoma Awareness, 2013. Skin Care Awareness.

Szoka, F., Papahadjopoulos, D., 1978. Procedure for preparation of liposomes with large internal aqueous space and high capture by reverse-phase evaporation. *Proceedings of the National Academy of Sciences of the United States of America* 75, 4194-4198.

Szoka Jr, F., Papahadjopoulos, D., 1980. Comparative properties and methods of preparation of lipid vesicles (liposomes). *Annual review of biophysics and bioengineering* 9, 467-508.

Tan, Z., Zhang, J., Wu, J., Fang, L., He, Z., 2009. The Enhancing Effect of Ion-pairing on the Skin Permeation of Glipizide. *Aaps Pharmscitech* 10, 967.

Tanigawa, T., Kanazawa, S., Ichibori, R., Fujiwara, T., Magome, T., Shingaki, K., Miyata, S., Hata, Y., Tomita, K., Matsuda, K., Kubo, T., Tohyama, M., Yano, K., Hosokawa, K., 2014. (+)-Catechin protects dermal fibroblasts against oxidative stress-induced apoptosis. *BMC complementary and alternative medicine* 14, 133.

ten Tije, A.J., Verweij, J., Loos, W.J., Sparreboom, A., 2003. Pharmacological effects of formulation vehicles: implications for cancer chemotherapy. *Clin Pharmacokinet* 42, 665-685.

Teow, H.M., Zhou, Z., Najlah, M., Yusof, S.R., Abbott, N.J., D'Emanuele, A., 2013. Delivery of paclitaxel across cellular barriers using a dendrimer-based nanocarrier. *Int J Pharm* 441, 701-711.

Thawonsuwan, J., Kiron, V., Satoh, S., Panigrahi, A., Verlhac, V., 2010. Epigallocatechin-3-gallate (EGCG) affects the antioxidant and immune defense of the rainbow trout, *Oncorhynchus mykiss*. *Fish physiology and biochemistry* 36, 687-697.

Thewalt, J.L., Bloom, M., 1992. Phosphatidylcholine. *Biophys J* 63, 1176-1181.

Thomas, B.J., Finnin, B.C., 2004. The transdermal revolution. *Drug discovery today* 9, 697-703.

Touitou, E., Dayan, N., Bergelson, L., Godin, B., Eliaz, M., 2000. Ethosomes—novel vesicular carriers for enhanced delivery: characterization and skin penetration properties. *J Control Release* 65, 403-418.

Touitou, E., Fabin, B., Dany, S., Almog, S., 1988. Transdermal delivery of tetrahydrocannabinol. *Int J Pharmaceut* 43, 9-15.

Trotta, M., Peira, E., Carlotti, M.E., Gallarate, M., 2004. Deformable liposomes for dermal administration of methotrexate. *Int J Pharm* 270, 119-125.

Trotta, M., Peira, E., Debernardi, F., Gallarate, M., 2002. Elastic liposomes for skin delivery of dipotassium glycyrrhizinate. *Int J Pharmaceut* 241, 319-327.

Trotta, M., Ugazio, E., Peira, E., Pulitano, C., 2003. Influence of ion pairing on topical delivery of retinoic acid from microemulsions. *J Control Release* 86, 315-321.

Trovatti, E., Silva, N.H., Duarte, I.F., Rosado, C.F., Almeida, I.F., Costa, P., Freire, C.S., Silvestre, A.J., Neto, C.P., 2011. Biocellulose membranes as supports for dermal release of lidocaine. *Biomacromolecules* 12, 4162-4168.

Tsai, M.J., Huang, Y.B., Fang, J.W., Fu, Y.S., Wu, P.C., 2015. Preparation and Characterization of Naringenin-Loaded Elastic Liposomes for Topical Application. *PloS one* 10, e0131026.

Urosevic, M., Dummer, R., 2002. Immunotherapy for nonmelanoma skin cancer: does it have a future? *Cancer* 94, 477-485.

Utreja, P., Jain, S., Tiwary, A.K., 2011. Localized delivery of paclitaxel using elastic liposomes: Formulation development and evaluation. *Drug Deliv* 18, 367-376.

- Vajjha, R.S., Das, D.K., Kulkarni, D.P., 2010. Development of new correlations for convective heat transfer and friction factor in turbulent regime for nanofluids. *International Journal of Heat and Mass Transfer* 53, 4607-4618.
- Valenta, C., Auner, B.G., 2004. The use of polymers for dermal and transdermal delivery. *Eur J Pharm Biopharm* 58, 279-289.
- van den Bergh, B.A., Vroom, J., Gerritsen, H., Junginger, H.E., Bouwstra, J.A., 1999. Interactions of elastic and rigid vesicles with human skin in vitro: electron microscopy and two-photon excitation microscopy. *Biochimica et Biophysica Acta (BBA)-Biomembranes* 1461, 155-173.
- van der Merwe, D., Brooks, J.D., Gehring, R., Baynes, R.E., Monteiro-Riviere, N.A., Riviere, J.E., 2006. A physiologically based pharmacokinetic model of organophosphate dermal absorption. *Toxicological sciences : an official journal of the Society of Toxicology* 89, 188-204.
- van Kuijk-Meuwissen, M.E., Junginger, H.E., Bouwstra, J.A., 1998. Interactions between liposomes and human skin in vitro, a confocal laser scanning microscopy study. *Biochimica et Biophysica Acta (BBA)-Biomembranes* 1371, 31-39.
- van Winden, E.C.A., Zhang, W., Crommelin, D.J.A., 1997. Effect of Freezing Rate on the Stability of Liposomes During Freeze-Drying and Rehydration. *Pharm Res-Dord* 14, 1151-1160.
- Vázquez-González, M.L., Bernad, R., Calpena, A.C., Domènech, O., Montero, M., Hernández-Borrell, J., 2014. Improving ex vivo skin permeation of non-steroidal anti-inflammatory drugs: enhancing extemporaneous transformation of liposomes into planar lipid bilayers. *Int J Pharmaceut* 461, 427-436.
- Verma, D.D., Verma, S., Blume, G., Fahr, A., 2003. Particle size of liposomes influences dermal delivery of substances into skin. *Int J Pharmaceut* 258, 141-151.
- Vilar, G., Tulla-Puche, J., Albericio, F., 2012. Polymers and drug delivery systems. *Current drug delivery* 9, 367-394.
- Vivero-Escoto, J.L., Slowing, I.I., Wu, C.-W., Lin, V.S.-Y., 2009. Photoinduced intracellular controlled release drug delivery in human cells by gold-capped mesoporous silica nanosphere. *Journal of the American Chemical Society* 131, 3462-3463.
- Vogt, A., Blume-Peytavi, U., 2014. Selective hair therapy: bringing science to the fiction. *Experimental dermatology* 23, 83-86.
- Voss, N., Kim-Sing, C., 1998. Radiotherapy in the treatment of dermatologic malignancies. *Dermatologic clinics* 16, 313-320.
- Wadajkar, A.S., Bhavsar, Z., Ko, C.-Y., Koppolu, B., Cui, W., Tang, L., Nguyen, K.T., 2012. Multifunctional particles for melanoma-targeted drug delivery. *Acta biomaterialia* 8, 2996-3004.
- Wang, Y., Wang, S., Firempong, C.K., Zhang, H., Wang, M., Zhang, Y., Zhu, Y., Yu, J., Xu, X., 2016. Enhanced Solubility and Bioavailability of Naringenin via Liposomal Nanoformulation: Preparation and In Vitro and In Vivo Evaluations. *Aaps Pharmscitech*.
- Warner, R., Lilly, N., 1994. Correlation of water content with ultrastructure in the stratum corneum. *Bioengineering of the skin. Water and the stratum corneum* 1, 3-12.
- Weiner, N., Egbaria, K., Ramachandran, C., 1992. Topical Delivery of Liposomally Encapsulated Interferon Evaluated by In Vitro Diffusion Studies and in a Cutaneous Herpes Guinea Pig Model, in: Braun-Falco, O., Korting, H.C., Maibach, H.I. (Eds.), *Liposome Dermatics: Griesbach Conference*. Springer Berlin Heidelberg, Berlin, Heidelberg, pp. 242-250.
- Wen, J., Liu, B., Yuan, E., Ma, Y., Zhu, Y., 2010a. Preparation and physicochemical properties of the complex of naringenin with hydroxypropyl-beta-cyclodextrin. *Molecules* 15, 4401-4407.
- Wen, J., Liu, B., Yuan, E., Ma, Y., Zhu, Y., 2010b. Preparation and physicochemical properties of the complex of naringenin with hydroxypropyl-β-cyclodextrin. *Molecules* 15, 4401-4407.
- Wiig, H., Swartz, M.A., 2012. Interstitial fluid and lymph formation and transport: physiological regulation and roles in inflammation and cancer. *Physiological reviews* 92, 1005-1060.
- Yamashita, F., Bando, H., Koyama, Y., Kitagawa, S., Takakura, Y., Hashida, M., 1994. In vivo and in vitro analysis of skin penetration enhancement based on a two-layer diffusion model with polar and nonpolar routes in the stratum corneum. *Pharm Res* 11, 185-191.
- Yang, C.S., Maliakal, P., Meng, X., 2002. Inhibition of carcinogenesis by tea. *Annual review of pharmacology and toxicology* 42, 25-54.
- Yanyu, X., Yunmei, S., Zhipeng, C., Qineng, P., 2006. The preparation of silybin-phospholipid complex and the study on its pharmacokinetics in rats. *Int J Pharmaceut* 307, 77-82.

- Yong, C.S., Jung, S.H., Rhee, J.D., Choi, H.G., Lee, B.J., Kim, D.C., Choi, Y.W., Kim, C.K., 2003. Improved solubility and in vitro dissolution of Ibuprofen from poloxamer gel using eutectic mixture with menthol. *Drug Deliv* 10, 179-183.
- Zuidam, N.J., Barenholz, Y., 1997. Electrostatic parameters of cationic liposomes commonly used for gene delivery as determined by 4-heptadecyl-7-hydroxycoumarin1. *Biochimica et Biophysica Acta (BBA) - Biomembranes* 1329, 211-222.